Characterisation and toxicological evaluation of hydrogel-type polymeric biomaterials pre- and post-sterilisation with a novel pulsed plasma gas-discharge system

A thesis submitted for the degree of

Doctor of Philosophy

To the

Higher Education and Training Awards Council

By

Dominik Kirf

May 2010

Based on research carried out under the supervision of

Dr. Sinéad Devery,

Dr. Neil Rowan & Dr. Clement Higginbotham

Declaration

I hereby declare that this thesis submitted to the Higher Education and Training Awards Council for the degree of Doctor of Philosophy, is a result of my own work and has not in the same or altered form, been presented to this institute or any other institute in support of any degree other than which I am now a candidate.

Dominik Kirf
B.Sc. (Hons)
Dipl.-Wirtsch.-Ing. (FH)

Date,
Athlone Institue of Technology

"If we were logical, the future would be bleak, indeed. But we are more than logical. We are human beings, and we have faith, and we have hope, and we can work."

Jacques-Yves Cousteau (1910-1997)

Acknowledgements

I would like to express my sincere appreciation to the people who contributed to the completion of this thesis.

First of all I would like to thank my supervisors, Sinéad Devery, Neil Rowan and Clement Higginbotham, for their knowledge, experience and guidance throughout the duration of this study. I'd like to thank my lead supervisor Sinéad for her guidance and profound expertise in the field of toxicology and for her valuable input into the development of this written thesis. Thank you to Neil for his guidance coupled with all the essential advice and expertise and the contributions relating to the area of microbiology/sterilisation. Thank you to Clem for taking me onboard his AIT-flagship of biopolymer research, for all the valuable discussions and advice in the field of polymer chemistry/technology and for finally getting that fine piece of a piano!

A very big thank you goes to Sinéad Lordan, not only for the detailed proof reading of this document, but also for all the valuable and enjoyable conversations, scientific or otherwise.

I would also like to thank my colleagues in the polymer research group, especially Luke Geever, Thomas Smith and Sean Lyons for repeatedly showing me how to press the "right" buttons on their delicate material characterisation instruments – I'm afraid you will have to show me that again at one stage!

Thanks to Mary McGee and Alan Murphy for their assistance in the set up of analytical chemistry equipment. I would also like to thank Declan Devine and Jessica Hayes from the AO Research Institute, Davos, Switzerland, for providing the scanning electron micrographs.

Furthermore, I would like to extend my gratitude to my old friends from Germany and all the new friends and helpful people I met during my time in Ireland, which are far too many to name on this short page. This includes many researchers of the AIT bioscience and biopolymer research groups and many fellow divers of the Athlone Sub-Aqua Club. Thanks for making me find the time to relax and for introducing me to a great country with an amazing culture!

Of course I won't forget to mention Spooky, the immortal 1930s jazz spirit, who took me and my fellow musicians Luke and Clem on so many musical vacations. It was an honour to have played with you all.

A very special thank you goes to Mary for her unwavering support and encouragement especially at the times when it was needed most. Go raibh míle maith agat. Táim buioch diot as do chúnamh.

Last but not least, my sincere appreciation goes to my family, especially to my mother Marlene and my father Heribert, for their support and belief in me throughout the years. Herzlichen Dank Euch allen!

Abstract

This study investigated the *in vitro* biocompatibility and important physicochemical properties of unique *N*-vinyl-2-pyrrolidone–acrylic acid based copolymer hydrogels intended for use in biomedical applications. Moreover, the suitability of a novel pulsed plasma gas-discharge (PPGD) technology for the nonthermal sterilisation of such hydrogels was also evaluated. Physical hydrogels were synthesised using varying monomer concentrations in conjunction with UV_{340nm} photopolymerisation and the photoinitiator Irgacure® 184. In addition, covalently crosslinked chemical hydrogels were prepared by supplementing the polymerisation reaction with ethylene glycol dimethacrylate based crosslinking agents. The hydrogels were analysed and characterised using a variety of appropriate analytical and mechanical testing techniques.

Initial swelling and degradation studies revealed that the physical hydrogels dissolved after a short swelling period. Further analytical testing showed that considerable amounts of residual monomeric material still remained in the gels post-polymerisation. Subsequently, *in vitro* biocompatibility testing was performed to determine the cytotoxic and genotoxic potential of the hydrogels following direct and indirect contact with human hepatoma (HepG2) and human ileocecal adenocarcinoma (HCT-8) cells, chosen as model cell lines. More specifically, dissolved physical hydrogels were tested in appropriate cytotoxicity assays using MTT and neutral red endpoints. The presence of unreacted components in the physical networks induced severe cytotoxicity following direct cellular exposure to concentrations above 1.25 mg/ml of hydrogel solutions in cell culture medium. In addition, the cell morphology was adversely affected. Similar results were observed following cellular exposure to solid hydrogel discs in the indirect contact (agarose overlay) assay. In the alkaline comet assay the highest tested concentration of physical hydrogels (2.5 mg/ml) resulted in a slight but significant increase in DNA migration. However, this effect was believed to be exerted by the hydrogels' cytotoxic potential rather than through an active genotoxic mechanism. Investigations carried out at the nucleotide level using the Ames assay provided no evidence of mutagenic activity associated with the physical hydrogels.

Chemical hydrogels were shown to be water insoluble and their swelling capacity permitted the retention of high amounts of aqueous solution (over 20-35 times their own weight depending on the monomeric composition), yet still maintaining structural integrity. Chemical analysis suggested that the unreacted monomeric base material was efficiently removed post-polymerisation by applying an additional purification process. An investigation into the gels' mechanical properties revealed that they may find use in wound healing applications. Promising biocompatibility data was obtained during direct and indirect contact exposure of the purified polymers to human keratinocytes (HaCaT) and HepG2 cells. No indication of significant cell death was observed using MTT, neutral red and fluorescence-based toxicity endpoint indicators. In addition, the alkaline comet assay and the Ames assay showed no genotoxic effects following cell exposure to hydrogel extracts. Findings from this study demonstrated that these chemical hydrogels are noncyto- and nongenotoxic and further work should be carried out to investigate their potential as a wound healing device.

Seminal investigations were carried out on the development and subsequent optimisation of the prototype PPGD system for the novel decontamination of hydrogels

under varying operating conditions. Significant calibration and modification of this PPGD system were undertaken in order to apply this emerging technology for hydrogel sterilisation. After considerable and intensive investigations it was discovered that using O_2- and N_2-mediated discharges produced significant antimicrobial activities in test media at varying applied voltages. When artificially inoculated with a high microbial cell density (reaching 4.6 cfu/cm^2 of either *Escherichia coli* or *Staphylococcus aureus*), PPGD effectively decontaminated the chemical hydrogels within 16 minutes of exposure at 16 kV. Preliminary material characterisation suggested that the treatment had no adverse impact on the functional material properties. However, studies into the toxicological safety showed that reactive chemical species and/or electrode degradation products can adversely influence the biocompatibility of treated hydrogels if operated for ≥30 min at 16 kV. Although no genotoxic effects were observed, cytotoxic changes were introduced during prolonged PPGD treatment regimes (at ≥30 min exposures) that were aimed at extreme microbial contamination conditions. The negative impact on the hydrogels biocompatibility was reduced by simply preincubating the hydrogels for 7 days prior to testing thus allowing reactive species to dissipate.

This multidisciplinary project constitutes the first study to report on the development of novel pulsed power electrotechnologies for the nonthermal decontamination of important hydrogels. Specifically, development of PPGD as an alternative or complementary approach to hydrogel sterilisation will increase the available methods of effective decontamination. Development of this PPGD is both pressing and timely as it also coincides with a marked reduction in the amount and intensity of existing decontamination approaches that are effective, as attested by the commensurate rise in unwanted community and healthcare related infections. Findings from this project have also been presented at leading international conferences and published in leading journals.

Abbreviations

AA	Acrylic acid
2-AmAn	2-aminoanthracene
ANOVA	Analysis of variance
AOP	Advanced oxidation processes
AP	Apurinic and apyrimidinic site
ATR	Attenuated total reflectance
CCS	Corona stabilised switch
cfu	Colony-forming unit
DMSO	Dimethlysulfoxide
DNA	Deoxyribonucleic acid
EGDMA	Ethylene glycol dimethacrylate
EDTA	Ethylenediamine tetra-acetic acid
EtBr	Ethidium bromide
EtO	Ethylene oxide
EWC	Equilibrium water content
FCS	Fetal calf serum
FDA	Food and Drug Administration
Fda	Fluorescein diacetate
FTIR	Fourier transform infrared spectroscopy
G’	Storage modulus
G’’	Loss modulus
HaCaT	Human keratinocyte cell line
HCT-8	Human ileocecal adenocarcinoma cell line
HepG2	Human hepatoma cell line
HPLC	High performance liquid chromatography
HV	High voltage
IEC	Ion exchange chromatography
IR	Infrared spectroscopy
Irgacure184®	1-Hydroxycyclohexylphenylketone

ISO	International Organization for Standardization
LMP	Low melting point
MTT	3-(4,5-Dimethylthiazol-2yl)-2,5-diphenyl-2H-tetrazoliumbromid
MW	Molecular weight
4-NQO	4-nitroquinoline-*N*-oxide
2-NF	2-nitrofluorene
NR	Neutral red
NVP	*N*-vinyl-2-pyrrolidone
OD	Optical density
OPA	Ortho-phthalaldehyde
PBS	Phosphate buffered saline
PAA	Poly(acrylic Acid)
PEF	Pulsed electric fields
PEGDMA	Poly(ethylene glycol) dimethacrylate
PFN	Pulse forming network
PPGD	Pulsed plasma gas-discharge
pps	pulse per second
PVC	Poly(vinyl chloride)
PVP	Poly(vinylpyrrolidone)
PPGD	Pulsed plasma gas-discharge
Rf	Radio-frequency
RMC	Residual monomer content
rpm	Revolutions per minute
ScEM	Scanning electron microscopy
SD	Standard deviation
SEM	Standard error of mean
Tris	Tris(hydroxymethyl)aminomethane
UV	Ultraviolet
vis	Visible
Ø	Diameter

Table of Contents

Chapter 1: Introduction

1.1 Biomaterials

Biomaterials are defined as nonviable materials of natural or manmade origin that are used in medical practice to direct, supplement or replace the function of living tissues of the human body (Black, 1992). Biomaterials may be distinguished from other materials in that they possess a combination of properties, including chemical, mechanical, physical and biological properties that render them suitable for safe, effective and reliable use within a physiological environment (Williams, 1987). They can be segmented into three categories: synthetic polymers (plastics), natural polymers (biomolecular materials) and inorganic materials (metals, alloys, ceramic, glass).

The application of biomaterials is not a modern phenomenon. The use of biomaterials can be traced back to the early days of civilisation with artificial eyes, ears, teeth and noses found on Egyptian mummies (Williams and Cunningham, 1979). There is also evidence to suggest that the Chinese and Indians used waxes, glues and tissues in the reconstruction of missing or defective body parts (Ramakrishna *et al*., 2001). However, due to the increased risk of infections associated with biomaterials, their use did not become practical until aseptic surgical techniques were developed by Joseph Lister in the 19th century (Das, 2000; Rimondini *et al.,* 2005). The earliest successful implants were introduced to support the skeletal system and these still accounts for a large portion of modern biomaterial implants. Bone plates were introduced in the early 20th century to aid the fixation of fractures.

Today, biomaterial devices range from relatively simple devices requiring one material, such as pure titanium dental implants, to highly complex assemblies such as a cardiac pacemaker. However, the main application of biomaterials is still found in the form of implants and medical devices. Such implants and medical devices are being widely used to replace and/or restore the function of damaged tissues or organs, to assist in the healing process and to improve function or correct abnormalities, thus leading to an overall improvement in a patient's quality of life. Over the century dramatic advancement in synthetic materials, surgical techniques and sterilisation methods have permitted the use of biomaterials in new and innovative ways (Griffith, 2000). A host of new applications are emerging as a result of major advances in the sciences of molecular cell biology and development biology. An array of novel pharmaceutical agents such as proteins and nucleic

acid based drugs, which cannot be administered via classical delivery formulations, are providing impetus for new implantable biomaterials for controlled drug delivery and gene therapy. Also applications in the relatively new field of tissue engineering, using novel biomaterials as scaffolds to assist regeneration of three-dimensional tissue and organ structures, became possible during the last decades (Stoop, 2008).

1.1.2 The use of polymers as biomaterials

A polymer is a long-chain molecule that consists of a number of small repeating units. Although a wide variety of polymers includes both synthetic and natural materials (Ratner *et al.,* 1996), there is a tendency to forget that the human body is composed of polymers such as proteins, polysaccharides and nucleic acids which are present as basic components in all living organic systems (Dang and Leong, 2006). Indeed, pseudo-poly(amino acid)s are a class of polymers based on natural amino acids linked by nonamide bonds including ester, urethane, and carbonate (Kohn and Langer, 1984, 1987). They offer improved mechanical properties, processing, stability and ease of synthesis over poly amino acids joined by traditional peptide bonds.

However, during the development of the fast expanding polymer industries, new synthetic polymers became available as solids, tubes, fibres, films and textiles (Recum *et al.,* 1998). Today, synthetic polymers are used for numerous other applications mainly because they are available in various compositions, properties, and forms which can be readily fabricated into complex shapes and structures (Ramakrishna *et al.*, 2001).

While the first synthetic polymers were not used for biological applications, the need for new biocompatible materials has led to the introduction of polymers in the field of biomaterials (Recum *et al.,* 1998). Review articles have reported that synthetic polymers such as nylon, poly(methyl methacrylate), Dacron polyester and poly(vinyl chloride) (PVC) found their application in medical surgeries during the early 1940s (Griffith, 2000).

These polymers are still important in the area of clinical medicine today as essential components of permanent prosthetic devices including hip implants, artificial lenses, large diameter vascular grafts, catheters, etc. (Griffith, 2000). In addition, polymers are now used for numerous other medical applications including soft and hard tissue replacement

therapies, dental applications, vascular grafting, medical instrumentations and for a wide variety of novel controlled drug delivery devices (Ramakrishna *et al.,* 2001).

1.1.3 Polymeric biomaterials for controlled drug release

The collaboration between biomaterial science and pharmaceutical science has led to the introduction of natural and synthetic polymers in the field of drug delivery. Basically the term 'drug delivery system' can be defined as a technique that is used to administer therapeutic compounds inside the body (Hillery *et al.,* 2001). In the middle of the last century the increased manufacturing of synthetic and semi-synthetic materials coupled with the new trends and strategies in drug discovery such as the advent of highly potent substances prompted the development of alternative drug systems which attempt to address the requirements of rate and extent of drug release (Karsa and Stephenson, 1996). The versatility of polymers together with the huge possibilities to tailor the interaction between different polymers, polymers and a certain pharmaceutical agent, as well as polymers and the physiological medium led to the development of a wide range of polymeric drug delivery systems for controlled drug release. Controlled drug delivery occurs when a polymer is judiciously combined with a drug or any other active pharmaceutical agent in such a way that the active agent is released from the material in a predesigned manner (Brannon-Peppas, 1997).

The purpose of any controlled delivery system is to enhance or facilitate the action of therapeutic compounds and to minimise side effects. Therefore, a controlled drug delivery system should be able to deliver the correct amount of drug to the site of action at the correct rate and over a specified period of time, in order to maximise the desired therapeutic response. Hence, improved efficiency combined with reduced toxicity and improved patient convenience of new delivery devices has a number of advantages over traditional systems. In contrast to conventional therapeutic drug formulation, controlled release systems typically require smaller and less frequent dosages to maintain the desired pharmacokinetics (Brannon-Peppas, 1997). Another important issue in controlled drug delivery is drug targeting. Drug targeting is the delivery of a drug to specific cells and organs in the body and the subsequent release of the drug to the desired target site. Delivery of therapeutic agents to particular cells also minimises exposure of other cells to

the agents and thereby reduces toxic side effects (Park *et al.,* 1993). Within the body and certain tissues each drug has a specific therapeutic concentration range above which it is toxic and below which it is ineffective. As shown in Figure 1.1, during conventional drug delivery the drug concentration in the blood and tissue rises immediately after administration reaching a peak which may lead to adverse effects (e.g. hypotension in patients taking fast-release nifedipine products), then declines rapidly to produce the therapeutic concentration. However, further periodic administrations of therapeutic agent are required to maintain required drug levels (Lee and Robinson, 2000). Controlled release devices are able to deliver the drug in the desired therapeutic range without reaching a high initial peak while also keeping a constant therapeutic plasma concentration (Kost and Langer, 2001).

The release pattern from such a device may vary from continuous to two or more pulses (Alderborn, 2002). However, one of the major goals of a controlled release device is to maintain zero-order release kinetics, a phenomena where the rate of drug release is independent of drug amount in the system. Zero-order controlled release offers the advantage that risks of side effects are minimised due to the avoidance of toxic drug plasma levels. This kind of controlled drug release also reduces the possibility of symptom breakout which may occur if blood plasma concentrations drop too low, while patient compliance is improved due to the reduction in the number and frequencies of doses required to maintain therapeutic effects (Hillery *et al.*, 2001).

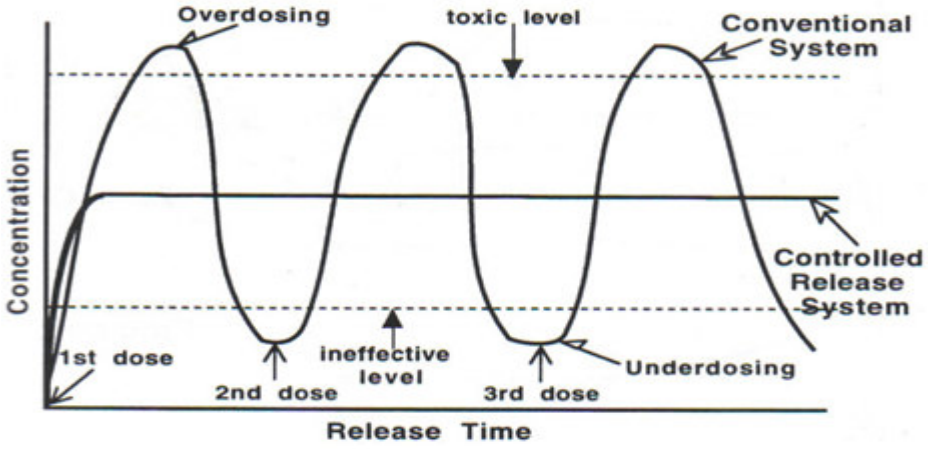

Figure 1.1: Comparison of controlled release with conventional release.

Zero-order release kinetics of drug delivery devices may be achieved in several ways including passive diffusion through a rate determining barrier, dissolution controlled release and osmotic regulated release mechanisms (Okano, 1998). However, the physiochemical properties of the delivery system combined with the bioactive agent ultimately regulates the rate of drug release. This process may also be dependent on environmental factors such as temperature, pH and ionic strength at the site of drug release (Mallapragada and Narasimhan, 1998). Recently developed additional properties of new drug delivery technologies also cover other specific needs such as obtaining slow release of water soluble drugs, improving the bioavailability of low water soluble drugs, delivering two or more agents in the same formulation, and improvements in targeting to specific target tissues and the possibility to control the release of highly toxic drugs (Simo *et al.,* 2003). Today, modern release devices offer different methods for systemically administering therapeutic agents. The most common approaches still include devices which are administered via conventional routes into the body including oral, nasal and vaginal drug administration, but implanted, injected, and transdermal delivery devices are also used in modern therapy (LaPorte, 1997).

Although there are different polymeric products available for controlled drug release, in general most of these release mechanisms are maintained by diffusion and polymer degradation processes (Figure 1.2). It is also possible that these processes may occur singly or combined in a given release system (Hillery *et al.,* 2001).

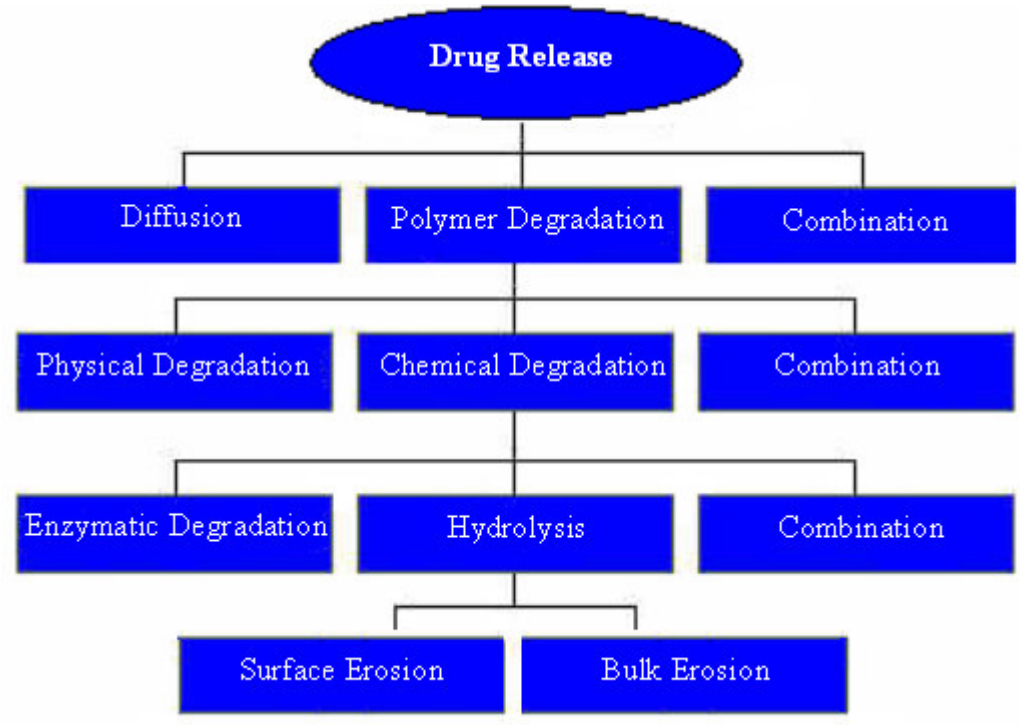

Figure 1.2: Possible drug release mechanisms for polymeric drug delivery devices.

Diffusive transport from a polymer network is a concentration gradient driven process that governs drug transport in most controlled release devices (Mallapragada and Narasimhan, 1998). The rate of diffusion is dependent on the partition and diffusion coefficients of the drug within the polymer network, the available surface area and the thickness of the membrane (Okano, 1998). Furthermore, the geometry of the device strongly influences the drug release characteristics with slab, cylindrical and spherical configurations commonly used for appropriate release pattern (Hillery *et al.,* 2001). However, in cases where the polymer network is swellable, due to the absorption of aqueous solutions from its surroundings, rather complex diffusion processes are present as swelling changes the dimension and/or physical properties of the system and therefore the release kinetics (Okano, 1998). The dry polymer starts to swell when placed in an aqueous medium thereby increasing its aqueous solvent content within the formulation as well as the polymer mesh size. This, in turn, allows the incorporated drug to diffuse out of the polymer network into the surrounding environment. A typical swelling-controlled release is illustrated in Figure 1.3.

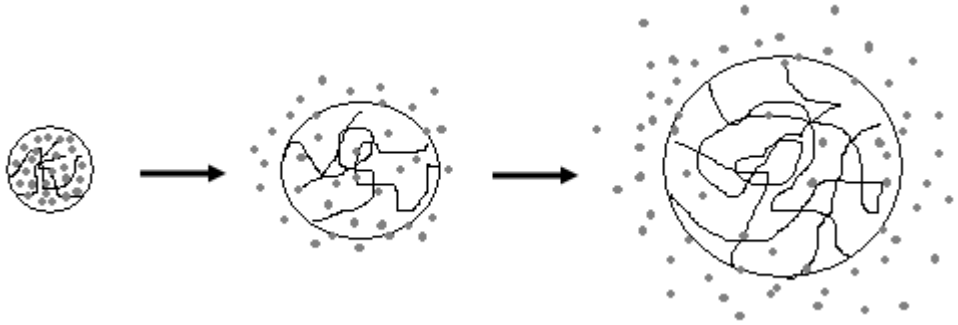

Figure 1.3: Drug release through polymer swelling

The simplest form of polymeric degradation is due to physical erosion and dissolution processes. Hydrophilic materials start to dissolve into low molecular weigth (MW) compounds when in contact with water (Park *et al.,* 1993). Hence, the rate at which the active agent dissolves in the surrounding liquid is the release controlling process. It is possible to obtain controlled release by using drugs and/or polymeric materials with an appropriate dissolution rate. Biochemical degradation results from backbone hydrolysis and enzymatic breakdown of the whole polymer molecule (Wu, 1996). It leads to erosion of the polymer network by cleavage processes with the polymer chains cleaved into smaller polymer fragments, such as oligomers and monomers. Drug molecules that are present in the matrix are released in response to this fragmentation (Siepmann and Goepferich, 2001). Surface erosion occurs when the rate of erosion at the outer coating of the device exceeds the rate of water permeation into the bulk of the polymer. This form of polymer degradation is much faster and may not lead to drug release which follows zero-order kinetics, because the size of the matrix decreases during the dissolution process and the amount of drug which is released due to this process also decreases with time. Bulk erosion occurs when the rate of water permeation inside the polymer is faster than surface erosion. The polymer decays inside the body, thus exhibiting complex release kinetics (Uhrich *et al.,* 1999). Surface and bulk erosion may occur simultaneously when suitable materials and geometries are chosen (Siepmann and Goepferich, 2001). Figure 1.4 illustrates the release of an active agent by erosion processes.

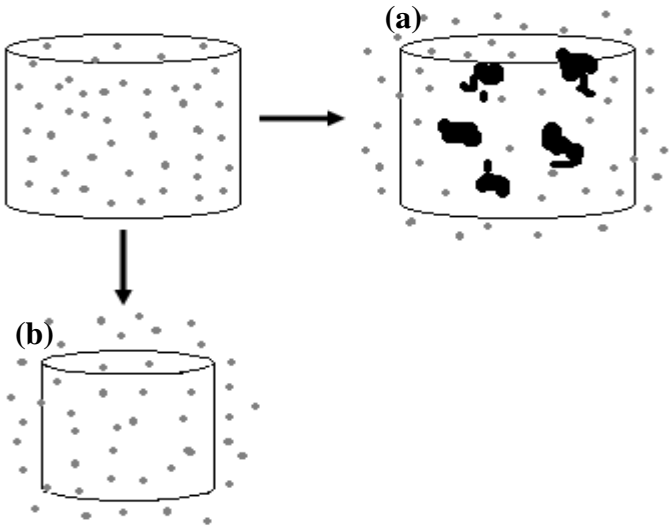

Figure 1.4: Drug release through polymer erosion: (a) bulk erosion (b) surface erosion.

1.2 Hydrogels

Certain biomaterials are able to swell rapidly and retain large volumes of water in their three-dimensional networks when placed in aqueous solution. Such networks are known as hydrogels. Sufficient interstitial space exists within the hydrogel network and water molecules can become trapped and immobilised, thus filling the available free volume. The term hydrogel implies that the material is already swollen in aqueous solution and a dried hydrogel is known as a xerogel (Park and Park, 1996). The hydrogel's affinity to absorb water is attributed to the presence of hydrophilic chemical groups in their polymer networks such as –OH, –CONH–, $–CONH_2–$, and $–SO_3H$ (Peppas and Kahre, 1993). Depending on the nature of the aqueous environment and polymer composition, hydrogels can be hydrated to different degrees, sometimes to more than 90% of their initial dry weight (Hamidi *et al.,* 2008).

Since their first production by Wichterle and Lim (1960) for use as contact lenses, hydrogels have played a vital role in numerous biomedical and pharmaceutical applications. These applications are often combined with the excellent controlled drug release properties of hydrogels. Due to their aqueous nature, pharmaceutical agents can diffuse into (drug loading), and out (drug release) of hydrogels (Satish *et al.,* 2006). Thus, hydrogels have a high permeability for water soluble drugs and the most common mechanism of drug release from such a system is swelling controlled diffusion, which can be combined with drug release by erosion processes if the polymer is biodegradable (Lee

and Kim, 1985; Park *et al.,* 1993; Hoffman, 2002). In addition, due to the presence of large amounts of water in their networks, hydrogels resemble the physical characteristics of soft tissues. The soft and rubbery nature of the gels minimises mechanical and frictional irritation to the body tissue with which they are in contact. Furthermore, the hydrophilic and high mobility polymer chains at the hydrogels surface contribute to the prevention of undesired protein adsorption and cell adhesion (Park *et al*., 1993; Luck *et al*., 1998). However, a major disadvantage of hydrogels is their poor mechanical strength and toughness after reaching a swelling maximum. This disadvantage can be overcome by either grafting a hydrogel onto a supportive substrate or by changing the degree of network bonding.

Hydrogels are usually made of homopolymer or copolymer molecules, with their networks being either physically bonded (physical hydrogels) or chemically crosslinked (chemical hydrogel) (Peppas *et al*., 2000). Physical hydrogels are comprised of an amorphous hydrophilic polymer phase held together by noncovalent secondary molecular forces (such as van der Waals forces) in conjunction with a range of other types of molecular interactions (hydrogen bonding, ionic association, hydrophobic interaction, crosslinking by crystalline segments, and solvent complexation) (Bordi *et al.,* 2002). Since physical gels are not covalently crosslinked, they behave as networks only for a short time and will often dissolve in water or solvents (LaPorte, 1997). This characteristic makes physical gels an excellent candidate for controlled drug delivery by degradation processes. Moreover, physical gels have gained much of the recent attention in the field of drug delivery as they need no recovery or further manipulation after introduction into the body (Kamath and Park, 1993; Park *et al.,* 1993).

Chemical hydrogels are defined as three-dimensional molecular networks formed from the introduction of primary covalent crosslinks. Chemical gels will not dissolve in water or any other organic solvents unless the covalent bond can be broken by chemical or physical cleavage processes (Schacht, 2004). They are observed to swell achieving much higher swelling ratios than physical gels and find major application in novel implant and regenerative tissue technology often combined with their excellent drug delivery properties (Hoffman, 2002).

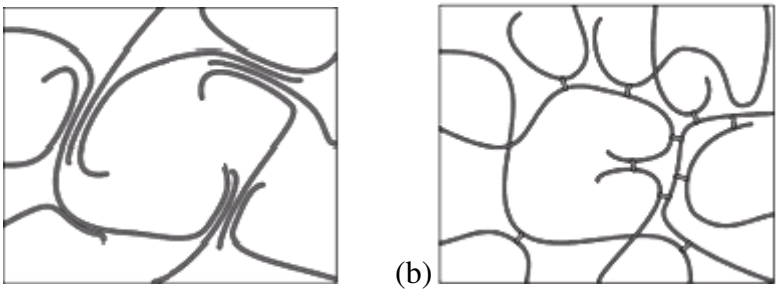

Figure 1.5: Schematic description of the general structure of (a) physical hydrogels with multiple junction zones and (b) chemical hydrogels with point crosslinks.

1.2.1 Hydrogels in biomedical applications

Due to their interesting dynamic structural properties hydrogels are commonly used in numerous applications in important areas such as agriculture, cosmetics, food industry, photography and instrumentation (Kulicke and Nottelmann, 1989). Particular interest emerged in the medical and pharmaceutical sector where a wide range of biomedical applications of hydrogels were found due to the materials excellent performance when in contact to human tissue (Peppas, 1986; Park and Park, 1996; Hoffman, 2002; Deligkaris *et al.,* 2010). Indeed, their range of biomedical applications is ever growing and includes coatings for medical devices, intravascular and urinary tract catheters, intraocular lenses, wound and burn dressings, soft tissue replacements and artificial organ supplements (Ratner and Hoffman, 1976; Rosiak and Yoshii, 1999; Hoffman, 2002). It is beyond the scope of this thesis to give a comprehensive assessment of all hydrogel applications, as they are far too vast. Excellent reviews in relation to this topic are readily available (Peppas *et al.,* 2000; Qiu and Park 2001; Hoffman, 2002; Lin and Metters, 2006; Rzaev *et al.,* 2007). These applications are often combined with customisable controlled drug delivery mechanisms as some hydrogels have the ability to respond to an external signal (e.g. swell and shrink) thereby influencing the rate of drug release (Qiu and Park, 2001; Kopeček and Yang, 2007). These types of environment sensitive hydrogels are known as 'intelligent' or 'smart' hydrogels and many external stimuli including pH and temperature changes have been applied to induce various responses of those smart hydrogel systems (Gupta *et al.,* 2002; Geever *et al.,* 2006; Kopeček and Yang, 2007).

Hydrogel based drug delivery devices can be administered via various routes that include oral, rectal, ocular epidermal and subcutaneous routes (Figure 1.6). Hydrogels also

exhibit a high permeability to biological nutrients and minerals making these materials attractive for the use in cell encapsulation and tissue engineering applications (Biondi *et al.,* 2008).

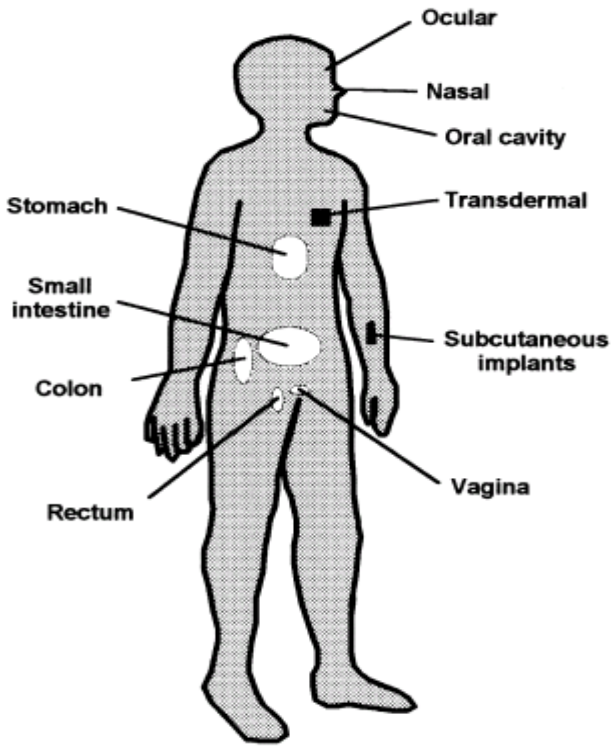

Figure 1.6: Tissue locations applicable for hydrogel-based drug delivery systems (Peppas *et al.,* 2000).

1.2.2 Hydrogels for moist wound healing applications

Hydrogels have found particular attention in the field of wound healing (Jones and Vaughan, 2005). In humans, skin is the largest organ with essential physical, chemical, and biological barrier properties. Skin damage such as trauma, disease, burns or surgery brings dramatic consequences for the whole organism (Korkina *et al.,* 2009). During the 20th century, wounds were thought to heal quicker if left under a scab. However, this process created surface desiccation and crust formation which could deepen the wound. The thinking back then was that the scab would protect the wound from outside influence. This thinking was reasonable at the time given the fact that the most severe effect of wound damage was infection. Also no advanced therapies or suitable antibacterial agents were available for treatment (Demling *et al.,* 2000) and this concept remained popular until work

carried out by Winter (1962) reported that healing in a moist environment is faster than in a dry environment. The research of Winter (1965) initiated the concept of an active involvement of a wound dressing in establishing and maintaining an optimal environment for wound repair. This attention led to the advancement of wound dressings from being traditionally passive materials to functional active dressings which create and maintain a moist and healing environment through the interaction with the wounds they covered. This is due to the fact that renewed skin, without the formation of a dry crust, takes place during healing in a moist environment. Besides maintaining a moist environment, an ideal wound dressing should protect the wound from infectious particles, stimulate the growth factors, prevent wound desiccation and absorb excess wound fluids and exudates (Purna and Babu, 2000; Lin *et al.,* 2001). Due to their unique features, special attention has been paid to the use of hydrogels for wound healing applications. Hydrogels deliver a moist wound environment, can absorb excess wound exudates, act as an antimicrobial barrier and moreover can be designed to deliver appropriate amounts of pharmaceutical agents such as anti-inflammatory agent, antimicrobial agents and various growth factors to the wound site (Jones and Vaughan, 2005; Chen *et al.,* 2006; Hori *et al.,* 2007; Mehyar *et al.,* 2008).

The first hydrogel was used for wound healing applications in the late 80s by Rosiak *et al.* (1989). Since then, several hydrogel wound dressings were successfully commercialised under trade names such as Ivalon™, Vigilon™, Aquagel™, Hypergel™, Nu-gel™ (Razzak *et al.,* 2001; Jones and Vaughan, 2005). Nevertheless, some of the hydrogels do not satisfy the ideal dressing requirements as their fragile networks are not able to resist the pressure of a wound bandage or they adhere to the wound surface and cannot be removed without causing further wound damage (Kokabi *et al.,* 2007). Hence, the search for improved hydrogel wound dressings is still ongoing (Murakami *et al.,* 2010; Sung *et al.,* 2010).

1.2.3 Synthesis of polymeric hydrogels

A wide range of hydrophilic monomers can be used to synthesise polymeric hydrogels and the literature on the synthesis of novel polymeric hydrogels has exploded since the first biomedical application of poly(hydroxyl methacrylate) hydrogels by Wichterle and Lim (1960). A summary of monomers most commonly used for the synthesis of polymeric

hydrogels for biomedical applications was given in a review paper by Peppas *et al.* (2000) and is listed in Table 1.

Table 1.1: Monomers most often used in the synthesis of polymeric hydrogels for biomedical applications (Peppas *et al.,* 2000).

Monomer abbreviation	Monomer
HEMA	Hydroxyethyl methacrylate
HEEMA	Hydroxyethoxyethyl methacrylate
HDEEMA	Hydroxydiethoxyethyl methacrylate
MEMA	Methoxyethyl methacrylate
MEEMA	Methoxyethoxyethyl methacrylate
MDEEMA	Methoxydiethoxyethyl methacrylate
EGDMA	Ethylene glycol dimethacrylate
NVP	*N*-vinyl-2-pyrrolidone
NIPAAm	*N*-isopropylacrylamide
Vac	Vinyl acetate
AA	Acrylic acid
MAA	Metharcylic acid
HPMA	*N*-(2-hydroxypropyl) methacrylamide
EG	Ethylene glycol
PEGA	Poly(ethylene glycol) acrylate
PEGMA	Poly(ethylene glycol) methacrylate
PEGDA	Poly(ethylene glycol) diacrylate
PEGDMA	Poly(ethylene glycol) dimethacrylate

The polymerisation reactions used for the synthesis of hydrogels can be divided into the following categories: step-growth, chain-growth, or mixed-mode chain and step-growth (Mathur *et al.,* 1996; Lin and Anseth, 2009; Miller *et al.,* 2010). Step-growth polymerisation reactions generally occur between bi- and multifunctional monomers which first form dimers, then trimers, longer oligomers and ultimately long chain polymers. A characteristic step-growth polymerisation is the rapid disappearance of the monomer at an

early stage of the reaction and the existence of a broad molecular weight distribution in the later stages of the reaction (Rudin, 1999; Long and Turner, 2000; Billiet *et al.,* 2009).

Chain-growth polymerisation, however, takes place in three distinctive steps involving initiation of active molecules, their propagation and termination of the active chain ends (Madden *et al.,* 1999; Lü and Ding, 2005). Initiation often requires the presence of an initiator to create a free radical which reacts with an unsaturated monomer (e.g. vinyl monomer). The activated monomer will bind to another monomer molecule and in turn activate it. During propagation, a polymer chain starts to form by rapid addition of monomer to the activated polymer chain ends. The chain polymerisation will not continue until all the participating monomers are used up as the free radicals involved are so reactive that they find a variety of ways of losing their activity. Thus, the polymer chain terminates by disproportionation or combination reaction. The disproportionation reaction occurs by the interaction of two radical species, whereby one molecule abstracts a hydrogen atom from the other and the other molecule forms a double bond. The combination reaction occurs when two radicals join together. In contrast to step-growth polymerisation, chain-growth reactions are more frequently used for the synthesis of hydrogels and most of the monomers summarised in Table 1.1 are polymerised by this method (Schacht, 2004; Nuttelman *et al.,* 2008).

A common way to initiate the chain-growth reaction is the use of a photoinitiator which is activated upon radiation with visible (vis) or ultraviolet (UV) light. More specifically, this reaction type is known as photopolymerisation and an excellent review of photopolymerised hydrogels for biomedical applications was published by Nguyen and West (2002). Photopolymerisation schemes generally use a photoinitiator having a high absorption at a specific wavelength of light to produce the free radical initiating species (Seet *et al.,* 2006). Suitable light sources for photopolymerisation normally emit in the wavelength range from 254 to 450 nm (Kidernay *et al.,* 2002). Over the last decade, various photoinitiators have been investigated to achieve suitable photopolymerisation for the production of biomaterials. In this regard, photoinitiators based on aromatic carbonyl compounds such as benzoin derivatives, benziketals, acetophenone derivatives, and hydroxyalkylphenones were found useful (Nguyen and West, 2002).

1.2.4 *N*-vinyl-2-pyrrolidone and acrylic acid based hydrogels

Polymers based on *N*-vinyl-2-pyrrolidone (NVP) have proven useful for the development of a variety of hydrogels particularly in combination with other polymers, as the NVP based homopolymer possesses fragile mechanical properties and low swelling capabilities (Shantha and Harding, 2003; Benamer *et al.,* 2006 Wang *et al.,* 2007a; Geever *et al.,* 2008). Initially, some NVP based hydrogels have been synthesised in the presence of agar as an additional component to enhance the mechanical properties (Himly *et al.,* 1993). However, it was suggested that the presence of agar may evoke the penetration of microorganisms into the hydrogel matrix; therefore poly(ethlylene glycol), poly(vinyl alcohol) and a range of polysaccharides were further investigated as suitable components aiming to overcome the abovementioned limitations (Razzak *et al.,* 2001; Zhao *et al.,* 2003; Ajji *et al.,* 2005).

Research previously conducted in our laboratories focused on hydrogel synthesis by polymerising NVP with various amounts of acrylic acid (AA), which is a monomeric combination chosen due to its high water affinity and fast copolymerisation characteristics (Devine and Higginbotham, 2003, 2005). Physical hydrogels were prepared in the absence of a crosslinking agent (Devine and Higginbotham, 2003) to obtain a biodegradable drug delivery system. Nondegradable chemical hydrogels were synthesized via the addition of chemical crosslinking agents based on ethylene glycol dimethacrylate (EGDMA) and this proved useful to further enhance the polymers mechanical stability (Devine and Higginbotham, 2005) and controlled drug release properties (Devine *et al.,* 2006).

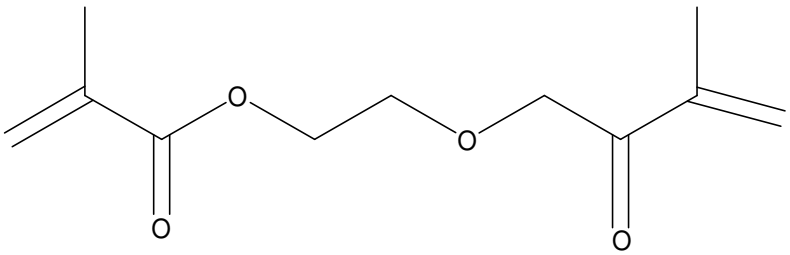

Figure 1.7: Chemical structure of the crosslinker ethylene glycol dimethacrylate.

The chosen method for production of the hydrogels was free radical photopolymerisation as it has been previously investigated for numerous biomedical

applications (Nguyen and West, 2000). The photoinitiator of choice was 1-hydroxycyclohexylphenylketone also known as Irgacure® 184.

1.2.4.1 *N*-vinyl-2-pyrrolidone

The monomer NVP is highly hydrophilic and appears as a colourless to yellow liquid at room temperature. It belongs to the family of organic heterocyclic compounds but is not aromatic. The pendent ring structure of the molecule contains nitrogen and oxygen, which impart polarity and the ability to form hydrogen bonds.

NVP and its polymeric form poly(vinylpyrrolidone) PVP were firstly synthesised in Germany at I.G. Farben by Walter Reppe and colleagues during the 1930s (Robinson *et al.*, 1990) using a chemical reaction now commonly known as Reppe-synthesis. NVP is mainly used to achieve PVP-homopolymer and copolymer based products including hydrogels for the biomedical field. Currently, polymerisation of NVP is possible using conventional polymerising techniques including free radical polymerisation, plasma electron beam irradiation and gamma radiation (LaPorte, 1997).

In contrast to the biocompatible PVP polymer, several scientific publications are available proving the toxicity of the monomer NVP. Although extensive *in vitro* testing did not reveal any mutagenic and genotoxic potential of the monomer (Simmon and Baden, 1980, Knapp *et al*., 1985), it induced tumours in long term animal inhalation studies using rats. The types of tumours concerned being adenomas and adenocarcinomas of the nasal cavity, and hepatocellular carcinomas. The tumours were believed to arise via a nongenotoxic mechanism of NVP exposure (Klimisch *et al*., 1997a). Furthermore, noncarcinogenic haematotoxicity, hepatoxicity and irritation to the rodents' nasal cavity were observed in subchronic inhalation studies (Klimisch *et al*., 1997b).

Interestingly, the homopolymer PVP was widely used during World War II as a blood substitute or plasma volume expander. In this context it offered the advantage of being nonantigenic, requiring no cross matching and avoiding the dangers of blood-borne infection (Robinson *et al*., 1990). Indeed, PVP is still widely utilised due to its unique combination of properties, including solubility in water and in organic solvents, very low toxicity, high complexing ability, good film-forming characteristics and the ability to adhere to a variety of substrates. As might be expected, minute quantities of the unreacted

monomer and other reaction products such as 2-pyrrolidone are commonly present in the final PVP product (Robinson *et al.*, 1990). PVP has been subjected to extensive investigation due to its utilisation as a plasma volume expander. An extensive body of toxicological data in animals supports the biological inertness of PVP. A lot of this data dates back to the 1950s, 60s and 70s including subchronic toxicity in mice, rats, dogs and cats (Scheffner, 1955; Kirsch *et al.*, 1972, 1975a, 1975b), as well as intravenous administration to human patients (Honda *et al.,* 1966). In addition, six independent investigations of the mutagenic potential of PVP have been performed, all of which indicate that PVP is without mutagenic activity. These included *in vitro* assays such as the Ames Assay (Zeiger *et al.*, 1987), Mouse lymphoma and cell transformation test (Kessler *et al.*, 1980), while *in vivo* assays included dominant lethal tests (Zeller & Engelhardt, 1977) and bone marrow chromosomal aberration assay (BASF, 1980). Research conducted by Ravichandran *et al*. (1997) showed that PVP undergoes very slow hydrolytic degradation in the physiological environment to yield nontoxic normal metabolites.

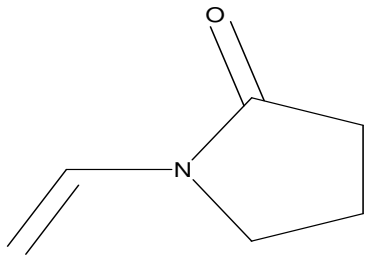

Figure 1.9: Chemical structure of the *N*-vinyl-pyrrolidone.

1.2.4.2 Acrylic acid

Acrylic acid is the simplest unsaturated carboxylic acid and appears as a clear, colourless liquid with a characteristic acrid smell. Josef Redtenbacher (1843) reported the first synthesis of AA by air oxidation of acrolein obtained from the high temperature cracking of glycerine. However, it was not until 1930 that the technical obstacles for the profitable manufacture and handling of this reactive monomer were overcome.

AA and its esters are primarily used in the preparation of polymers and copolymers. The polymeric products can be made to vary widely in physical properties by controlling the ratio of different monomers employed in their preparation and the degree of crosslinking. Poly(acrylic acid) (PAA) has been widely studied for its pH dependent

swelling characteristics and has been utilised in the production of hydrogels (Devine and Higginbotham, 2003). Within the body AA is metabolised as a short-chained fatty acid by the liver (ACGIH, 1991) with carbon dioxide being its major metabolite (US EPA, 1984). Deposition studies, using radio-labelled AA administered by several routes, show that nearly all of the acrylic acid is absorbed and metabolised to carbon dioxide with very little radioactivity in the urine or the faeces. However, metabolism and excretion do not appear to be sufficiently fast to prevent widespread distribution of unchanged AA in the body. After oral exposure in the rat, the highest concentrations of the chemical were found in the liver, adipose tissue, small intestine, brain, and kidneys (US EPA, 1984). From a toxicological perspective most of the data relating to acute and chronic exposure are via inhalation tests on AA vapour, which is a strong eye and skin irritant (ACGIH, 1986, 1991). Additional information regarding the chronic toxicity of acrylic acid to humans is not currently available.

Conflicting positive and negative results have been obtained by *in vitro* genotoxicity tests. Notably, acrylic acid was negative in the Ames test and the *in vitro* unscheduled deoxyribonucleic acid (DNA) synthesis assay (Johannsen, 2008), but appeared positive in a chromosome aberration assay and in the *in vitro* lymphoma cell assay (Cameron *et al.,* 1990; Moore *et al.,* 1988).

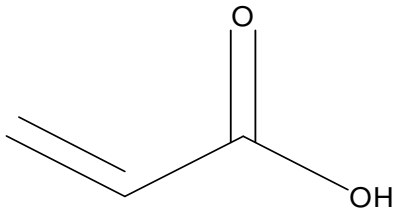

Figure 1.10: Chemical structure of AA.

1.3 Biocompatibility evaluation

An ideal biomaterial should not induce an inflammatory response, should resist bacterial colonisation, and promote normal differentiation in the surrounding tissues – characteristics which led to the introduction of the term biocompatibility. In general, biocompatibility describes the ability of a material to perform with an appropriate host response in a specific

application or to exist in harmony with the living system without eliciting any undesirable local or systemic effects (Williams, 1987).

It is often believed, however, that a polymer based material does not produce any toxic effects when in contact with living organisms. The basis for this assumption is that molecules greater than approximately 10,000 molecular mass cannot be absorbed into the body cells by traditional routes of exposure. However, the fact that only a few polymers are the products of reactions that have gone to completion and that their manufacturing process may lead to the introduction of other toxic substances into the polymeric material provides enough evidence to reject this hypothesis (Gad, 1988).

Biocompatibility testing is an essential requirement for the critical evaluation of any material intended to be used in biomedical applications. Biomaterials must be compatible with the biological tissues with which they come in contact, and should not have any adverse affect on the body. More specifically, the material should not produce adverse local and systemic effects, be carcinogenic, or produce reproductive and developmental effects (Ciarkowski and Mueller, 1998). Toxicological analysis of biomaterials is therefore important to ensure that the manufacturing process has not significantly altered the physicochemical properties of a biomedical product and that no toxic additives were introduced. The addition of toxic substances to the polymeric material may be intentional or unintentional. Intentional additives are those substances consciously added to the formulation for a particular purpose such as plastizisers, stabilisers, colourants, and polymerisation initiators. Unintentional additives would include contaminants from impure raw materials, further processing, sterilant residues and undesired and unexpected products of polymer degradation (Recum *et al.,* 1998).

Also the degradation of the polymer in the biological environment is of particular relevance because degradation products may have different behaviours than the parent polymer in terms of biological response. Indeed, due to their decreased molecular mass they may also be more likely to be absorbed from the body and gain entry to the systemic circulation (Braybrook, 1997). Even when the industrial components and degradation products of a formulation are declared as safe for human use, it is necessary to be sure that further processing does not lead to any unpredicted changes in the formulation which might produce any adverse effects in humans. Particular physical and chemical production

processes that use high energetic conditions such as high temperatures, pressure and radiation for the development of the end product may have potential to cause harmful cross interaction within different raw materials.

1.3.1 Guidelines for biocompatibility evaluation

Depending on the kind of product and country distribution, a biomaterial can be regulated as a medical device, tissue, drug, biologic or combination product (Heller and Howe, 1998; Grosskinsky, 2006). In the European Union (EU) biomaterials are subject to current Good Manufacturing Practice (EU directive 2003/94/EC) current Good Laboratory Practice (EU Directive 2001/83/EC), other regulations (EU Directive 2004/23/EC; EU Directive 93/42/EEC) and quality management systems (ISO EN DIN 9001; ISO EN DIN 13485). Based on the material characteristics and its application, several standards for testing of biomaterial properties including biocompatibility are available such as European Pharmacopoeia, standards by the International Organization for Standardization (ISO) and the National Institute of Standards and Technology (Ciarkowski and Mueller, 1998; Grosskinsky, 2006).

In particular, the ISO developed their standard for biological evaluation of medical devices (ISO 10993) in an effort to harmonise biocompatibility testing. The scope of this 20-part document is to evaluate the effects of medical device materials on the body. The ISO 10993-1 guideline outlines the principles of the safety evaluation from a descriptive toxicological perspective (ISO 10993-3-6,-11,-20) and furthermore includes a requirement to characterise and identify the composition of the biomaterial and any potential impurities (ISO 10993-18-19) or degradation products (ISO 10993-9, 13-15). More specifically, Part 5 of the guidance (ISO 10993-5) calls for an *in vitro* cytotoxicity evaluation and a number of test approaches are discussed to screen the material (Section 1.3.2.1). In addition, the ISO standard identifies the need to assess the *in vitro* genotoxicity (ISO 10993-3) of a novel material in order to ensure that no adverse effects are introduced to the body cells' genetic components (Section 1.3.2.2). Moreover, the physicochemical characterisation is clearly identified by ISO 10993-1 as one of the first steps in the overall biological evaluation. Part 18 covers the requirements for providing information on the chemical composition of materials, the potential release of leachable substances (which are further

specified in ISO 10993-16-17) and the predictive biological charaterisation of devices. Part 19, however, addresses the physical, mechanical and morphological characteristics.

1.3.2 *In vitro* testing

In the past, product safety assessments were mainly conducted via the performance of *in vivo* tests. Indeed, *in vivo* studies are still an essential requirement; however, many *in vitro* methods have been developed to substitute the need for testing on laboratory animals (Gupta *et al.,* 2005). *In vitro* methods are now required by regulatory agencies to serve as testing alternatives to animal-based methods in order to refine, reduce, or replace animal use (Russel and Burch, 1959). Current scientific advances, including *in vitro* methods such as cell and tissue culture systems, are often able to describe more effectively the lesion seen within *in vivo* studies and through their high degree of sensitivity it may be possible to give a better definition of the safe concentrations of test materials (Gupta *et al.,* 2005).

The rationale behind the use of mammalian cell culture systems for biocompatibility evaluations rests on the fact that the actions of toxic chemicals are ultimately exerted at the cellular level. Thus, investigation of cellular response is the cornerstone for establishing biological response to foreign materials (Northup and Cammack, 1998; Zucco *et al.,* 2004). Several types of mammalian cell culture systems of animal or human origin are available routinely for toxicity studies *in vitro.* These systems include freshly isolated primary cell cultures and continuous cell lines (Frazier, 1992). Primary cell cultures are obtained from fresh isolated cells by allowing the cells to migrate out of fragments of tissue adhering to a suitable substrate or by disaggregating the tissue mechanically or enzymatically to produce a suspension of cells, some of which will ultimately attach to the substrate. The fresh isolated and attached cells usually contain a variety of different cell types representative of the tissue of origin. Some cells may be able to survive or even proliferate under the particular culture conditions used and finally one cell type will become predominant. Further growth of the determined cell type may be obtained by subculturing in fresh nutrients, but as the primary cell culture ages, growth becomes slower and the culture will eventually die (Stacy and MacDonald, 2001).

Continuous cell lines can be obtained from primary cultures that have adapted to grow *in vitro* via an implied phenotypic change (spontaneous, chemical or viral induced

transformation) or due to cell isolation techniques from malignant tumours. The ability of cells to grow continuously and indefinitely probably reflects their capacity to undergo genetic changes. Continuous cell lines are usually aneuploid and often have a chromosome complement between the diploid and tetraploid value. Advantages of continuous cell lines over primary cultures are that, under appropriate conditions, they may be cultured indefinitely and are obtainable via commercial supply. A major disadvantage is that with increased culture time the cells may irreversibly lose their specialised properties; an effect known as dedifferentiation. Furthermore, systemic effects in relation to the pharmacokinetics of a xenobiotic cannot be evaluated (Freshney, 1987). *In vitro* cultured cells are generally more sensitive to toxic substances than *in vivo* tissues. Therefore, a material toxic in an *in vitro* cell system may not be particularly toxic to the tissues *in vivo*, while a material harmless to the cells in culture is also likely to be inert *in vivo* (Cenni *et al*., 1999). Today various mammalian cell lines, including gastrointestinal, bladder, kidney, skin and liver cells are commonly used in toxicity testing *in vitro* (Northup and Cammack, 1998; O'Hare and Atterwill**,** 1995).

1.3.2.1 Cytotoxicity assessment

Cytotoxicity is the expression of toxic effects on the structural and/or functional properties of one or more body cell components. A wide range of toxic substances can cause direct damage to body tissues and certain organs which may lead to reversible (short-lived or repairable) effects or irreversible events ultimately leading to cell death. Cell death, in turn, can take the form of necrosis or apoptosis (a programmed form of cell death). Typically, necrosis involves irreversible changes within the nuclei (such as karyolysis), loss of cytoplasmic structure, dysfunction in various organelles (especially mitochondria), and, finally, cytolysis as a result of high-amplitude swelling. The release of cell contents into the extracellular space can cause further injury or even death of neighbouring cells, and may result in inflammation or infiltration of proinflammatory cells into the lesion, leading to further tissue damage (Haslett, 1992). Apoptosis has been described as a form of cellular suicide, since cell death appears to result from induction of active processes within the cell itself. Although apoptosis is a normal physiological process, it can also be induced by a number of exogenous factors, such as xenobiotic chemicals, oxidative stress, anoxia, and

radiation (Hodgson, 2004). Typically, apoptosis involves margination and condensation of nuclear chromatin (pyknosis), cytoplasmic shrinkage, membrane blebbing, nuclear fragmentation, and finally, formation of apoptotic bodies. The apoptotic bodies are removed in an orderly manner by phagocytes without eliciting inflammatory events (Hart *et al.,* 2008).

Many different process are involved in cellular injury which are as of yet, not fully understood and are still the subject of extensive research. The stages that cause the cell to undergo necrosis or apoptosis after exposure to a cytotoxic substance can be classified in three dependent events. *Primary events* result in initial injury to the cell from exposure to toxicants, (e.g. lipid peroxidation, enzyme inhibition and covalent binding to macromolecules), *secondary events* describe further cellular changes followed from the initial damage (e.g. changes in membrane structure and function, mitochondrial damage and depletion of ATP and other cofactors) and *tertiary events* are the final changes observable under clinical investigation (e.g. cell death and adaptive changes) (Timbrell, 2009).

Considering the aforementioned, a cytotoxicity assessment is the study of the toxic effects of substances at the cellular level. Most of the existing guidance documents require *in vitro* cytotoxicity test as first part of a sequenced program to evaluate a materials biocompatibility. The ISO 10993-1 "Evaluation and testing within a risk management process" for instance states that cytotoxicity tests are indispensable requirements for the performance of appropriate biocompatibility evaluations. Essentially, cytotoxicity assays can be used to screen materials and substances to investigate their potential to cause cellular damage. Methods for the evaluation of cytotoxicity are known to be sensitive, economical, and quick to conduct and a wide range of assays can be conducted, primarily as a tool to rank materials against each other in terms of their potential to cause cellular damage (Weiner and Kotkoskie, 1996). Currently, cell culture systems are commonly used as bioindicator targets in cytotoxicity assays. Because many of the distinguishing characteristics related to cytotoxicity cannot be detected via a single cell culture based assay, several methods and various cell lines have been designed to assess the complex cellular response to a toxic stimulus (Babich and Borenfreund, 1990).

1.3.2.2 Genotoxicity assessment

The correlation between mutagenicity and carcinogenicity is a major concern in genetic toxicology and the identification of chemicals that have the possibility to damage genetic material is of growing scientific interest (Kappas, 1990). Cancer is thought to be a mutational event occurring either directly or indirectly from DNA damage. Genotoxic mechanisms are mostly held responsible for the initiation of cancer and the evaluation of genotoxic effects plays an important role in risk assessment of carcinogenesis. Furthermore, initial DNA damage leading to genetic alterations is also thought to be the basis for many hereditary diseases.

Damage to the genetic material can be classified in to three main categories known as point mutations (changes in the base sequence of DNA), structural chromosome aberrations (deficiencies, duplications, insertions, inversions and translocations) and numerical chromosome aberrations (gain or losses of whole chromosomes such as trisomy and monosomie, or sets of chromosomes such as haploidy or polyploidy) (Cohrrsen and Covello, 1989). These irreversible events are mostly caused by the induction of DNA base modifications, DNA strand breaks, apurinic and apyrimidinic (AP) lesions, DNA cross-links, and intercalations. DNA base modification usually occurs via DNA adducts, resulting from electrophilic substances or organisms reacting with nucleophilic sites on DNA molecules (Olinski *et al.,* 1995). Also reactive chemical species (e.g. reactive oxygen species) and UV-radiation can cause base modifications (Jaruga *et al.,* 2000).

DNA strand breaks can be categorised as either single or double stranded. DNA single strand breaks occur frequently in the course of physiological, endogenous processes and as a consequence of exposure to xenobiotics. They are usually easily repaired because the opposite strand of the double helix holds the two ends in close proximity. If the single strand breaks are simple discontinuities in the phosphodiester backbone of the DNA, the phosphate and the hydroxyl group can be directly repaired. Other single strand breaks may involve gaps in one strand or structures altered by xenobiotic damage. The latter must be removed before polymerases and ligases can repair the break.

DNA double strand breaks are lesions placed in direct or close opposition in the two phosphodiester backbones of duplex DNA. Therefore, under nondenaturing conditions, they will cause one double helical DNA molecule to form two shorter ones. Theoretically,

one unrepaired double strand break in the functional copy of an essential gene can lead to the loss of information contained within the particular gene, malignant transformation and cell death. However, in many cases, error free repair of double strand breaks may reconstitute the physiological DNA structure (Vamvakas, 1997).

One of the most frequent DNA lesion in cells is due to the formation of AP sites. Significant amounts of AP lesions are spontaneously generated via hydrolytic depurination and have been observed in cells that have been exposed to oxidative stress or to genotoxic agents (Loeb and Preston, 1986).

The covalent crosslinking between DNA and proteins or interstrand-crosslinks is another form of DNA damage induced by a number of chemical and physical agents. Interstrand-crosslinks are caused by bifunctional electrophiles inducing crosslinks between both DNA strands, but also links between two bases of the same DNA strand can occur. DNA–protein crosslinks are created when a protein becomes covalently bound to DNA through oxidative free radical mechanisms or indirectly through aldehydes generated by oxidative stress. Proteins that are crosslinked to DNA have also been observed through a chemical or drug linker or through co-ordination with a metal atom (Barker *et al.,* 2005).

Intercalators are typically planar fused aromatic cations that have the potential to slide between the base pairs of DNA. Here, they fill the space formed between base pairs when the helix is locally elongated and partially unwound. Intercalated molecules interact with adjacent base pairs through van der Waals forces coupled with electrostatic stabilisation, or by forming hydrogen bonds with base pairs (Sinha *et al.,* 2005).

In vitro genotoxicity tests can be defined as tests designed to detect a compound's potential to induce damage to the cellular genetic material. In the last decades genotoxicity assays have gained a widespread acceptance as an important and useful indicator of carcinogenicity. All new chemicals and especially those in the pharmaceutical area must be tested in appropriate *in vitro* tests as part of their genotoxicity assessment (Balls *et al.,* 1991).

The ISO 10993-3 standard series identifies the need to assess the genotoxicity of biomaterials in more than one model. In order to increase the likelihood of detecting a genotoxic event, a battery of *in vitro* tests must be performed on mammalian cells. Hepatocyte cultures are often preferred due to their metabolising activity for detecting

bioactivated carcinogens (Dierickx, 1998). Most genotoxicity assay systems employed *in vitro* cultured cells as both the drug metabolising cells and the target cells for DNA damage (Gad, 1988). Furthermore, the ISO 10993 guidelines recommend that *in vitro* tests other than mammalian cell culture based assay should be conducted to address different genotoxic mechanisms. Today, a great variety of *in vitro* test systems are available to identify and quantify the genotoxic effects of a broad range of chemicals. Apart from mammalian cells, different organisms including bacteria and insects are used to determine substances potential to damage genetic material (Balls *et al.,* 1991). A notable gene mutation test using bacteria strains of *Salmonella typhimurium* (*S. typhimurium*) is the Ames assay which has the potential for the rapid detection of point and frameshift mutations with a high degree of sensitivity (Ames *et al.,* 1975). Genotoxicity assays may be initiated and proposed as an alternative to an *in vivo* tumourgenicity bioassay, but they may also be considered as initial screening procedures owing to their sensitivity and the desire to reduce the use of animals for testing. However, the ISO 10993-3 states that if any *in vitro* test leads to a positive result throughout a genotoxicological investigation, further *in vivo* assays are required depending on which assay gave the positive result (Gad, 1988).

1.4 Microbial decontamination of biomaterials

Biomaterials and medical devices are subject to microbial contamination that can represent a health hazard to the patient during end-use. Microbial contamination of biomaterials may originate from raw materials and can be introduced during the manufacturing process or storage of the material (Clontz, 1998). Naturally, to render a biomaterial suitable for end use, it is of outermost importance to reduce the microbial contamination to a safe level. In this regard, the following terms were defined by Ayliffe (1997):

- **Decontamination** is a general term used for the removal or destruction of micro-organisms, soil and other unwanted contaminates which may prejudice the safe use of a biomaterial or medical device. It includes cleaning, disinfection and sterilisation
- **Cleaning** is a process which removes contaminants, including organic matter and most microorganisms and is always required before disinfection or sterilisation,

especially when processing at low temperatures, as the presence of proteins may protect microorganisms from destruction by chemical agents.

- **Disinfection** reduces numbers of viable microbes present on a surface or medical device to a previously specified safe level as appropriate for handling or its intended further use.
- **Sterilisation** is a process which renders an object free of all viable micro-organisms including spores.

Depending on the risk of infection involved in their use, biomedical devices can be classified into three groups based on system first proposed by Spaulding (1972): critical items, semicritical items and noncritical items. Critical items come into contact with sterile tissue or the vascular system and thus have a high risk to cause infection if they are contaminated with pathogenic organisms. Critical items require sterilisation treatment (ISO 14937). Semicritical objects come into contact with mucous membranes or skin that is not intact and thus require a high level of disinfection or preferably sterilisation. Noncritical items are namely those used externally which do not come in contact with damaged skin or mucous membranes. Noncritical items require cleaning or low level disinfection if necessary (Spaulding, 1972).

1.4.1 Limitation of conventional sterilisation methods for biomaterials

Numerous documented incidences of acquired infections, resulting from improper decontamination of biomaterials and medical devices, highlight the need for appropriate sterilisation and disinfection methods. However, difficulties in eradicating infectious agents safely from such materials are not only present due to the wide variety of pathogenic microorganisms and their steadily adapting resistance to current decontamination methods, but also as a result of the increasing number of different polymeric biomaterials with various physicochemical properties. The importance of determining the appropriate decontamination treatment for medical equipment is not only dependent on its efficiency to eliminate microbial contamination from the often complex surface structures, but also to avoid changes, resulting from the decontamination process, in the material itself which may cause dysfunction, or even worse, the introduction of toxic alterations. A variety of

conventional sterilisation methods using chemical or physical agents can be considered for the sterilisation of particular medical devices and include the use of dry or moist heat, chemicals and radiation (Chamberlain *et al.,* 1998). Apart from inactivating microorganisms, these sterilisation agents can interact with the material of a medical device itself and negatively affect its functionality. Steam sterilisation by autoclaving at appropriate high temperatures is probably the most widely employed method today, but might induce hydrolysis and/or melting of the polymer matrix which limits its application for the treatment of a vast range of polymeric biomaterials including heat sensitive hydrogels (Nair, 1995; Stoy, 1999; Jiménez *et al.,* 2008). The use of chemical agents such as ethylene oxide (EtO) gas, formaldehyde, glutaraldehyde and ortho-phthalaldehyde (OPA) offer the advantage of elective treatment at suitable temperatures and are useful for hydrolytically unstable polymers. However, due to its well-known toxicity (esp. carcinogenicity) and flammability the popularity of EtO gas is decreasing. There are also worries about the safety of operators when opening the EtO sterilisers before the end of the required vent time, which is much longer than the actual sterilisation time (Steelman, 1992). Moreover, EtO gas residues act as strong alkylating agents which sometimes react with functional groups on the polymer surface thereby altering the materials biological properties (Mendes *et al.,* 2007; Tarafa *et al.,* 2010). OPA, the successor of glutharaldehyde, expresses excellent material compatibility. Its major drawbacks are that it is more expensive and will stain proteins (including skin) gray in colour. Radiation sterilisation, including X-rays, gamma rays, electron beam and to a certain extent also UV-radiation, express good effectiveness, negligible thermal effects, and can even allow for packaging prior to treatment. On the other hand, radiation tends to induce degradation by random chain scission and/or cross linking in several polymeric materials resulting in changes of mechanical stability which may also interfere with the biocompatibility (Deng and Shalaby, 1995 Hirata *et al.,* 1995; Nair, 1995; Moreira *et al.,* 2004; Mrad *et al.,* 2010).

1.4.2 Modern plasma technologies for the sterilisation of temperature sensitive polymeric biomaterials

The limitation of conventional decontamination methods, especially regarding temperature sensitive polymeric materials, encouraged the search for novel techniques. The ideal

sterilisation technique should provide a sterilisation time equal or shorter than the actual processing time required for classical heat sterilisation methods (approximately 60 min). The processing temperature should be equal or lower than the maximum temperature encountered during EtO sterilisation (55^{o}C or less). Moreover, it should be possible to sterilise a wide range of materials without introducing harmful material changes or compromising the safety of the process operators (Moisan *et al.,* 2001).

Considering the aforementioned, the recent developments in the area of plasma technologies opened a new field for sterilisation of temperature sensitive biomaterials and medical devises. The plasma state is frequently called the fourth state of matter, because it is more activated than the solid, liquid or gas state. The plasmas used for low-temperature sterilisation often fall in the category of gas-discharge plasmas. These plasmas are formed by applying an electric field to a suitable gas. Plasmas for low-temperature sterilisation can be obtained by using radio-frequency (RF; typically 1-100 MHz) and microwave discharges (≥300 MHz) under low current and low pressure conditions respectively, or by creating pulsed or constant electric fields of high voltage (HV) magnitudes between electrodes even under atmospheric conditions (Moisan *et al.,* 2001; Moreau *et al.,* 2008). Under the right circumstances the electric field will lead to events that cause the neutral particles in the gas to dissociate and cause the formation of charged ions, electrons as well as neutral species (Bogaerts *et al.,* 2002). Plasma created by electric field induction is typically not in thermal equilibrium as the temperature of the different generated plasma species varies from each other. More precisely, the free electrons have much higher temperatures than heavy particles such as ions, atoms and molecules. Excited particles eventually lose their energy (de-excitation) either by spontaneously emitting a photon or through collisions with other particles or surfaces. It is the sum of the activated particles and other physical events including UV-radiation that can inactivate microbes at relatively fast rates.

Although interest in plasma sterilisation of heat sensitive materials has increased over the last two decades, the method is known since the late 60s. The first two patents regarding plasma sterilisation came from Menashi (1968) and Ashman and Menashi (1972). The Menashi (1968) patent described the use of a pulsed radio frequent (RF) field to form argon plasma for the microbial inactivation of polymeric containers such as plastic

bottles. It was found that the plasma must come in contact with the interior plastic surface of the bottles and it was thought that the biocidal action was due to intense heating of the microorganism – this mechanism was later termed microincineration by Peeples and Anderson (1985). However, a careful timing was required to create and extinguish the plasma to avoid substantial damage to the plastic material resulting from the localised temperature increases. The second Ashman and Menashi (1972) patent tried to address this problem by using a low pressure system with a range of different gases such as chlorine, bromine, hydrochloric acid and iodine and also mentioned trials with plasmas from hydrogen, oxygen and nitrogen. During the early 70s Brumfield *et al.* (1970a, 1970b) issued two plasma patents designed to treat unpackaged and packaged products using a microwave power source. Again, similar to the aforementioned patents, temperature increases were the main problem associated with this technique. In the following period several patents were issued using plasmas as sterilising agent but the temperature problem remained a critical issue (Fraser *et al.,* 1974, 1976; Tensmeyer, 1976, 1977). In an attempt to overcome the temperature problems Bithell (1982) used RF oxygen plasma to sterilise objects sealed in packages.

Boucher (1980) submitted a patent which described the use of antimicrobial agents combined with plasma effects. In this work plasma was formed from an oxygen gas mixture containing at least one aldehyde. The resulting sterilisation process was found to be more effective than using the plasma gas or the aldehyde vapour on its own. A similar approach was used by Jacobs and Lin (1987) whereby highly reactive plasma was generated form a vapour formed by evaporating a hydrogen peroxide (H_2O_2) solution. However, the Boucher (1980) and Jacobs and Lin (1987) patents required that the object to be sterilised had to be subjected to the electromagnetic field and this caused problems with the uniformity of the treatment (Martens *et al.,* 1998). Moreau *et al.* (2000) used the afterglow of a plasma to inactivate microbial spores. The term afterglow plasma (also known as remote plasma) describes the nonthermal action of residual long-lifetime species present in the gas after the plasma initiating source, the electromagnetic field, is removed (Tendero *et al.,* 2006).

Further development of plasma sterilisation methods using antimicrobial agents for the creation of plasma led to the production of the two commercially available plasma-

based sterilisers in the 1990s. They are the Sterrad® sterilisers (available models: Sterrad® 50, 100, 100S and 200, Advanced Sterilisation Products, Johnson and Johnson, Irvine, California) and the Plazlyte™ sterilisation system (AbTox Inc. Mundelein, Illinois). The Sterrad® process uses H_2O_2 vapour and water vapour to create its sterilising effects, while the Plazlyte™ uses a mixture of argon, oxygen and hydrogen plasma combined with peracetic acid vapour (Martens *et al.,* 1998). Both methods protect the object being sterilised from the electromagnetic plasma source and the treatment is alternated between afterglow plasma exposures and using the vapour of the respective antimicrobial chemical on its own. Although the Sterrad® and Plazlyte™ methods are sometimes criticised as not to belong to true plasma sterilisation methods, a vast amount of investigations were conducted to evaluate their sterilisation performance on polymeric biomaterials including hydrogels (Kurtz *et al.,* 1999; Lerouge *et al.,* 2001; Calvet *et al.,* 2008; Kanjickal *et al.,* 2008).

In the last decades a vast amount of experimental plasma techniques were investigated for the safe microbial decontamination of heat sensitive materials and this work was summarised in excellent review papers (Lerouge *et al.,* 2001; Moisan *et al.,* 2001, 2002; Bogaerts *et al.,* 2002; Laroussi, 2005; Rossi *et al.,* 2006; Moreau *et al.,* 2008).

1.4.2.1 Pulsed plasma gas-discharge for the antimicrobial decontamination of hydrogels

Recent advances in the field of pulse power technology provided suitable methods for the creation of low temperature plasma discharges at atmospheric conditions for sterilisation purposes (Marsili *et al.,* 2002; Satoh *et al.,* 2007; Rowan *et al.,* 2008). Pulsed power systems deliver a high peak power to a load in the form of a pulse. This is achieved by accumulating energy over a relatively long period of time which is then delivered in extremely short bursts (in the ns -µs timescale) with voltage magnitudes in the range of few kV to several MV. During each pulse, very high levels of peak power are generated and treatment is achieved using the required number of pulses. Under the right conditions, a pulse discharge directed into a suitable gas can cause an efficient ionisation and excitation of the gas to form plasma. In addition, as the 'pulse-on'-period compared to the 'pulse-off'-period is very small, excessive heat effects can be avoided (Bogaerts *et al.,* 2002).

Recent research has shown that due to their high water content and the resulting fragile polymer scaffold, hydrogels can be sensitive to common conventional sterilisation techniques based on high temperatures, chemicals and ionising radiation (Elijarra-Binstock *et al.*, 2007; Jiménez *et al.,* 2008; Kanjickal *et al.,* 2008). Hence, in the present study the suitability of a novel HV induced pulse plasma gas-discharge (PPGD) technology for the microbial decontamination of the developed hydrogels is investigated. In this setup the electrical discharge is generated above a liquid medium wherein the hydrogels are submerged and thus are protected from direct thermal effects of the discharge. Detailed information about this novel PPGD technology, its electrical parameters and inactivation mechanisms will be discussed throughout this study.

1.5 Aims and objectives of this study

The increasing demand for new medical treatment regimes has led to an elevated interest in the development of novel biomaterials with sophisticated functions such as controlled drug delivery. Since their introduction into the biomedical field, hydrogels have played a vital role in the manufacture of advanced treatment devices for a range of medical conditions and this role is constantly expanding due to the increasing applications of these adaptable materials. Thus, one of the major objectives of this investigation was the synthesis, functional characterisation and biocompatibility assessment of physical and chemical hydrogels based on NVP and AA.

Due to the current problems associated with the sterilisation of delicate hydrogel biomaterials, another major objective of this study was to determine the suitability of a novel PPGD based treatment method for the safe microbial decontamination of hydrogels. Surprisingly, although plasma based treatment methods have the potential to reduce the biocompatibility of certain biomaterials, there is only a limited amount of toxicological data available especially concerning the area of genotoxicological evaluations. Hence, the impact of PPGD treatment on the hydrogels' biocompatibility was further determined using suitable *in vitro* cyto- and genotoxicological tests. The main aims of this study are summarised as follows:

Aims

Development and characterisation of novel NVP-AA based hydrogels intended for drug delivery applications

- To determine the efficiency of the photopolymerisation process for the development of NVP and AA based hydrogels

- To determine swelling and degradation behaviour of these hydrogels

- To analyse the extent of unpolymerised residuals still present in the hydrogel networks using HPLC methods

- To determine important mechanical characteristics

In vitro biocompatibility evaluation of novel NVP-AA based hydrogels

- To investigate the cytotoxic potential of NVP-AA based hydrogels in direct and indirect contact assays in conjunction with MTT, neutral red and fluorescence based endpoints

- To determine the extent of DNA strand breakage and point mutation induction following exposure to NVP-AA based hydrogels

Investigations into the suitability of a novel plasma based technology for the safe microbial decontamination of hydrogels

- To optimise and characterise a novel PPGD technology for the efficient low temperature sterilisation of hydrogels

- To evaluate the impact of PPGD treatment on the hydrogels' material properties

- To evaluate the impact of PPGD treatment on the hydrogels' biocompatibility performance

Chapter 2: Experimental Details

2.1 Hydrogel synthesis

Physical and chemical hydrogels were prepared by free radical photopolymerisation according to a method developed by Devine *et al.* (2003 and 2005). The monomers used in polymeric hydrogel synthesis were *N*-vinyl-2-pyrrolidone (NVP, Lancaster synthesis, UK) and acrylic acid (AA, Merck-Schuchardt, Germany) with both monomers used as received. The initial monomeric feed ratios were 100 wt% NVP (100-0), 75 wt% NVP-25 wt% AA (75-25), 50 wt% NVP-50 wt% AA (50-50), and 25 wt% NVP- 75 wt% AA (25-75). Chemical hydrogels where fabricated with the addition of an appropriate crosslinking agent at 0.1 wt% of the total monomer content. Two different crosslinkers, ethylene glycol dimethacrylate (EGDMA, Sigma-Aldrich, Ireland) and poly(ethylene glycol) dimethacrylate (PEGDMA, Sigma-Aldrich, Ireland) with a molecular mass of 400 were compared for their suitability to generate water insoluble hydrogels.

To initiate the polymerisation reactions the UV light sensitive initiator 1-hydroxycyclohexylphenylketone (Irgacure® 184, Ciba specialty chemicals, UK) was added at 3 wt% of the total monomer weight and stirred continuously until completely dissolved. Subsequently, the mixtures were transferred into a silicon mould (W.P. Notcutt, UK) that contained disk impressions of 25 mm diameter and 3 mm depth. The mould was positioned horizontally to the gravity direction under two UVA lamps (Q-panel products, UK) and the solution was irradiated with 280 $\mu W/cm^2$ of UVA_{340nm} light (UVX Radiometer, Ultra-Violet Products, Davidson & Hardy Laboratory Supplies Ltd, Ireland) for 2 h. The cured samples were then dried in a vacuum oven at 40^{o}C, 400 mmHg for 24 h prior to use. Due to their insoluble character, chemical hydrogels were subjected to further purification to facilitate the removal of unreacted material (e.g. monomers). This involved submerging the chemical hydrogels in a phosphate buffered saline solution or PBS (0.01 M phosphate buffer; 0.0027 M KCL; 0.137 M NaCl pH 7.4; Sigma-Aldrich, Ireland) for 15 days at 37^{o}C and 125 rpm agitation with the PBS solution replaced on a daily basis.

The name and composition of the samples used throughout this investigation are outlined in Table 2.1.

Table 2.1: Name and composition of hydrogels synthesised via photopolymerisation using Irgacure® 184 (3 wt% of base monomer content). The abbreviation phys, xP and xE indicates for physical gels, PEGDMA and EGDMA crosslinked hydrogels, respectively.

Hydrogel	NVP (wt%)	AA (wt%)	EGDMA (wt%)	PEGDMA (wt%)
100-0phys	100	-	-	-
75-25phys	75	25	-	-
50-50phys	50	50	-	-
25-75phys	25	75	-	-
100-0xP	100	-	-	0.1
75-25xP	75	25	-	0.1
50-50xP	50	50	-	0.1
25-75xP	25	75	-	0.1
100-0xE	100	-	0.1	-
75-25xE	75	25	0.1	-
50-50xE	50	50	0.1	-
25-75xE	25	75	0.1	-

2.2 Hydrogel characterisation

2.2.1 Fourier transform infrared spectroscopy

Fourier transform infrared spectroscopy (FTIR) was used to determine the presence of specific chemical groups in the hydrogels after photopolymerisation. Such analysis was carried out on all hydrogel samples shortly after completing the 24 h vacuum drying process. A Nicolet Avatar 360 FTIR (Nicolet Instrument Corporation, US) linked to OMNIC 5.1 software was used in the attenuated total reflectance (ATR) mode in the range of 4000 to 650 cm^{-1} with 32 scans obtained per sample. A rectangular shaped zinc selenid crystal was employed to allow for ATR mode. The obtained FTIR spectra were normalised and major vibration bands were associated with chemical groups.

2.2.2 Swelling and stability studies

The following swelling and degradation experiments were conducted on both the physical and chemical hydrogels. This was considered necessary to gain knowledge of the materials'

performance when in contact with body fluids. Therefore, all experiments were carried out under physiological conditions (37^{o}C and pH 7.4) using PBS as the swelling medium.

2.2.2.1 Swelling and solubility of physical hydrogels

The swelling and solubility properties of physical hydrogels were evaluated by fully immersing a hydrogel disk, with a mass of 1.15 ±0.15g, in 30 ml of PBS in a plastic petri dish (Ø = 7.5 cm) and incubating at 37^{o}C. At predetermined time intervals excess buffer solution was removed and the samples were carefully surface-dried, using absorbent tissue, and subsequently weighed (Sartorius Scale, Germany). The samples were then re-submerged in fresh buffer solution and the swelling experiment continued until the polymer had completely dissolved. The *swelling ratio* was determined as outlined in Equation 2.1 where *Wt* is the weight of the swollen hydrogel at a predetermined time, and *Wo* is the weight of the dry hydrogel (xerogel) before swelling experiments.

$$Swelling\ ratio\ (g/g) = Wt / Wo$$

Equation 2.1: Swelling ratio.

2.2.2.2 Swelling and degradation of chemical hydrogels

The swelling and degradation characteristics of covalently crosslinked hydrogels were studied by fully immersing a hydrogel disk, with a mass of 1.15 ±0.15 g, in 100 ml of PBS in a 1000 ml glass beaker and incubating at 37^{o}C. As with the physical hydrogels, at predetermined time intervals, excess buffer solution was removed and the samples were carefully surface-dried, using absorbent tissue, and weighed. The samples were then re-submerged in fresh buffer solution and the swelling experiments were carried out for 15 days until a stable equilibrium water content (EWC) was obtained. The swelling ratio and the *EWC* were determined by using Equations 2.1 and 2.2.

$$(EWC) = ((Wt - Wo) / Wt) \times 100$$

Equation 2.2: Equilibrium water content.

For degradation studies, chemical hydrogel samples which were previously hydrated for 15 days in PBS were placed in a sealed container with a known quantity of sterile PBS. Following incubation at 37^{o}C, the EWC (Equation 2.2) of the samples was determined at 5 day intervals for up to 15 days.

2.2.3 Reverse phase HPLC analysis of residual monomers

High-performance liquid chromatography (HPLC) was the chosen method for analysing the residual monomer content (RMC) of the hydrogels. The chromatographic system was composed of a Shimadzu LC-6A HPLC pump, a Waters^{TM} 486 UV/vis tunable absorbance detector and a Shimadzu C-R6A chromatopac for system and data management. The mobile phase consisted of methanol in 10 mM aqueous ammonium acetate (ratio 25:75). The standards for the calibration curves were prepared from monomer stock solutions containing 100 µg/ml of either NVP or AA in mobile phase. The final standard concentrations were obtained by appropriate quantitative dilution from the stock solution using the mobile phase as diluent.

2.2.3.1 Hydrogel preparation

To evaluate the RMC of physical hydrogels, solutions containing 10 mg/ml of solubilised hydrogel sample in mobile phase were prepared and diluted 1:100 to obtain a final concentration of 100 µg/ml. Before injection onto the HPLC system, solutions were filtered using a 0.45 µm pore sized syringe filter to protect the injection valve and analytical column from sample particulate matter.

In accordance with the procedure for hydrogel preparation for biocompatibility studies (as outlined in Section 2.4.1), extracts of unpurified and purified chemical hydrogels were also prepared for analysis of residual monomer. Extracts of unwashed chemical hydrogels were prepared by placing a 250 ±10 mg one-piece sample in a sealed container with 30 ml of PBS for 5 days at 37^{o}C and 125 rpm agitation. Conversely, extracts of washed chemical hydrogels were prepared by also placing 250 ±10mg one-piece samples in a sealed container which was subsequently washed with 100 ml PBS for 15 days at 37^{o}C and 125 rpm agitation, with the PBS replaced on a daily basis. Subsequently, the gels were dried at 37^{o}C for 24 h in a laboratory oven (Humboldt H-30100, Eckardt & Sohn GmbH, Germany). The extracts of the washed samples were obtained by incubating

the prewashed networks for a further 5 day period in 30 ml of PBS for 5 days at 37^{o}C and 125 rpm agitation. Before injection to the HPLC system, the extract solutions were filtered using a 0.45 µm pore sized syringe filter.

2.2.3.2 Injection and performance settings

A sample volume of 10 µl was injected onto the chromatographic system, with separation was performed in isocratic mode at a 1.0 ml/min flow rate and ambient temperature on a Phenomenex® C8 (2) Luna 5µM analytical column (150 x 4.60 mm), with a total run time of 20 min. For both monomers analysed, detection was performed at 234 nm. The limit of detection for each monomer was predetermined by injecting appropriate monomer dilutions resulting in a signal less than twice the noise level of the base line. Ultimately, the total residual monomer content in the analysed specimens was calculated using linear regression analysis of peak areas interpolated from the calibration curves.

2.2.4 Mechanical testing of chemical hydrogels

Mechanical properties of EWC preswollen chemical hydrogels were investigated via rheometry and compression testing, to determine the intra-comparative strength of gels synthesised from different monomeric feed ratios. Prior to testing, the surface of the test samples was blotted dry from excess water using filter paper to minimise slippage during testing and all tests were performed in triplicate using individual hydrogel samples.

2.2.4.1 Rheological measurements

Oscillatory parallel plate rheological measurements were carried out on chemical hydrogels using an Advanced Rheometer AR1000 (TA Instruments, Germany) fitted with a Peltier temperature control (set to 37°C) and a 60 mm diameter parallel steel plate. The hydrated samples were subjected to a low strain range sweep from 1.88 x 10^{-4} to 1 x 10^{-3} at a frequency of 1 Hz, while a constant normal force of 5 ±0.5 N was exerted on the samples to ensure proper contact between the gels and the surface plates of the instrument. The shear storage (elastic) modulus G' and the shear loss (viscous) modulus G'' were noted for determining the comparative strength of the hydrogels.

2.2.4.2 Compression testing

The compressive properties of the chemical hydrogels were examined using an Instron® 3300 testing system computer controlled by Bluehill® software (Instron® GmbH, Germany). The tests were conducted in the compressive failure mode to determine the point where hydrated samples experienced a nonreversible plastic deformation under an experimental load i.e. the point of destruction of the hydrogels three-dimensional network. A compressive stress of 0.1 MP and a compressive strain of 50% were used as maximal compression parameters. During the analysis, the compressive strain (%) was continuously recorded in relation to an increase of applied pressure defined as compressive stress (MPa).

2.3 Management of continuous cell lines

In vitro biocompatibility evaluation of the hydrogels was performed with human hepatoma (HepG2), human colon carcinoma (HCT-8) and the human normal keratinocyte (HaCaT) cell lines. For physical hydrogels HepG2 and the HCT-8 were the cell line models of choice, with the biological response to chemical gels evaluated with the HepG2 and HaCaT cell lines. The HepG2 and HCT-8 cell lines were obtained from the American Type Culture Collection (ATCC, US) while the HaCaT cell line was obtained from Cell Lines Service (CLS, Germany).

2.3.1 Routine cell culture quality control

Cell lines were grown from frozen ampoules and routinely subcultured according to standard procedures (Freshney, 1987). In order to maintain a sterile working environment, all cell culture manipulations were carried out in a class II laminar flow cabinet in a dedicated cell culture laboratory. In order to achieve a satisfactory level of sterility, aseptic technique was strictly adhered according to standard procedures. At regular intervals the humidified carbon dioxide (CO_2) incubator and the laminar flow unit were cleaned using 70% aqueous ethanol solution to minimise the risk of contamination. The deionised water (dH_2O) used for cell culture manipulations was sourced from an Elix 5 water system connected to Milli-Q ultrapurifier (Millipore, VWR, Ireland). To ensure sterility, all media and cell line manipulations were conducted using tissue culture grade plastics, with all glassware autoclaved before use. Routinely, 5-10 ml of media was aseptically transferred to a sterile universal, incubated for 48 h at 37°C and examined for the presence of overt

bacterial and fungal contamination. When necessary, 100 µl of media was examined for the presence of bacterial/fungal contamination using a compound microscope and suspect media was disposed off.

2.3.2 Culture medium preparation

Complete cell culture media for all cell lines was prepared in 100 ml volumes in sterile 75 cm^2 tissue culture flasks under aseptic conditions and stored at 4°C. All cell culture consumables and media components were sourced from Sarstedt (Ireland) and Sigma-Aldrich (Ireland), respectively. Media constituents for HepG2 and HaCaT cells are outlined in Table 2.2. Prior to use all media constituents were preheated in a 37°C water bath.

Table 2.2: HepG2 and HaCaT cell culture medium constituents and storage temperature**.**

Medium component	Storage temperature (°C)	HepG2 Medium constituents Volume (ml)	HaCaT Medium constituents Volume (ml)
Foetal calf serum (FCS)	- 20	10	10
L-Glutamine (200 mM)	- 20	1	1
Penicillin - Streptomycin (5000 U - 5 mg/ml)	- 20	0.5	0.5
Amphotericin B (200 mM)	- 20	0.5	0.5
DMEM (Hepes modification)	+ 4	44	88
HAMS F-12 (Hepes modification)	+ 4	44	-

The HCT-8 cell line was cultured in RPMI 1640 media prepared by dissolving the RPMI powder (16 g/l) in 889 ml of sterile dH_2O, followed by the addition of 1 ml L-Glutamine, 5 ml amphotericin B solution, 5 ml penicillin-streptomycin solution and 100 ml FCS to give a final volume of 1 l of media containing 10% FCS. Subsequently, 2 g of sodium bicarbonate was added to the media. The media was then filter-sterilised using 1 l cell culture filters (Nunc™, VWR, Ireland) and the pH adjusted to 7.4 using 1 M hydrochloric acid (HCl) as required; pH measurements were taken before and after filtration using a calibrated pH meter (pH-510, Eutech Instruments, Fisher Scientific, Ireland). All media was stored at 4°C and heated to 37 °C before use.

2.3.3 Reconstitution of frozen cell cultures

A frozen ampoule of cells was removed from liquid nitrogen storage (-196^{o}C) and thawed quickly in a 37^{o}C water bath. The cells were then aseptically transferred to a sterile universal containing 10 ml of prewarmed culture medium and centrifuged at 1300 rpm for 5 min to pellet the cells. The supernatant was aspirated off and the cell pellet resuspended in 1 ml of cell culture medium before the addition of a further 4 ml of culture medium and aseptic transfer to a 25 cm^2 culture flask. The cells were then incubated at 37°C until the desired degree of confluency (80%) was obtained.

2.3.4 Harvesting and subculture

Upon reaching 80% confluency, the medium was aspirated off prior to rinsing cultures with sterile PBS. Subsequently, 2 ml of 0.25% trypsin-ethylenediamine tetra-acetic acid (EDTA) solution (0.05% trypsin-EDTA for HaCaT cells) was added to the flask swirling gently prior to the removal of all but 0.5 ml of trypsin-EDTA. The culture flask was then incubated at 37^{o}C for 5 min or until complete cellular detachment had occurred. Subsequently, the cells were collected in 5 ml of complete medium, transferred to a sterile universal and centrifuged at 1300 rpm for 5 min. The supernatant was discarded and the pellet resuspended in 4 ml of culture medium. If required, a cell count was performed, otherwise the resuspended cell pellet was split equally between two tissue culture flasks which were incubated at the appropriate temperature of 37^{o}C with 5 % relative humidity.

2.3.5 Cell viability and enumeration

Mammalian cells were harvested as previously described and the pellet was resuspended in a predetermined amount of cell culture medium. Next, 100 µl of cell suspension was transferred to a sterile universal to which 150 µl sterile PBS and 250 µl filter sterilised trypan blue was added. The suspension was mixed by inverting several times to allow for even distribution of cells. Subsequently, 10 µl of the cell suspension was then loaded onto a Neubauer haemocytometer which was covered with a cover glass slip. All viable cells (cells excluding trypan blue) were counted in the five larger 1 x 1 mm squares. The cell concentration per ml of culture media was determined as outlined in Equation 2.3, where N is the mean value for the obtained cell count, df is the dilution factor and S is the number of haemocytometer squares counted.

$$\textit{Number of cells per ml of culture media} = \frac{N \times df \times 10^4}{S}$$

Equation 2.3: Cell enumeration.

2.3.6 Cryopreservation

To facilitate cell banking and ensure a continuous supply of low-passage number cells, cultures were harvested using 0.25% trypsin-EDTA solution (0.05% trypsin-EDTA for HaCaT cells) followed by centrifugation at 1300 rpm for 5 min prior to resuspending the resultant cell pellet in freeze medium containing 50% FCS, 40% DMEM and 10% dimethyl-sulphoxide (DMSO) to a final cell concentration of 1 x 10^6 cells/ml. Subsequently, 1.8 ml of the cell suspension was transferred into cryovials and the vials placed within a polystyrene cryobox in a -80°C freezer. After 24 h the cryovials were removed from the freezer and placed in liquid nitrogen (-196ºC) for long term storage.

2.4 *In vitro* assessment of cytotoxicity

2.4.1 Preparation of hydrogels for biocompatibility testing

Prior to biocompatibility testing, physical and chemical hydrogel samples were prepared according to their physicochemical properties to obtain reproducible and valid samples for testing. The risk of microbial contamination was reduced by briefly submerging the gels for 10 s in 70% ethanol solution prior to drying under aseptic conditions, to remove residual ethanol, and UV-irradiating at the germicidal wavelength of 263 nm for 10 min.

Physical hydrogels

Stock solutions containing 25 mg/ml of solubilised hydrogel samples were prepared in complete culture medium. The AA content of the hydrogels induced a substantial pH change to the culture medium which needed to be adjusted to physiological conditions (pH 7.4) by the addition of 3 M NaOH. The solutions were further diluted with appropriate cell culture medium to obtain concentrations in the range of 0–25mg/ml for biocompatibility studies.

Chemical hydrogels

Extracts of unwashed chemical hydrogels were prepared by placing a 250 mg (±10 mg) one-piece sample in a sealed container with 30 ml of culture medium for 5 days at 37^{o}C and 125 rpm agitation. As with the physical hydrogels, the induced pH change was adjusted to physiological conditions (pH 7.4) by the addition of 3 M NaOH.

To facilitate the removal of unbound material, a 250 mg (±10 mg) one-piece sample was washed for 15 days in a sealed container with 50 ml of sterile PBS at 37^{o}C and 125 rpm agitation, with the PBS replaced on a daily basis. Subsequently, the gels were dried at 37^{o}C for 24 h in a laboratory oven (Humboldt H-30100). The extracts of the prewashed samples were obtained by a further 5 day incubation period in 30 ml of culture medium at 37^{o}C and 125 rpm agitation. A pH adjustment was not necessary for these extracts.

In accordance with the ISO 10993-5 standard series the recommended *in vitro* cytotoxicity assays, i.e. indirect and direct cell contact assays, were chosen to determine the relative sensitivities of the different cell types to the test materials. Subsequently, dose-response curves were constructed from which toxicity indices were obtained.

2.4.2 Direct contact assay (MTT endpoint)

Cytotoxic effects on cell growth and viability were determined via the MTT assay. This assay was originally developed by Mosmann (1983) and determines the ability of viable cells to convert the soluble tetrazolium salt 3-[4,5-dimethlythiazol-2-yl]-2,5-diphenyltetrazolium bromide (MTT) into a formazan precipitate. The conversion of the tetrazolium ring to the formazan product is maintained by the mitochondrial enzyme succinate dehydrogenase and the cofactors NADH and NADPH (O'Hare and Atterwill, 1995; Fotakis and Timbrell, 2006). The possibility to quantify the purple coloured formazan crystals spectrophotometrically makes this assay rapid and highly reproducible for the determination of toxicity and proliferation in cultured cell lines (O'Hare and Atterwill, 1995) as the amount of formazan produced is directly proportional to the number of viable cells (Bernhard *et al*., 2003).

Procedure

For cytotoxicity testing in this study, a 5 mg/ml MTT stock solution was prepared by adding 50 mg MTT to 10 ml PBS in a sterile universal and the solution was stored in the dark at 4^{o}C. Prior to use, this mixture was incubated at 37^{o}C for 1 h and filter sterilised using a 0.2 µm pore-sized syringe filter to remove any crystals which had formed. The assay was performed in 96 well microplates seeded at 1-1.5 x 10^4 of respective cells in 200 µl of complete culture medium. The plates were then incubated for 12-24 h (depending on cell type) at 37^{o}C until the desired percentage of confluency (40-60%) was observed.

Depending on the type of hydrogel tested, the cells were exposed to various concentrations of physical hydrogel solutions, extracts from unpurified and purified chemical hydrogels and to the reference chemicals NVP, AA and PVP for predetermined time periods (6, 12, 24 h) at 37^{o}C. Subsequently, the medium containing test chemicals was discarded and the wells were washed twice with warm PBS (37^{o}C). Following this, 180 µl of fresh media and 20 µl of MTT solution was added to each well to obtain a final MTT concentration of 0.5 mg/ml. After a further 4 h incubation at 37ºC, the medium containing the MTT was carefully aspirated off and the resulting blue formazan crystals were solubilised by the addition of 100 µl of DMSO to each well. To assist thorough solubilisation, the plates were shaken gently. Finally, the optical densities (OD) of each well were recorded using a multiwell plate reader (Anthos HTIII, Labtec Instruments GmbH, Germany) at a test wavelength of 540 nm and a reference wavelength of 690 nm. Results are presented as percentage of untreated controls against test chemical concentrations.

2.4.3 Direct contact assay (neutral red endpoint)

The neutral red (NR) cytotoxicity assay is based on the ability of viable cells to incorporate and accumulate the weakly cationic supravital dye NR (Borenfreund and Puerner, 1985). The dye readily penetrates the cell membranes of viable cells by nonionic diffusion and binds with anionic sites in the intracellular lysosomal matrix (Lullmann-Rauch, 1979). In general, the dye is not incorporated in damaged or dead cells, but may appear as a diffuse stain throughout the cytoplasm. Similar to the MTT assay, the amount of dye retained is

directly proportional to the number of viable cells which can be quantitated via spectrophotometry.

Procedure

A 1 mg/ml NR stock solution was prepared and the solution was acidified with 2 drops of glacial acetic acid, autoclaved and stored in the dark at 4^{o}C. Immediately before use, a working solution was prepared by diluting the NR stock solution 1:10 with prewarmed sterile PBS. The solution was filter sterilised, using a 0.2 µm pore-sized syringe filter to remove any crystals that had formed.

Cells were seeded in 96 well microplates at a density of 1-1.5 x 10^4 cells in 200 µl of complete culture medium and then further incubated for 12-24 h (depending on cell type) at 37^{o}C until the desired percentage of confluency (40-60%) was observed. In accordance with the previously described MTT test, the cells were exposed to various concentrations of physical hydrogel solutions, extracts from unpurified and purified chemical hydrogels and to the reference chemicals NVP, AA and PVP for a predetermined time period at 37^{o}C. After the cell exposure, the medium containing test chemicals was discarded and the wells were washed twice with warmed PBS. Subsequently, 100 µl of the freshly prepared and prewarmed NR working solution (100 µg/ml) was added to each well and further incubated for 80 min at 37ºC. The NR solution was carefully aspirated off and the cells were washed twice with 200 µl of prewarmed PBS before the dye was extracted by adding 100 µl of the NR extract solution (1% glacial acetic acid/ 50% ethanol (v/v)). To support dye solubilisation the plates were shaken gently and the OD recorded using a multiwell plate reader (Anthos HTIII) at a test wavelength of 540 nm and a reference wavelength of 690 nm. Wells exposed to NR solution without cells were used as blanks and were subtracted from the obtained optical densities obtained. The results are presented as percentage of untreated controls against test chemical concentrations.

2.4.4 The indirect contact (agarose overlay) assay

The agarose overlay assay used in this study was derived from the agar overlay assay originally developed by Guess *et al.* (1965) for *in vitro* toxicity screening of plastics destined for medical use. Since then, this method has been modified several times to

facilitate the cytotoxicity evaluation of numerous products including a wide range of biomaterials. The main principle of the agarose overlay assay is based on the migration or diffusion of toxic substances from the test material through the protective agarose cushion to the underlying cell monolayer. The slow diffusion of leachable substances through the agarose results in a zone of dead cells around and beyond the test samples if the leachable substances are cytotoxic. The main function of the agarose layer is to protect the cells from physical damage caused by solid test materials and to overcome some of the difficulties associated with the direct contact assays i.e. low-density samples tend to float in culture medium and result in poor contact with the monolayer surface, whilst high-density samples cause physical disruption of the cells due to their weight and hard surface. Zones of cytotoxicity can be visualised and measured via colour changes after staining the cell layer with vital dyes e.g. NR, MTT, Sudan black or Giemsa (Northup and Cammack, 1998).

Procedure

For this study, the method was modified to allow for the use of HepG2 and HaCaT cells. A low melting point agarose was utilised to prevent the thermal cell shock associated with preparations of conventional agar. Also agarose does not significantly alter the diffusion rate of charged compounds because it lacks agraopectin (Wilsnack *et al.,* 1973). To assess the final outcome of the assay, the MTT cell viability method was the preferred endpoint in this study, as it resulted in a greater contrast between zones of discolouration compared to other vital stains.

An agarose overlay gel was prepared by dissolving 3% low melting point agarose in sterile PBS. The dissolved agarose was autoclaved, cooled, and further diluted with appropriate cell culture medium to obtain a final agarose gel concentration of 1.5%. The solution was maintained at 40^{o}C using a water bath to prevent solidification. Cells were seeded at 2 x 10^{5} cells in 4 ml culture medium in 60 mm tissue culture plates and incubated for 48 h at 37ºC until a complete confluent monolayer was obtained. Following this, the culture medium was then replaced with 4 ml of evenly distributed agarose overlay mixture on top of the monolayer. After 30 min incubation at 37^{o}C to allow for agarose-gel solidification, perfectly round discs (Ø = 20 mm) of, in complete culture medium, pre-swollen, un-purified and purified chemical hydrogel tests samples were placed in the centre

of the culture plates and incubated for a further 24 h at 37ºC. One agarose plate was used for each individual test sample. Subsequently, each test sample was carefully removed from the gel layer and 4 ml of 0.5 mg/ml MTT solution was added and further incubated for 2 h to allow for formazan production in viable cells. Finally, the MTT solution was aspirated off and the plates were examined for zones of reactivity. The grading of these zones is outlined in Table 2.3.

Table 2.3: Reactivity grades for Agar Overlay assay.

Grade	Reactivity	Description of Reactivity Zone
0	No toxicity	No detectable zone around or under sample
1	Slight toxicity	Some malformed or degenerated cells under sample
2	Mild toxicity	Zone limited to area under sample
3	Moderate toxicity	Zone extends 0.5-1.0 cm beyond sample
4	Severe toxicity	Zone extends greater than 1.0 cm beyond sample but does not involve entire dish
5	Maximum toxicity	Zone involves entire dish

2.4.5 Morphological examination of cells in direct contact with chemical hydrogels

The method used in this study for the morphological examination of cells is derived from a method described by Rosenbluth *et al.* (1965) and involves the microscopic evaluation of cells cultured in direct contact with the test article. The assay is not only used to detect the cell damaging potential of a test material, but is also a sensitive method for evaluating the ability of cells to adhere and to proliferate on the surface or in the presence of a biomaterial. The technique is especially important for assessing the cytotoxic potential of solid test materials, as the presence of unleachable toxic substances that do not pass into the extraction medium can be detected.

2.4.5.1 Light microscopy

Chemical hydrogels preswollen for 24 h in cell culture medium were evaluated in their unpurified and purified state to determine the cells' ability to grow in the presence of the hydrogel networks. Cells were seeded in 12 microwell plates at a density of 2 x 10^4 cells in

800 µl culture media containing 10% FCS and left to adhere for 2 h. Subsequently, round discs (Ø = 20 mm) of chemical hydrogel test samples were carefully placed on top of the cells and incubated for a further 24 h at 37ºC before final morphological examination. In addition, to evaluate the ability of cells to adhere and proliferate on the surface of the hydrogels, round discs (Ø = 20 mm) of chemical hydrogel test samples were placed into wells of a 12 microwell plate. Subsequently, 3 x 10^4 cells in 300 µl of complete culture medium were carefully seeded onto the hydrogel's surface and left to adhere for 2 h at 37^{o}C. The hydrogels were then carefully submerged in complete cell culture medium before additional 24 h incubation at 37ºC. The morphological changes indicating cytotoxicity and cell growth characteristics were recorded using a compound and inverted microscope (Leitz, Germany) attached to a digital camera (Hamamatsu Photonics 3CCD, Germany).

2.4.5.2 The fluorochrome-mediated viability assay

Furthermore, the viability of HepG2 and HaCaT cells was monitored using a modification of the fluorochrome-mediated viability assay, as described by Strauss (1991). The cells were exposed to the hydrogels as described in Section 2.4.5.1 and then incubated for 5 min with a fluorescein diacetate (Fda) - ethidium bromide (EtBr) (30µg/ml-8µg/ml) solution (Sigma-Aldrich, Ireland) which was freshly prepared in PBS. By utilising fluorescence microscopy (Leitz Diaplan, Germany) with an excitation filter of 515–560 nm it was observed that viable cells hydrolysed the Fda and appeared green while dead cells absorbed the EtBr and their nuclei appeared red. At least 200 cells were scored from each data point and the percentage of viable cells was calculated.

2.5 *In vitro* genotoxicity evaluation

Genotoxicity testing was included as part of the *in vitro* biocompatibility assessment of the hydrogels. More specifically, the highly sensitive, alkaline, single cell gel electrophoresis (comet) assay was used to determine the hydrogels' potential to induced DNA damage in the form of single strand breaks and alkali-labile sites. In addition the *S. typhimurium* reverse mutation (Ames) assay was employed to investigate the hydrogels' ability to induce point mutations thus ensuring that DNA damage or mutagenic potential was investigated at both the chromosomal and nucleotide levels respectively.

2.5.1 The comet assay

The comet assay is a widely adopted rapid and sensitive technique for detecting and analysing the potential of substances to cause DNA damage which includes strand breaks, alkali-labile sites, DNA crosslinks, and incomplete excision repair sites in virtually all single cells (Singh *et al.,* 1988). The basic principle of the comet assay is the migration of different sized DNA molecules in an agarose gel under an electrophoretic current. More specifically, induced DNA strand breakage leads to fragmentation of the supercoiled duplex DNA which can be stretched out by electrophoresis. Under an electric current, due to their reduced molecular size, fragments of damaged DNA move further within the pores of the agarose gel than intact DNA. This process leads to the microscopic appearance of the cell as a comet-like shape as the broken strands of the negatively charged DNA molecule become free to migrate in the electric field toward the anode. The intact DNA of the nucleus forms the head of the comet and the small DNA fragments appear as the tail. Therefore, the presence of strand breaks is visualised by the emergence of comet tails from the nuclei of cells treated with genotoxic agents (Sparrow *et al*., 2003). The assay, as first introduced by Östling and Johanson (1984), was performed under neutral pH conditions. This prevents DNA strand separation and therefore is more sensitive to the detection of double strand DNA damage. Subsequently, the method was modified by applying highly alkaline denaturing conditions combined with unwinding of the DNA duplex. This resulted in a more detailed visualisation of comet tails due to enhanced DNA fragmentation by single and double strand breaks, including the indirect single strand breaks produced as alkaline labile AP sites (Singh *et al.,* 1988; Olive, 1990).

2.5.1.1 The comet assay procedure

The alkaline comet assay procedure described by Singh (1996) was used in the present study with slight modifications. Cells were suspended at a density of 2 x 10^4 cells per ml and 2 ml aliquots of the cell suspension were added to individual wells of a 24 well plate. Following 12 h incubation at 37^{o}C, the residual culture medium was replaced with physical hydrogel solutions or extracts prepared from prewashed chemical hydrogels and the cells were exposed for a further 24 h at 37^{o}C. A 100 mM working stock of H_2O_2 was prepared as a positive control agent and diluted in cold PBS to give the following final assay

concentrations: 10, 50 and 100 µM H_2O_2. Each H_2O_2 concentration was added to duplicate wells prior to 40 min incubation at 4°C. Subsequently, the medium containing the test substances was removed and the wells were rinsed twice with 1 ml cold PBS. The cells were harvested by adding 300 µl of ice cold 0.25% trypsin-EDTA (0.05% trypsin-EDTA for HaCaT) to each well for 5 min at 4ºC followed by the addition of 700 µl of cold culture medium. The cell suspensions were centrifuged at 2000 rpm for 5 min and cells were then resuspended in 200 µl of ice-cold PBS and stored on ice prior to assessing cell viability (≥80% for all test concentrations) was determined via trypan blue exclusion to avoid false positive responses due to cytotoxicity. A 1% low melting point (LMP) agarose in PBS solution was prepared by dissolving 0.2 g agarose in 20 ml PBS and stored at 40°C to prevent solidification. Next, 200 µl aliquots of cells were mixed with 400 µl of LMP agarose and 100 µl were pipetted onto individual gel bond strips (GelBond™ Electrophoresis Film, Sigma-Aldrich, Ireland), coverslipped and stored at 4°C for 5-10 min or until the gel had set. Under dim light conditions to avoid the introduction of additional DNA damage, coverslips were removed and the strips were placed in Quadriperm plates (Sigma-Aldrich, Ireland). Cells were then subjected to lysis by immersion in ice cold lysis buffer pH 10 for 40 min at 4°C followed by rinsing 5 times in tris(hydroxymethyl)aminomethane (tris)-Cl buffer pH 7.4 to remove residual salt. The strips were then exposed to proteinase K solution for 2 h at 37°C.

Alkaline electrophoresis was preceded by a 20 min unwinding step in electrophoresis buffer pH 13. Electrophoresis was performed at 25 V and 300 mA for 12 min in a 2 l capacity 35 cm tank connected to Power Pac 300 (Bio-Rad), with gelbond strips placed horizontally side by side avoiding gaps. Cells were neutralised by rinsing 3 times with Tris-Cl buffer pH 7.4 before fixation in 100% methanol for a minimum of 3 h at 4°C. Prior to analysis, DNA was stained by placing gelbond strips in freshly prepared SYBR® Gold nucleic acid stain (Invitrogen GmbH, Germany) for 40 min at room temperature. Finally, the gels were coverslipped and viewed at 400x magnifications using a fluorescent microscope (Leitz Diaplan) equipped with an excitation filter of 475 - 490 nm. The tail moment and percentage tail DNA (% tail DNA) parameters were analysed for 50 randomly selected single cells per duplicate slide using Comet Assay IV image analysis software (Perceptive Instruments, UK). Unless otherwise stated, the reagents used for the

comet assay were sourced from Sigma-Aldrich, Dublin, Ireland. The solutions used for the comet assay were prepared as outlined in Table 2.4.

Table 2.4: Preparation of comet assay buffer and reagents

Solution / Buffer	Component	Concen-tration	Amount added	Final volume
Lysis solution	EDTA	100 mM	37.22 g	1 l
pH 10	Tris-Cl (pH 10)	10 mM	1.21 g	
(using 3 M NaOH)	NaCl	2.5 M	146.1 g	
	Triton X-100	1%	10 ml	
	DMSO	10%	100 ml	
Tris-Cl buffer	Tris	400 mM	48.4 g	1 l
pH 7.4 (using HCl)				
Electrophoresis	NaOH	0.3 M	24.0 g	2 l
Buffer	EDTA	10 mM	7.44 g	
pH 13	DMSO	2%	40 ml	
(using 3 M NaOH or 3 M HCl)	8-hydroxy-quinoline	0.1%	20 ml	
Proteinase K solution	Proteinase K	0.1%	0.1 g	0.1 l
pH 10	EDTA	100 mM	3.72 g	
	Tris-Cl	10 mM	0.121 g	
	NaCl	2.5 M	14.61 g	

2.5.2 The Ames assay

The Ames assay, a short term bacterial reverse mutation assay, was specifically designed by Ames and colleagues to detect a wide range of chemical substances that can produce genetic damage resulting in gene mutations (Ames *et al.,* 1975). The assay is now a widely recognised *in vitro* method to screen for chemical carcinogens on the basis that most mutagens prove to be carcinogenic in subsequent animal tests (Zeiger, 1987). The assay uses *S. typhimurium* bacterial strains with pre-existing single base mutations positioned at strategic points within the histidine gene operon rendering the bacteria incapable of producing the amino acid histidine. Hence, such pre-existing mutations result in organisms

that can only grow on histidine-supplemented growth medium. However, when a mutagenic event occurs, certain base substitutions (reverse mutations) within the histidine gene operon can cause the bacteria to revert back to wild type. Within the assay, a chemical's mutagenic potential is assessed by exposing these organisms to varying concentrations of the chemical and selecting for reversion events i.e. counting the presence of bacteria growing in the absence of histidine. In a variation of the assay, the *S. typhimurium* strains are exposed to the test chemicals in the presence of S9 mix, an animal liver homogenate containing active liver microsomes, capable of converting promutagens into active mutagens by simulating metabolic activation.

2.5.2.1 Preparation of Ames II^{TM} assay strains, solutions and reagents

The assay system employed in the present study was the Ames II^{TM} Mutagenicity Assay (Xenometrix AG, Switzerland), utilising the *S. typhimurium* tester strains TA98 and TAMix (a mixture of strains TA7001, TA7002, TA7003, TA7004, TA7005, and TA7006) (Gee *et al*., 1994; Flueckiger-Isler *et al*., 2004). The genotypic characteristic of the employed bacterial strains is illustrated in Table 2.5.

The bacterial culture TA98 and TAMix (treated as an individual strain) were resuscitated in Ames growth medium containing 50 µg/ml ampicillin for 12 h using a shaking incubator (Lab Companion, SI-600, Wolf laboratories Ltd, UK) at 37^{o}C and 250 rpm. Subsequently, appropriate cell density was confirmed via optical density measurements at 600 nm according to manufacturers' instructions. Before conducting the Ames assay the cytotoxic potential of the test samples towards the bacterial strains was evaluated according to manufacturers' instructions by exposing a defined bacterial cell density of the TA98 strain for 90 min at 37^{o}C to the test solutions. The visual turbidity of the bacterial test solutions was then used as an indicator of cytotoxicity.

Table 2.5: Characterisation of *S. typhimurium* strains (Ames II^{TM} Mutagenicity Assay).

Strain	Mutation	Type	Target	Cell wall[1]	Repair[2]	pKM101[3]
TA98	*hisD3052*	Frameshift	GC	*Rfa*	*uvrB*	Yes
TA7001	*hisG1775*	Missense	A:T>G:C	*Rfa*	*uvrB*	Yes
TA7002	*hisC9138*	Missense	T:A>A:T	*Rfa*	*uvrB*	Yes
TA7003	*hisG9074*	Missense	T:A>G:C	*Rfa*	*uvrB*	Yes
TA7004	*hisG9133*	Missense	G:C>A:T	*Rfa*	*uvrB*	Yes
TA7005	*hisG9130*	Missense	C:G>A:T	*Rfa*	*uvrB*	Yes
TA7006	*hisC9070*	Missense	C:G>G:C	*Rfa*	*uvrB*	Yes

[1] These mutations affect the lipopolysaccharides component of the cell envelope. Strains have increased permeability for bulky molecules.
[2] Strains carrying the uvrB mutation are deficient in excision repair of bulky lesions as measured by their lack of survival following irradiation with UV light at 254 nm.
[3] This R factor plasmid carries the mucA and mucB genes to compensate for the weak mutagenic activities of the *umu* operon in *S. typhimurium*.

For treatments without S9 mix, a positive control chemical stock solution containing 12.5 μg/ml 4-nitroquinoline-*N*-oxide (4-NQO) and 50 μg/ml 2-nitrofluorene (2-NF) in DMSO was prepared to ensure assay conditions were optimal. Such concentrations resulted in a final assay concentration of 500 ηg/ml for 4-NQO and 2000 ηg/ml for 2-NF. For treatment with S9 mix, a positive chemical control stock solution of 125 μg/ml 2-aminoanthracene (2-AmAn) in DMSO was prepared resulting in a final assay concentration of 5 μg/ml.

A stock solution of 30% S9 mix from Aroclor 1254 induced Rat Liver (Moltox, US) was prepared immediately prior to use and stored on ice with the final S9 concentration in the assay being 4.5%. Composition of the S9 liver homogenate stock solution is outlined in Table 2.6.

Table 2.6: Composition of 30% S9 liver homogenate solution.

Concentration (M)	Reagent	Volume (ml)
1.00	KCL [1]	0.083
0.25	$MgCl_2 \bullet 6H_2O$ [1]	0.080
0.20	Glucose-6-phosphate [2]	0.063
0.04	NADP [2]	0.250
0.20	NaH_2PO_4 buffer [1]	1.250
	Sterile water [1]	0.025
	S9 fraction	0.755

[1] autoclaved, [2] filter sterilised

2.5.2.2 The Ames II^{TM} assay procedure

All assays were preformed in triplicate according to the manufacturer's instructions with slight modifications.

Physical hydrogels

Three concentrations of the physical hydrogels (0.025, 0.25, 2.5 mg/ml solubilised in PBS), plus a negative control and a positive control (Section 2.5.2.1) were tested. The hydrogel concentrations were prepared 25 times more concentrated to achieve the desired assay concentration during bacterial strain exposure. Bacteria exposure was performed in triplicate by transferring 10 µl of each test concentration into 3 single wells of a 24 well plate. Subsequently, 215 µl of Ames exposure medium and 25 µl of previously resuscitated bacterial strains were added to each well. For tests performed in the presence of S9 mix, 177.5 µl of Ames exposure Medium, 25 µl of bacterial strains and 37.5 µl of 30% S9 mix were added to the wells. The mixture was then incubated for 90 min at 37^{o}C with agitation at 250 rpm.

Chemical hydrogels

Extracts from previously washed hydrogels were prepared as outlined in Section 2.4.1 using 30 ml of Ames exposure medium instead of culture medium as extract liquid.

Exposure of bacterial strains was performed in triplicate by transferring 225 µl of treated Ames exposure medium and 25 µl of bacterial strains to each of the single wells of a 24 well plate. For tests performed in the presence of S9 mix, 187.5 µl of Ames exposure medium, 25 µl of bacterial strains and 37.5 µl of 30% S9 mix were added to the wells. The plates were then incubated for 90 min at 37^{o}C with agitation at 250 rpm. Exposure to negative control (untreated Ames exposure medium) and positive controls were also performed as described for the physical hydrogels.

Following 90 min incubation, 2.8 ml of indicator medium, which selects for prototrophic reversion, was added to each well of the 24 well plates prior to transferring 50 µl aliquots to 48 wells of a 384 well plate. The plates were then incubated at 37^{o}C for 48 h. Bromocresol purple, an essential constituent of the indicator medium, turns yellow as the pH drops (pK = 5.2) due to catabolic activity of revertant cells which grow in the absence of histidine. The number of positive (yellow) wells were scored and compared with the number of spontaneous revertants obtained for the negative control. The average number of revertants per culture and concentration was calculated, and the increase above the zero-dose was determined at each concentration of the test chemicals.

2.6 Optimisation of a novel pulsed plasma gas-discharge (PPGD)-prototype technology for microbial inactivation of hydrogel surfaces

The HV pulsed power generator used to create the biocidal PPGD is a prototype which was designed and developed by Samtech Ltd (Glasgow, UK). The system was built solely for the laboratory environment to drive experimental loads such as plasma reactors for microbial treatments. The unit is comprised of a number of discrete components housed within a 19 inch racking cabinet. The racking acts as a Farady cage which prevents electromagnetic interference with other equipment in the laboratory and protects the operator of the system from the high electromagnetic fields. The input voltage is delivered by the main AC power supply specified at 230 V, 13 A and 50 Hz. The output voltage ranges from 0–30 kV depending on pulse outputs used. It is possible to trigger the output pulses in manual delivered single pulse, or via an automated mode ranging from 1–15 pulses per second (pps). The main components are the HV power supply, a set of charging resistors, a trigger generator linked to a corona stabilised switch (CCS) and the pulse

generator. The pulse generator has three pulse outputs: two pulse outputs having impedances of 100 Ω, and a DC output with an impedance of 8.25 Ω. The heart of the pulse generator is composed of a set of pulse forming network (PFN) transmission lines (URM67 coaxial cable). This is of a Blumlein configuration where the matched load impedance is twice the transmission line's characteristic impedance. The Blumlein generator works on the basis that the pulse forming lines are charged simultaneously and then discharged via the CCS to obtain a sharp high energetic pulse.

The system is operated by setting the desired level of output voltage via the dial on the HV power supply unit. The pulse rate can be preset (single or automated pulse mode) and is monitored at the LCD display on the front panel of the trigger generator unit. Figure 2.1 shows the pulse generator while Figure 2.2 represents a simplified scheme of the internal layout.

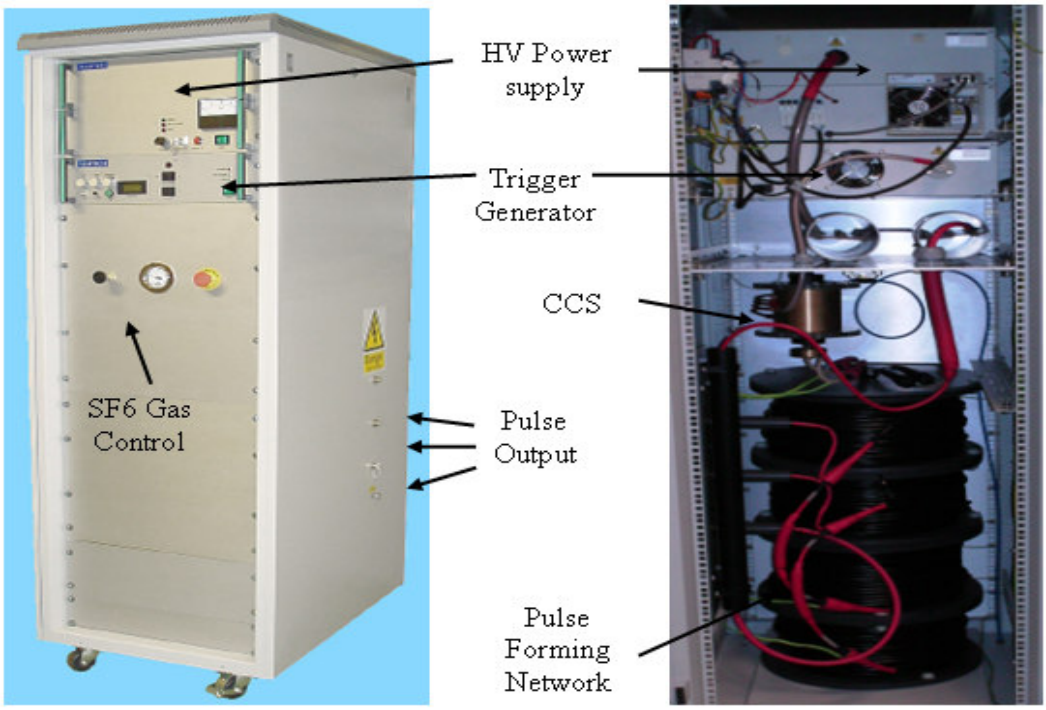

Figure 2.1: Pulse generator front view and internal elements.

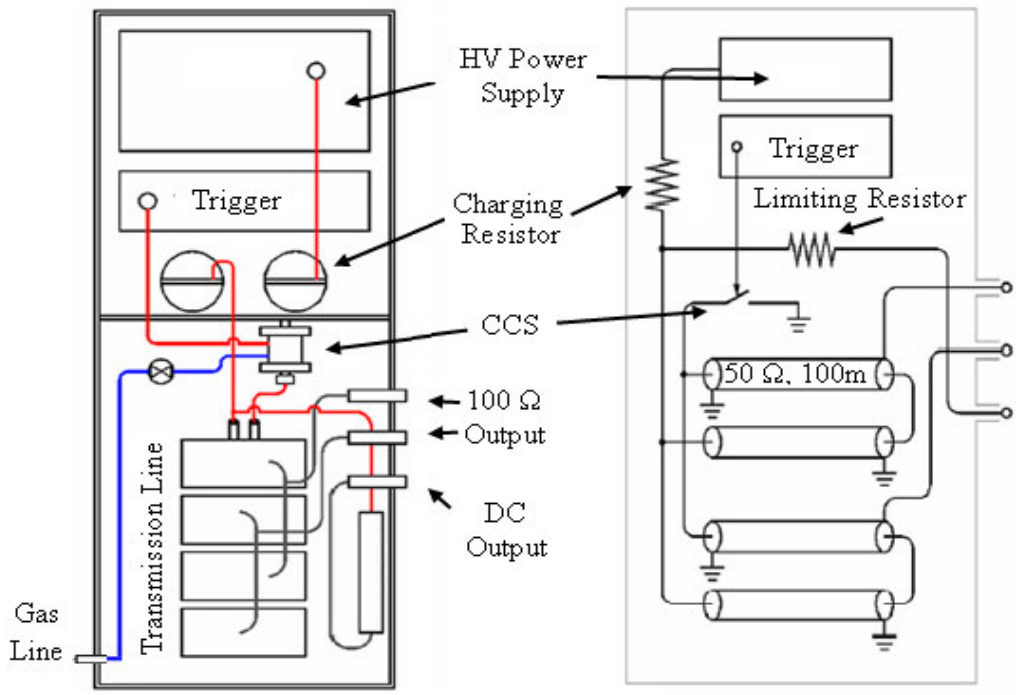

Figure 2.2: General internal layout and simplified schematic of pulse generator.

2.6.1 Operation of the PPGD treatment chamber

The treatment chamber was designed and fabricated (Samtech, Glasgow) to house a defined volume of aqueous treatment solution. The system comprises two electrodes separated by a PVC spacer cylinder of 98 mm internal diameter and 100 mm height. The upper lid was also made from PVC while the upper electrode was entirely composed of stainless steel BS316S11, consisting of six stainless steel needles of 10 mm length mounted onto the upper electrode in a circular arrangement to create the gas-discharge above the test liquid. Conversely, the lower earth electrode was composed of aluminium alloy 6082. The chamber was adjusted to accommodate a volume of 100 ml of test solution sufficient to submerge the hydrogels in the chamber. The gap length, defined as the vertical distance between the tips of the needle electrodes and the surface of the test liquid, was adjusted to 5 mm. A transparent perspex spacer cylinder was employed to visualise the discharge for control and demonstration purposes. The HV electrode was connected to the two 100 Ω outputs of the pulse generator. A separate earth connection was also connected from the lower earth electrode to the earth connection of the pulse generator. This earth point was

further connected to the main laboratory earth point. Figure 2.3 shows the variations of PPGD treatment chamber used in this study and the HV electrode.

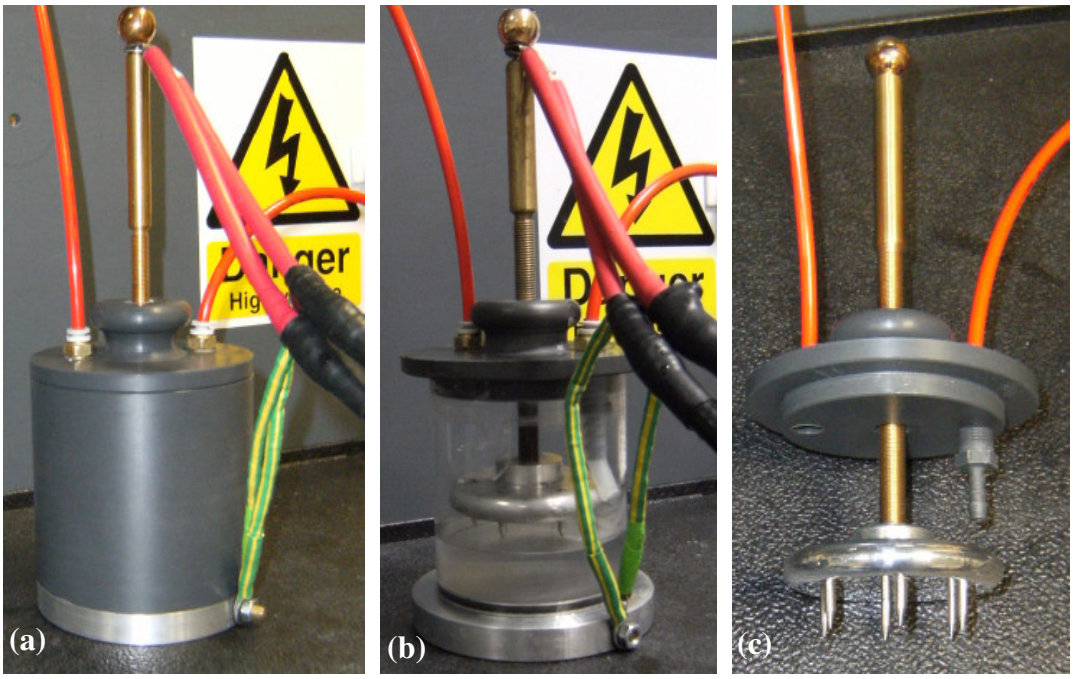

Figure 2.3: (a) PPGD treatment chamber with pulse cable connected to HV and earth points; (b) treatment chamber with perspex spacer cylinder which allows for direct pulse observation; (c) the HV electrode displaying the multi-needle arrangements.

2.6.2 Adjustment and maintenance of the internal corona stabilised switch

The internal CSS was used to activate the pulse-forming network. This switch design is particularly suitable for applications that require moderate energy per pulse (several tens of joules) and moderate pulse repetition rate. The CCS is activated by a HV trigger generator which enables the operation in single shot mode or at selective pulse frequencies between 1-15 pps. To minimise arcing within the switch and resulting pulse misfiring of the system, the CCS is needed to be insulated with sulphur hexafluoride (SF_6) gas. Before the switch was pressurised via an external compressed SF_6 gas cylinder (BOC Gases, Ireland), residual gas was evacuated with a vacuum pump (V-700, Buchi, Switzerland). As the gas pressure within the switch depends strongly on the desired charging voltage of the system, great care must be taken to fill the switch to its correct gas pressure. The relationship between the SF_6 gas pressure and the power supply charging voltage is illustrated in Figure 2.4. The SF_6 gas was changed periodically to maintain a proper switching performance.

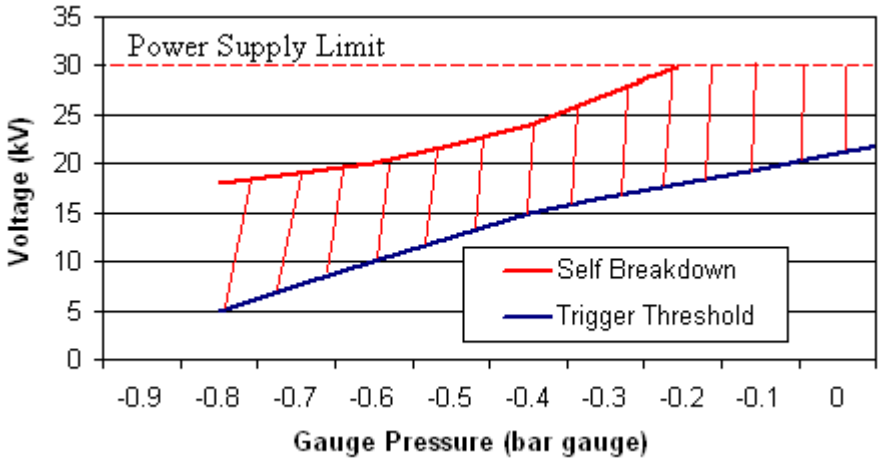

Figure 2.4: Power supply charging voltage with corresponding SF_6 gas pressure.

Prolonged usage of the PPGD system (especially at high pulse rates) caused internal arcing which lead to the breakdown of SF_6 gas within the switch. A consequence of the gas breakdown was the settlement of debris and arc root burn marks on the switch electrodes (Figure 2.5). This had a detrimental impact on the triggering performance and required the switching element to be removed from the system and cleaned. Before removing the switch, it was flushed several times with air to remove residual SF_6 breakdown gases and the body of the switch and the HV terminal were completely discharged via an earthling stick (Samtech, Glasgow). After removal, the switch was opened and the internal electrodes were cleaned of debris and burn marks by using abrasive paper with increasing grit sizes (P220–P600). As some of the SF_6 breakdown products are highly reactive, corrosive and toxic (Tsai, 2007), the use of appropriate safety equipment (rubber gloves, coveralls and a suitable dusk mask) was necessary throughout the cleaning process. However, repeated maintenance did not fully prevent the switch from being subjected to irreversible damage. During the time course of this study, the electrode insulators failed and the electrical tracking caused a short-circuit within the pulse generator (Figure 2.6). Thus, the system was nonoperational as no voltage potential could be established due to the charge being able to flow directly to the earth connections. Ultimately, a new CCS was manufactured by Samtech (Glasgow).

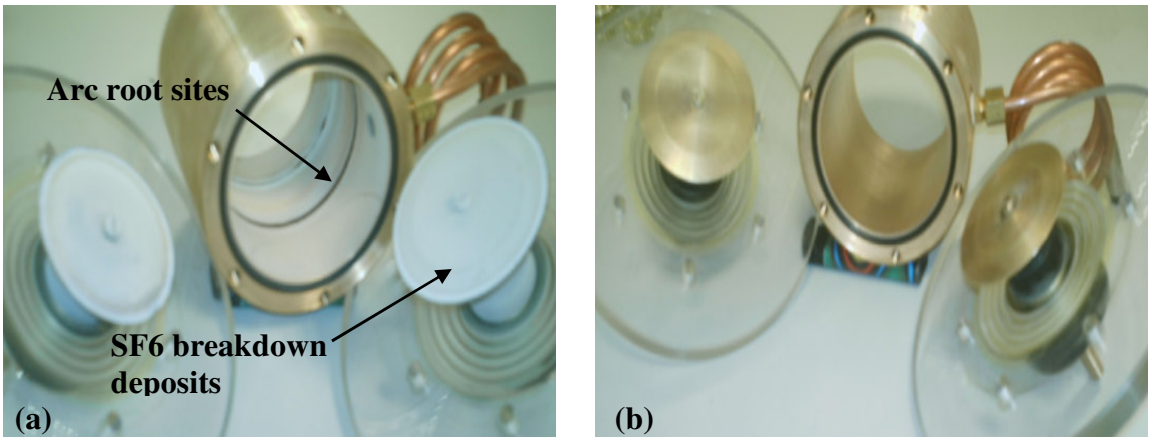

Figure 2.5: Breakdown deposits and arc root sites on the CCS switching elements after prolonged usage (a). The switching elements after thorough cleaning (b).

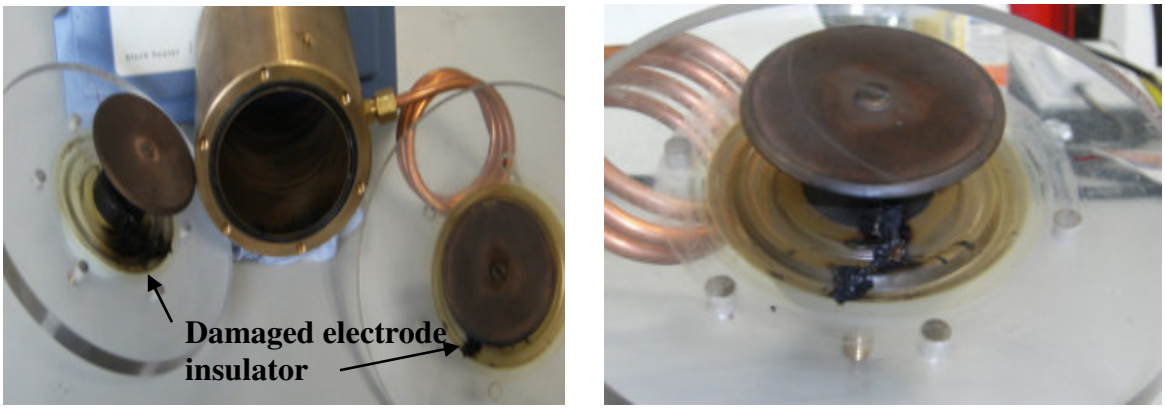

Figure 2.6: Irreversibly damaged CCS: The electrode insulators have failed causing the formation of a short-circuit.

2.6.3 Discharge gas selection and pulse characterisation

Two gases were investigated to compare their HV gas-discharge profile. Pure oxygen (O_2) or nitrogen (N_2) (BOC Gases, Ireland) were fed into, and vented from the plasma chamber near ambient pressure through a linear low density poly(ethylene) (LLDPE) tubing of 6 mm internal diameter (Hudson Extrusions Inc., US). The tubing was attached to the PVC chamber lid via brass quick fittings (SMC Pneumatics Ltd, Ireland). The flow rate was controlled via a Rate-Master® flow-meter (Dwyer Instruments Inc., UK) adjustable to a gas flow of 0.5–5 l/min. Subsequently, the output pulse formed at the treatment chamber was monitored via a digital oscilloscope attached to a resistive probe at the HV connection of the treatment chamber. The oscilloscope used for the acquisition, view and storage of the

voltage data was a Tektronix TDS 3022 oscilloscope (input resistance of 1 MΩ; bandwidth of 300 MHz and peak sample rate of 1.25 GS/s) while the high voltage probe used was a Tektronix P6015A, 1000:1, resistor-capacitor compensated voltage divider (100 MΩ, 3.0 pF input characteristics with a maximum input voltage of 20 kV DC, 40 kV pulsed and a frequency response of up to 75 MHz).

2.6.4 Corrosion and maintenance of electrodes

During treatment, both electrodes were subjected to wear and corrosion, visualised via a Wild M3Z stereo-zoom microscope (Leica, Germany) using an optical ring illuminator system at ten times magnification. On the HV electrode the creation of plasma arcs resulted in the slow but steady shortening of the individual needles via etching mechanisms necessitating periodic needle replacement to maintain a consistent working system. In addition, the lower earthed electrode was prone to a build up of what appeared to be salt deposits and oxide layers. Hence, the earthed electrode was periodically maintained by polishing the surface using fine abrasive paper with increasing grit sizes (P800–P1200) followed by rinsing the surface with dH_2O.

2.6.5 Treatment fluid characteristics

The treatment chamber was attuned to house a treatment volume of 100 ml with the top of the needle electrodes arranged exactly 5 mm above the test liquid. Subsequently, the chamber was thoroughly rinsed with ice cold dH_2O to ensure that there was time for the chamber to cool down. The chamber was filled with 95 ml of ice cold dH_2O and 5 ml of ice cold PBS treatment fluid. The PBS was added to increase the conductivity thereby supporting discharge stability (Sato *et al.,* 1999; Satoh *et al.,* 2007; Zhang *et al.,* 2009). Furthermore, the resultant increase in osmolarity provided a suitable medium for suspending test microorganisms. The treatment liquid was composed of 5×10^{-4} M phosphate buffer, 1.35×10^{-4} M potassium chloride and 6.85×10^{-3} M sodium chloride. After connecting the treatment chamber to the treatment gas (N_2, O_2), the required gas flow rate was adjusted via the Rate-Master® flow-meter. The pulse generator was started with the SF_6 pressure within the CCS matched to the desired charging voltage, while the pulse repetition rate was set on the trigger unit panel. The treatment experiment was started immediately after the capacitors were fully charged.

2.6.5.1 Temperature, pH and conductivity changes

Before and during the PPGD treatment the critical physicochemical parameters of the treatment fluid were periodically monitored to ascertain the potential mechanisms that would underlie microbial inactivation. Temperature and pH were monitored by using an Eutech® CyberScan pH 510 pH/mV meter with automated temperature control adjustment (Thermo Fischer Scientific, UK). The conductivity of the fluid was measured via an electrical conductivity meter using the temperature compensations mode for natural water (R 720 Cond, Reagecon, Ireland).

2.6.5.2 Dissolved ozone concentration

The dissolved ozone (O_3) concentration of gas-discharge-treated water was analysed via the dipropyl-p-phenylenediamine (DPD) colorimetric method (Spectroquant® 1.00607, Merck Chemicals, VWR, Ireland), which detects the presence of dissolved O_3 in water within the concentration range 0.01-4.00 mg/l. According to the manufacturer's instruction, the Spectroquant® reagents were dissolved in a 10 ml water sample, incubated for 3 min and analysed at a test wavelength of 528 nm (Jenway 6300 spectrophotometer, Lennox Laboratory Supplies Ltd, Ireland). This test method requires that the pH of the testing solution is between pH 4 and 8, therefore, where necessary, pH adjustments were made using 2 M HCl or sodium hydroxide (NaOH). For comparative purposes a 2.00 mg/l O_3 standard solution was prepared according to DIN EN ISO 7393, whereby 1.005 g potassium iodate (KIO_3) was dissolved in 1000 ml of dH_2O. Subsequently, 1 g potassium iodite (KI) was added to 14.8 ml of the KIO_3 stock before diluting to a final volume of 1000 ml with dH_2O. Next, 2 ml of 0.5 M sulfuric acid (H_2SO_4) was added to 20 ml of the working stock and the pH adjusted using 2 M (NaOH) until the solution lost its colour. Finally, dH_2O was added to obtain a volume of 1000 ml and an O_3 standard curve was obtained via the DPD colorimetric method.

2.6.5.3 Detection of nitrogen fixation byproducts via ion exchange chromatography

When N_2 was employed as the discharge gas, the pH of the treatment solution was drastically reduced following PPGD treatment. Therefore, byproducts of nitrogen fixation, which were believed to be responsible for the pH reduction, were detected and quantified. More specifically, ion exchange chromatography (IEC) was used to determine the presence

of nitric acid (HNO_3) and nitrous acid (HNO_2) in the gas-discharge-treated water at different treatment times and discharge settings. The chromatographic system was composed of a 761 Compact IC (Metrohm, Ireland) including a conductometric detector and suppressor with peristaltic pump. The system and data was managed by the 761 Compact IC Control and Data Acquisition System Version 1.1 (Metrohm, Ireland). The utilised mobile phase consisted of 1 mM sodium bicarbonate ($NaHCO_3$) and 3.5 mM sodium carbonate (Na_2CO_3) in aqueous solution, with ion separation performed in isocratic mode at a 1.2 ml/min flow rate and ambient temperature on a Transgenomic® IC Sep AN2 analytical column (250 x 4.60 mm). The conductivity detector was operated in anion regenerating suppressor mode using 20 mM H_2SO_4 as regenerating solution and dH_2O for ion removal. The calibration standards contained nitrate ($N0_3^-$) and nitrite (NO_2^-) in addition to chloride and phosphate at a broad concentration range, to allow for linearity confirmation. All injections were performed in duplicate, with an injection volume of 20 µl and a total run time of 15 min.

2.6.5.4 Presence of electrode degradation products

The presence of elemental metal contaminate released from the electrodes into the treatment fluid during HV treatment was also determined. The electrodes were made of two materials. The upper HV electrode and the needle arrangements were made of stainless steel BS316S11 (predominately iron (Fe) with 16.5–18.5% chromium (Cr), 11–14% nickel, 2–5% molybdenum, a maximum of 2% manganese (Mn), 1% silicon, 0.045% phosphorous, 0.03% sulphur, and 0.03% carbon) while the lower earth electrode comprised aluminium alloy 6082 (predominately aluminium (Al) with 0.7–1.3% silicon, 0.4–1% Mn, 0.6–1.2% magnesium, a maximum of 0.5% Fe, 0.25% Cr, 0.2% zinc, 0.1% copper, and 0.1% titanium).

Prior to analysis, the electrodes were maintained and thoroughly rinsed with dH_2O. The test chamber was filled with 100 ml of ice cold dilute PBS solution (5 x 10^{-4} M phosphate buffer, 1.35 x 10^{-4} M potassium chloride and 6.85 x 10^{-3} M sodium chloride) followed by HV treatment at 16 kV, 10 pps for 30 and 90 min with over streaming O_2 or N_2 gas at 2.5 l/min. A control test was conducted without discharge treatment for water resident in the chamber for the same duration as the longest test run. For all samples, the

temperature, pH and conductivity were determined. The samples were analysed for their content of four indicator elements, namely aluminium, chromium, iron and manganese by City Analyst Ltd, Ireland.

2.7 Evaluation of the biocidal efficacy of the PPGD system

2.7.1 Microbial test strains

Two different bacterial test strains were used to determine the biocidal potential of the PPGD method. Gram negative *Escherichia coli* (*E. coli*) ATCC 25922 and the Gram-positive *Staphylococcus aureus* (*S. aureus*) ATCC 25923 were obtained from the American Type Culture Collection (ATCC), with fresh slope cultures of each test strain used each week to maintain key characteristics and stored at 5^{o}C until required. Single colony isolation of pure cultures was performed using the streak-plate method in conjunction with relevant selective and nonselective media. Broth cultures required incubation at 37^{o}C in an orbital shaking incubator (Lab Companion, SI-600) at 125rpm to improve aeration and ensure homogenous distribution. For long term storage all strains were stored in microbanks® (Pro-Lab Diagnostics, UK) at -80^{o}C by inoculating separate microbank® vials, comprising 10 porous beads with a nutrient broth suspension (10^7 colony-forming units (cfu)/ml), with subsequent removal of the suspension fluid surrounding the beads. All agar and broth media used in this study were sterilised by conventional autoclaving. The bacterial strains with their respective growth requirements are illustrated in Table 2.7.

The identity of all test organisms was confirmed before and after PPGD treatments by performing specific morphological, biochemical and physiological tests on randomly selected colonies from nonselective agar plates, as previously described by Cowan and Steel (2003). Morphological and physiological testing included standard Gram staining, motility and IMViC testing, catalase, oxidase, lactose and glucose testing. More specific biochemical tests involved culturing *E. coli* on MacConkey agar and performing API 20E tests (BioMerieux, Germany), while *S. aureus* was confirmed by performing coagulase testing, DNAase activity and growth on Baird Parker agar and by performing API 20 STAPH tests (BioMerieux, Germany).

Table 2.7: Growth requirements of bacterial tester strains

Bacterium	Clinical Significance[1]	Growth Media		Incubation conditions[2]
		Nonselective	Selective	
Escherichia coli ATCC 25922	Clinical isolate	Nutrient broth/agar (Oxoid, UK)	MacConkey agar (Oxoid, UK)	37°C aerobic
Staphylococcus aureus ATCC 25923	Clinical isolate	Nutrient broth/agar (Oxoid, UK)	Baird Parker agar (Oxoid, UK)	37°C aerobic

[1] Clinical significance designates clinical sample and/or symptoms from which respective test strains were isolated or associated within humans.
[2] Incubation of broth cultures required agitation in an orbital shaker at 125 rpm to ensure homogenous distribution of sample and to improve aeration.

2.7.2 Preparation of microbe-containing test liquid for PPGD treatment

The microorganisms were prepared for PPGD inactivation by culturing in 50 ml of nutrient broth at 37°C and 125 rpm agitation, until they reached an approximate density of 3 x 10^9 cfu/ml (12-17 h depending on cell type). Bacterial cells were then harvested by transferring 10 ml of the bacterial cell suspension into sterile universals and centrifuging at 4000 rpm for 10 min at 10°C, prior to resuspending cell pellets in 7-15 ml of cold sterile PBS. Furthermore, to standardise the bacterial cell density (1.5-2.5 x 10^9 cfu/ ml), OD_{600nm} measurements of such bacterial suspensions were recorded. Next, the PPGD test liquid was prepared by transferring 1 ml of the bacterial suspension into 95 ml of ice cold dH_2O combined with 4 ml of ice cold PBS. The PBS was added to increase the conductivity of the test liquid as this provided stability for the pulse discharge and reduced osmotic stress towards the organisms. The final composition of the test liquid was as follows: 1.5–2.5 x 10^7 cfu/ml of test organisms, 5 x 10^{-4} M phosphate buffer, 1.35 x 10^{-4} M potassium chloride and 6.85 x 10^{-3} M sodium chloride.

2.7.3 Enumeration of microbial survivors and determination of the inactivation rate

The spread plate technique was employed to facilitate bacterial cell enumeration before and during the PPGD treatment process and involved spreading 100 µl aliquots and respective dilutions of microbial test liquid on nutrient agar plates followed by incubation at 37°C for

a minimum of 24 h. As necessary, 1 ml of sample was pour plated to confirm complete microbial inactivation. Untreated and surviving populations were then determined by enumeration of colonies per ml of sample (cfu/ml) as outlined in Equation 2.4 where *N* is the mean value for the obtained colony count, *df* is the dilution factor and the factor *10* was used to revert the amount of counted colonies to a sample volume of 1 ml.

$$cfu/ml = N \times 10 \times df$$

Equation 2.4: Number of colonies per ml sample.

Samples were examined in duplicate from triplicate trials and results were transformed to $\log_{10}$ cfu/ml values with mean and standard deviation (SD) reported for each test. In order to demonstrate the overall susceptibility of the two test strains to various discharge conditions, the observed microbial inactivation results were transformed using a pseudo first-order disinfection model developed by Chick (1908) and Watson (1908) where N_0 represents the initial number of microorganisms prior to treatment, N_t is the number of microorganisms at time t and k is an empirical inactivation rate constant descriptive for the microorganism at certain inactivation conditions.

$$\log_{10}[N_t / N_0] = - k \times t$$

Equation 2.5: The Chick-Watson model of microbial inactivation.

The inactivation rate constant k is the average $\log_{10}$ reduction in microbial cell viability as a function of PPGD treatment time. Therefore, the rate constant k defines the sensitivity of a microorganism to the PPGD treatment and is unique to each microbial species and the utilised treatment condition.

2.7.4 PPGD treatment procedure

The treatment chamber was attuned to house a treatment volume of 100 ml with the top of the needle electrodes arranged exactly 5 mm above the test liquid. Subsequently, the chamber was cleaned with a 70-30% ethanol-water (v/v) solution followed by thorough rinsing with ice cold sterile dH_2O, ensuring that there was time for the chamber to cool down. The prepared test liquid containing microbial species was aseptically transferred into

the treatment chamber. The chamber was connected to the respective discharge gas (N_2, O_2) and the required gas flow rate was adjusted via the Rate-Master® flowmeter. The pulse generator was started and the SF_6 pressure within the CCS was matched to the desired charging voltage, while the pulse repetition rate was set on the trigger unit panel. The treatment experiment was started after the capacitors were fully charged. Periodically, a 100 µl sample was aseptically withdrawn to determine the number of surviving bacteria cells.

2.7.4.1 Effect of varying the applied voltage on decontamination efficacy

The first electrical parameter examined was the effect of varying the applied voltage on the inactivation of microorganisms suspended in the test liquid. These studies were primarily conducted over a wide range of PFN charging voltages (10-25 kV). However, due to thermal effects and problems associated with the durability of the CCS, the treatment range was narrowed to a range below a charging voltage of 18 kV. Other adjustable electrical parameters were kept constant. The suitability of both N_2 and O_2 gases was also examined. A cell concentration of 1 x 10^7 cfu/ml of *E. coli* or *S. aureus* was prepared separately as previously outlined in Section 2.7.2. The cultures were subjected to a PFN charging voltage of 14, 16 and 18 kV at 10 pps at a constant gas flow rate of 2.5 l/min. These parameters were subsequently employed in the hydrogel decontamination studies, hence, using settings which were deemed optimal for microbial inactivation without imposing detrimental thermal effects.

2.7.4.2 Effect of varying pulse frequency

The effect of varying the pulse frequency on microbial inactivation of the test liquid was also investigated. After a preliminary range finding experiment, the microorganisms were subjected to a pulse frequency of 7.5, 10 and 12.5 pps while the treatment voltage was kept constant at 16 kV. The suitability of both N_2 and O_2 gases was examined at a constant flow rate of 2.5 l/min

2.7.4.3 Effect of various treatment gases and flow rates

The effect of the different nature of gases supplied for the HV discharge on the microbial inactivation was examined by using N_2 and O_2 gas. The impact of varying the flow rate on

inactivation profiles was also assessed by adjusting the gas flow rate to 1, 2.5 and 5 l/min while the PFN charging voltage and pulse frequency were kept constant at 16 kV and 10 pps respectively.

2.8 Evaluation of the toxic potential of the PPGD system

Since the PPGD treatment is a novel procedure of microbial decontamination of biomedical hydrogels, verification of the toxicological safety of the method is a necessary requirement. The potential generation of toxic byproducts within the treatment liquid during the gas-discharge process required investigation, as residues of the liquid can potentially diffuse into the hydrogels' matrix during treatment and affect the gels' biological performance. Therefore, PPGD-treated liquid was subjected to a range of biocompatibility assessment methods, including assays for cyto- and genotoxicity.

2.8.1 Preparation of a representative liquid test sample

Preparation of the test liquid for toxicological analysis following PPGD treatment was performed as previously described in Section 2.7.2, but without the addition of microorganisms to the test system. The sample liquid was treated for 30 min at a charging voltage of 16 kV and a pulse repetition rate of 10 pps. For comparative purposes, N_2 and O_2 gases were also utilised as discharge gases at a flow rate of 2.5 l/min. Finally, a 10 ml sample of the HV gas-discharge-treated test liquid was taken aseptically at the end of each treatment and transferred into a sterile universal, before being subjected to toxicity testing. The liquid was also tested after an incubation period of 7 days at 37^{o}C to determine if a possible reduction of toxic free radicals may have occurred. An untreated liquid sample was used as a control reference.

2.8.2 Cytotoxicity of PPGD-treated test liquid

The cytotoxic potential of the HV treated test liquid was determined on HaCaT cells via MTT and NR endpoints as previously outlined in Section 2.4.2 and 2.4.3. The PPGD-treated test liquid was serially diluted with complete cell culture medium to a suitable concentration range and the cells were exposed to the test liquid for 24 h at 37^{o}C. After treating the cells with the relevant viability dye (MTT or NR) the OD of each well was recorded using a multiwell plate reader (Anthos HTIII) at a test wavelength of 540 nm and

a reference wavelength of 690 nm. Results are presented as percentage of untreated controls against test chemical concentrations.

2.8.3 Genotoxicity of PPGD-treated test liquid

2.8.3.1 DNA strand breakage

The DNA damaging/clastogenic potential of the HV treated test liquid was also determined on HaCaT cells via the comet assay. The assay was performed as previously described in Section 2.5.1.1. However, the PPGD-treated test liquid was diluted in complete cell culture medium to a suitable concentration range prior to cellular exposure for 12 h at 37^{o}C, with H_2O_2 (100 µM in PBS) used as a positive control by addition to duplicate wells prior to incubation for 40 min at 4^{o}C. Again, following treatment, cells were harvested and cell viability (≥80% for all test concentrations) was determined by trypan blue exclusion to avoid false positive responses due to cytotoxicity.

2.8.3.2 Single nucleotide alterations or point mutations

The Ames II^{TM} Mutagenicity assay was also used, as previously outlined in Section 2.5.2.2 with minor modifications to detect the mutagenic potential of the PPGD-treated test liquid. The bacterial culture TA98 and TAMix were exposed to the PPGD-treated test liquid in the presence and absence of S9 mix. Exposure to negative control (untreated Ames exposure Medium) and positive control chemicals were performed in accordance with the procedure used to determine the mutagenic potential of the hydrogels (Section 2.5.2.1). For the exposure of PPGD-treated test liquid, a 10 fold concentrated exposure medium (Xenometrix, Switzerland) was diluted with appropriate volumes of treated liquid, dH_2O and 25 µl of previously resuscitated bacterial suspension to obtain the desired concentration ranges at a final volume of 250 µl per test well (for tests performed with the addition of S9 mix the volume of dH_2O was reduced to allow for a final S9 assay concentration of 4.5%). The mixture was then incubated for 90 min at 37^{o}C with agitation at 250 rpm and the consecutive steps were performed in accordance with Section 2.5.2.2. The average number of revertants per culture and concentration was then calculated, and the increase above the zero-dose was determined for each concentration of the test chemicals.

2.9 PPGD-mediated inactivation of microorganisms on selected hydrogel surfaces

Ultimately, the suitability of the PPGD method for the inactivation of microbial contamination on the surface of the hydrogels was examined. Optimised discharge conditions, determined from preliminary microbial inactivation testing, were used to treat hydrogels which were previously inoculated with two test bacteria, *E. coli* and *S. aureus*. The PPGD treatment was conducted with the hydrogels fully submerged in the treatment liquid which protected the hydrogel surface from the direct and deleterious thermal effects of the HV discharge. Microbial inactivation was achieved via indirect biocidal effects transmitted through the liquid medium to the hydrogel surface. The representative sample chosen for this investigation was the purified crosslinked 75-25xP hydrogel.

2.9.1 Microbial inoculation of hydrogel surface

Samples of dry 75-25xP type hydrogel samples each with a mass of 250 ±10 mg were disinfected as outlined in Section 2.4.1. To enhance the biocompatibility, the samples were also purified by incubating for 15 days in a sealed container with 30 ml of sterile PBS at 37^{o}C and 125 rpm agitation, with the PBS replaced daily. At the end of the purification, the preswollen gels were aseptically divided with a sterile scalpel into two equally sized pieces weighing 3.25 ±0.25 g. This corresponded to a calculated free surface area of 12.5 ±1 cm^2 per portion. For microbial inoculation of the hydrogels, *E. coli* and *S. aureus* were prepared as described in Section 2.7.2 until they reached an approximate density of 1 x 10^9 cfu/ml. Subsequently, the solution containing the microorganisms was divided into 20 ml volumes and placed in sterile universals, with the surface of the hydrogels inoculated by submerging each sample into the microbial solution for 90 min at 37^{o}C and 75 rpm agitation. After the incubation period, the gels were transferred from the universals and gently rinsed twice with PBS to remove unbound bacteria.

2.9.2 PPGD treatment of hydrogel

The treatment chamber was prepared as previously outlined in Section 2.7.3 and the chamber filled with 92 ml of cold dH_2O and 4.75 ml of cold PBS with the inoculated hydrogel sample carefully submerged in the center. The chamber was connected to the respective discharge gas (N_2, O_2) and the optimised gas flow rate was adjusted to 2.5 l/min via the Rate-Master® flowmeter. The pulse generator was started and the SF_6 pressure

within the CCS was matched to the desired charging voltage. The pulse repetition rate was set to 10 pps on the trigger unit panel. The experiment was started after the capacitors were fully charged to 16 kV. The sample was aseptically removed at predetermined time intervals for enumeration of bacterial cell survivors.

2.9.3 Recovery and enumeration of viable test organisms

At the end of each PPGD treatment, the hydrogel sample was carefully removed from the treatment chamber and transferred to a sterile stomacher bag preloaded with 3.25 ±0.25 ml of PBS, and bacteria dislodged by completely homogenising the hydrogel (Seward Stomacher®, Biomaster Lab system, UK) for 2.5 min at the high intensity setting. The spread plate technique was then used to enumerate bacterial cell density, by spreading 100 µl aliquots of the homogenised hydrogel samples on nutrient agar plates. As necessary, 1 ml of sample was pour plated to confirm complete microbial inactivation. The agar plates were incubated at 37°C for a minimum of 12 h, with surviving populations determined by enumeration of colonies as per formula described in Section 2.7.3. Additionally, the number of viable bacterial cells per hydrogel unit surface area (cfu/cm^2) was determined as outlined below in Equation 2.6, where *N* is the mean value for the obtained colony count, *df* is the dilution factor, the factor *10* was used to revert the amount of counted colonies to the sample volume of 1 ml, V_{hydr} stands for the volume (ml) of the hydrogel sample, V_{PBS} is the volume of PBS added to the stomacher bag and S_{hydr} is the free surface area (cm^2) of the hydrogel sample.

$$cfu/cm^2 = \frac{N \times 10 \times df \times (V_{hydr} + V_{PBS})}{S_{hydr}}$$

Equation 2.6: Number of colonies per surface area of hydrogel.

2.10 Impact of PPGD on the physicochemical and biological properties of hydrogels

To determine whether the PPGD treatment had a negative impact on the hydrogels' physicochemical and biocompatibility characteristics, a series of experiments were performed. Purified and in PBS preswollen (Section 2.4.1) 75-25xP type hydrogels with a mass of 6.5 ±0.5 g were treated at the optimised discharge conditions of 16 kV, 10 pps and a gas flow (N_2, O_2) of 2.5 l/min. The gel strength of the treated gel samples was

investigated via rheological measurements and compression tests while surface changes of dehydrated samples were qualitatively analysed by scanning electron microscopy (ScEM).

2.10.1 Rheological measurements

The gel strength of PPGD-treated hydrogels compared to untreated hydogels was examined via oscillatory parallel plate rheology as described in Section 2.2.4.1. The hydrated samples were subjected to a low strain range sweep from 1.88 x 10^{-4} to 1 x 10^{-3} at a frequency of 1 Hz, while a constant normal force of 5 ±0.5 N was exerted on the samples to ensure proper contact between the gels and the surface plates of the instrument. The G' and the G'' were noted for determining the comparative strength of the hydrogels.

2.10.2 Compression studies

The compressive properties of PPGD-treated hydrogels compared to untreated hydrogels were examined as described in Section 2.2.4.2. A compressive stress of 0.1 MPa and a compressive strain of 50% were used as maximal compression parameters. During the analysis, the compressive strain (%) was continuously recorded in relation to an increase of applied pressure defined as compressive stress (MPa).

2.10.3 Surface topography analysis using scanning electron microscopy

The surface topography of dehydrated, untreated and PPGD-treated hydrogel samples was evaluated by the AO Research Institute in Davos, Switzerland via a Hitachi S-4700 field emission scanning electron microscope. Surface images were taken in secondary electron mode with an accelerating voltage of 0.7 kV. An emission current of 25 A and a working distance of 10 mm were used. Prior to ScEM imaging, the samples were placed on a stub using double sided tape. The section was then sputter coated (E1010, Hitachi) with an 8 nm thick coating of gold/palladium mixture to increase the conductivity of the sample.

2.10.4 PPGD effects on hydrogel biocompatibility

The impact of the PPGD treatment on hydrogel biocompatibility was investigated via a select range of previously outlined *in vitro* toxicity test methods. The PPGD-treated chemical hydrogel type 75-25xP was used as a representative sample throughout the biocompatibility testing and the findings were compared to untreated samples. Prior to

testing, the hydrogel was prepared and purified in PBS as described in Section 2.4.1. The risk of microbial contamination was reduced by briefly submerging (for 10 s) a 250 ±10 mg sample of hydrogel in a biocidal 70-30% ethanol-water (v/v) solution followed by drying to remove residual ethanol and UV-radiation at the germicidal wavelength of 263 nm for 10 min. Aseptically, the samples were swollen and further purified for 15 days in a sealed container with 30 ml of PBS at 37^{o}C and 125 rpm agitation, with the PBS replaced daily. After purification, one-piece 75-25xP type hydrogels with a mass of 6.5 ±0.5 g were treated at optimised discharge conditions with the impact of both O_2 and N_2 as discharge gases investigated at a flow rate of 2.5 l/min, a pulse repetition rate of 10 pps and at a charging voltage of 16 kV. The treatment was started after the capacitors were fully charged to 16 kV. After 30 min, the sample was aseptically removed and rinsed with sterile PBS and the extracts required for toxicity evaluation were incubated for a further 3 days in 15 ml of culture medium at 37^{o}C and 125 rpm agitation.

2.10.4.1 Cytotoxicity of PPGD-treated hydrogels

The cytotoxic potential of PPGD-treated hydrogel extracts was determined on HaCaT cells via the direct contact and the agarose overlay assays with MTT and NR endpoints. The direct contact assays were performed in 96 well microplates seeded at 1.5 x 10^4 cells in 200 µl of complete culture medium incubated for 12 h at 37^{o}C until the desired percentage of confluency (40-60%) was observed. Extracts of the treated gels were exposed to the cells for a further 24 h at 37^{o}C. After addition of the viability dye (MTT or NR), the OD of each well was recorded using a multiwell plate reader (Anthos HTIII) at a test wavelength of 540 nm and a reference wavelength of 690 nm. Results are presented as a percentage of untreated controls against test chemical concentrations.

The agarose overlay assay was conducted using HaCaT cells with minor modifications to the method previously explained in section 2.4.4. The hydrogels were PPGD-treated as described in Section 2.9.2 with perfectly round discs (Ø = 20 mm) being placed in the centre of the agarose dish. As the PPGD-treated hydrogels were not preconditioned in complete culture medium the incubation time was reduced to 12 h at 37^{o}C to avoid adverse cell effects resulting from decreased nutrient supply. Lastly, the

hydrogel test sample was carefully removed and MTT was added before conducting the final examination according to Table 2.3.

2.10.4.2 Genotoxicity of PPGD-treated hydrogels

The genotoxic potential of the PPGD-treated hydrogel extracts was determined on HaCaT cells via the comet assay as previously described in Section 2.5.1.1, using 100 µM H_2O_2 as positive control. Following cellular exposure to the hydrogel extracts for 12 h at 37°C, the cells were harvested and cell viability (≥80% for all test concentrations) was determined by trypan blue exclusion to avoid false positive results due to cytotoxicity.

The Ames II™ mutagenicity assay was also used to investigate the mutagenic potential of PPGD-treated hydrogel extracts as described in Section 2.5.2.2. Extracts from PPGD-treated hydrogels were prepared similar to the method outlined in Section 2.4.1 except that 15 ml of Ames exposure medium was used as the extract liquid. Exposure to the TA98 and TAMix bacterial strains were performed in triplicate by transferring 225 µl of the hydrogel extract medium and 25 µl of bacterial strains to single wells of a 24 well plate (for tests +S9 mix, 187.5 µl of Ames exposure medium, 25 µl of bacterial strains and 37.5 µl of 30% S9 mix were added to the wells). The mixture was then incubated for 90 min at 37°C with agitation at 250 rpm and the assay was performed in accordance with Section 2.5.2.2. The average number of revertants per culture and concentration was then calculated, and the increase above the zero-dose was determined at each concentration of the test chemicals.

2.11 Statistical analysis

Indirect contact cytotoxicity assays (MTT and NR) were conducted using four to six replicates per test sample in three independent experiments, with mean absorbance values expressed as a percentage of untreated control cell values ± standard error of the mean (SEM). The fluorochrome-mediated viability test was performed in triplicate with at least 200 cells counted per data point. The rheological analysis to determine comparative hydrogel strength was performed in three independent experiments with 75 data points collected per sample. For the above assays and tests, homogeneity of variances and normality of data were confirmed with the Levene's test and the Kolmogorov-Smirnov test respectively. Statistical differences compared to control groups were evaluated by one-way

analysis of variance (ANOVA) followed by Dunnett's post-hoc test at 95% and 99% confidence level. The comet assay was conducted on duplicate slides with 50 cells scored per slide. Statistical differences between control and treated cells was evaluated with the nonparametric Mann-Whitney test using untransformed tail moment and percentage tail DNA values. The Ames II™ mutagenicity test was performed as per manufacturers' instruction in triplicate with statistical differences between treatment groups determined using a one tailed t-test. The bacterial inactivation studies were conducted in triplicates and expressed in Log_{10} cfu/ml ± standard deviation (SD) with statistical differences between treatment groups determined using a one tailed t-test. The means of the inactivation rate constants (k) ±SD were compared using ANOVA followed by Dunnett's post-hoc test and two sample t-tests at 95% confidence level. All statistical analyses were performed using Minitab® Version 15.

Chapter 3: Results and Discussion

3.1 Synthesis, characterisation and biocompatibility of *N*-vinyl-2-pyrrolidone - acrylic acid based physical hydrogels

3.1.1 Preface

Hydrogels' three-dimensional networks are usually made of hydrophilic polymer chains that are held together by chemically-induced crosslinking or via physical bonding forces. In contrast to chemical hydrogels, most physical hydrogels are noncovalently bonded networks which are capable of swelling after been placed in aqueous solutions. Physical hydrogels are composed of weak and potentially reversible forms of chain-chain interactions between the polymer backbones which act as physical bonding associations rather than crosslinking points (Bae *et al.,* 2000). These noncovalent associations are typically reversible and much weaker than chemical crosslinks; hence, physical gels eventually degrade in water or solvents after an initial swelling period. Most natural and many synthetic physical hydrogels degrade by dissolving in aqueous solutions due to their elevated hydrophilicity. Polar physical hydrogels, such as those based on NVP polymers, dissolve in water by forming hydrogen bonds with water molecules while gels composed of polyelectrolytes, like AA based polymers, dissolve in water by interacting with the partial charge of water molecules (Park *et al.,* 1993). After complete dissolution in an aqueous solvent, the physical hydrogel is known as a hydrosol, which is a dispersion of colloidal particles within the solvent (Napper and Hunter, 1972). Due to their degradable characteristics, these gels have gained much attention in the development of novel drug delivery systems as well as other biomedical applications (Bae *et al.,* 2000).

Physical hydrogels based on photopolymerised monomers of NVP and AA were developed in our laboratory. Fundamental investigations of the material properties of these gels suggest that they have the potential to be used as biodegradable gastric drug delivery systems (Devine and Higginbotham*,* 2003). The photopolymerisation technique used in this study is based on a free radical polymerisation reaction, with the reaction being initiated by irradiating the liquid monomers with $UV_{340\ nm}$ light to obtain solid dry xerogels. This type of polymerisation can be conducted at room temperature and room pressure and has therefore been widely used for the synthesis of hydrogels destined for the biomedical field (Nguyen and West, 2002). In comparison to conventional polymerisation methods,

photopolymerisation proves to be fast and effective by avoiding the addition of otherwise commonly used and often hazardous organic or inorganic solvents. To initiate the free radical based polymerisation reaction, the photoinitator Irgacure®184 was mixed within the monomeric blend. Irgacure® 184 belongs to the chemical family of acetophenones and undergoes cleavage at the carbon (C-C) bond to form radicals when exposed to the UV light (Nguyen and West, 2002), as illustrated in Figure 3.1.

Figure 3.1: Chemical structure of the photoinitiator Irgacure® 184 which, upon exposure to UV light, undergoes cleavage to form radicals that promote the polymerisation reaction.

Although many NVP and AA based polymers are generally considered to be non-toxic and consequently have been used in biomedical applications (Wan *et al.,* 2005), it is still necessary to evaluate the biocompatibility of these novel copolymeric hydrogels as unreacted residues from the photopolymerisation process in addition to changes in physico-chemical properties may be harmful when applied to human tissue. Moreover, biocompatibility testing of biomaterials forms an integral part of preclinical product evaluation as well as being a prerequisite for regulatory approval. In this regard, the ISO guidelines for the biocompatibility testing of medical devices and biomaterials recommend materials characterisation (ISO 10993-13-19) and *in vitro* testing for cytotoxicity (ISO 10993-5) as part of a standard test battery. The former confirms the chemical composition, presence and nature of any leachates and/or extractables in addition to fitness for purpose, while the latter ensures no adverse effects on cellular morphology and function following cell exposure to such biomaterials. Additional tests for genotoxicity are also recommended depending on intended use and duration of exposure (ISO 10993-3).

Considering the aforementioned, the main focus of the following study was to define the *in vitro* biocompatibility of the NVP-AA based physical hydrogels for potential use in biomedical applications. More specifically, FTIR spectroscopy was used to verify the chemical composition of the monomers and polymers employed in hydrogel synthesis

while HPLC was employed to determine the presence and nature of any residual monomers following photopolymerisation. Additional swelling and solubility studies were also performed, under physiological conditions, to determine fitness for purpose and to ascertain the best approach for preparing the hydrogels for subsequent *in vitro* toxicity tests.

Following such material characterisation, specific *in vitro* cytotoxicity and genotoxicity tests were employed in conjunction with direct hydrogel exposure of two human-derived cell culture models. The HCT-8 ileocecal adenocarcinoma cell line was used as they represent the *in vivo* characteristics of the gastrointestinal tract, the point of prolonged exposure to a gastric drug delivery system. Additionally, the hepatoma HepG2 cell line was chosen owing to its drug metabolising capabilities and the potential of toxicants absorbed via the gastrointestinal tract to reach the liver via the hepatic portal vein, while also being mindful of the potential for enterohepatic recirculation (Dierickx, 1998; Knasmueller *et al.,* 1998). The hydrogels potential to induce chromosomal and single nucleotide point mutations was also evaluated via the single cell gel electrophoresis (comet) assay and the *S. typhimurium* reverse mutation (Ames) assay respectively.

3.1.2 Synthesis of physical hydrogels

Physical hydrogels based on different ratios of a liquid monomer blend of NVP and AA, were photopolymerised in the absence of a chemical crosslinking agent. The photoinitiator Irgacure® 184 was used at 3 wt% of the total monomer weight as this proved effective in previous studies (Devine and Higginbotham, 2003; Geever *et al.,* 2006). Ultimately, the photoinitiator was fully soluble within the monomer blend but did require stirring of the blend for approximately 10 min before transferring the mixtures into specially designed silicone moulds and irradiating with $UVA_{340\ nm}$ light at an intensity of 280 $\mu W/cm^2$ for exactly 2 h. This initiated the free radical polymerisation reaction through decomposition of the photoinitiator (Nguyen and West, 2002), thereby producing the desired solid xerogel which appeared transparent and glass like in their nonhydrated form (Figure 3.2). The 100-0phys samples cured with a uniform surface, which suggests that it could potentially be used for biomedical coating applications. With the addition of AA, the uniformity of the surface deteriorated forming an appearance best described as containing ridge-like

structures. This surface change increased with an increase in AA concentration (Figure 3.2). Furthermore, the surface of the 25-75phys hydrogel appeared slightly moist suggesting that the polymerisation was not as efficient for this sample. Devine and Higginbotham (2003) found that the addition of decreased amounts of AA (10-20 wt%) led to the formation of white solids at the surface of the polymerised hydrogels. These residues were also noted by Lau and Mi (2002) during the synthesis of copolymers based on a PVP-PAA complex and it was suggested that this was due to phase separation during the polymerisation process. However, in the present study, the monomeric ratios chosen for the polymerisation did not result in the formation of any visible signs of phase separation. The monomeric feed ratio combined with the polymerisation reaction appeared sufficient to produce homogeneously polymerised hydrogels.

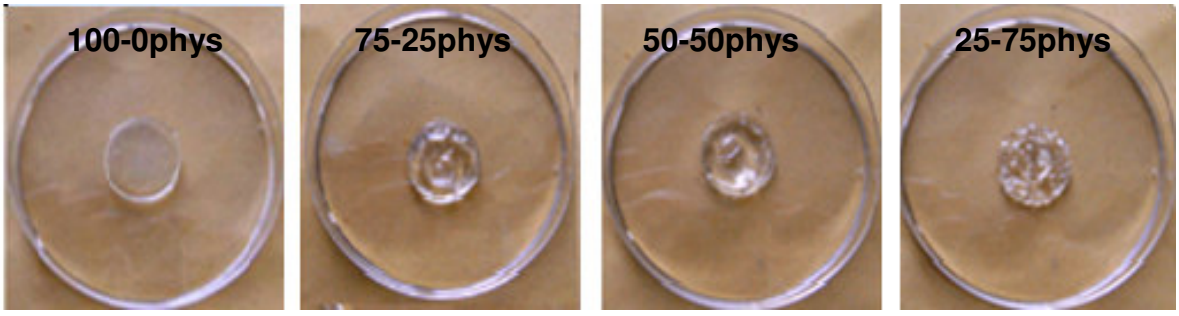

Figure 3.2: Appearance of the dry physical hydrogels (xerogels) with varying monomeric feed ratios and 3 wt% Irgacure® 184 after photopolymerisation.

3.1.3 Characterisation of physical hydrogels

3.1.3.1 FTIR spectroscopy

Infrared (IR) spectroscopy is commonly used for the structural identification and quality control of monomers and polymers. Indeed, in the last two decades, IR has also been extensively used to characterise hydrogels in their dehydrated form, based on the absorption or reflection of electromagnetic radiation in the IR of a test specimen (Devine *et al.,* 2006; Geever *et al.,* 2006). The absorption bands present in the IR frequency domain form a molecular fingerprint of the specimen and thus allows for the detection of compounds and the derivation of structural details. Such absorption bands originate from

the interaction of the electromagnetic wave at a specific frequency with the vibration of a chemical bond. If the vibration of the chemical bond oscillates at the same frequency as the electromagnetic radiation, than the electrical component of the wave can transfer its energy to the bond. Therefore, at the resonant frequency obtained absorption bands can be associated with a particular bond type. Although based on the same principle, FTIR has significantly altered the traditional approach to obtaining IR spectra. FTIR are single beam instruments which employ an interferometer that is placed between the light source and the sample. This technique imposes several advantages including the achievement of brighter signals with higher signal to noise ratios and a constant resolution throughout the studied IR domain.

In the present study, FTIR spectroscopy was used in the Attenuated Total Reflection (ATR) mode to confirm that photopolymerisation was effective in producing polymeric hydrogels. Thus, the IR spectra from the NVP and AA monomers were compared to spectra obtained from the dehydrated hydrogel samples. Furthermore, to provide a better overview, the spectra were examined in the range of 600-3000 cm^{-1} as the characteristic peaks for all samples tested appeared below 3000 cm^{-1}. However, the range of hydroxyl (OH) stretching vibration (3000–3700 cm^{-1}) could not be examined objectively due to the difficulty in removing residual water completely from the hydrophilic samples. Figures 3.3 and 3.4 illustrate the obtained FTIR spectra obtained for the base monomers and the physical hydrogels respectively.

The FTIR spectra obtained for both the NVP and AA monomers highly resembled their respective reference spectra illustrated in the Sadtler IR atlas of monomers and polymers (Sadtler, 1980). A publication by Száraz and Forsling (2000) states that pure liquid NVP displays two very strong stretch bands in the IR spectrum. The first band corresponds to the olefinic carbon bond (C=C), which is characteristic for the monomer and is usually found near 1630 cm^{-1}. The second band usually appears around 1700 cm^{-1} and assigns the carbonyl bond (C=O). In the present work, the distinct C=C stretch band of the vinyl group was determined at 1623 cm^{-1} and the C=O bond peaked at 1690 cm^{-1}.

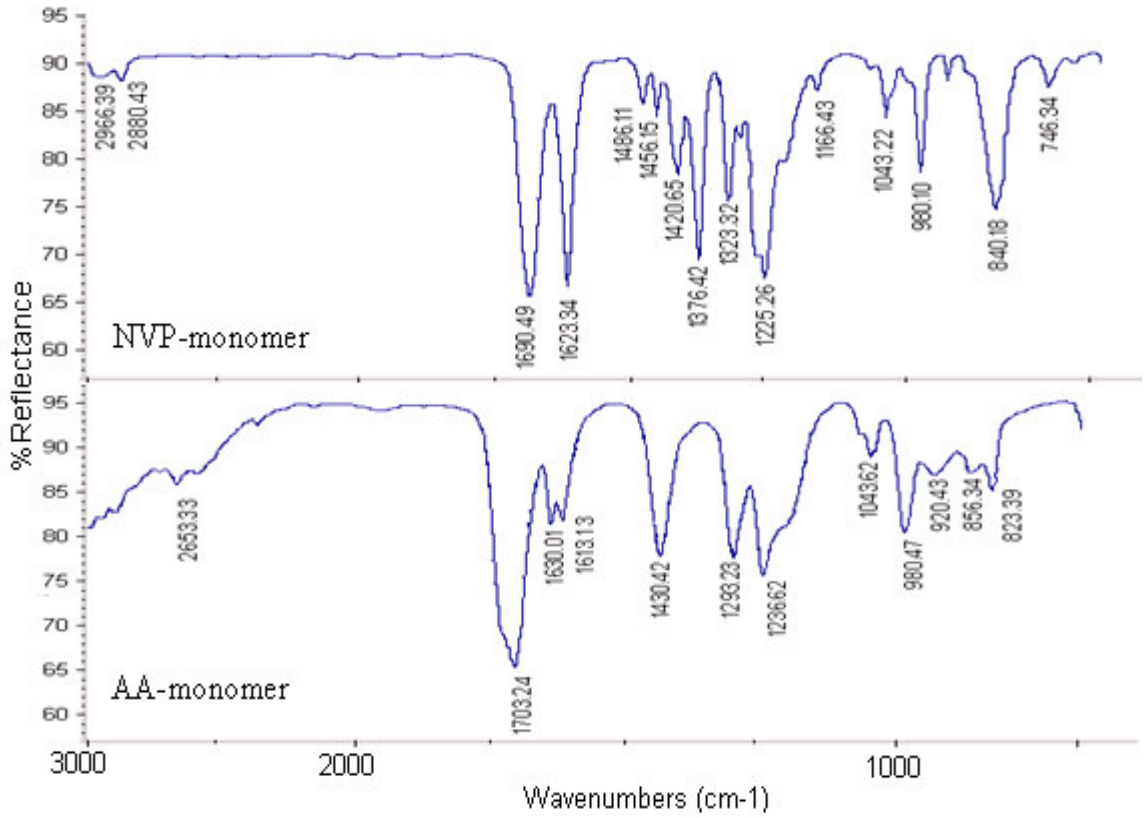

Figure 3.3: FTIR spectra of the NVP and AA monomers.

The IR spectrum of liquid AA has been thoroughly discussed in the scientific literature (Feairheller and Kanton, 1967; Charles *et al.,* 1987). The distinct band at 1703 cm^{-1} is assigned to a stretch of the C=O bond. The two peaks observed in the range of 1613 to 1630 cm^{-1} originate from a stretch of the vinyl C=C bond, a feature only observed in the monomeric form of AA. The characteristic carbon-oxygen bond (C-O) stretch is assigned to the band observed at 1430 cm^{-1}. The peaks shown at 1293 and 1236 cm^{-1} originate from a OH bend and a C-C stretch respectively. Further bands at 1043, 980 and 920 cm^{-1} indicated the presence of a bending vibration of the CH_2 group. Feairheller and Kanton (1967) also highlight the fact that the AA molecule can form dimeric species in which two carboxylic acid units are sufficiently coupled through hydrogen bonding. This formation can yield a spectrum close to that expected of an oligomer.

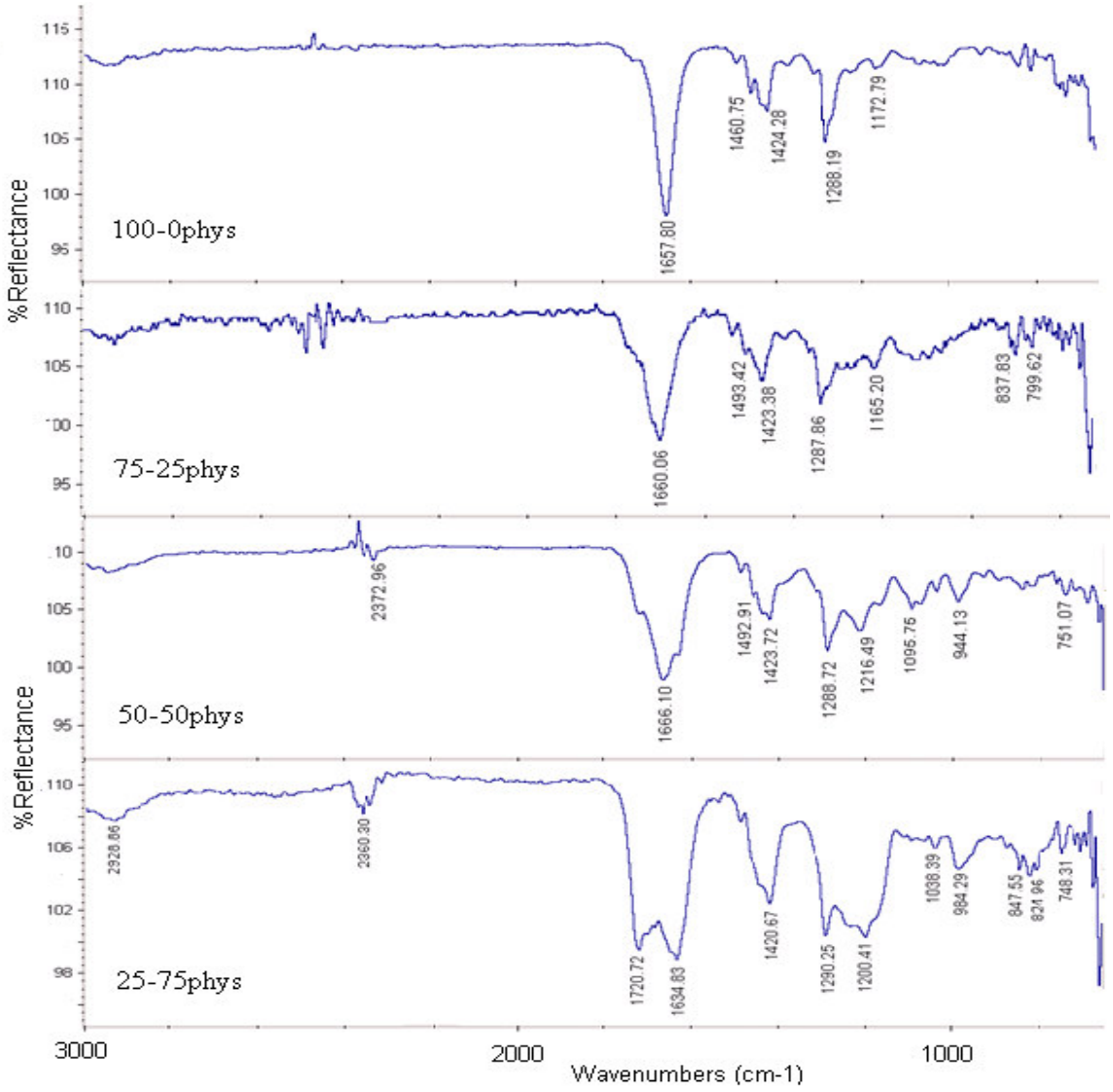

Figure 3.4: Comparison of the FTIR spectra of dehydrated physical hydrogel samples.

The characteristics of the FTIR spectra obtained for the physical hydrogel samples differed drastically from the monomer spectra thus indicating that polymerisation had occurred. In contrast to the NVP monomer spectra, the FTIR result obtained for the 100-0phys sample (Figure 3.4) resembled the respective PVP reference spectrum illustrated in the IR atlas by Sadtler (1980). Here, the NVP monomer's vinyl C=C stretch band typically seen at 1623 cm^{-1} (Figure 3.3) had completely disappeared. The strong peak observed at 1657 cm^{-1} corresponded to the C=O bond of the PVP polymer (Alla *et al.,* 2007). Additionally, Szaraz and Forstling (2000) confirm that the C=O peak in NVP based

polymers is usually found at a lower frequency than the corresponding peak in the liquid monomer solution. They also suggest that this frequency decrease results from intermolecular hydrogen bonds acting on the carbonyl group, which are stronger in the polymeric solid phase than in the NVP liquid. The peaks observed in the 1400-1500 cm^{-1} region are attributed to CH_2 deformation (Sadtler, 1980).

The interpretation of the spectra obtained for NVP-AA based hydogels is complicated because of the numerous possibilities of interactions between the two parent molecules. In this context, a study by Kaczmarek and his colleagues suggest that the intermolecular interactions between polymers of NVP and AA are most often due to hydrogen bonds (Kaczmarek *et al.,* 2001).

The spectra obtained for the polymerised monomer mixtures showed a strong C=O stretch band near 1660 cm^{-1}. This band could have originated from either the carbonyl group of the initial NVP or AA monomer. However, in accordance with previous findings for similar hydrogels, the C=O shift towards higher wavenumbers indicated the formation of copolymeric hydrogels (Jin *et al.,* 2006; Alla *et al.,* 2007). In addition, this band broadened with an increasing ratio of AA in the initial feed ratio and a shoulder effect towards higher wavenumbers was visible in the 75-25phys and 50-50phys samples. This shoulder developed into an absorption peak at 1720 cm^{-1} for the 25-75phys sample and has been attributed to the presence of carboxylic acid groups in their dimeric form (Yaung and Kwei, 1998; Devine and Higginbotham, 2003). On the other hand, results published by Kaczmarek *et al.* (2001) contradict this theory by suggesting that the carbonyl group of AA based polymers peaks at around 1710 cm^{-1} and therefore in turn could be responsible for the formation of the peak found in the present study at 1720 cm^{-1}. By increasing the AA content to 50% a second shoulder formed towards the lower wavenumber region. This shoulder, which started to peak at 1634 cm^{-1} for the 25-75phys hydrogel needs to be interpreted very cautiously. The formation of hydrogen bonding between the carboxylic acid group and the carbonyl group of NVP based polymers has previously been reported to shift the latter towards 1630–1640 cm^{-1} (Yaung and Kwei, 1998; Devine and Higginbotham 2003) and this may explain the absence of the C=O peak in the 1660 region for the 25-75phys samples. However, it is possible that this peak originated from the olefinic vinyl C=C bond of unpolymerised NVP or AA residuals. This correlates with the

observed moist surface of the sample after polymerisation, thereby indicating that increasing the AA content somewhat inhibited the polymerisation process.

The broad peak starting to appear at 2900 cm^{-1} originated from C-H stretching and the intensity of these bands increased with the increasing ratio of AA in the initial feeding ratio (Alla *et al.,* 2007). Also, with increasing amounts of AA, absorption bands in the region of 1290-1240 cm^{-1} and 984-940 cm^{-1} indicated the presence of characteristic bending vibrations of OH and CH_2 groups, respectively.

Overall, the spectra obtained for the physical hydrogel samples indicated that polymerisation and copolymerisation between the monomer molecules had occurred. However, an indicator of the efficiency of the polymerisation process could not be achieved and the presence of unpolymerised residuals within the hydrogel matrices could not be excluded. Therefore, further testing to confirm the purity of the polymers was warranted.

3.1.3.2 HPLC analysis of residual monomers

Optimisation and calibration of HPLC

Polymeric devices can contain harmful residuals such as monomers, oligomers and polymerisation additives. The presence and quantity of these residuals often plays a major role in determining the efficiency of the polymerisation reaction and overall biocompatibility. Indeed, the residual monomer content of a polymer can be considered as an indicator of the devices purity. Reverse phase HPLC is one of the most common analytical methods for quantitative measurements of organic compounds, and was therefore used for the determination of residual monomer in solutions produced from the physical hydrogels. The core of the HPLC system consisted of a C8 column in conjunction with a mobile phase composed of methanol in aqueous ammonium acetate (25:75). Detection was performed at 234 nm. Figure 3.5 shows the chromatogram obtained after injection of a standard mixture containing 4 µg/ml AA and NVP, using the reverse phase HPLC parameters described in Section 2.2.3. Figure 3.6 illustrates the linear calibration graphs for AA and NVP.

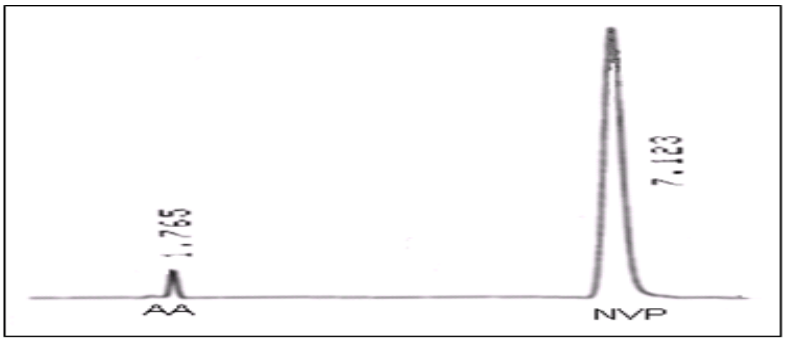

Figure 3.5: HPLC chromatogram of a prepared standard containing a mixture of AA and NVP (µg/ml). AA eluted at 1.76 min, NVP eluted at 7.123 min.

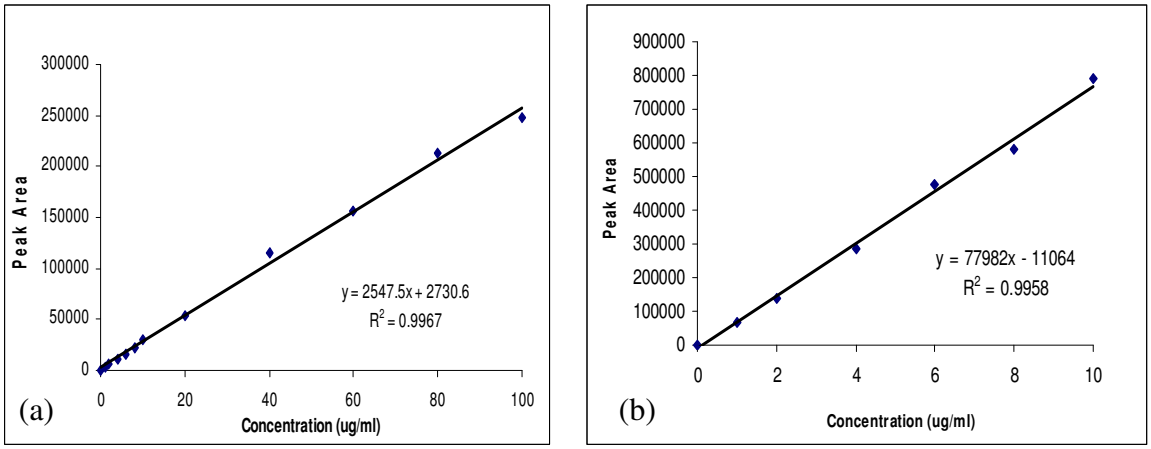

Figure 3.6: HPLC calibration graph for (a) AA (0.5-100 µg/ml) and (b) NVP (0.5–10 µg/ml) standards. Regression equation and correlation factor (R^2) displayed.

Table 3.1: Calibration data for AA (0.5-100 µg/ml) and NVP (0.5-10 µg/ml).

Concentration (µg/ml)	Mean Peak Area AA (±SD)	Mean Peak Area NVP (±SD)
1	3216.00 (±19.86)	68209.50 (±3544.73)
2	70332.00 (±18.38)	139077.50 (±2848.93)
4	11009.50 (±275.77)	285623.00 (±545.87)
6	16446.50 (±986.44)	476338.00 (±3481.79)
8	22581.00 (±1254.41)	581652.50 (±3772.42)
10	30270.50 (±362.75)	789093.50 (±4567.21)
20	53048.50 (±693.67)	-
40	109744.00 (±2035.05)	-
60	156869.00 (±1772.01)	-
80	213592.50 (±1723.22)	-
100	247185.50 (±5565.64)	-

The retention times obtained were 1.76 min and 7.123 min for AA and NVP respectively. Detection at 234 nm led to the appearance of a higher NVP peak compared to the AA peak as the highest absorbance values of the monomers determined by previously performed UV spectrometry were found to be 234 nm for NVP and 210 nm for AA. However, over the concentration ranges tested, both monomers resulted in a linear detection at 234 nm. The calibration graphs for the analysed monomers were plotted in the range of 1-100 µg/ml for AA and 1-10 µg/ml for NVP (Table 3.1). The standard concentration range response resulted in linear respective analyte concentration peaks. The regression equations were y = 2547.5x + 2730.6 for the AA and y = 77982x - 11064 for the NVP standard plot, where y denotes peak area and x the concentration of analyte in µg/ml. The correlation factors were not less than 0.9967 for AA and not less than 0.9958 for NVP (Figure 3.6).

Determination of residual monomers in physical hydrogels in solution

The use of HPLC for analysing the residual monomer content present in polymeric material solubilised by an appropriate solvent has been previously reported (Viljanen *et al.,* 2006). In the present study, the physical hydrogels were solubilised at 37^{o}C using HPLC mobile phase as the solvent. Similar to the swelling studies, the hydrogel samples containing 75 wt% AA were not fully dissolvable in the mobile phase and thus were eliminated from the HPLC analysis. To obtain HPLC peaks in the range of the calibration curve, the hydrogel solutions were further diluted with mobile phase to achieve a hydrogel-hydrosol solution with a final concentration of 100 µg/ml. The amount of residual monomer was determined on the basis of peak area values interpolated from previously constructed calibration curves (Figure 3.6). Detection was performed at a wavelength of 234 nm. The data is presented as the mean of two independent experiments.

Table 3.2: Retention time, peak area, residual monomer quantity (µg/ml) in diluted sample and calculated final concentration (wt%) in hydrogel matrix of (a) NVP and (b) AA present in physical hydrogels as obtained via reverse phase HPLC.

(a)

Dissolved Hydrogel (100 µg/ml)	Mean Ret. Time	Mean Peak Area NVP (±SD)	Conc. in diluted sample (µg/ml)	Final conc. in hydrogel (wt%)
100-0 wt%	7.407	476584 (±1862.52)	6.25	6.25
75-25 wt%	7.410	3014.5 (±443.36)	0.18	0.18
50-50 wt%	7.383	642.5 (±146.37)	0.15	0.15

(b)

Dissolved Hydrogel (100 µg/ml)	Mean Ret. Time	Mean Peak Area AA (±SD)	Conc. in diluted sample (µg/ml)	Final conc. in hydrogel (wt%)
100-0 wt%	N/A	N/A	0	0
75-25 wt%	1.730	15226 (±12446.13)	4.58	4.58
50-50 wt%	1.729	8908 (±946.11)	2.26	2.26

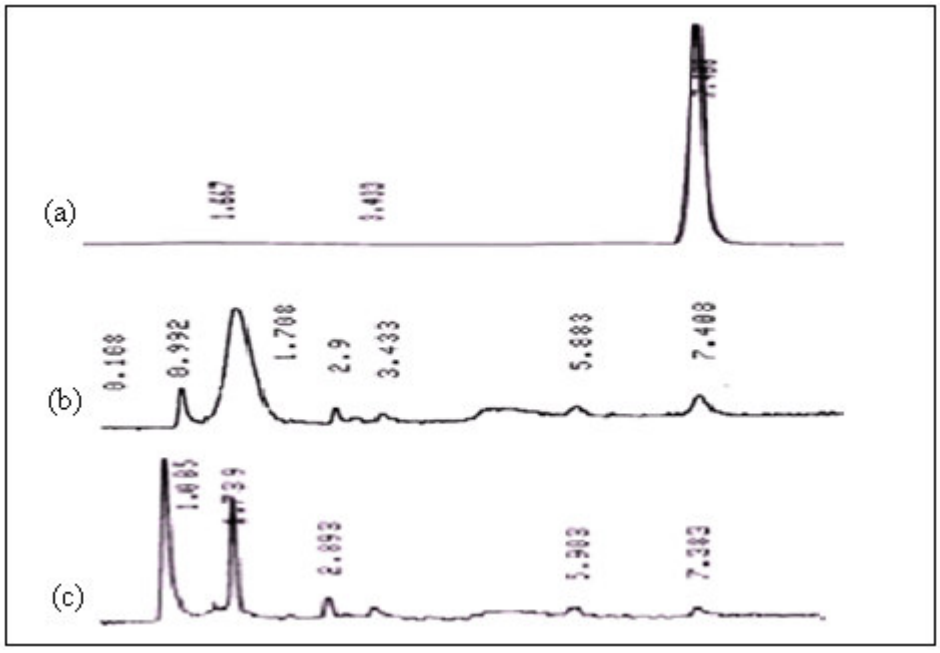

Figure 3.7: HPLC chromatogram of hydrogel solutions dissolved in mobile phase. (a) 100-0phys, (b) 75-25phys, and (c) 50-50phys.

The results obtained following HPLC analysis of the residual monomer content in physical hydrogel solutions are illustrated in Table 3.2 and HPLC chromatograms are shown in Figure 3.7. Compared to the monomer standards (Figure 3.5), the respective retention times revealed the presence of a considerable amount of residual monomers (AA

and NVP) in the networks. The monomeric NVP concentration in 100-0 hydrogel solutions containing 100 µg/ml of the dissolved hydrogel was 6.25 µg/ml. This correlates to a final concentration of 6.25 wt% residual NVP in the hydrogel network.

Also, the presence of considerable amounts of both base monomers was detected for hydrogel networks prepared with the addition of AA. The analyte samples based on 75-25phys gel contained 4.58% of unbound AA monomer while the 50-50phys contained 2.26% of residual AA. For both AA containing networks the detectable concentration of unbound NVP was below 0.2 wt%. Furthermore, as shown in Figures 3.7b and 3.7c numerous smaller peaks were observed with a retention time below that of the NVP monomer. These peaks may indicate the presence of unpolymerised breakdown products of the initial base monomer or the photoinitiator. However, the findings obtained from AA containing analytes have to be treated cautiously. Due to the polyelectrolytic nature of AA based polymers (Fujimori and Trainor, 1983), solutions from hydrogels prepared in the presence of AA as base monomer were highly viscose. The viscosity proved problematic during filtration of the analyte, which is an essential requirement before injections to the HPLC system. It appeared that, in solution, the AA based polymer chains unfolded due to polyelectrolytic mechanisms and gradually blocked the filter membrane, thereby possibly influencing the residual monomeric composition of the hydrogel filtrate. This also resulted in somewhat inconsistent results for the residual monomer detection of these gels. A fact which is also reflected in the high SD values obtained for these results compared to values obtained from respective calibration standards. Hence, the performance of an additional monomer analysis using a different approach is strongly recommended to verify the findings for AA based physical hydrogels. Another effective but rather intricate method to identify and quantify the monomeric residual in solid NVP based polymers is headspace solid-phase microextraction linked gas chromatography-mass spectrometry (Mehdinia *et al.,* 2007).

From the results obtained, it appears that the photopolymerisation process utilised in the present study was not efficient enough to reduce the monomeric residues to an acceptable level. The NVP content in the 100-0phys hydrogels was found to be unexpectedly high. Although an accurate determination could not be achieved for the physical hydrogels containing AA as second base monomer, the obtained results indicate

the presence of unpolymerised materials. For that reason, further optimisation of the polymerisation process is advised to achieve a substantial reduction of unpolymerised residues within the hydrogel matrices. Future investigations may include the use of different types and varying amounts of photoinitiator. Furthermore, the gel geometry could be changed to allow for an enhanced UV light absorption. This could be combined with maximising the UV light intensity to obtain an increased penetration of UV light.

3.1.3.3 Swelling and solubility studies

The swelling and solubility tests on the physical hydrogel networks were conducted in PBS at 37^{o}C to simulate physiological conditions. The swelling profile obtained from physical hydrogels submerged in PBS is illustrated in Figure 3.8. Representative images of hydrogels in different swelling states are shown in Figure 3.9. The samples prepared from 100 wt% NVP swelled to twice their initial mass and dissolved rapidly within 8 h. As the AA content was increased, the hydrogels were capable of reaching higher swelling ratios. They also tended to dissolve at a slower rate compared to those prepared from 100 wt% NVP. The 25-75phys hydrogel reached the highest maximum swelling ratio by exceeding a value of 5.12 and resisted complete dissolution for more than 160 h. However, this network did not fully dissolve in the swelling medium but resulted in the formation of small polymer aggregates which were removed by the addition of fresh swelling medium.

A similar swelling trend was observed with the 50-50phys samples and although the maximum swelling ratio was reduced to about 3.4, the gel network resisted complete dissolution for more than 168 h. Gels synthesised with 75 parts of NVP and 25 parts of AA reached their maximum swelling ratio of 4.6 within 12 h, but degraded within the following 36 h.

The dissolution process of the hydrogel networks can be explained by the transformation from entangled polymer chains in the gel phase to disentangled polymer chains in the liquid solution. More precisely, when in contact with aqueous solution, the hydrophilic solid polymer networks absorb water and swell to form a hydrogel. Once a gel is formed, water molecules diffuse freely through the rather loose network and noncovalent polymer contacts are broken. Subsequently, individual polymer molecules of the

hydrophilic polymer chains are dissolved in the water (Park *et al.,* 1993). Water continues to penetrate towards the core and finally the gel is converted to a viscous solution in the form of a hydrosol (Napper and Hunter, 1972).

The degree of swelling and dissolution varies depending on the hydrophilicity and the molecular weight of the polymer. Furthermore, environmental variations in pH, ionic strength, or temperature may also influence the solubilisation process (Kamath and Park, 1993). In the present study, the extreme hydrophilic nature of NVP and its polymerisation products facilitated the rapid dissolution of 100 wt% NVP based hydrogels. Due to their polarity, NVP based polymers readily dissolve in water by forming hydrogen bonds with water molecules and this property could make the 100-0phys hydrogel a suitable candidate for use as lubricous drug eluting coatings on medical devices such as catheters and internal probes. Devine and Higginbotham (2003) suggest that an increase in intermolecular hydrogen bonding is caused by the addition of AA to the hydrogel systems, which in turn leads to the enhanced swelling profile and higher dissolution resistance. Furthermore, Park *et al.* (1993) imply that the solubility of a polyelectrolyte, such as AA based polymers, is strongly depended on the pH of the swelling medium. At low pH, these polymers appear less hydrophilic because the carboxyl groups are protonated i.e. not ionised. When the pH of the solution is increased, these functional groups release hydrogen atoms, become ionised and the AA molecule gains hydrophilic properties by interacting with the partial charge on water molecules.

Although the PBS solution used displays excellent buffer capacities, a decrease in the pH of the solution surrounding the hydrogel (to approximately pH 4) was evident resulting from the acidic nature of AA. The reduced pH was believed to significantly alter the hydrogels swelling and degradation process and may explain the formation of the small insoluble polymer aggregates within the swelling medium of the 25-75phys gel.

Due to the pH sensitive swelling and solution properties of the NVP and AA based copolymerised hydrogels, it has been suggested that they may find a suitable application in the field of gastric drug delivery (Devine and Higginbotham, 2003). By using different monomer ratios the hydrogel could be tailored to deliver a suitable amount of a pharmaceutical agent to specific target sites within the gastrointestinal tract.

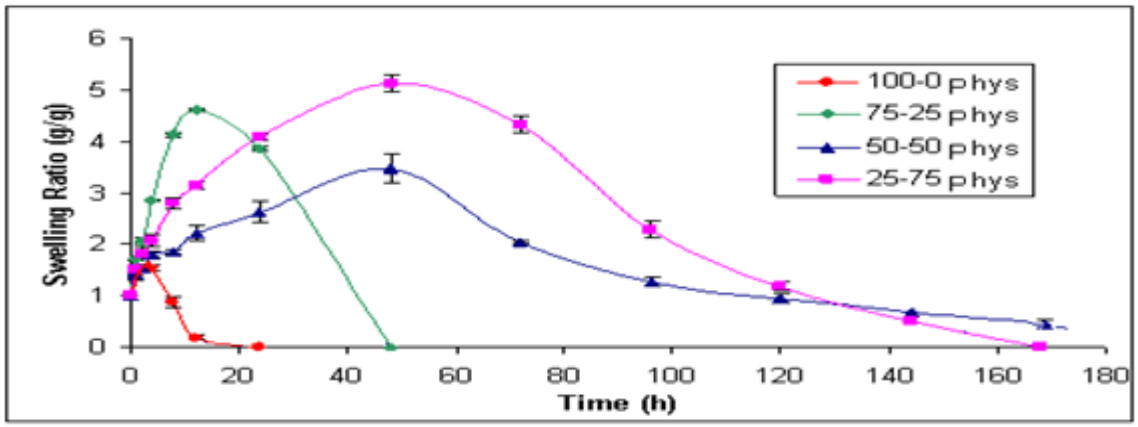

Figure 3.8: Swelling ratio (g/g) of physical hydrogels submerged in PBS monitored over a time period of 168 h at 37°C. Data presented is the mean of three independent experiments (±SEM).

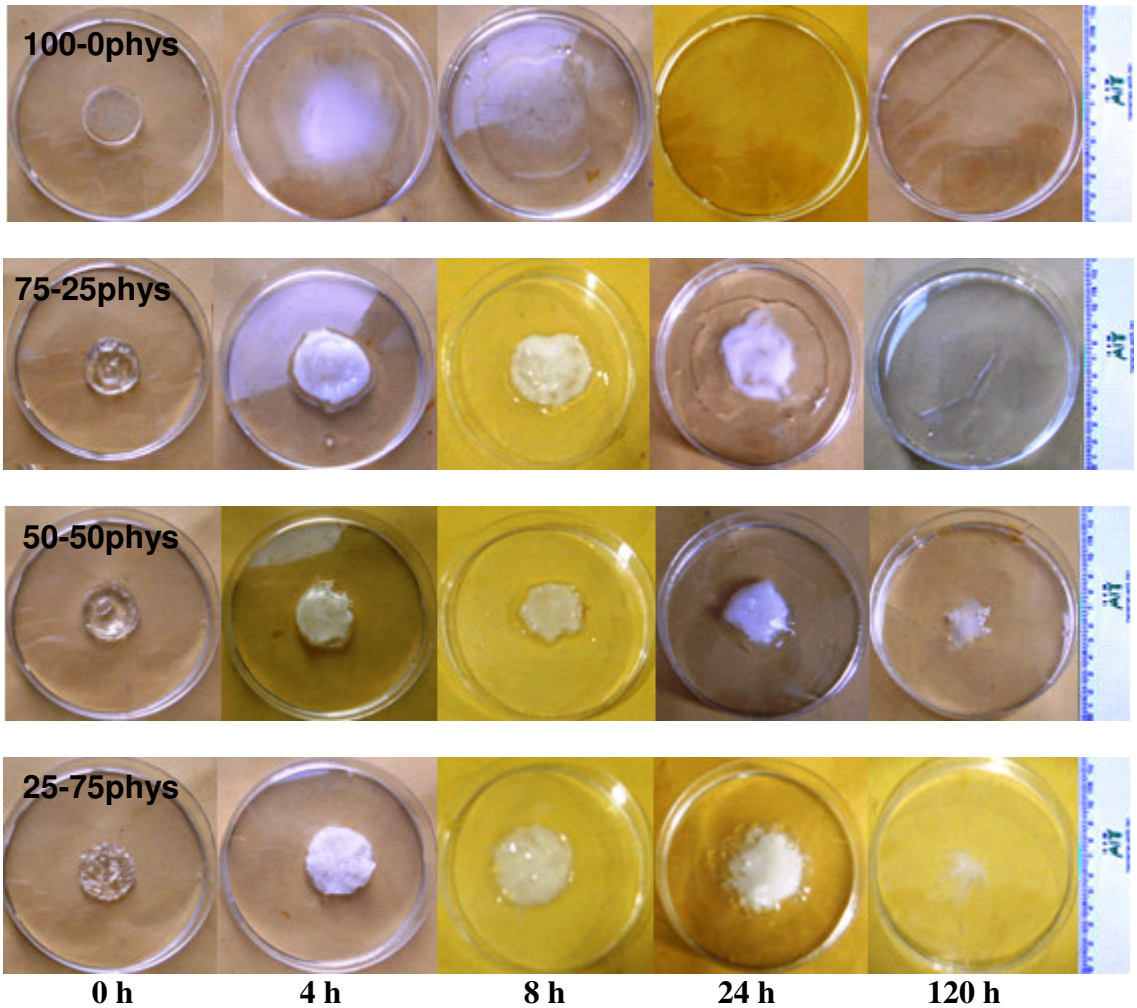

Figure 3.9: Swelling characteristics of physical hydrogels in PBS over a time period of 120 h at 37°C.

3.1.4 Cytotoxicity assessment of physical hydrogels and base monomers

Owing to the soluble nature of the physical hydrogels the direct contact assay, in conjunction with MTT and neutral red endpoints, was the cytotoxicity assay of choice used to screen the hydrogels for their potential to cause cellular damage. Such cytotoxicity endpoints are known to be sensitive and economical to perform and, since they report different endpoints of cytotoxicity, can also provide mechanistic information regarding the toxic potential of the physical hydrogels (Mosmann, 1983; Borenfreund and Puerner, 1985). Moreover, such assays can be conducted primarily as a means of ranking the varying material compositions against each other in terms of their potential to cause cell damage. The MTT endpoint measures mitochondrial function as an indicator of cytotoxicity (Fotakis and Timbrell, 2006), whereas the NR endpoint assesses the ability of viable cells to incorporate and accumulate the supravital dye NR within lysosomes (Borenfreund and Puerner, 1985). Thus, the MTT endpoint is more sensitive to mitochondrial cell damage whereas the NR endpoint is particularly sensitive to chemicals that have direct effects on lysosomes (Weyermann *et al.*, 2005). Furthermore, tissue specific cytotoxicity can involve undesirable effects on particular types of differentiated cells in culture. Hence, comparative studies on the HepG2 and HCT-8 cell line were performed. The HepG2 hepatoma cells were chosen because of their metabolic activity and anatomical characteristics comparable with primary human hepatocytes (Knasmueller *et al.,* 1998; Devery and Tomkins, 1999). These cells display many genotypic and phenotypic features of normal liver cells and retained the ability to produce bioactivated metabolites as it possesses many of the specialised functions relating to drug metabolising enzyme activities (Dierickx, 1998; Knasmueller *et al.,* 1998). The HCT-8 cell line is of human intestinal origin and was chosen to evaluate the cytotoxic potential of the physical hydrogels due to their potential use as gastric drug delivery systems.

3.1.4.1 The direct contact assay (MTT endpoint)

The conversion of a yellow tetrazolium salt to a purple formazan product has several desirable properties for assaying cell survival and proliferation following exposure to test materials. MTT is transformed to its formazan product only by living metabolically active cells and since the untransformed substrate does not interfere with measurement of the

product, this allows the assay to be conducted with minimal washing steps thus increasing the speed of the assay and reproducibility. The distinct advantage that many samples can be processed and analysed simultaneously within a reasonable time period (Mosmann, 1983), made the MTT assay a suitable test system for the cytotoxicity investigation of hydrogel samples. HepG2 and HCT-8 cells were seeded at an appropriate cell density to achieve the desired level of cell growth (40-60% confluency) prior to direct exposure to the solubilsed hydrogels. To facilitate formazan production, a final MTT concentration of 0.5 mg/ml was used at an exposure time of 4 h. Due to the difference in growth rate and probable varying number of mitochondria of each cell type, the formazan production differed slightly for each cell line. The resulting formazan was solubilised using DMSO before recording optical densities at 540 nm. Indeed, the use of DMSO as a solvent for the MTT assay offers significant advantages over the commonly used acidified isopropanol in terms of interference with spectral properties and rapidness of solubilisation (Twentyman and Luscombe, 1987).

The physical hydrogels and respective monomers were diluted in complete cell culture medium to achieve a concentration range representing the toxic effects of the test material (0-25 mg/ml). Due to the acidity of AA containing samples, the final exposure dilutions needed to be pH adjusted (pH 7.4) by the addition of small amounts of 3 M NaOH. The addition of NaOH substantially enhanced the solubility of these samples via ionisation and subsequent unfolding (due to repulsive charges) of the polyelectrolytic AA based polymer chains (Jianqi and Lixia, 2002). Despite enhanced solubility for AA based hydrogels the 25-75phys sample could not be solubilised completely, with small polymer aggregates present in the solution which would have significantly altered the samples availability during exposure. Therefore, it was decided to exclude this matrix from the following toxicity assessment. Despite the fact that the pH manipulation has the potential to influence the cell toxicity data, it was essential as the cells proved to be highly sensitive to the reduction in pH caused by unbuffered solutions making a proper evaluation difficult. The results obtained from the absorbance readings were transformed as percentage of untreated control cell values. The mean percentage viability of replicate results and the SEM were calculated for each cell line.

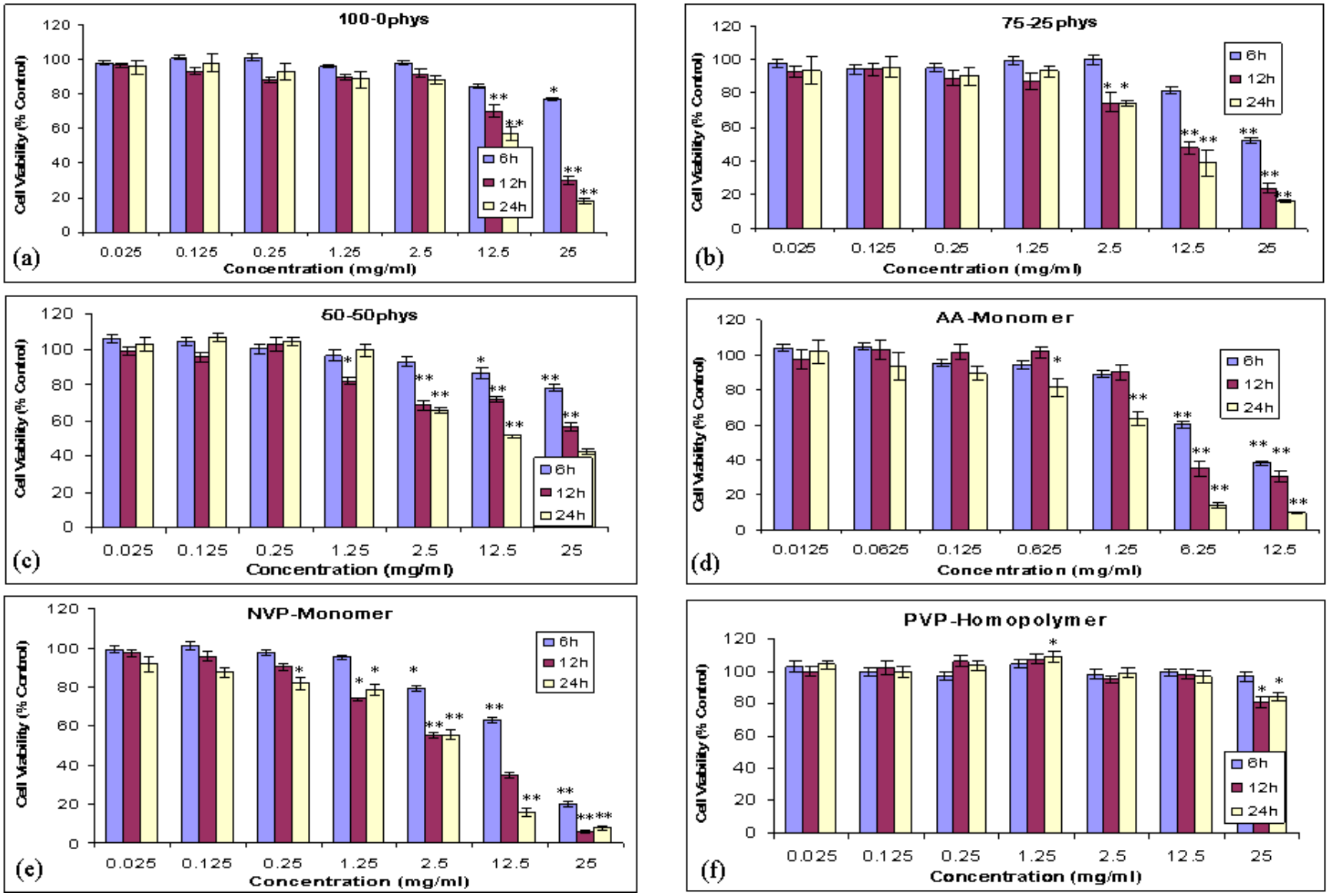

Figure 3.10: Effect of various concentrations of physical hydrogels and monomers on the viability of HepG2 cells following 6, 12 and 24 h exposure at 37°C as assessed in the direct contact assay with MTT endpoint (n=12 ±SEM, * denotes a significant difference from the control **=p<0.01, *=p<0.05).

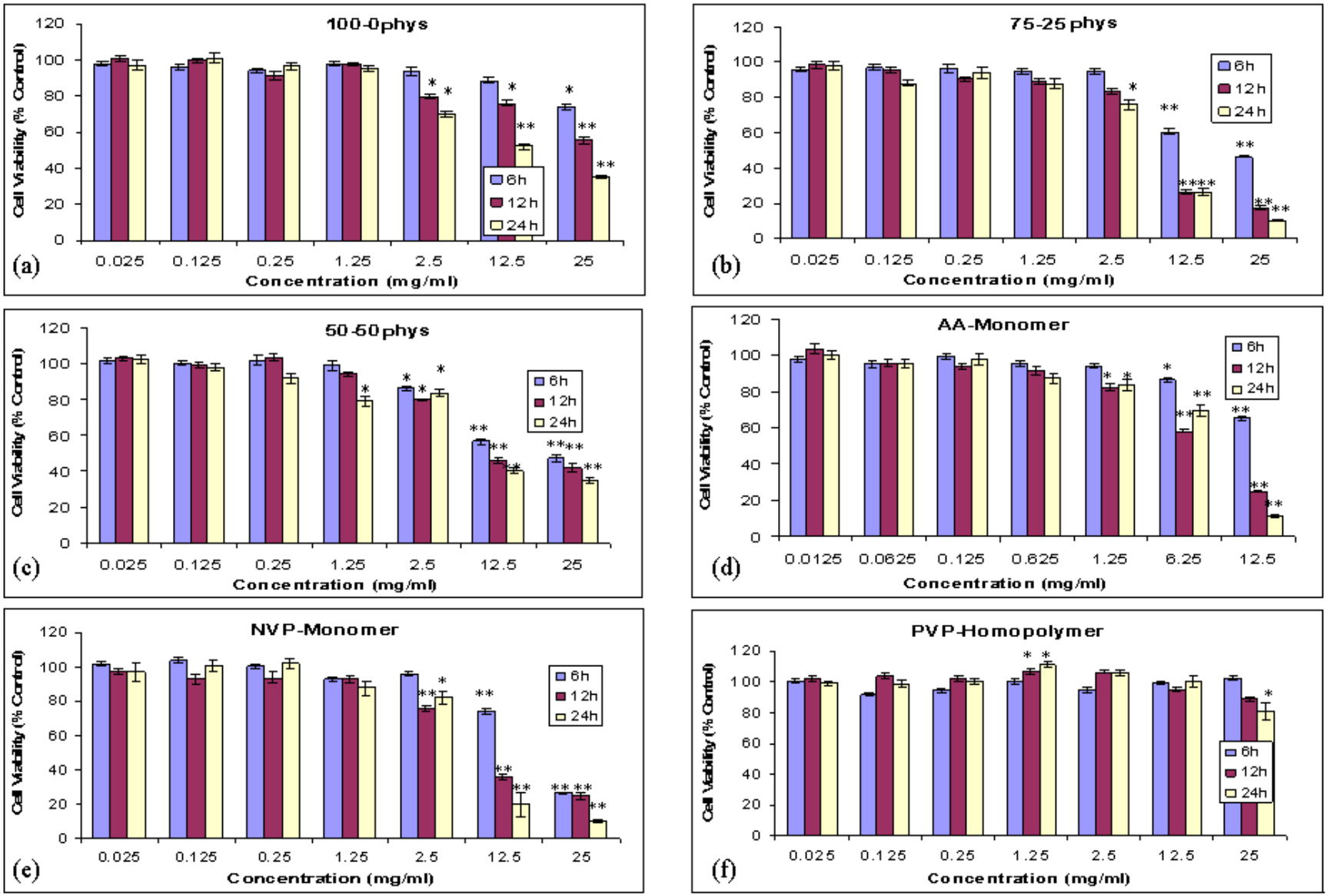

Figure 3.11: Effect of various concentrations of physical hydrogels and monomers on the viability of HCT-8 cells following 6 h, 12 h and 24 h exposure at 37^{o}C as assessed in the direct contact assay with MTT endpoint (n=12 ±SEM, * denotes a significant difference from the control **=p<0.01, *=p<0.05).

The results for the MTT viability assessment of HepG2 and HCT-8 cells following 6, 12, and 24h exposure to physical hydrogel-containing culture medium and the respective control chemicals, AA, NVP and PVP are shown in Figures 3.10 and 3.11. For both cell lines a high degree of reproducibility was achieved as indicated by the relatively small SEM error bars.

In general, both hydrogel samples and the monomeric control chemicals produced a significant time dependent decrease in viability at concentrations ≥1.25 mg/ml. At longer exposure times, a slight but significant ($p<0.05$) inhibition of formazan production was observed at 2.5 mg/ml (Figures 3.10a-e and 3.11a-e). This effect became more pronounced when the concentration was increased to 25 mg/ml, where all tested hydrogel samples induced severe cell death ($p<0.01$). Moreover, the 100-0phys and 75-25phys samples induced the highest level of cell death by reducing the viability values below 20% at the 24 h exposure (Figures 3.10a and b). In comparison, the hydrogel matrices produced with lesser amounts of NVP as base material (50-50phys) were less toxic following 24 h with 25 mg/ml (Figures 3.10c and 3.11c). As expected, both monomeric controls proved to be highly cytotoxic at concentrations above 1.25 mg/ml for AA and 2.5 mg/ml for NVP. Similar to the hydrogel samples, the observed cellular toxicity was time dependent and reached its maximum at the highest exposure concentrations (Figures 3.10d and e, 3.11d and e). At the prolonged exposure times of 12 and 24 h, the AA monomer appeared to be more toxic than the NVP to both cell line systems. The maximum AA concentration tested (12.5 mg/ml) induced highly significant ($p<0.01$) levels of cell death at all time-points tested (Figures 3.10d, 3.11d and e).

In contrast, the PVP homopolymer did not induce severe cytotoxicity to either cell line utilised in this study (Figures 3.10 and 3.11f). In fact, minor cell growth stimulating effects were evident at intermediate concentrations after prolonged exposure times. However, a slight inhibition of cell growth was observed in the form of reduced formazan production at the highest exposure.

Surprisingly, the toxicity profile of all tested hydrogels resembled the trends obtained from the cytotoxic monomeric controls rather than the profile obtained for the biocompatible PVP homopolymer reference control. These findings in turn correlate with the results obtained from HPLC analysis, where high concentrations of monomers were

detected in the hydrogel matrix (Table 3.2). Although the monomers AA and NVP are widely used for the synthesis of polymeric hydrogel synthesis, they have proven to be toxic to both culture systems at the concentrations tested in this study. Several studies have reported the toxicity of the monomer NVP and the potential of the monomer AA to interfere with mitochondrial metabolism (Custodio *et al.,* 1998). Loo-Teck and Swami (2005) attribute the AA toxicity to the acidic nature of the molecule, where the hydrogen of the carboxylic acid group dissociates within the culture medium, thereby altering the pH of the immediate cellular environment. In the present study, however, the pH of the cell culture medium was neutralised with the addition of sterile NaOH prior to cell exposure. Thus, a negative effect on the cell viability resulting from pH changes is questionable in this instance. The monomer NVP has been shown to be toxic in subchronic and long term *in vivo* inhalation studies indicating the liver and the upper respiratory tract as the main target organs (Klimisch *et al.,* 1997a, 1997b). However, a specific mechanism of toxicity remains unknown. In contrast to the monomers, the PVP polymer appeared to be compatible with the cells in culture. This was not surprising as the nontoxic properties of the polymer are well established and described in scientific literature (Scheffner, 1955; Kirch *et al.*, 1972; Robinson *et al*., 1990). PVP has been extensively utilised in the medical field for numerous applications ranging from a blood plasma expander (Honda *et al.,* 1966), extensive use as a pharmaceutical excipient (Albertini *et al.,* 2003) to more complex biomaterials (Tunney and Gorman, 2002). The cytotoxicity of the photoinitiator Irgacure® 184 has also been tested *in vitro* in two previous investigations (Byrant *et al.,* 2000; Williams *et al.,* 2005). Both studies concluded that unreacted Irgacure® 184 is potentially cytotoxic. Williams and his colleagues suggested that the toxicity of the photoinitiator is related to its hydrophobicity and its uptake through the phospholipid bilayer of cellular membranes. Inside the cell, the formation of radicals is believed to result in damage to the cells vital proteins and DNA (Williams *et al.,* 2005).

Only a limited amount of studies have investigated the cytotoxic potential of physical hydrogels in solution. A preliminary investigation by Devine *et al.* (2006) showed that physical hydrogels based on NVP combined with either EGDMA or PEGDMA induced significant cell death to HepG2 cells in the direct contact assay (MTT endpoint). Comparable to the current study, these findings where obtained at a concentration above

2.5 mg/ml and an exposure time of 24 h and the assumption was raised that unpolymerised residues could have caused the cytotoxic effect. Similar results were obtained by Geever *et al.* (2008) following direct exposure of HepG2 cells to physical hydrogels based on varying ratios of NVP and *N*-isopropylacrylamide also using the MTT endpoint. Here a dose-dependent decease in cell viability was obtained following 24 h exposure at concentrations exceeding 1.25 mg/ml.

Overall, in the current study the physical hydrogels appeared to be cytotoxic in a time and dose-dependent manner. Supported by the results obtained during the HPLC analysis (Section 3.1.3.2), it is suggested that unreacted residuals from the base materials (monomers and photoinitiator) may have caused the toxic effects. In respect to the HepG2 and HCT-8 cell lines tested, no cell specific toxicity was evident. Due to the biodegrading properties of the physical hydrogels, no successful procedure for washing the unreacted monomers and possible photoinitiator residuals from the hydrogel networks can be implemented. It appears that a reduction in the toxic residuals may only be achieved via further optimisation of the polymerisation process including enhanced adjustments of photoinitiator ratios.

3.1.4.2 The direct contact assay (neutral red endpoint)

As mentioned earlier, the sensitivity of a cytotoxicity assay differs depending on the mechanisms leading to cell death. In order to obtain a deeper insight into such mechanisms following exposure to the hydrogels, a second cytotoxicity endpoint or viability dye, NR, was employed. Neutral red is a weakly cationic dye that is bound to anionic sites on intracytoplasmic vacuoles and granules. It accumulates in lysosomes and other intracellular vacuoles of living cells. The ability to retain this dye is lost when cells die. Therefore, the NR endpoint seems particularly sensitive to chemicals that have a direct lysosomal effect, whereas the MTT endpoint is more sensitive to mitochondrial cell damage (Weyermann *et al.,* 2005). Once the assay is complete, the NR dye needs to be extracted from the cells and therefore cells are lysed before absorbance is measured at 540 nm. A mixture of 1% glacial acetic acid/50% ethanol proved to be efficient to extract the dye. The direct contac assay puls NR endpoint was performed under similar conditions as the MTT endpoint to obtain comparable results. Again, the physical hydrogels and respective monomers were diluted in

cell culture medium to achieve a representative concentration. As previously mentioned, the AA containing samples were pH neutralised (pH 7.4) using 3M NaOH. The results obtained from the absorbance readings at a wavelength of 540 nm were expressed as a percentage of untreated controls against tested hydrogel extracts. The mean percentage viability of replicate results and SEM were calculated for each cell line.

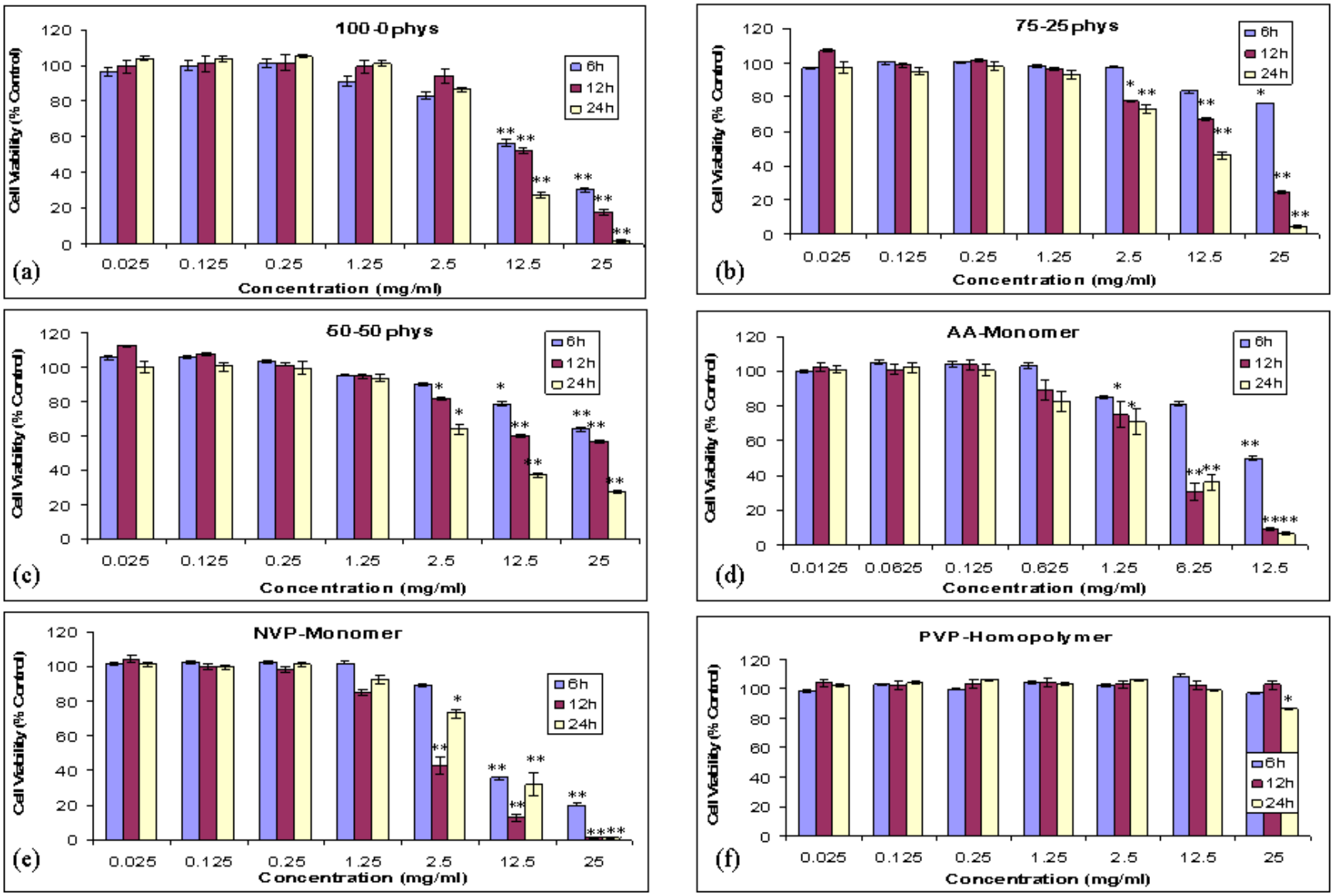

Figure 3.12: Effect of various concentrations of physical hydrogels and monomers on the viability of HepG2 cells following 6, 12 and 24 h exposure at 37°C as assessed in the direct contact assay with the NR endpoint (n=12 ±SEM, * denotes a significant difference from the control **=p<0.01, *=p<0.05).

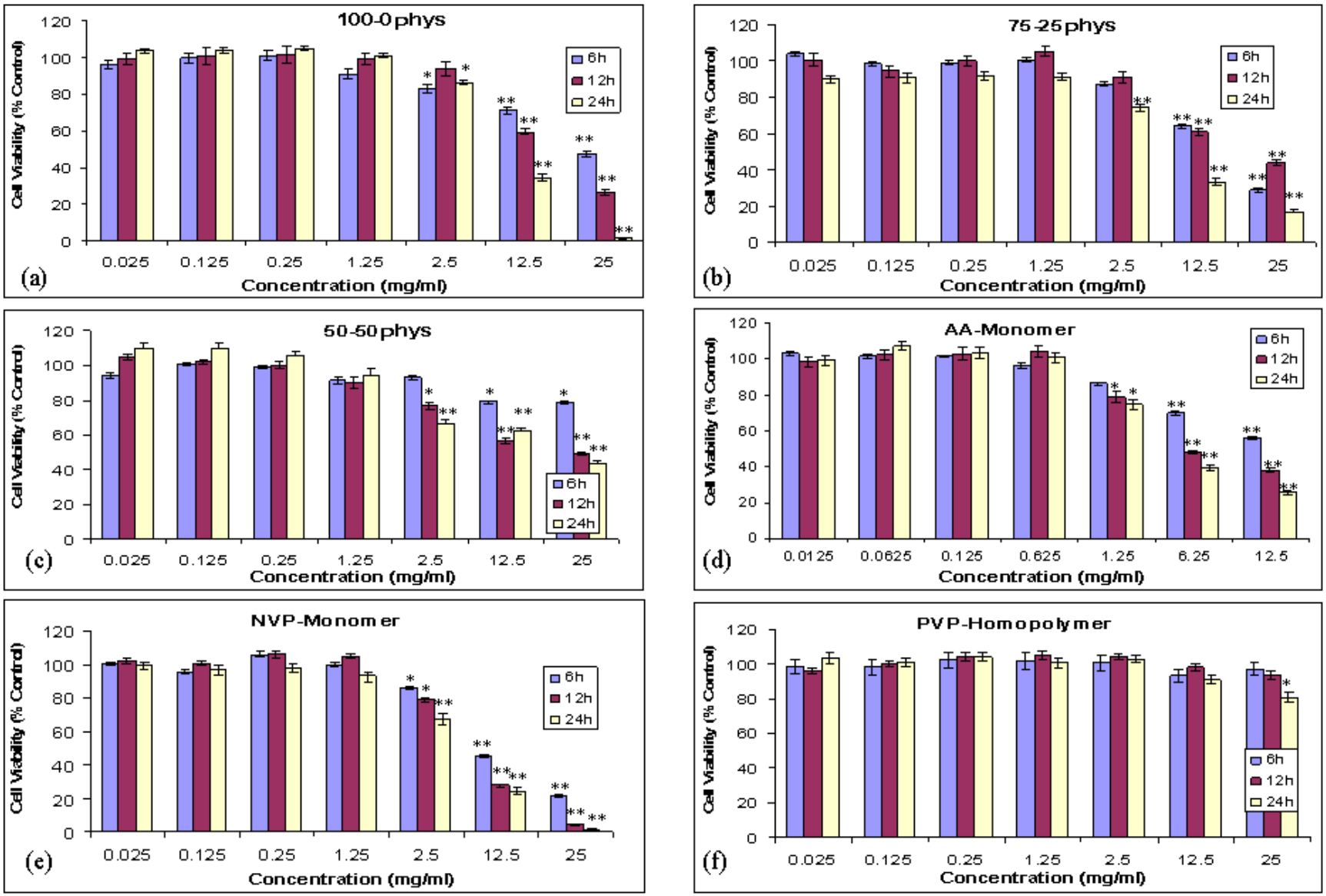

Figure 3.13: Effect of various concentrations of physical hydrogels and monomers on the viability of HCT-8 cells following 6, 12 and 24 h exposure at 37°C as assessed in the direct contact assay with the NR endpoint (n=12 ±SEM, * denotes a significant difference from the control **=p<0.01, *=p<0.05),

The results for the NR viability assessment of HepG2 and HCT-8 cells following 6, 12, and 24 h exposure to physical hydrogel-containing culture medium and respective control chemicals AA, NVP and PVP are shown in Figures 3.12 and 3.13. Similar to the MTT endpoint, a high degree of reproducibility was achieved for both cell lines as indicated by the relatively small SEM values.

The results obtained in the NR assay showed similar trends to those obtained with the previously performed MTT assay, with a dose- and time-dependent reduction in HepG2 and HCT-8 viability observed over the concentration range tested. However, it appeared that the NR was generally more sensitive in detecting the toxic response of the test samples at the highest concentrations and extended exposure times. (Figures 3.10a-c, 3.11a-c, and Figures 3.12a-c, 3.13a-c). More specifically, using the NR endpoint, direct cell exposure to the highest concentration of 100-0phys hydrogels and the respective NVP monomer control almost completely reduced the cell viability and this effect was observed for both the HepG2 and the HCT-8 cell lines (Figures 3.12a and e, 3.13a and e). Again, the hydrogels prepared with the addition of AA as base monomer were slightly less cytotoxic than the gels composed of 100 wt% NVP (Figures 3.12b and c and 3.13b and c). Furthermore, it appeared that the HCT-8 cell line (Figure 3.13b and c) was more resistant to the effect of AA containing hydrogels and the AA monomer than the HepG2 cell line (Figure 3.12b and c). As observed previously in the MTT assay, the exposure of both cell lines to solutions of the PVP-homopolymer led to enhanced cell growth. However, no distinctive proliferation effects were obtained via the NR endpoint and only minor growth inhibitory effects were observed at the highest exposure concentration with prolonged exposure times when compared to the MTT results (Figures 3.10f and 3.11f, Figures 3.12f and 3.13f).

Overall, the results obtained from the NR assay support the findings from the MTT assay. The higher concentrations of the physical hydrogel solutions produced comparable cytotoxic effects in both assays. More specifically, the NR endpoint appeared somewhat more sensitive in detecting cell toxicity. Although this may indicate that certain sub-cellular structures (e.g. lysosomes) were more susceptible to the cytotoxic effects of the test samples than other organelles (e.g. mitochondria), more information is required to elucidate such mechanistic-toxicological implications. Again, the cell exposure to hydrogels resembled the toxicity profiles of the monomeric controls rather than those obtained for the

nontoxic PVP polymer. The need for an enhanced polymerisation process to reduce the amount of unreacted residuals is emphasised.

3.1.4.3 Morphological examination of cells in contact with physical hydrogels

The effect of physical hydrogels and respective monomers on the morphology of HepG2 and HCT-8 cells was also assessed. Microscopic examinations were carried out on cells exposed to 100-0phys and 50-50phys hydrogel solutions prepared in accordance to the previously performed cytotoxicity analysis (Sections 3.1.4.1 and 3.1.4.2). The cell cultures were exposed to hydrogel solutions, AA, NVP, and PVP control chemicals for 24 h at 37°C.

HepG2

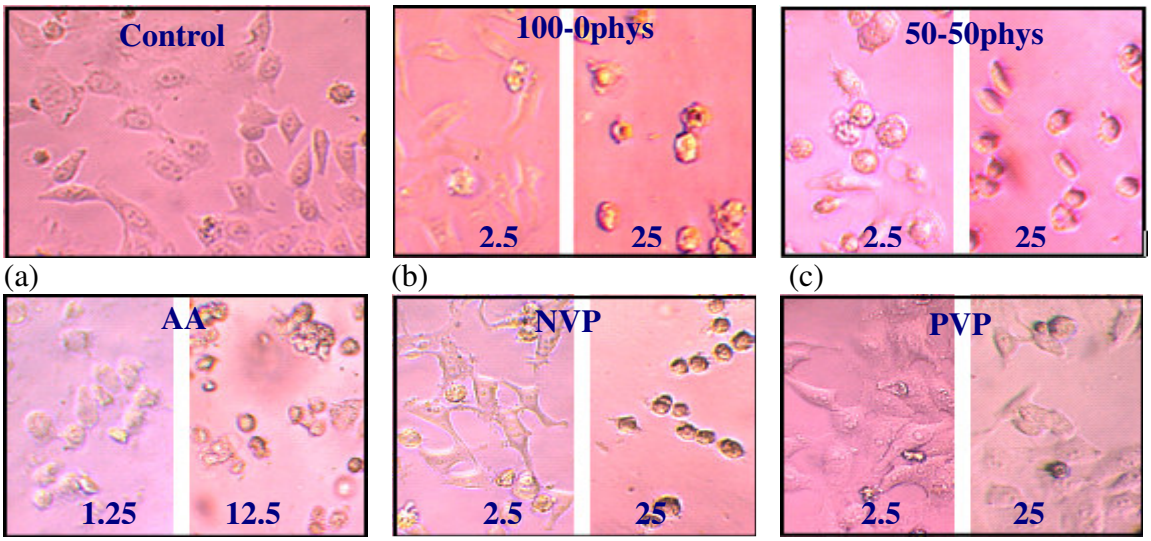

Figure 3.14: Representative images of the morphology of HepG2 cells in direct contact with higher-end concentrations of solubilised physical hydrogels and respective monomers for 24 h. (a) complete culture medium control; (b) 2.5 and 25 mg/ml 100-0phys hydrogel sample; (c) 2.5 and 25 mg/ml 50-50phys hydrogel sample; (d) 1.25 and 12.5 mg/ml AA; (e) 2.5 and 25 mg/ml NVP; (f) 2.5 and 25 mg/ml PVP.

HCT-8

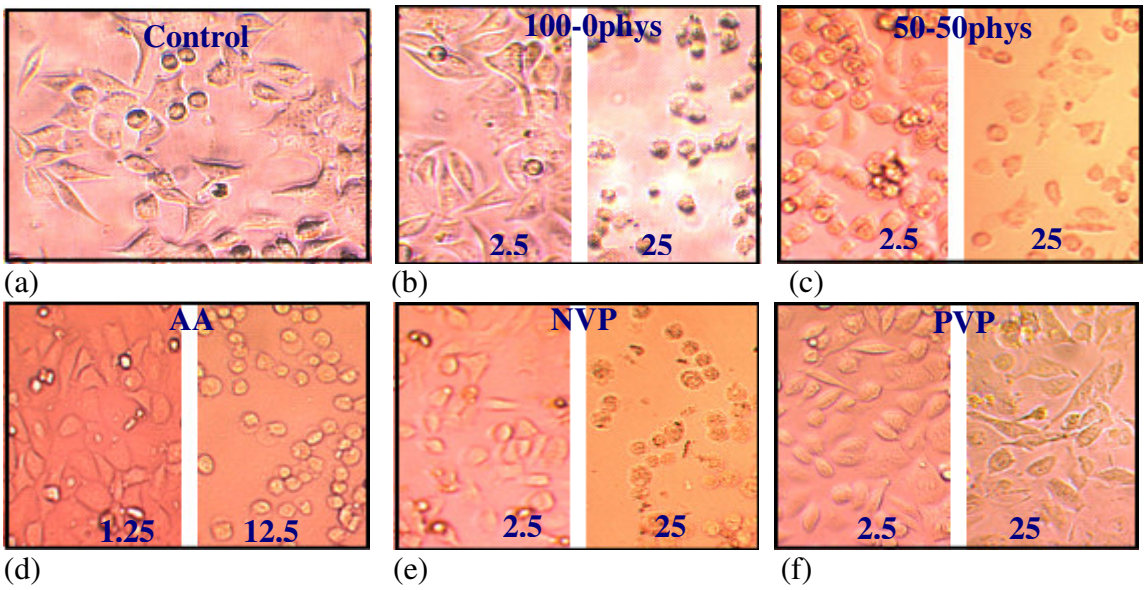

Figure 3.15: Representative images of the morphology of HCT-8 cells in direct contact with higher-end concentrations of solubilised physical hydrogels and monomers for 24 h. (a) complete culture medium control; (b) 2.5 and 25 mg/ml 100-0phys hydogel sample; (c) 2.5 and 25 mg/ml 50-50phys hydrogel sample; (d) 1.25 and 12.5 mg/ml AA; (e) 2.5 and 25 mg/ml NVP; (f) 2.5 and 25 mg/ml PVP.

Figures 3.14 and 3.15 show representative images of the morphology of HepG2 and HCT-8 cells cultured for 24 h in the presence of solubilised hydrogels and monomeric controls. The untreated media controls for the HepG2 and the HCT-8 cells, illustrated in Figures 3.14a and 3.15a, were used as a reference to determine any morphological alterations. In general, the morphology changes of cells exposed to the test material were in accordance with the previously performed MTT and NR cytotoxicity assays. Overall, the majority of HepG2 and HCT-8 cells exposed to the lower concentration of hydrogels (2.5 mg/ml), composed of 100 wt% NVP as base material, were still attached to the culture dish and only minor morphology changes, such as detachment of single cells, occurred (3.14b and 3.15b). In contrast, by increasing the concentration to 25 mg/ml, numerous cells detached and died as indicated by the deteriorated cell monolayer. Residual cells which were still able to attach to the culture dish appeared damaged and rounded. A similar picture was obtained for the cells exposed to NVP monomer (3.14e and 3.15e). In contrast to the previously obtained cytotoxicity data (Figures 3.10-3.12a-c), the hydrogel solutions

containing additional amounts of AA as base monomer proved more detrimental to the cell morphology, even at the lower concentration of 2.5 mg/ml (3.14c and 3.15c). Higher concentrations of AA based hydrogels (25 mg/ml) induced severe cytotoxic effects on both cell lines with only a fragmented cell layer composed of damaged cells remaining. A similar effect was observed following exposure to solutions of AA monomer. The AA concentration of 1.25 mg/ml produced observable changes to HepG2 and HCT-8 cell morphology and increasing the concentration to 12.5 mg/ml proved highly cytotoxic (3.14d and 3.15d). In contrast, cells exposed to similar concentrations of PVP were still attached and appeared healthy (3.14f and 3.15f), thus indicating the homopolymer had no adverse effect on either HepG2 or HCT-8 cell morphology.

Again, these results are in agreement with previously obtained HPLC data during the residual monomer analysis thereby indicating that the presence of unpolymerised residues is reducing the cytocompatibility of physical hydrogels. Although the morphological examination confirmed the results obtained from the MTT and NR endpoint studies, it was not possible to determine any cell-specific or mechanistic toxicity effects.

3.1.5 Genotoxicity evaluation of physical hydrogels and base monomers

Prior to determining the hydrogels' potential to damage DNA, the previously conducted cytotoxicity tests were used to establish an appropriate test concentration range as genetic effects are more relevant if determined at subcytotoxic levels. Indeed, genotoxicity results are not conclusive unless testing has first been performed to determine cytotoxic levels (Gad, 2000). Traditionally, genotoxicity testing has been performed *in vivo*, but with the development of suitable metabolically active *in vitro* test systems, such as mammalian cell cultures and metabolically activated bacterial assays, testing is more frequently performed *in vitro*. *In vitro* genotoxicity assays are appropriate for the rapid and reproducible detection of the genotoxic potential of chemicals. Further advantages of *in vitro* test systems also include their high degree of sensitivity, the ability to ensure adequate exposure to the test substance, the possibility to evaluate cell specific effects and the reduction in animal testing. *In vitro* genotoxicity tests can, thanks to well defined endpoints, also provide a suitable method for elucidating the mode of action of genotoxic substances. Hence, two assay systems evaluating different genotoxic endpoints were used

in the present study. The comet assay and the Ames assay were chosen because they measure different genotoxic endpoints, allowing for a broader assessment of the genotoxic potential of test samples to induce DNA strand breakage and point mutations respectively. As already mentioned, a prerequisite for *in vitro* genotoxicity assessments is the capacity for metabolism, as quite often it is the metabolites of parent compounds that are in fact genotoxic. For instance, a wide range of substances are responsible for damaging genetic material due to the presence of procarcinogens which require metabolic activation (Lu, 1991). To ensure metabolic competence in the comet assay HepG2 cells were employed for the evaluation of physical and chemical hydrogels. As previously mentioned, this cell line retains many of the morphological characteristics of liver parenchymal cells and the major enzyme systems such as cytochrome P450-mixed function oxidases, epoxide hydrolase, glucuronyltransferase, and glutathione transferase, responsible for activating various classes of indirect mutagens (Knasmueller *et al.,* 1998; Duthie and Collins, 1996). The Ames assay was performed with and without the addition of mammalian liver S9 fraction to ensure metabolic competence.

3.1.5.1 The comet assay

The alkaline version of the comet assay is an appropriate method to detect a wide variety of DNA lesions, including DNA strand breaks, alkali labile sites, crosslinks and incomplete repair sites (Tice *et al.,* 2000). In addition, this assay shows clear advantages in its applicability to almost all mammalian cell types and has been previously demonstrated as a fast and sensitive technique for determining the genotoxic potential of polymeric hydrogels using the HepG2 cell line (Devine *et al.,* 2006). Therefore, the alkaline method was chosen in the present study to assess if solutions of physical hydrogels had the potential to induce genetic alterations. The 'percentage tail DNA' and the 'tail moment' (product of the tail length and percentage tail DNA) were the chosen parameters to quantify and compare the level of DNA damage in exposed cells. Although the tail moment is considered to be a sensitive indicator of DNA damage, this parameter is not standardised and tends to be calculated differently by various image analysis software making interlaboratory comparisons difficult (Tice *et al.,* 2000; Collins *et al.,* 2008). Percentage tail DNA covers the widest range of damage and over most of this range it is linearly related to strand break

frequency (Collins *et al.,* 2008). It also has the advantage that it can be standardised and there is increasing emphasis on the use of this parameter as the preferred primary endpoint (Lovell and Omori, 2008). A H_2O_2 concentration range of 10-100 µM was utilised as a positive control to ensure optimal assay conditions. The comet assay was used to assess the DNA damaging potential of solubilised 100-0phys and 50-50phys hydrogels on HepG2 and HCT-8 cells. The test was conducted using solubilised 100-0phys and 50-50phys hydrogels as representative samples. The AA and NVP monomers and the PVP homopolymer, dissolved in culture medium, were used as additional reference chemicals. Cells were exposed to both the hydrogel and reference chemicals for 24 h at a concentration range of 0.025, 0.25 and 2.5 mg/ml, with concentrations exceeding 2.5 mg/ml excluded due to their previously associated cytotoxic potential evaluated in the MTT and NR assays (Section 3.1.4). In the present study, both the mean of the tail moment and percentage tail DNA values were reported for each test sample (Table 3.3), calculated by scoring 50 individual cells per duplicate slides per concentration tested. The box plots illustrated in Figures 3.17 and 3.18 show transformed results obtained from analysing the percentage tail DNA values. The 25-75 percentiles and the median were presented as they are usually highly correlated (Lovell and Omori, 2008) and visualise the distribution of DNA migration values for the cell population under investigation. For the comet assay, the majority of the data obtained was not normally distributed (Anderson-Darling method) and statistical difference between control and treated cells was evaluated with nonparametric tests.

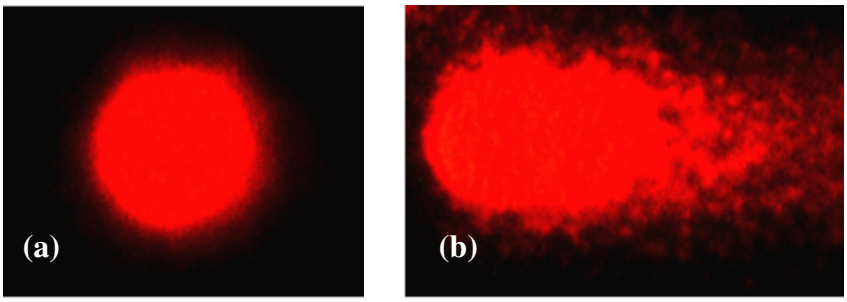

Figure 3.16: HepG2 cell images obtained in the alkaline comet assay following SYBR Gold staining. (a) exposure to 2.5 mg/ml of 100-0phys hydrogel solution for 24 h, (b) exposure to 100 µM H_2O_2 positive control clastogen for 40 min.

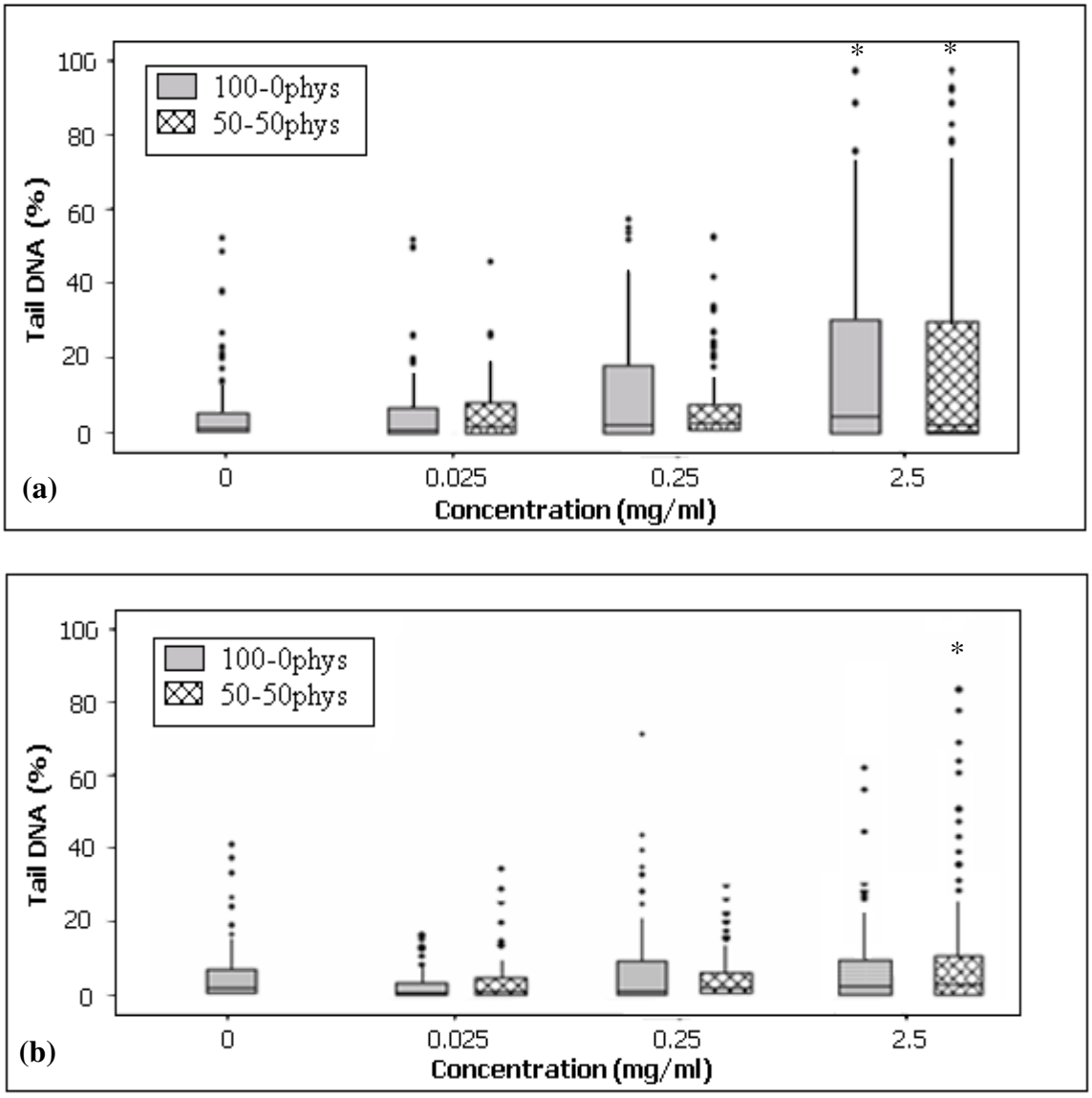

Figure 3.17: Box plot presents percentage tail DNA values of (a) HepG2 cells and (b) HCT-8 cells exposed to increasing concentrations of physical hydrogel solutions for 24 h at 37^{o}C in the comet assay. Each box corresponds to 100 single cells measured on two slides and represents 25-75 percentiles, middle line = median, whisker extends to the maximum/minimum data point within 1.5 box heights from the top/bottom of the box. Dots above and below boxes indicate outliers. * denotes a significant difference from the control ($p<0.05$).

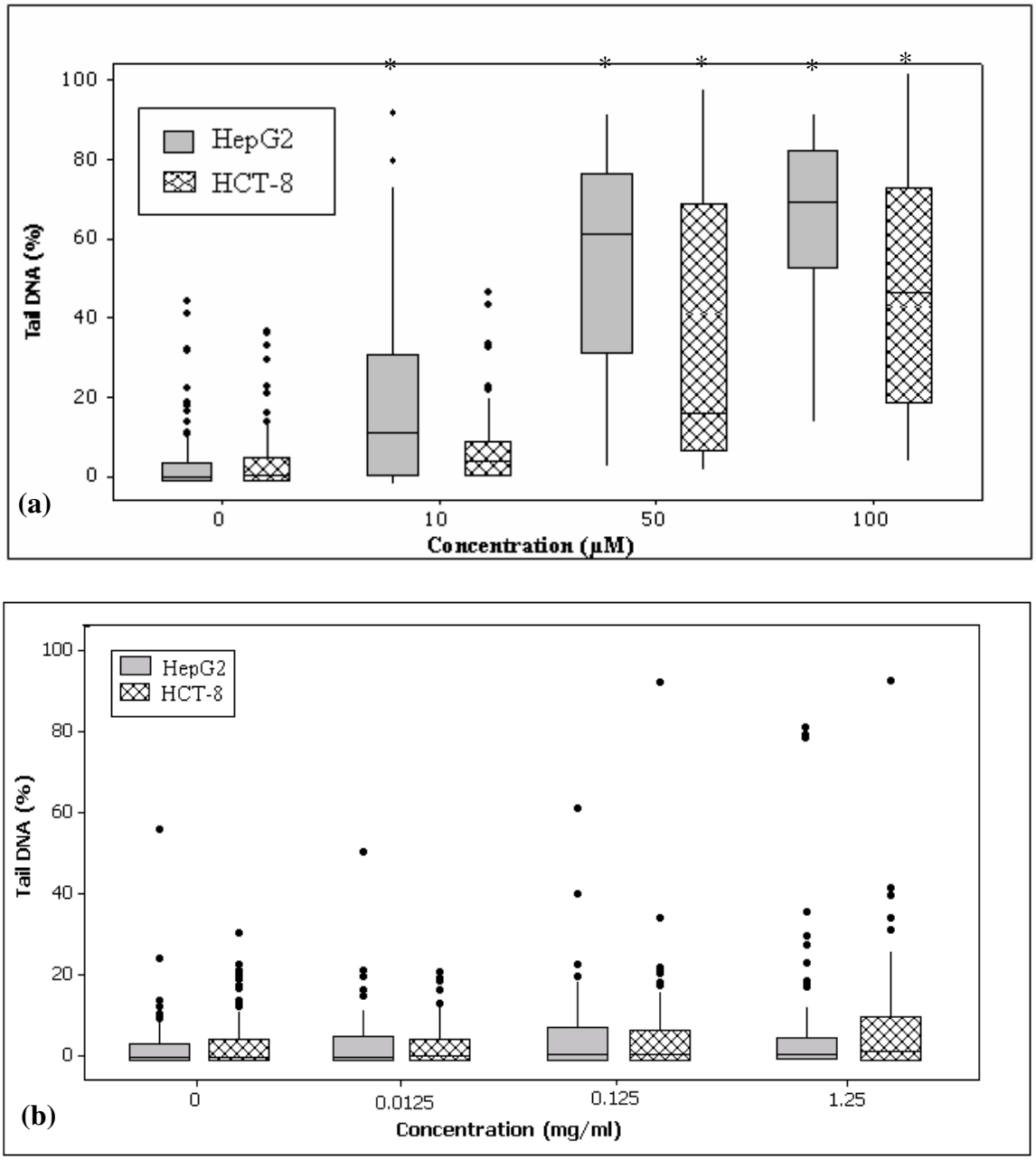

Figure 3.18: Box plot presents percentage tail DNA values of HepG2 and HCT-8 cells exposed to increasing concentrations of (a) the positive control H_2O_2 for 40 min at 4°C and (b) AA for 24 h at 37°C in the comet assay. Each box corresponds to 100 single cells measured on two slides and represents 25-75 percentiles, middle line = median, whisker extends to the maximum/minimum data point within 1.5 box heights from the top/bottom of the box. Dots above and below boxes indicate outliers. * denotes a significant difference from the control ($p<0.05$).

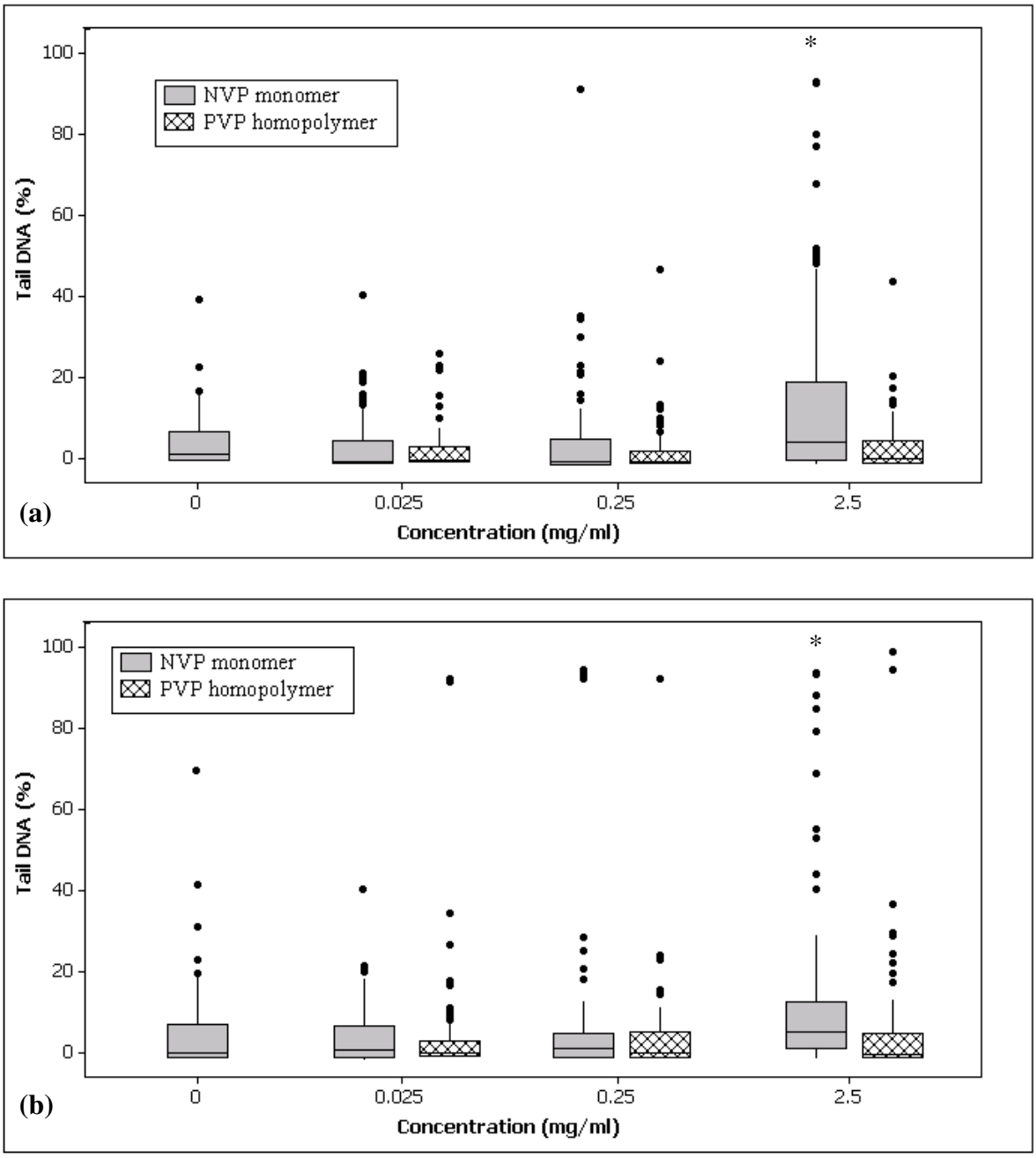

Figure 3.19: Box plot presents percentage tail DNA values of (a) HepG2 cells and (b) HCT-8 cells exposed to increasing concentrations of NVP monomer and PVP homopolymer solutions for 24 h at 37^{o}C in the comet assay. Each box corresponds to 100 single cells measured on two slides and represents 25-75 percentiles, middle line = median, whisker extends to the maximum/minimum data point within 1.5 box heights from the top/bottom of the box. Dots above and below boxes indicate outliers. * denotes a significant difference from the control ($p<0.05$).

Table 3.3: Mean tail moment and mean percentage tail DNA obtained in the comet assay after exposure of HepG2 and HCT-8 cells to increasing concentrations of physical hydrogels, AA, NVP and PVP solutions for 24 h and increasing concentrations of H_2O_2 for 40 min. Results shown are the mean (±SEM) of 100 single cells from duplicate slides. * denotes a significant difference from the untreated control ($p<0.05$).

	HepG2 Cells		HCT-8 Cells	
Sample (mg/ml)	**Tail moment** (±SEM)	**% Tail DNA** (±SEM)	**Tail moment** (±SEM)	**% Tail DNA** (±SEM)
Control	0.65 (±0.13)	4.66 (±0.87)	0.55 (±0.09)	4.66(±0.74)
Phys 100-0				
0.025	0.65 (±0.12)	4.35 (±0.79)	0.27 (±0.05)	2.10 (±0.35)
0.25	1.20 (±0.16)	10.11 (±1.36)	0.70 (±0.11)	6.15 (±1.05)
2.5	2.01 (±0.27) *	15.71 (±1.96) *	1.43 (±0.12)	8.75 (±1.10)
Phys 50-50				
0.025	0.61 (±0.09)	4.40 (±0.65)	0.36 (±0.06)	3.12 (±0.53)
0.25	0.57 (±0.11)	4.84 (±0.81)	0.46 (±0.07)	3.73 (±0.59)
2.5	2.54 (±0.48) *	15.25 (±2.31) *	1.77 (±0.32)*	11.29 (±1.82) *
AA				
0.0125	0.59 (±0.12)	3.69 (±0.64)	0.79 (±0.12)	3.46 (±0.65)
0.125	0.58 (±0.11)	5.33 (±1.11)	0.86 (±0.37)	5.60 (±1.10)
1.25	1.03 (±0.15)	6.88 (±1.64)	1.45 (±0.33)	7.39 (±1.23)
NVP				
0.025	0.55 (±0.10)	3.86 (±0.68)	0.63 (±0.08)	4.57 (±0.59)
0.25	0.67 (±0.13)	5.38 (±1.19)	0.85 (±0.18)	6.70 (±1.65)
2.5	2.25 (±0.40)	14.75 (±2.13)	2.88 (±1.02)	13.20 (±2.11)
PVP				
0.025	0.36 (±0.06)	2.63 (±0.40)	0.51 (±0.13)	4.72 (±1.38)
0.25	0.37 (±0.10)	3.02 (±0.98)	0.72 (±0.24)	6.04 (±1.41)
2.5	0.59 (±0.12)	4.68 (±1.09)	1.08 (±0.31)	7.18 (±1.75)
H_2O_2 (µM)				
10	3.46 (±0.40) *	20.49 (±2.12) *	0.98 (±0.14)	6.95 (±0.96)
50	14.98 (±1.23) *	55.93 (±2.70) *	9.00 (±1.34) *	32.55 (±3.45) *
100	16.23 (±1.42) *	65.58 (±1.84) *	12.08 (±1.96) *	42.91 (±3.04) *

The results for physical hydrogels following exposure of HepG2 and HCT-8 cells in the alkaline comet assay are illustrated in Figure 3.17. For comparative purposes, the comet assay results obtained from cell exposure to the positive control chemical H_2O_2 and the AA monomer are illustrated in Figure 3.18. The effects of the NVP monomer and the PVP

homoploymer are also displayed in Figure 3.19. The results are further summarised in Table 3.3. Both hydrogel types caused a slight elevation in DNA migration values with the HepG2 cells appearing more sensitive to DNA strand breakage than HCT-8 cells. Concentrations of solubilised physical hydrogels below 2.5 mg/ml did not induce DNA damage as both of the evaluated DNA migration parameters did not significantly differ from the untreated control. In contrast, the only significant levels of DNA damage, when compared to untreated control cell values, occurred following exposure to the solubilised hydrogels and the monomer sample at concentrations higher than 2.5 mg/ml. More precisely, a three to five fold increase in mean tail moment values and a three fold increase in mean percentage tail DNA values compared to untreated cells were obtained (Table 3.3). The reference solution containing NVP monomer also induced similar DNA migration values as obtained for the hydrogel solutions. Here, significant DNA tailing was observed for concentrations higher than 2.5 mg/ml. Increasing concentrations of the AA monomer solution also lead to a slight increase in DNA migration although this was not found to be statistically relevant for the dose range tested (0.0125-1.25 mg/ml).

Interestingly, these findings are somewhat similar to those previously reported, where HepG2 cells were exposed to solubilised NVP based physical hydrogels containing 0.1 wt% EGDMA over a concentration range of 0.25-25mg/ml for 3 h (Devine *et al.,* 2006). This study reported a four to six fold increase in tail moment values compared to untreated cells. In the current study, 2.5 mg/ml concentrations of copolymeric hydrogels based on a mixture of NVP and AA monomers were found to produce a slightly increased DNA tailing effect compared to those solely made from NVP at 2.5 mg/ml.

However, these results need to be interpreted cautiously. For the higher concentrations tested within the comet assay, both the hydrogels and the monomeric control solutions significantly reduced the viability of the treated cells. Within the conducted trypan blue exclusion method the reduction was found to be close to, or even slightly below the recommended viability value of 80%. It is known that the comet assay can be sensitive to nongenotoxic cell killing and in some cases it can be difficult to distinguish between direct, chemically-induced genotoxicity and DNA damage that occurs secondary to chemically induced cytotoxicity (Hartmann and Speit, 1997). It has also been shown that necrotic cells produce strand breaks by unspecific nuclease degradation that can

increase the overall DNA migration values (Tice *et al.,* 2000; Morley, 2006; Collins *et al.,* 2008). Also the presence of cells undergoing earliest stages of apoptosis induced by a cytotoxic insult can lead to highly elevated DNA migration measurements on single cells, where the DNA is ultimately broken down into nucleosome sized pieces (Choucroun *et al.,* 2001; Collins *et al.,* 2008).

In this study, it is believed that the significant increase in mean DNA migration values for hydrogel and monomer treated cells was a result of the cytotoxic potential of the residual monomers rather than an active genotoxic mechanism. This belief is strengthened by the fact that the 24 h exposure to hydrogel concentrations of 2.5 mg/ml led to a slight but significant reduction in cell viability in the previously performed MTT and NR assays (Figures 3.12 and 3.13). Such cytotoxicity data is similar to effects observed in the comet assay, with the addition of AA as base monomer, the cytotoxic potential of the hydrogels was enhanced at this particular concentration. Furthermore, the distribution of percentage tail DNA values observed for the hydrogel and monomeric control treatments are indicative of a cytotoxic insult. The results obtained for the higher-end concentrations in Figures 3.17 and 3.19, show a widely distributed range of percentage tail DNA while numerous outliers were observed. Here the box plots revealed that most of the measured cells did not experience a substantial DNA tailing effect with the median values been comparable to values obtained for untreated control cell populations. However, the elevated 75 percentile values and the numerous outliers observed for cells exposed to concentrations of hydrogels and monomers above 2.5 mg/ml indicate that the DNA for a minority of cells was highly fragmented. This in turn resulted in the formation of the significantly increased mean tail moment values. The possibility that single cells underwent necrotic processes that led to enhanced DNA migration was also substantiated via direct microscopic observation. The majority of cells within a treated cell population appeared undamaged while a small number of fragmented cells were present.

As expected the PVP homopolymer, used as a control reference due to its well described biocompatibility (Robinson *et al.*, 1990; Wan *et al.,* 2005), did not induce any elevated DNA migration compared to untreated control cells (Figure 3.19 and Table 3.3). In contrast, the clastogenic agent H_2O_2 proved to be a useful positive control in the present study as shown in the Figure 3.18a and summarised in Table 3.3. With increasing

noncytotoxic doses of H_2O_2 (10 µM, 50 µM and 100 µM) at an exposure time of 40 min, a significant dose-dependent increase in DNA damage was observed for both cell lines. The HepG2 cells proved to be slightly more susceptible than the HCT-8 cells especially to lower concentrations of the established clastogen. Furthermore, both of the evaluated DNA damage parameters (tail moment and percentage tail DNA) proved sensitive for the detection of DNA migration and resulted in similar trends. This observation is in accordance with previous investigations using mammalian cells in culture as it is well documented that H_2O_2 generates DNA strand breaks at concentrations as low as 10 µM while exposed for less than 60 min and produces a clear dose effect relationship at higher concentrations (McNamee *et al.,* 2000; Petersen *et al.,* 2000; Diaz-Llera *et al.,* 2002). H_2O_2 is able to penetrate freely across cell membranes and single and double DNA strand breakages are the predominate lesion caused by exposure to this agent (Collins *et al.,* 1997; Barbouti *et al.,* 2002; Ito *et al.,* 2005). Indeed, the species expected to be mainly responsible for the DNA damage is the hydroxyl radical (·OH) which possibly generated during intra- or extracellular redox cycling of the parent compound by free or cell-bound transition metals (Spencer *et al.,* 1995; Diaz-Llera *et al.,* 2002; Kawanishi *et al.,* 2001; Ohshima, 2003; Ito *et al.,* 2005). Overall, the results obtained from H_2O_2 exposure confirmed that the assay conditions were appropriate.

3.1.5.2 The Ames mutagenicity test

As DNA damage can result via several mechanisms, no single *in vitro* based test assay is capable of detecting all relevant genotoxic/mutagenic agents. The transformation of primary DNA damage into a permanent gene-mutation is usually not an immediate process, requiring the replication or fixation of such damaged DNA and is consequently undetectable via the comet assay. Furthermore, a genotoxic effect in the comet assay, if successfully repaired, may not be directly related to mutagenesis and carcinogenesis. As mentioned before, DNA effects in the comet assay can be based on various types of DNA damage with neither the shape of the comet nor the extent of DNA migration reflecting the actual mutagenic potential of a chemical (Collins, 2004). Therefore, further studies exploring the mutagenic potential of the hydrogels were evaluated with the Ames

mutagenicity test, which remains one of the most widely used tests for assessing the mutagenic properties of chemicals.

The Ames assay is one of the most widely used gene mutation test and is routinely used as a screening agent to identify possible carcinogens due to the high correlation between mutagenicity and carcinogenicity (Williams *et al.,* 2000). The mutagenic potential of solubilised physical hydrogels was assessed with the Ames II^{TM} Mutagenicity test, a microtiter modification of the Ames assay (Flueckiger-Isler *et al*., 2004). The *S. typhimurium* strain TA98 and a strain mixture of TA7001-TA7006 (TAMix) were chosen to detect the ability of the test material to introduce DNA base-pair substitutions and frame shift mutations. To facilitate comparison with the comet assay, the mutagenic potential of physical hydrogels prepared via photopolymerisation of 100 wt% NVP and 50-50 wt% NVP-AA was also evaluated via the Ames assay. A concentration range of 0-2.5 mg/ml of the solubilised polymers was used as this proved to be noncytotoxic to the bacterial strains as evaluated via the prescreen test (Section 2.5.2.1). All chemicals were exposed for 90 min to approximately 10^7 bacteria cells allowing for two cell divisions as recommended by the manufacturer. Bacterial cell exposure was performed in the presence and absence of liver S9 fraction using respective positive control chemicals (in the absence of S9 the positive control used was 4-NQO:2-NF 500:2000 ηg/ml and in the presence of S9 the positive control used was 2-AmAn 125 μg/ml). The average number of wells containing revertants, as indicated by a change in the colour of indicator medium, was calculated.

Figure 3.20 and Table 3.4 illustrate the observed reversion events obtained following 90 min exposure of *S. typhimurium* TA98 and TAMix strains (±S9) to increasing concentrations of physical hydrogel solutions, control monomers and the positive control chemicals. Figure 3.20 illustrates that exposure to the tested hydrogels did not result in a significantly elevated reversion response for any of the strains tested (±S9) as the mean values of positive wells were found to be within the range of the untreated control i.e. not exceeding a value of 3 for both the negative control and tested hydrogel extracts. Also, no significant difference between the obtained reversion rates of bacteria cells exposed to hydrogels made from NVP as the base monomer and those produced from NVP and AA was established. Also, the tested monomer solutions of NVP and AA did not induce any mutagenic effects in the Ames assay at the concentrations tested. Therefore, it can be

concluded that neither the hydrogel, nor the monomers induced any mutagenic activity on the strains used. This is in agreement with the comet assay where no genotoxicity of the hydrogels and the tested monomer control solution was determined (Table 3.3) and the elevated DNA migration values were believed to stem from the cytotoxic potential of unpolymerised residuals. In contrast to the cytotoxicity analysis, the residual monomer concentration within the hydrogels did not seem to affect the gels' mutagenic potential.

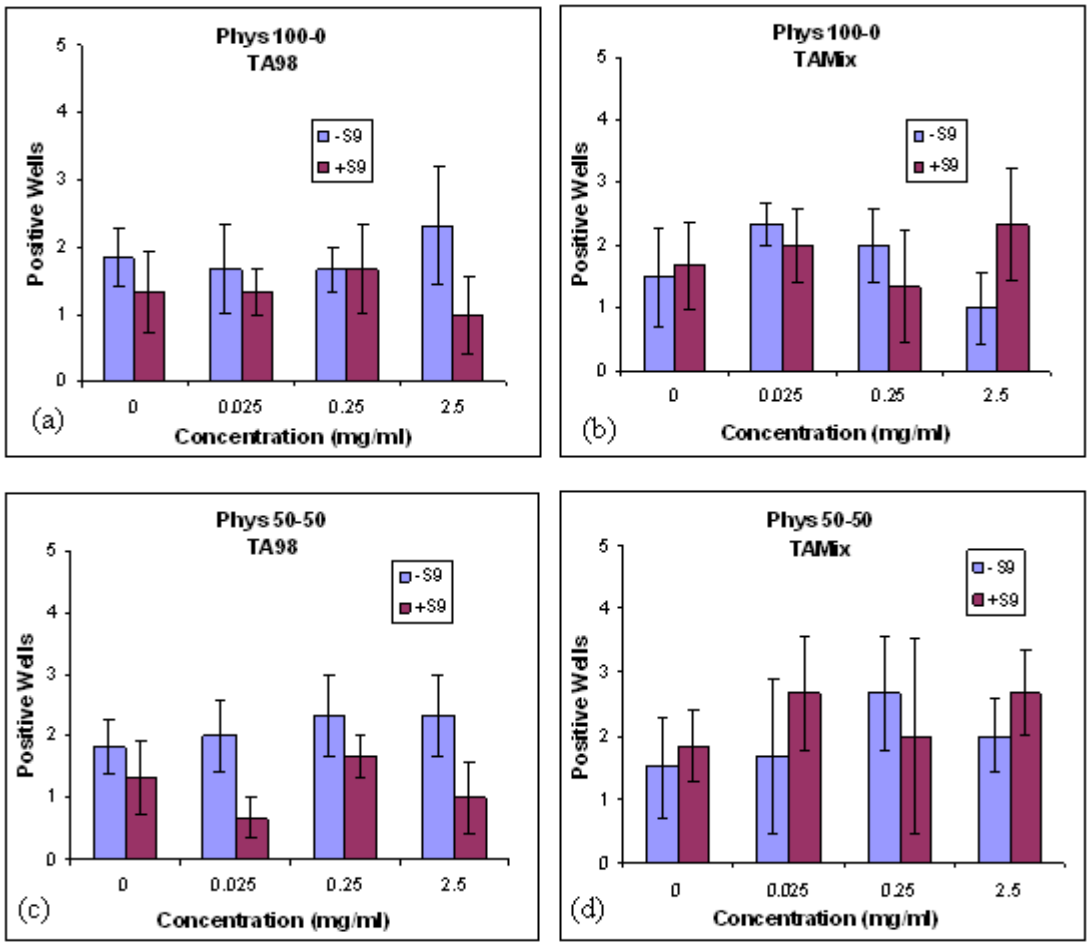

Figure 3.20: Reversion events observed following exposure of *S. typhimurium* strains to (a and b) 100-0phys and (c and d) 50-50phys sample. Results are a mean from three independent experiments (±SEM).

Table 3.4: Mean values of positive wells obtained from three independent experiments (±SEM) via the Ames mutagenicity assay following 90 min exposure to physical hydrogel solutions and positive control chemicals. * denotes a significant difference from the untreated control (0 mg/ml) ($p<0.05$).

Sample (mg/ml)	TA98 (±SEM)		TAMix (±SEM)	
	-S9	+S9	-S9	+S9
100-0phys				
0	1.83 (±0.43)	1.33 (±0.59)	1.50 (±0.79)	1.67 (±0.70)
0.025	1.67 (±0.66)	1.33 (±0.33)	1.33 (±0.88)	2.00 (±0.58)
0.25	1.67 (±0.33)	1.67 (±0.66)	2.00 (±0.58)	1.33 (±0.88)
2.5	2.33 (±0.88)	1.00 (±0.58)	1.00 (±0.58)	2.33 (±0.88)
Positive control	46.67 (±1.33)*	45.33 (±0.88)*	48.00 (±0.00)*	44.67 (±1.48)*
50-50phys				
0	1.67 (±0.47)	1.33 (±0.59)	1.67 (±0.88)	1.83 (±0.57)
0.025	2.00 (±0.58)	0.67 (±0.33)	1.67 (±1.20)	2.67 (±0.88)
0.25	1.67 (±0.66)	1.67 (±0.33)	2.67 (±0.88)	2.00 (±1.53)
2.5	2.33 (±0.66)	1.00 (±0.58)	2.00 (±0.58)	2.67 (±0.66)
Positive control	45.67 (±0.66) *	44.67 (±1.45)*	48.00 (±0.00) *	44.33 (±1.45)*
AA				
0	2.67 (±1.20)	0.33 (±0.33)	2.00 (±1.15)	3.00 (±1.00)
0.0125	1.33 (±0.33)	2.00 (±1.15)	1,67 (±0.33)	0.33 (±0.33)
0.125	1.33 (±0.66)	2.33 (±1.20)	2.67 (±1.20)	1.67 (±0.88)
1.25	0.00 (±0.00)	2.00 (±0.58)	2.00 (±1.53)	3.00 (±1.00)
Positive control	41.33 (±1.45)*	37.33 (±0.88)*	46.33 (±0.88)*	39.00 (±1.15)*
NVP				
0	2.00 (±0.58)	1.67 (±0.88)	2.00 (±0.58)	2.33 (±0.62)
0.025	1.67 (±0.33)	1.00 (±0.33)	1.33 (±0.47)	2.67 (±0.58)
0.25	1.33 (±0.47)	2.33 (±0.88)	2.33 (±0.33)	1.00 (±0.58)
2.5	2.67 (±0.33)	2.00 (±1.53)	1.00 (±0.58)	1.67 (±0.88)
Positive control	47.67 (±0.33)*	43.67 (±0.88)*	47.00 (±1.00)*	46.33 (±1.48)*
PVP				
0	1.33 (±0.33)	1.67 (±0.66)	1.67 (±0.88)	3.67 (±0.33)
0.025	0.00 (±0.00)	2.33 (±0.88)	1.33 (±0.44)	2.33 (±0.88)
0.25	1.33 (±0.47)	2.00 (±0.58)	1.33 (±0.33)	2.00 (±0.58)
2.5	1.00 (±0.58)	1.00 (±0.58)	2.33 (±0.33)	1.67 (±0.33)
Positive control	47.00 (±1.00) *	44.67 (±1.45)	48.00 (±0.00) *	39.33 (±1.45)

These results also correlate with previous findings of Simmon and Baden (1980) and Knapp *et al.* (1985), who found that the NVP monomer did not result in any mutagenic activity in the Ames assay. Regarding the mutagenicity of the polymerised NVP, Zeiger *et al.* (1987) conducted *in vitro* mutagenicity studies on the PVP homopolymer using the Ames Assay and found that PVP was also without mutagenic activity.

To date, the genotoxic potential of the AA monomer has been questionable due to conflicting results obtained using a range of assays with different genotoxicity endpoints. In accordance with the findings of the present study, AA was also found to be nonmutagenic in an Ames assay performed by Cameron *et al.,* (1990). However, as previously mentioned the chemical did prove to be weakly positive in a chromosome aberration assay and in the *in vitro* mouse lymphoma cell assay (Johannsen, 2008).

As shown in Table 3.4, the concurrent positive controls demonstrated the sensitivity of the assay and the metabolising activity of the S9 liver preparations. The induced reversions rate exceeded a value of 41 mean positive wells in the absence of S9 liver homogenate and a value of 37 in the presence of S9 for all strains tested.

3.1.8 Summary

Physical hydrogels were synthesised via free radical photopolymerisation utilising various ratios of NVP and AA as base monomers. The photoinitiator Irgacure® 184 was added to start the polymerisation reaction upon controlled UV light radiation, allowing phase changes from liquid monomer blend to the solid and glass like xerogels to take place. However, by increasing the amount of AA in the initial monomeric feed ratio, the surface of the xerogel started to deteriorate progressively and the matrices synthesised with the addition of 75 wt% AA appeared moist. The FTIR spectra of the dehydrated hydrogels indicate that polymerisation had taken place, although the presence of unpolymerised monomeric residuals could not be excluded. Hence, reverse phase HPLC analysis of physical hydrogel solutions was undertaken to estimate the residual monomer content and thereby indirectly assess the photopolymerisation efficiency. Although the tested hydrogels visually appeared successfully polymerised, a considerable amount of undesired residual monomers were present in their physical networks. Swelling and degradation studies conducted in PBS at 37^{o}C revealed different physical properties for the hydrogels with

varying monomeric feed ratios. After an initial and short swelling period, the physical gels degraded and finally dissolved into the swelling medium. It was found that a higher NVP base content led to reduced swelling but faster dissolution rates. In contrast, the incorporation of AA as a second base compound led to elevated swelling ratios. Devine *et al.* (2003) reported that this enhanced swelling can be influenced by the pH of the swelling medium and therefore suggested that these gels may be suitable as gastric drug delivery devices. Reverse phase HPLC analysis of physical hydrogel solutions was undertaken to estimate the residual monomer content and thereby indirectly assessing the photopolymerisation efficiency. Although the tested hydrogels visually appeared successfully polymerised, a considerable amount of undesired residual monomers were present in their physical networks.

The cytotoxic potential of the solubilised hydrogels was investigated via exposure to suitable *in vitro* cell culture systems using MTT and NR endpoints and cell morphological examinations. The base monomers and the commercially available and biocompatible PVP homopolymer were used as reference chemicals. For both endpoints, a highly significant concentration and time-dependent decrease in cell viability was observed. Comparison of the cytotoxicity data with reference chemicals suggests that the obtained loss in cell viability may have been a result of the presence of residual unpolymerised substances within the physical networks.

The hydrogels' and the monomers' potential to cause genotoxicity *in vitro* was evaluated using the alkaline comet assay with the same cell lines used for the cytotoxicity assessment and by the Ames II^{TM} mutagenicity test in the absence and presence of metabolic activation. The highest concentration of physical hydrogel and NVP monomer solution tested in the comet assay resulted in a slight but significant increase in DNA migration. However, this effect was believed to be exerted by their cytotoxic potential rather than through an active genotoxic mechanism. The Ames II^{TM} assay did not reveal any mutagenic potential for either physical hydrogels nor for the tested monomer control solutions. It appears that, in the case of the physical hydrogels, further optimisation of the polymerisation process is required in an attempt to decrease the amount of residual unreacted material and thus enhance the biocompatibility of the networks. Bearing this in mind, it must be stated that *in vitro* models tend to be highly sensitive and specific thereby

presenting an isolated environment unlike that which exists *in vivo*. Transformed cell lines are isolated routes of uptake so factors which influence the pharmacokinetics/toxicokinetics of a test agent (absorption, distribution, metabolism and excretion) are not always fully addressed (Hawksworth, 1994). In addition, those cell lines cannot fully demonstrate the differentiated functions of cells *in vivo*. Thus, on one side, adverse effects could be exaggerated due to concentration effects and the absence of protective mechanisms present in an intact body system. Conversely, there is always the possibility to overlook potentially adverse effects due to a lack of target elements in *in vitro* tests systems.

3.2 Synthesis, characterisation and biocompatibility of chemically crosslinked *N*-vinyl-2-pyrrolidone – acrylic acid based hydrogels

3.2.1 Preface

Chemical hydrogels are composed of covalently crosslinked three-dimensional polymer networks. In contrast to physical hydrogels, chemical hydrogels will not degrade when being placed in water or other organic solvent unless the covalent bonds can be broken by chemical or physical cleavage processes (LaPorte, 1997). Due to their hydrophilic nature chemical hydrogels will absorb water within their network and hence achieve much higher swelling ratios than physical gels. In their hydrated form, chemical hydrogels express an overall soft consistency which resembles natural living tissue more than any class of synthetic biomaterial, and when used within the human body, this property minimises irritation to the surrounding tissue (Peppas *et al.,* 2000). Furthermore, when in contact with body fluids, their hydrophilic surfaces prevent proteins and cells from adhering to the hydrogels, another property which contributes to their biocompatibility (Hennink and van Nostrum, 2002).

Because of these characteristics and the possibility to incorporate an active pharmaceutical ingredient within the hydrogels' network, chemical hydrogels have found widespread application in the medical sector. They have been used in numerous applications including contact lenses, support for artificial organs, matrices for cell-encapsulation, wound healing devices and as a diverse range of drug delivery devices (Peppas *et al.,* 2000; Hoffman, 2002; Hamidi *et al.,* 2008).

Two different approaches are often used to introduce covalent crosslinks in the polymeric networks. Firstly, chemical gels can be prepared by using typical organic synthesis whereby functional groups of the hydrogel polymers itself are used to form covalent crosslinks, or secondly, with the introduction of a bi- or multifunctional chemical crosslinking agents (Park *et al.,* 1993). A chemical crosslinker contains two or more reactive functional groups which joins the molecular components of the hydrogel polymers by covalent bonding (Hennink and van Nostrum, 2002). The efficiency of the crosslinker depends on the specificity of the functional polymer groups towards particular groups present in the crosslinker. Also, the molecular size of the crosslinking agent can vary

widely and is believed to play an important role in the resulting hydrogel's strength and its swelling characteristics (Park *et al*., 1993). Indeed, changing the degree of crosslinking has been used to tailor the desired mechanical properties of hydrogels. For instance, increasing the degree of crosslinking in the system will result in a stronger consistency for the swollen hydrogel (Jiang *et al.,* 1999). However, a high degree of crosslinking creates a more brittle gel structure. Hence, there is an optimum degree of crosslinking which leads to the formation of a relatively strong and yet elastic chemical hydrogel. Copolymerisation has also been used to influence the mechanical properties. Incorporation of a comonomer often contributes to a stronger hydrogel consistency by the introduction of additional hydrogen bonds (Peppas *et al.,* 2000).

In the previous section it was shown that physical hydrogels based on photopolymerised NVP and AA dissolved in aqueous solutions, however, a considerable amount of monomeric residues were still present within these gels post-polymerisation. As chemical hydrogels do not dissolve in water, it was expected that the problematic residual monomer content could be drastically reduced by washing the chemical hydrogels in an aqueous solution. Therefore, in this section chemical crosslinkers were added to the monomeric NVP-AA blend to improve the gels mechanical properties. The potential use of two different crosslinking agents, monomer EGDMA or PEGDMA, was also under investigation, as they have previously proven useful in the development of NVP-AA based chemical hydrogels within our laboratories (Devine and Higginbotham, 2005). Furthermore, Devine *et al.* (2006) showed that these types of hydrogels were capable of releasing various active pharmaceutical agents (e.g. Aspirin and Paracetamol) in a predictable and controllable fashion and they suggested that these type of hydrogels may find potential use as wound healing dressings in conjunction with drug delivery.

In the present study, chemical hydrogels were synthesised using suitable ratios of NVP and AA. These chemical hydrogels were developed in accordance with the physical hydrogels previously discussed but with the introduction of the chemical crosslinking agents prior to photopolymerisation. Subsequent characterisation of such chemical gels again involved FTIR spectroscopy in order to confirm chemical composition and/or molecular structure. The swelling behavior and water equilibrium content of such insoluble gels was also investigated under physiological conditions. The chemical hydrogels were

then subjected to various washing steps, in order to reduce the amount of unreacted monomer, with HPLC analysis subsequently used to determine the residual monomer content post-washing, Additional parallel plate rheometry and compression studies were also carried out to investigate the comparative strength of such fully hydrated hydrogels.

The main focus of the present study, however, was to define the biocompatibility of these novel chemical hydrogels with respect to their potential use in wound healing applications. *In vitro* cytotoxicity and genotoxicity assessment was undertaken by means of direct and indirect hydrogel exposure to two human cell culture models. The HaCaT cell line, obtained from spontaneously transformed keratinocytes, was employed as it shares characteristics and functions of human skin (Boukamp *et al.,* 1988) which may be the first site of contact to such chemical hydrogels *in vivo*, due to their potential to be used in wound healing applications. Additionally, HepG2 hepatoma cells were employed for their metabolic activity. The chemical hydrogels' potential to cause deleterious effects at the DNA level was investigated via the comet and Ames assay.

3.2.2 Synthesis of chemical hydrogels

Copolymeric chemical hydrogels were produced by photopolymerisation using various ratios of NVP and AA as base monomers. Irgacure® 184 was used at 3 wt% of the total monomer content to initiate polymerisation while been exposed to irradiation with UV_{340nm} light at an intensity of 280 $\mu W/cm^2$ for exactly 2 h. The copolymers were crosslinked using either EGDMA or PEGDMA. Throughout this study, the amount of crosslinker added was kept constant at 0.1 wt% of the total monomer content as this proved to be an effective concentration in previous studies (Devine and Higginbotham, 2005, 2006). Moreover, the incorporation of crosslinking agents at such low concentrations tends to result in hydrogels that have high swelling ratios which is often advantageous for many biomedical applications, as a high water content generally contributes to the hydrogels' biocompatibility (Yanfeng and Min, 2001; Panayiotou and Freitag, 2005).

Based on visual inspection, it was found that the addition of either crosslinker had no effect on the samples' appearance as they looked very similar to the physical gels described in Section 3.1.2. As shown in Figure 3.21, the photopolymerisation technique produced solid chemical crosslinked xerogels, which appeared transparent and glass-like in

their nonhydrated form. Again, with the addition of increasing amounts of AA monomer, the surface uniformity of the samples changed and the polymers adopted a ridge like appearance. Again, the surface of the 25-75phys hydrogel appeared slightly moist indicating that the polymerisation may not have been as efficient for this sample.

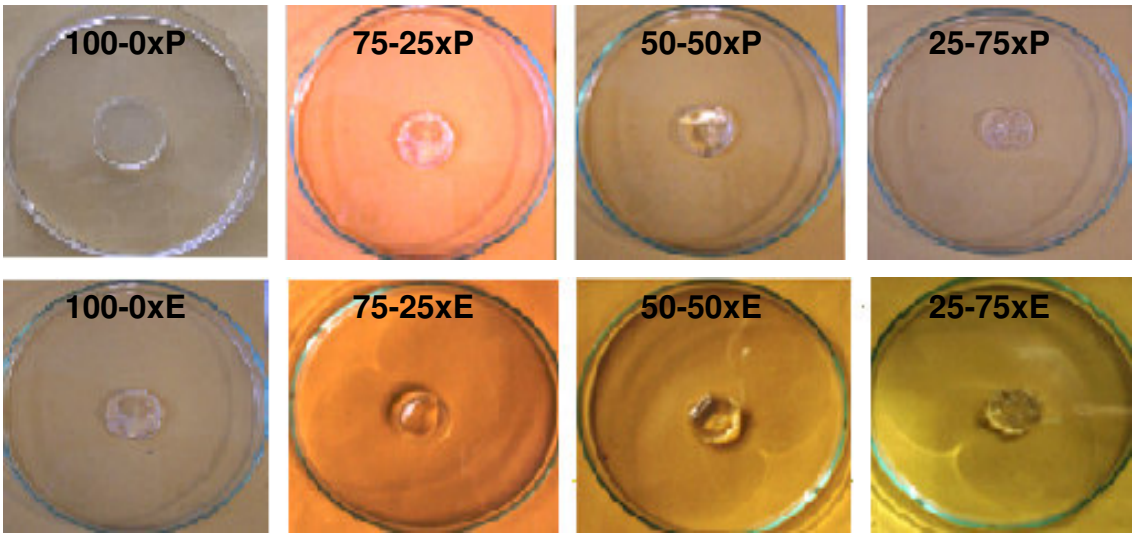

Figure 3.21: Appearance of the dry chemical hydrogels (xerogels) with varying monomeric feed ratios and 3 wt% Irgacure® 184 after photopolymerisation. The initial monomer compositions of the samples were: 100 wt% NVP (100-0), 75wt% NVP-25 wt% AA (75-25), 50 wt% NVP-50 wt% AA (50-50), and 25 wt% NVP-75 wt% AA (25-75). The symbol xP and xE indicate samples crosslinked with either PEGDMA or EGDMA respectively.

3.2.3 Characterisation of chemical hydrogels

3.2.3.1 FTIR spectroscopy

FTIR in the ATR mode was carried out on the chemical hydrogels to ascertain the efficiency of the photopolymerisation and the physicochemical interactions between the polymer chains and the chemical crosslinking agents, with the spectra obtained compared to the spectra of the physical hydrogels (Section 3.1.3.1). The FTIR results of the hydrogels crosslinked with PEGDMA and EGDMA are shown in Figures 3.22 and 3.23.

The FTIR spectra obtained for the chemical hydrogel samples (Figures 3.22 and 3.23) were almost indistinguishable from the spectra previously obtained for the physical hydrogels (Figure 3.4). The strong stretch bands observed in the region of 1650–1700 cm^{-1}

assigns the C=O group which is typical for polymerised NVP and AA (Jin *et al.,* 2006; Alla *et al.,* 2007). Once more, for the spectra obtained from hydrogels polymerised with higher initial feed ratios of NVP, the characteristic monomer peaks assigning the C=C bond (at 1623 cm^{-1} for NVP and 1613 and 1630 cm^{-1} for AA) were absent thus indicating that polymerisation had taken place.

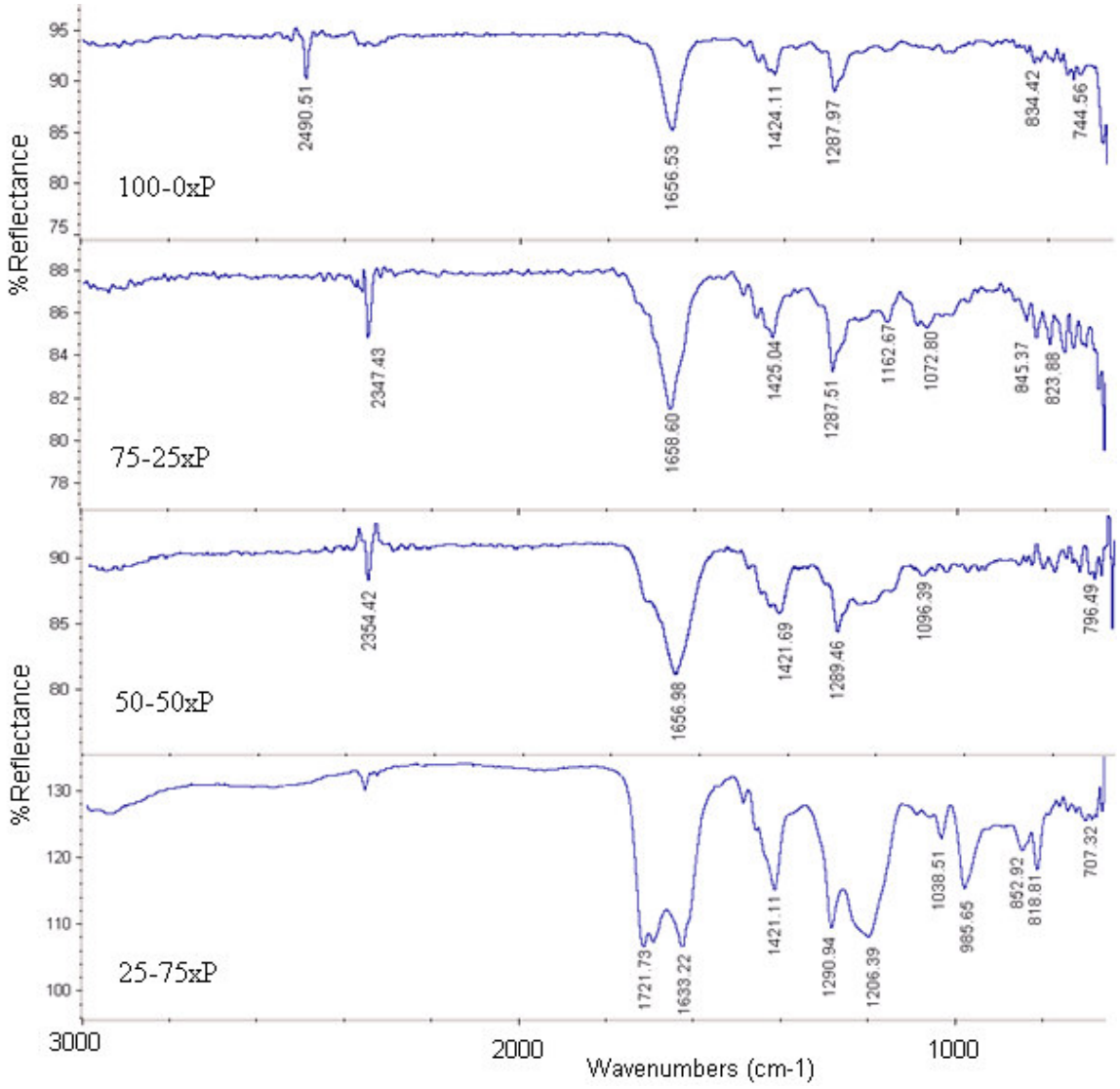

Figure 3.22: FTIR spectra of dehydrated hydrogel samples chemically crosslinked with 0.1 wt% PEGDMA.

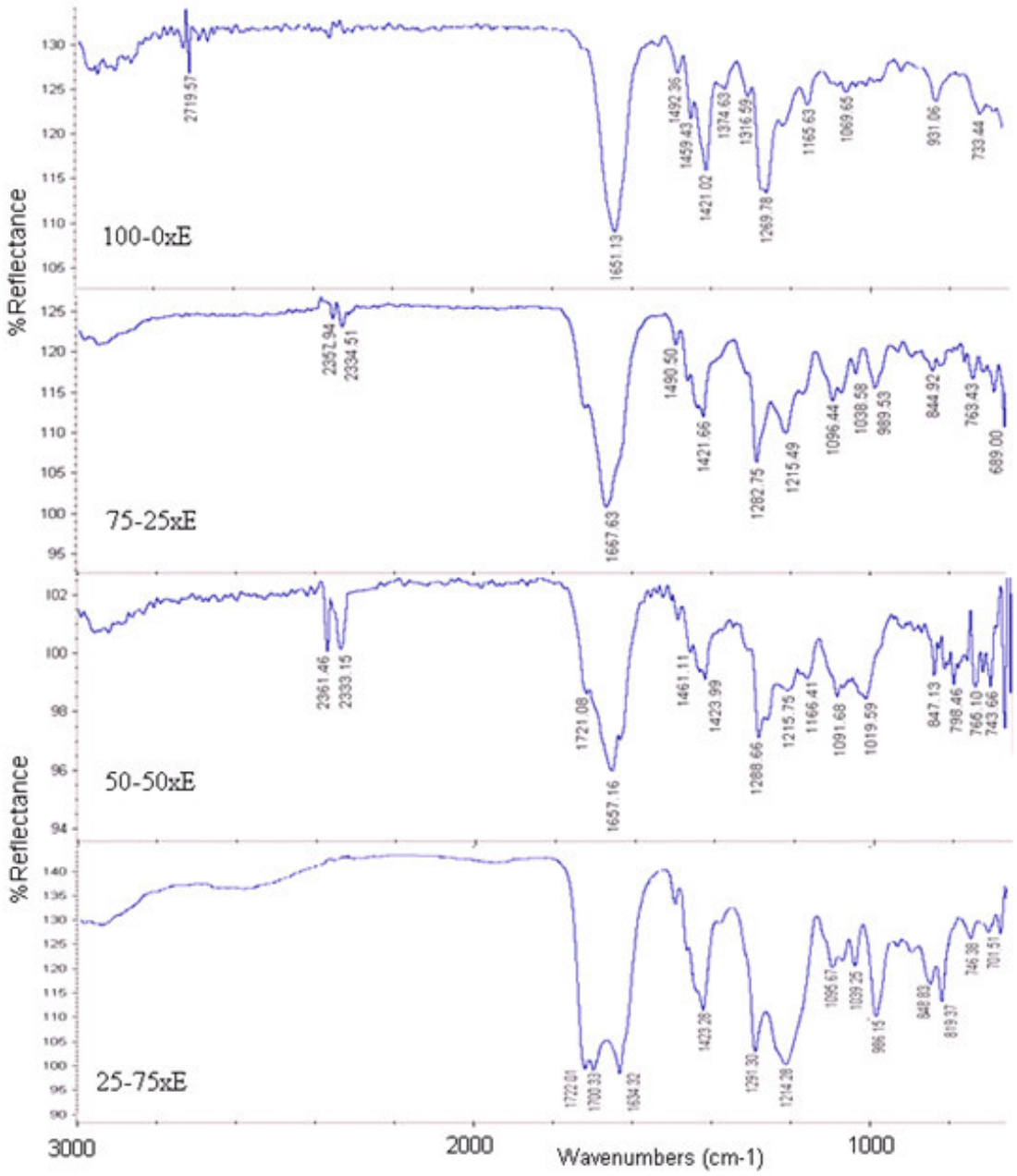

Figure 3.23: FTIR spectra of dehydrated hydrogel samples chemically crosslinked with 0.1 wt% EGDMA.

Moreover, as was seen in the spectra for the physical hydrogels, by increasing the AA content to 50% a shoulder towards the lower wavenumber region begins to form on the carbonyl peak (1650-1700 cm^{-1}). By increasing the initial AA feed content, this shoulder peaks at 1633-1634 cm^{-1} for both the 25-75xP and 25-75xE matrices. As previously discussed in Section 3.1.3.1, this peak could originate from a negative shift of the C=O

group of NVP based polymer due to hydrogen bonding (Yaung and Kwei, 1998; Devine and Higginbotham, 2003). This hypothesis may be further strengthened due to the fact that the C=O band for PVP at 1660 cm^{-1} disappeared while the C=O for AA based polymers at 1700 cm^{-1} was still present. However, as the olefinic C=C bond of the vinyl group from unpolymerised NVP and AA is also expected to appear in the region of 1630 cm^{-1}, possible presence of unpolymerised residues cannot be excluded at this point.

In terms of the incorporation of the crosslinking agent, FTIR proved inconclusive. No new peaks were observed which could be explicitly assigned to the presence of the crosslinking agents. It is believed that the concentration of crosslinker (0.1 wt% of initial monomer feed) was too low to be detected using the FTIR system. However, a study by Devine and Higginbotham (2005) which investigated comparable hydrogels, showed that the addition of EGDMA based crosslinking agent resulted in a shift to the right of the characteristic carbonyl stretch band. They further elaborate that this shift indicated that the crosslinking agent acted as a spacer that did not allow a high degree of intermolecular bonding to occur on the carbonyl group. This effect was not observed in the present study as the deviation between the peak location of physical and chemical hydrogels was only minimal.

3.2.3.2 Swelling and stability studies

Due to the addition of a chemical crosslinker, hydrogels are able to absorb and retain large quantities of water without undergoing subsequent degradation and dissolution (Hoffman, 2002). Therefore, the chemical gels synthesised in this study were expected to exhibit high swelling ratios while losing none of their integrity by dissolution. Considering the following biocompatibility evaluation, the swelling and degradation properties of the hydrogels were conducted simulating physiological conditions with PBS warmed to 37^{o}C being used as the submerging medium. The stability of the hydrogels was also investigated by placing fully swollen samples for a 15 day period in PBS, with particular attention being given to the effect of the two different crosslinkers on the hydrogels' degradability (Figures 3.24 and 3.25) .

The data reflects the effect of polymer composition on the ability to imbibe different levels of aqueous media within the hydrogel matrix. The hydrogel sample

consisting of 100 wt% NVP disintegrated upon a short exposure to the swelling medium, despite the incorporation of 0.1 wt% crosslinking agent, suggesting the extreme hydrophilicity of NVP based polymers requires a copolymeric network to achieve a covalently crosslinked hydrogel. Indeed, Ratner and Hoffman (1976) stated that high concentrations of crosslinker are required to produce insoluble materials based on homopolymerised NVP. Thus, as this gel type expressed the characteristics of a physical hydrogel rather than a chemical crosslinked hydrogel, it was decided to exclude these compositions from further testing.

As demonstrated in Figures 3.24 and 3.25 and visualised in images shown in Figure 3.26, the uptake of aqueous solution into the hydrogel matrix occurred very rapidly during the first stage of the swelling profile. In general, maximum swelling was reached between 100 and 150 h of incubation for both EGDMA and PEGDMA crosslinked gels. The hydrogels crosslinked with PEGDMA obtained a higher swelling ratio than the gels crosslinked with EGDMA indicating that the equilibrium swelling ratio of a hydrogel is influenced by the crosslinking agent used. It is believed that the internal structure of the three-dimensional hydrogel network may have become denser and more compact as the molecular mass of the crosslinking agent was reduced. The reduced length of the crosslinks would decrease the space between polymer chains, leading to a decrease in swelling (Gueven and Sen, 1991). Conversely, gels crosslinked with PEGDMA reached higher swelling ratios due to the presence of longer crosslinks acting as spacers between the polymer chains (Figure 3.26a).

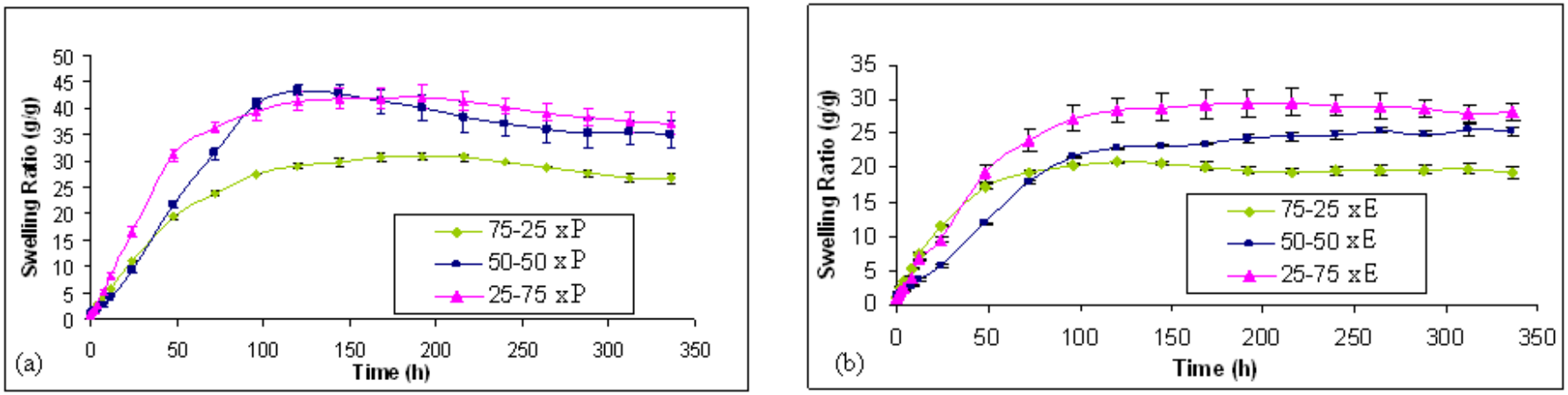

Figure 3.24: Swelling ratio (g/g) monitored over a time period of 350 h at 37°C for hydrogels synthesised using PEGDMA (a) and EGDMA (b) as crosslinking agents at 0.1 wt%. Data presented is the mean of three independent experiment ±SEM.

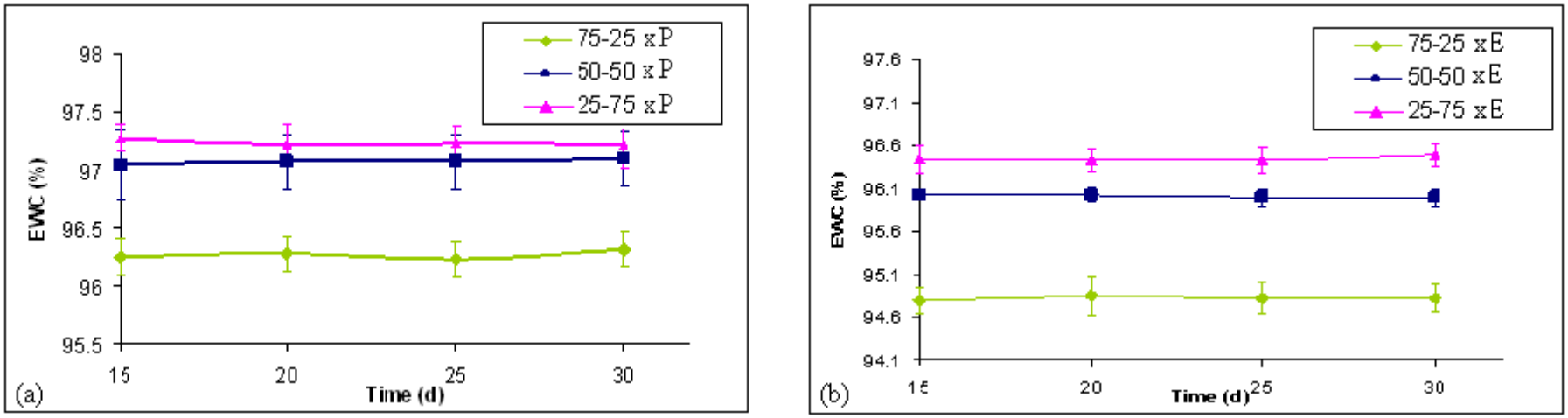

Figure 3.25: The EWC (%) values obtained for swollen gels synthesised using PEGDMA (a) and EGDMA (b) as crosslinking agents over additional 15 days incubation at 37°C in PBS. EWC values are used as an indicator of hydrogel stability. Data presented is the mean of three independent experiments (±SEM).

(a) *0.1 wt% PEGDMA*

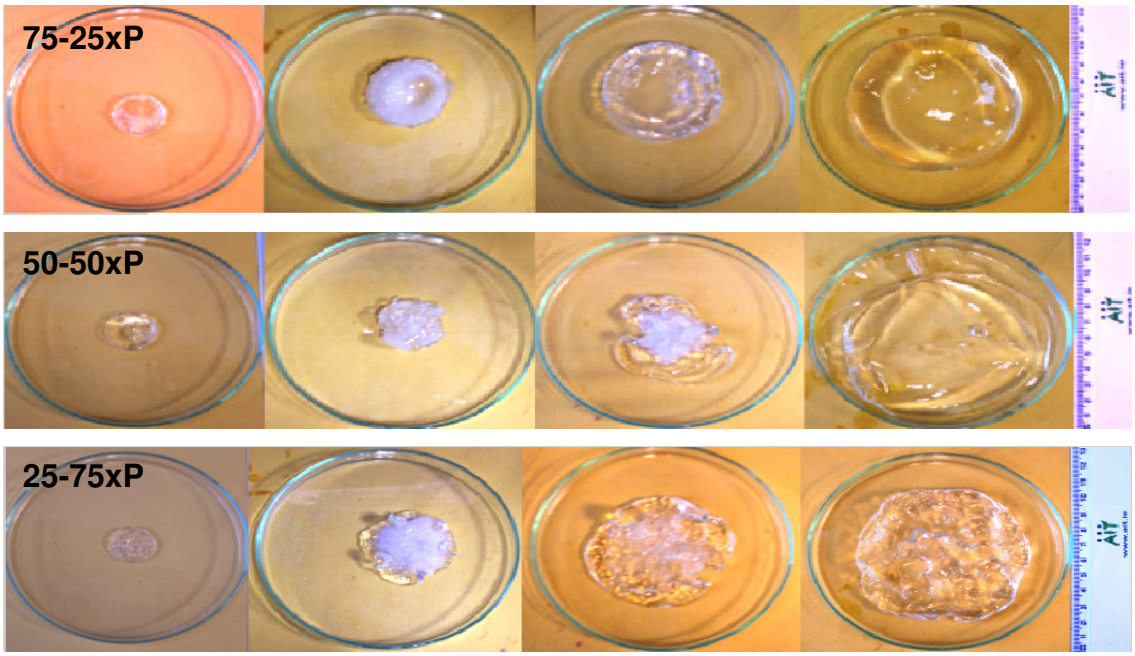

(b) *0.1 wt% EGDMA*

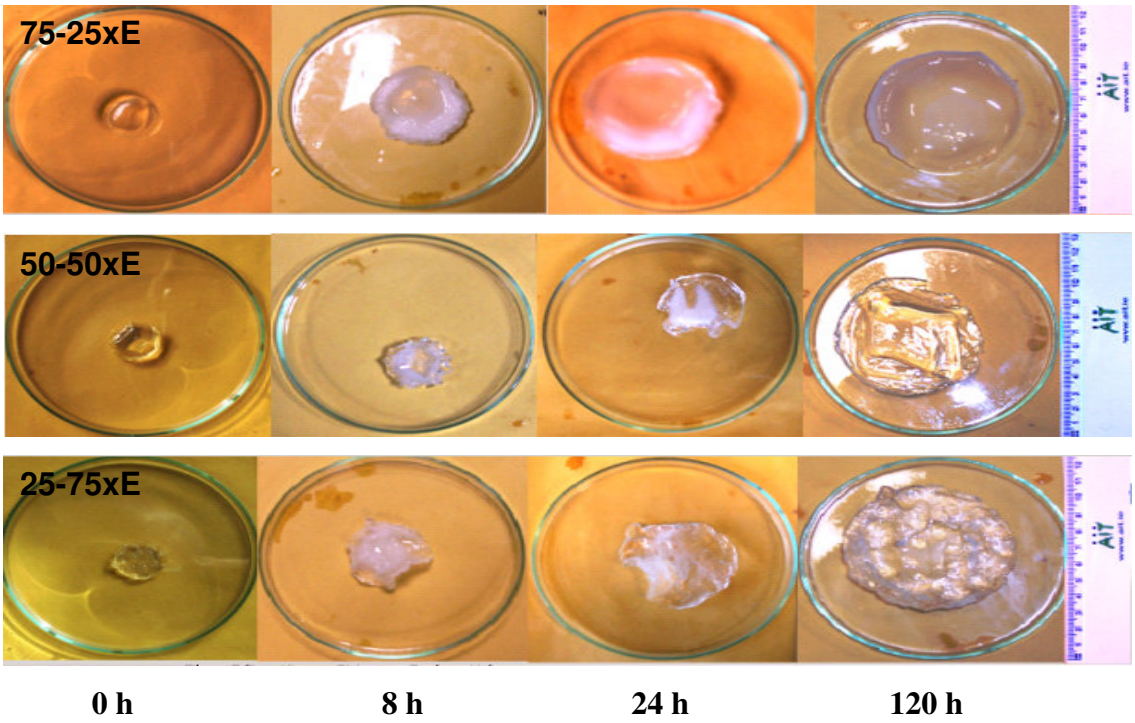

Figure 3.26: Images illustrating the swelling behaviour of hydrogels over 120 h at 37°C synthesised using (a) PEGDMA and (b) EGDMA at 0.1 wt% as crosslinking agents.

Furthermore, with increasing amounts of AA, the hydrogels' swelling capacity increased, reaching a swelling maximum of 37 and 28 times the weight of the dry gel for PEGDMA and EGDMA crosslinked gels respectively (Figures 3.26a and b). This effect was caused by the physiological pH of the swelling medium facilitating ionisation of the carboxylic acid groups which, in turn, raises the concentration of free ions inside the gel causing additional attraction of water molecules. Moreover, the dissociated carboxyl groups cause the gel to expand to minimise the repulsion (Jianqi and Lixia, 2002). This phenomenon also explains the change in swelling behaviour of NVP-AA based chemical hydrogels when placed in swelling media with different pH values, as observed by Devine and Higginbotham (2005). Similar to the xerogels, the surface ridges present on swollen gels also increased with increasing amounts of AA. Moreover, it also should be noted that the swelling trend obtained for most of the tested hydrogels showed a negative slope shortly after reaching maximum swelling. This effect may be an indicator of mass loss resulting from diffusion of unbound material into the swelling medium.

As illustrated in Figure 3.25, the EWC values stayed constant over an additional 15 day period in swelling medium and showed no evidence of hydrogel degradation or release of unbound material into the swelling media. As expected, the chemical crosslinks prevented dissolution and after reaching equilibrium, the gels maintained their integrity. It is also noteworthy that all hydrogels swelled to yield EWC values well above 90%, whereby most of the water is unbound and can effortlessly diffuse in and out of the polymer (Yin *et al.,* 2008). In agreement with the swelling ratios (Figure 3.24), the hydrogels crosslinked with PEGDMA reached higher water contents than corresponding gels crosslinked with EGDMA. Also the equilibrium swelling ratio increased as the monomer feed ratio of AA increased (Figure 3.25)

Overall, as expected, the swelling was found to drastically change the size and consistency of the original xerogel. By incorporating the swelling medium into the hydrogel matrix, UV-cured xerogel swelled to become soft and natural tissue-like while keeping its structural integrity. Compared to the swelling profile of physical hydrogels discussed in Section 3.1.3.3, the chemical hydrogels showed a much higher degree of swelling without dissolving within the swelling medium. After reaching maximum

swelling the hydrogels showed no evidence of degradation or further release of unbound material into the swelling media over an incubation period of 15 days.

3.2.3.3 HPLC analysis of residual monomers

Several studies have investigated the nature and quantity of compounds extracted from biopolymer-based hydrophilic materials using water and organic solvents (Kawahara *et al.,* 2004; Urban *et al.,* 2007). As mentioned earlier, these solvents penetrate the polymer network causing it to expand or swell, thereby mobilising residues of unbound monomers and breakdown products. In order to equalise the adjacent concentration gradient, these mobilised residues will readily diffuse from the material into the solvent. Because of the potential toxicity often associated with unbound materials, such as unreacted monomers, it is important to evaluate their leachability from the polymer network. As the hydrogels evaluated in this section are nonsoluble due to the insertion of covalent crosslinks, it was expected that the unbound monomer content could be drastically reduced by washing the gels within a suitable aqueous solution. In the present study, PBS was utilised as washing and extract medium at 37^{o}C to simulate physiological conditions and the residual monomer content in the extract solution was determined before and after 15 days of hydrogel washing. To determine if the washing step efficiently removed unbound material from the hydrogel matrix, the quantity of the base monomers, AA and NVP, present in extracts were analysed via HPLC described in Section 3.1.3.2. The quantities of released AA and NVP monomer were calculated on the basis of standard calibration curves previously shown in Figure 3.8. A chromatogram obtained from the HPLC analysis of the extracts before and after washing is illustrated in Figure 3.27. The retention time, peak area and respective quantity (µg/ml) of the analysed monomers are shown in Tables 3.5 and 3.6.

The HPLC analysis of the hydrogel extracts before and after the PBS wash step (Tables 3.5 and 3.6, and Figure 3.27) revealed that the washing process was efficient for the removal of unbound residues. A drastic reduction in the amount of analysed monomers and other nonidentifiable unbound substances was evident in extracts from washed hydrogels.

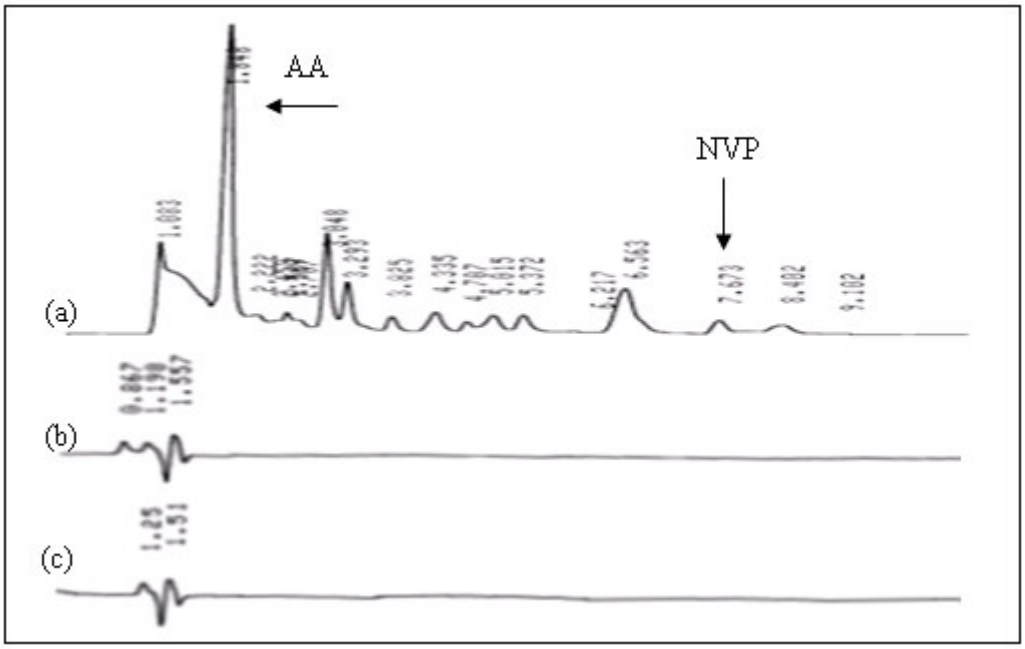

Figure 3.27: Chromatogram obtained during HPLC analysis: (a) PBS extract of unwashed 50-50xP samples, (b) PBS extract of washed 50-50xP samples, (c) untreated PBS as control.

Table 3.5: Retention time, peak area and respective quantity (µg/ml) of (a) AA and (b) NVP monomer present in extracts prepared from unwashed chemical hydrogels as determined via reverse phase HPLC.

(a) Extract Sample	Mean Ret. Time	Mean Peak Area AA (±SD)	Concentration (µg/ml)
75-25xP	1.855	24171.50 (±1672.31)	7.85
50-50xP	1.834	372884.00 (±8683.27)	135.56
25-75xP	1.803	594841.50 (±6614.98	216.84
75-25xE	1.881	15144.00 (±824.49)	4.55
50-50xE	1.796	235013.50 (±2044.25)	85.06
25-75xE	1.855	516997.50 (±2158.70)	188.33

(b) Extract Sample	Mean Ret. Time	Mean Peak Area NVP (±SD)	Concentration (µg/ml)
75-25xP	7.551	1994787.00 (±3393.41)	25.72
50-50xP	7.546	455166.00 (±1220.47)	5.95
25-75xP	7.485	212853.50 (±769.99)	2.87
75-25xE	7.374	1540505.50 (±13250.47)	19.90
50-50xE	7.266	325108.50 (±6062.03)	4.31
25-75xE	7.200	138083.00 (±1118.64)	1.91

Table 3.6: Retention time, peak area and respective quantity (µg/ml) of (a) NVP and (b) AA monomer present in extracts of previously washed chemical hydrogels as determined via reverse phase HPLC.

(a) Extract Sample	Mean Ret. Time	Mean Peak Area AA (±SD)	Concentration (µg/ml)
75-25xP	-	*No peak obtained*	*Not detectable*
50-50xP	-	*No peak observed*	*Not detectable*
25-75xP	-	*No peak observed*	*Not detectable*
75-25xE	-	*No peak observed*	*Not detectable*
50-50xE	-	*No peak observed*	*Not detectable*
25-75xE	-	*No peak observed*	*Not detectable*

(b) Extract Sample	Mean Ret. Time	Mean Peak Area (±SD)	Concentration (µg/ml)
75-25xP	-	*No peak observed*	*Not detectable*
50-50xP	-	*No peak observed*	*Not detectable*
25-75xP	-	*No peak observed*	*Not detectable*
75-25xE	-	*No peak observed*	*Not detectable*
50-50xE	-	*No peak observed*	*Not detectable*
25-75xE	-	*No peak observed*	*Not detectable*

More specifically, the amount of unreacted monomers in the extracts of washed hydrogels was too small to be detected – the chromatograms of the washed gels resembled the appearance of chromatograms obtained after injection of the neat extraction medium PBS (Figure 3.27b-c). In contrast, the residual monomer content analysed in extracts produced from unwashed hydrogels showed a similar trend for PEGDMA and EGDMA crosslinked samples, suggesting similar polymerisation reactivity for both types of crosslinked gels (Table 3.5). In general the residual monomer content increased with a respective increase of base monomer concentration in the samples. The highest amount of monomeric residues present in the hydrogel extracts was 216 µg/ml AA (25-75xP) and 25.72 µg/ml NVP (75-25xP). This was not surprising given the moist surface of some sample after the photopolymerisation and the presence of FTIR peaks potentially indicating the presence of unreacted monomers. The monomer amount in extracts from EGDMA crosslinked hydrogels was lower than those in extracts from PEGDMA crosslinked material. This may be explained by the lower swelling ratio of EGDMA crosslinked gels (Figure 3.24) as the diffusion of unbound material into the surrounding solution is related

to the amount of water taken up by the network. In addition, several unidentifiable peaks were obtained from extracts of unwashed hydrogels as shown in Figure 3.27. These peaks were believed to originate from other substances used to support the synthesis of the hydrogels i.e. photoinitiator and crosslinkers, from breakdown products of the base materials or from unbound polymer fragments of lesser chain length not covalently embedded in the hydrogel matrix. Furthermore, this finding strengthened the assumption that mass loss was the cause of the negative slopes observed in swelling curves after reaching maximum swelling (Figure 3.24).

Overall, a reduction in unbound material such as monomers or residues from the polymerisation reaction was successfully achieved. Due to the addition of chemical crosslinkers, it was possible to develop insoluble hydrogels. These gels could be further purified of unwanted residues which proved to be problematic in the biocompatibility evaluation of physical hydrogels. Preliminary HPLC studies performed to investigate the residual photoinitiator content and respective breakdown products were unsuccessful due to difficulties solubilising the chemical in a range of mobile phases. Hence, additional work is advised to investigate the suitability of headspace gas chromatography-mass spectrometry for the detection of residual photoinitiator material within the gels.

3.2.3.4 Mechanical testing

An understanding of the hydrogels' mechanical properties is important to provide information on their gel strength and stability. Overall, to determine if a hydrogel has potential to be used as a biomedical device, knowledge of the material properties must be established to ensure suitable and reliable structures. A variety of mechanical testing techniques have been used to study the functional behaviour of hydrogels. The most popular include oscillatory rheometry and compression analysis as these techniques provide critical information on the hydrogels' strength expressed as viscosity or elasticity in relation to the gels stability (Stammen *et al.,* 2001; Meyvis *et al.,* 2002). Both of these techniques belong to the field of dynamical mechanical characterisation, i.e. the response of the sample is measured when it is deformed under a certain stress or strain. This gives information about to what extent, if any, the mechanical gel properties change when stress is applied. This in turn provides further information on the gels' possible application within

the biomedical field. Importantly, these techniques are also very useful for investigating the inter-comparative strength between different hydrogel formulations.

Rheological analysis

Oscillatory parallel plate rheology was carried out at 37^{o}C to determine the viscoelastic properties of the chemical hydrogel networks. The fully hydrated samples were subjected to a strain sweep ranging from 1.88 x 10^{-4} to 1 x 10^{-3} at a strain rate frequency of 1 Hz while simultaneously measuring the shear storage (or elastic) modulus G' and the shear loss (viscous) modulus G''. The G' provides information about the elasticity or the energy stored in the material during deformation, whereas G'' describes the viscous character or the energy dissipated as heat (Borzacciello and Ambrosio, 2009). To be characterised as a gel, the storage modulus G' obtained during an oscillatory shear experiment should be considerably higher than the loss modulus G'' (Kavanagh and Ross-Murphy, 1998). An overall of 75 measuring points for each respective modulus value were collected per sample. The graph shown in Figure 3.28 illustrates that the obtained G' was much higher than the G''. This effect was observed for all the hydrogel samples tested within this study and indicates that the elastic response of the material is stronger than the viscous response - a common character for hydrogels (Borzacciello and Ambrosio, 2009). During the experiment, the increase in applied strain did not cause a significant alteration of G' and almost no dependence of the G' to the applied strain could be observed within the range tested. These features can be interpreted as indicative of a "strong" gel which could withstand the applied strain without experiencing a change in its mechanical properties. Cabane *et al.* (1996) states that the higher the G' value of the hydrogel, the greater the gel strength. Hence, the obtained storage modulus values of the various hydrogel formulations tested were used to evaluate the comparative gel strength as shown in Figure 3.29.

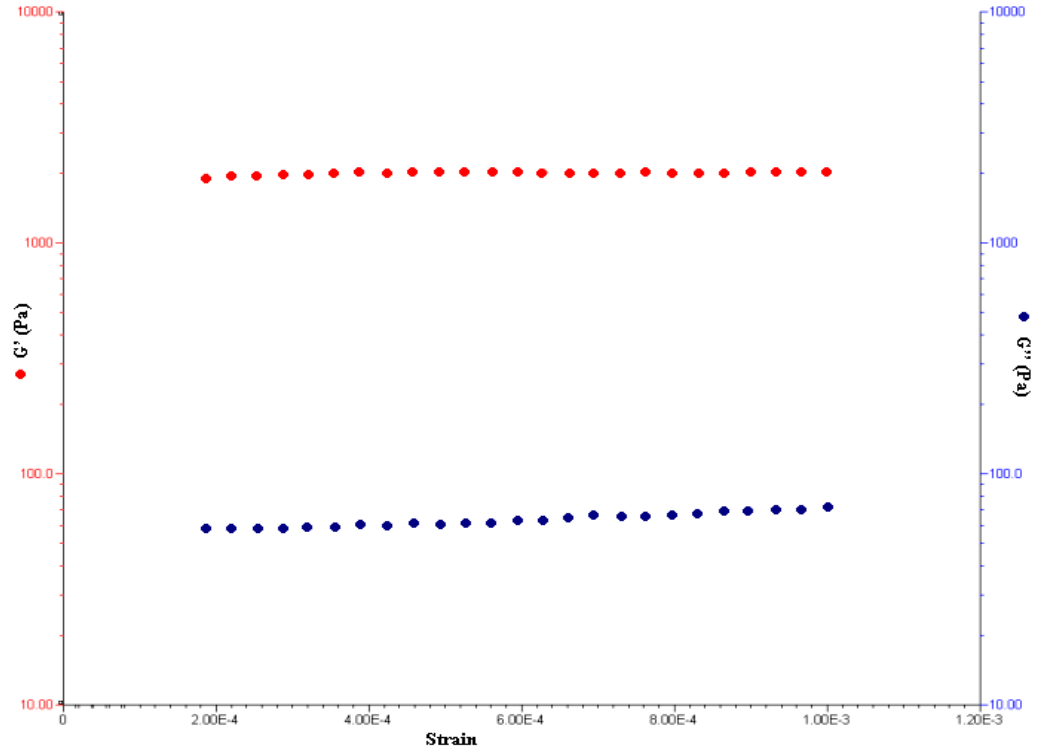

Figure 3.28: Typical result obtained during the rheological analysis of hydrated 50-50xP hydrogel samples.

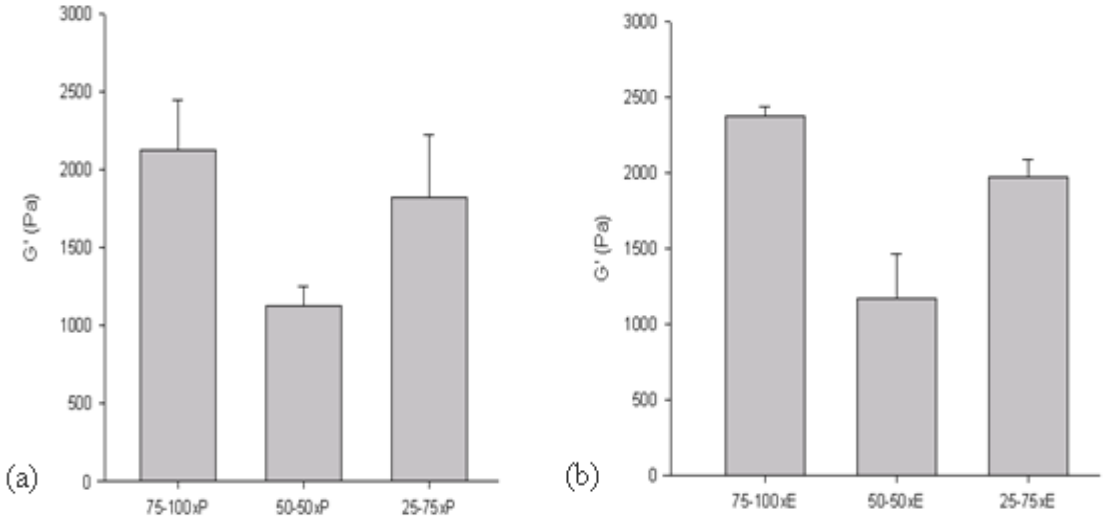

Figure 3.29: Storage modulus of fully hydrated chemical hydrogels crosslinked with (a) PEGDMA and (b) EGDMA.

As shown in Figure 3.29, the crosslinked 75-25xP hydrogel exhibited a G' value of 2129 Pa, while 50-50xP and the 25-75xP type hydrogels reached reduced G' values of

1122 Pa and 1818 Pa, respectively. In relation to the different crosslinkers utilised, the storage moduli were comparable (Figure 3.29). Although the results obtained from the PEGDMA crosslinked gels were not found to differ significantly from results obtained for the EGDMA gels, latter gels achieved slightly higher G' with the exception of the 25-75xE sample. The 75-25xE displayed the highest G' value with 2375 Pa, while the 50-50xE and 25-75xE reached lower values of 1173 Pa and 1762 Pa, respectively.

The obtained storage modulus values indicated that the hydrogel strength was significantly ($p<0.05$) affected by the monomeric feed ratio, and this appeared to be the case for both crosslinker types used. The hydrogels synthesised with the addition of 75 wt% NVP proved to be the strongest gels. Taking the decreased EWC values of the 75-25xP and 75-25xE type gels into account, it was not unexpected that these samples reached higher G' values as this resulted in an increased amount of gel strengthening polymer content per hydrated hydrogel volume. In comparison, as the gels containing higher amounts of AA (50-50xP, 50-50xE, 25-75xP and 25-75xE) produced higher swelling ratios, less polymer molecules were available per hydrogel volume to strengthen their structure. Thus, when equal parts of NVP and AA were added as base monomer, the gel strength was significantly reduced, whereas when the AA content was increased to 75 wt%, the gel strength appeared to recover. This was surprising, as it was assumed that an AA feed ratio higher than 50 wt% would result in a further deterioration of the gel strength. At this point, it can be speculated that the increased amount of carboxylic acid groups within the 25-75xP and 25-75xE polymers caused an increase of inter-molecular hydrogen bonding.

With regards to the hydrogels' potential application, all the tested samples reached storage modulus values comparable with those for commercially available gels used in wound healing applications. Interestingly, Jones and Vaughan (2005) quote storage modulus values for a number of established hydrogel wound dressings and such values were found in the in the range of 340 and 2490 Pa. Therefore, it can be concluded that based on the results obtained from the present rheological assessment, the tested hydrogels have favourable mechanical properties for the use in wound healing applications where they would be expected to provide structural support to damaged tissue.

Compression testing

The compressive failure behaviour of the swollen hydrogels was evaluated using a single compressive cycle. The compressive failure is defined as the point at which the sample experiences a nonreversible plastic deformation under an experimental load, i.e. the point at which the applied load leads to destruction of the hydrogels three-dimensional network. During the analysis, the compressive strain was continuously recorded in relation to increasing applied pressure defined as compressive stress expressed as MPa. The compressive strain indicates the compressive deformation of the hydrogel sample during compression and is expressed as a percentage of the decrease in sample thickness to the initial sample thickness before the force was applied. To find use in the field of wound healing, the hydrogels must be able to withstand a certain amount of applied pressure; hydrogels are often fixated above a wound by applying pressure with a sterile bandage or suitable medical tape. However, while the soft consistency of hydrogels is considered a key property for their use in wound healing, low mechanical properties have severely limited their use in load bearing medical applications (Hoffman, 2002). Therefore, the compression analysis conducted in the present study was used to examine whether the hydrated hydrogel samples were able to withstand a certain pressure load. Additionally, a better insight into the samples inter-comparative strength was gained. The results obtained from the compression evaluation are shown in Figure 3.30.

As expected, the compressive failure analysis conducted on the fully hydrated hydrogels showed that with increasing compressive stress load, the percentage compressive strain increased. The values obtained for the compressive strain, which is an indicator of the extent of reversible sample deformation experienced during the compression, reached 40.71%, the highest value for the 50-50xE gels. The lowest value for sample deformation was obtained for the 25-75xE samples which was determined at 15.38% prior to the gel breaking down. In general, after reaching a critical pressure point all samples began to deform rapidly.

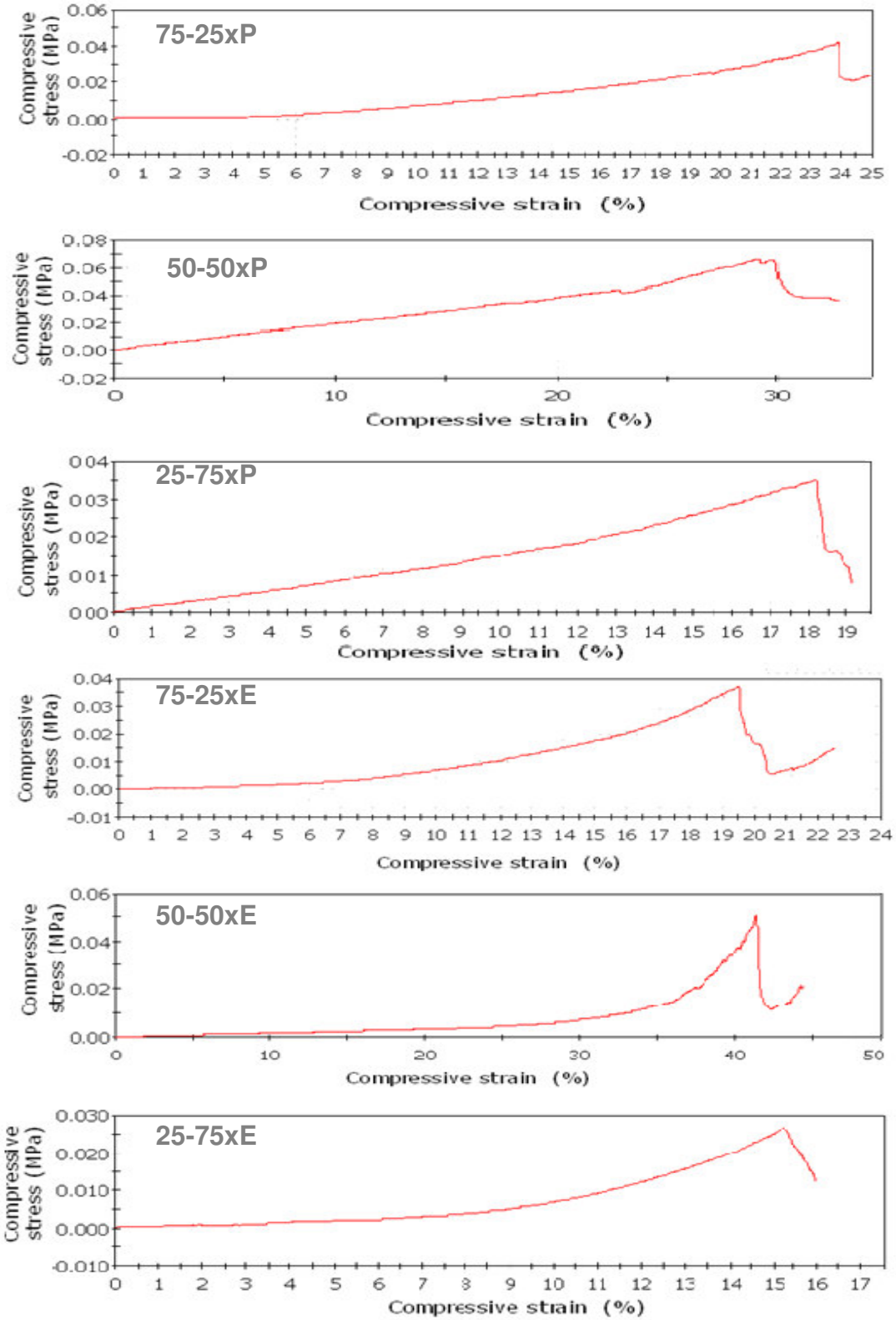

Figure 3.30: Results obtained during compression testing of hydrated chemical hydrogels.

Depending on the monomeric feed ratio and different crosslinker used, the samples tested were able to resist a compressive stress between 0.0264 and 0.0640 MPa. The results illustrated in Figure 3.30 suggest that the samples composed of equal parts of NVP and AA were able to resist the highest compressive stress load. The 50-50xP samples reached a value of 0.0640 MPa and the 50-50xE samples reached a value of 0.0512 MPa before they began to disintegrate. The compression of the 75-25xP and 75-25xE samples led to reduced maximum compressive stress values of 0.0409 and 0.0375 MPa respectively. The smallest compression stress value at the gel breaking point was achieved with the gels produced with higher amounts of AA. The 25-75xP reached a maximum compressive stress value of 0.0350 while the 25-75xE gels reached the lowest value of 0.0264.

In terms of the different crosslinkers used, it appears that the gels synthesised with the addition of PEGDMA were able to withstand a slightly higher load than the samples crosslinked with EGDMA. In comparison to the data obtained from the rheological analysis, the compressive failure results led to surprising findings. The gels with the lowest storage modulus values obtained during oscillatory rheological analysis were able to withstand the highest compressive load, and vice versa. At the first view, this finding may appear contradictory, as one might expect that a gel which proved to be the strongest during rheological testing should also be able to withstand the highest compressive load. However, it has been previously suggested that the introduction of crosslinks to the hydrogel network can improve the gel strength but conversely this may be at the cost of creating a more brittle structure (Jiang *et al.,* 1999; Peppas *et al.,* 2000).

With regards to wound healing devices, only a very limited number of scientific publications discuss the actual pressure values applied to open wounds. A recent paper published by Fonder *et al.* (2008) states that compression therapy is the superior treatment method for open ulcer-type wounds. However, the applied compression should not be in excess of 0.008 MPa. During the compression study conducted, all the tested hydrogels were able to resist a much higher compressive load before their network broke down. In terms of their compressive properties, it appears that these hydrogels are suitable for use in wound healing applications.

3.2.4 Cytotoxicity assessment of chemical hydrogels

The potential of chemical hydrogels to induce cytotoxicity in HepG2 and HaCaT cell lines was evaluated using *in vitro* based cell culture assays performed in a similar manner to those employed for the biocompatibility assessment of the physical gels (Section 3.1.4) but with slight modifications, due to the insoluble nature of the chemical gels. More specifically, the elution test, direct and indirect contact (agarose overlay) assays were used in conjunction with MTT and NR endpoints to quantitatively and qualitatively evaluate the cytotoxic potential of residual monomers and breakdown products from unwashed and washed chemical hydrogels. More specifically, quantitative evaluation of cell viability following exposure to hydrogel extracts was confirmed with elution tests, while the viability of cells directly exposed to hydrogel samples was evaluated quantitatively and qualitatively via the Fluorochrome-mediated (Fda/EtBr) viability test and morphological examination respectively. In addition, the cytotoxic potential of the swollen hydrogel matrices was measured by indirectly exposing cells within the agarose overlay assay.

3.2.4.1 Elution test (MTT endpoint)

For comparative purposes the elution test, in conjunction with an MTT endpoint, was conducted with extracts prepared from unwashed and washed chemical hydrogels to further confirm such purification wash steps, post-polymerisation, were effective. The extracts of unwashed hydrogels were prepared by incubating untreated 250 ±10 mg samples in 30 ml of culture medium for 5 days at 37^{o}C with 125 rpm agitation. The AA content of the hydrogels induced a substantial pH change to the culture medium which was adjusted to physiological conditions (pH 7.4) by the addition of small amounts of alkaline 3 M NaOH. Purified chemical hydrogels were produced by washing samples of the same weight for 15 days with 30 ml of PBS at 37^{o}C and 125 rpm agitation before subjecting them to the cell culture extract medium. For these samples, the pH of the extract medium was not found to be reduced as the majority of unbound hydrogen ions may have been removed during the washing. Subsequently, both extract types were exposed to HepG2 and HaCaT cells for 24 h at 37^{o}C before the endpoint was evaluated via the MTT endpoint. The results obtained were analysed as outlined earlier in the evaluation of the physical hydrogels (Section 3.1.4).

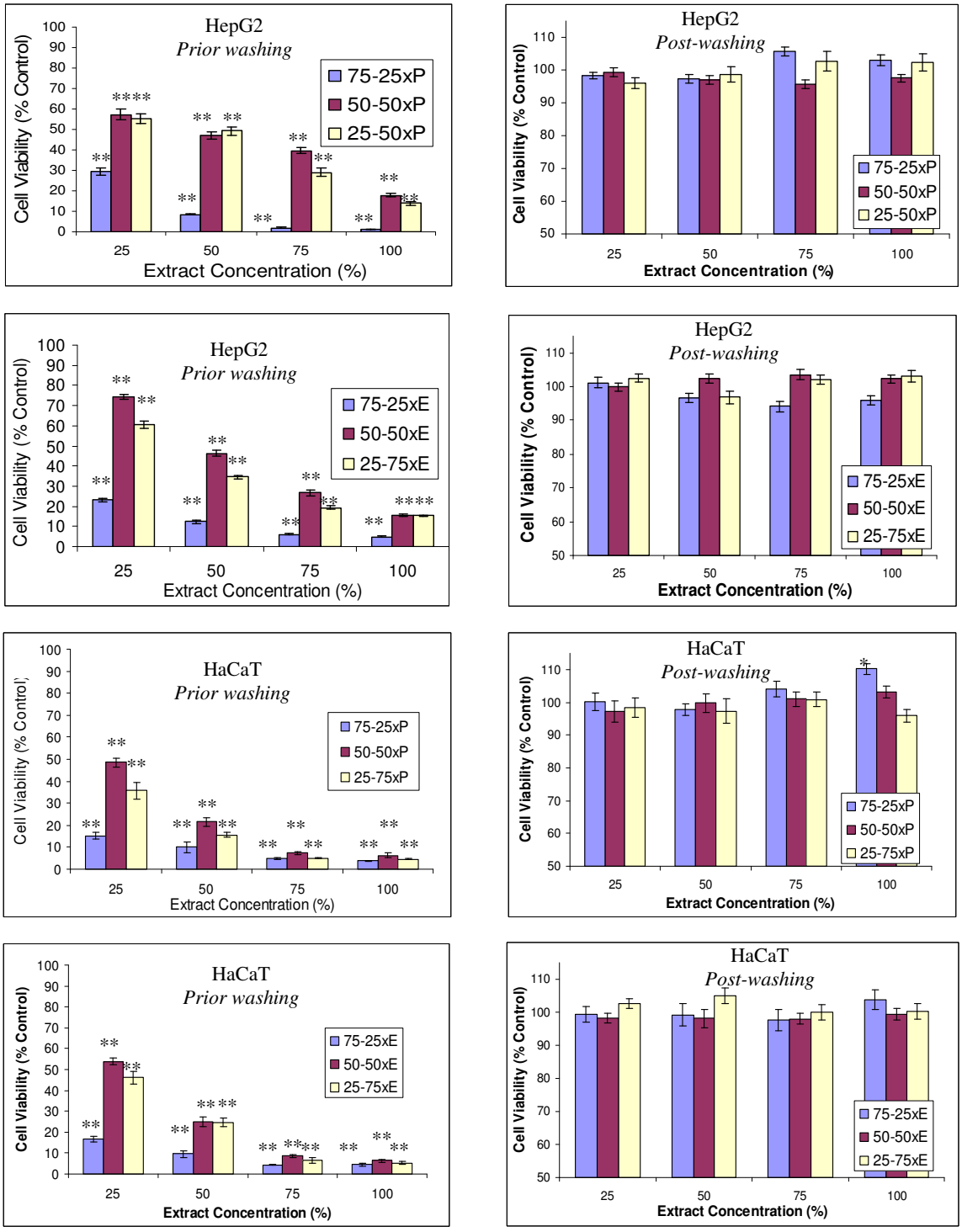

Figure 3.31: The effect of washing on the viability of HepG2 and HaCaT cells as assessed in the elution test plus the MTT endpoint following 24 h exposure at 37°C to various concentrations of extracts of PEGDMA (xP) and EGDMA (xE) crosslinked hydrogels (n=12 for extracts produced prior to washing, n=18 for extracts produced post-washing, ±SEM, * denotes a significant difference from the control **=p<0.01, *=p<0.05).

Table 3.7: Viability (% of control cells) of HepG2 cells after 24 h exposure at 37°C to undiluted extracts of PEGDMA (xP) and EGDMA (xE) crosslinked hydrogels as assessed in the elution test with the MTT endpoint (n=12 for extracts produced prior washing, n=18 for extracts produced post-washing, ±SEM, * denotes a significant difference from the control **=p<0.01).

Hydrogel Sample	Undiluted Extract before washing	Undiluted Extract post-washing
	% Viability (±SEM)	% Viability (±SEM)
75-25xP	2 (±0.29)**	103 (±1.90)
50-50xP	18 (±1.00)**	98 (±1.18)
25-75xP	14 (±0.89)**	102 (±2.72)
75x25xE	5 (±0.38)**	96 (±1.30)
50-50xE	16 (±0.81)**	102 (±1.24)
25-75xE	15 (±0.55)**	103 (±1.66)

Table 3.8: Viability (% of control cells) of HaCaT cells after 24 h exposure at 37°C to undiluted extracts of PEGDMA (xP) and EGDMA (xE) crosslinked hydrogels as assessed in the elution test with the MTT endpoint (n=12 for extracts produced prior washing, n=18 for extracts produced post-washing, ±SEM, * denotes a significant difference from the control **=p<0.01, *=p<0.05).

Hydrogel Sample	Undiluted Extract before washing	Undiluted Extract, post-washing
	% Viability (±SEM)	% Viability (±SEM)
75-25xP	4 (±0.22)**	110 (±1.77)*
50-50xP	6 (±0.98)**	103 (±1.70)
25-75xP	5 (±0.20)**	96 (±1.86)
75-25xE	4 (±0.56)**	104 (±3.04)
50-50xE	6 (±0.76)**	99 (±1.71)
25-75xE	5 (±0.74)**	100 (±2.39)

The results for the viability assessment of HepG2 and HaCaT cells following 24 h exposure to hydrogel extracts of unwashed and washed chemical hydrogel samples using the MTT endpoint are shown in Figure 3.31 and summarised in Tables 3.7 and 3.8. A high degree of reproducibility was obtained as evidenced by SEM values in Tables 3.7 and 3.8 and the relatively small error bars in Figure 3.31.

The results clearly indicate that the purification procedure performed on the chemical hydrogel samples had a major impact on the cytotoxic potential of the tested extracts. In contrast to extracts obtained from unwashed hydrogels, the extracts produced from washed hydrogels did not exert any cytotoxic behaviour. Overall, the viability of the HepG2 and HaCaT monolayer did not significantly vary from the untreated control monolayer indicating that no loss of viability occurred following treatment with extracts of

prewashed hydrogels crosslinked with 0.1 wt% of either PEGDMA or EGDMA. However, the highest tested concentration of extracts obtained from washed PEGDMA crosslinked hydrogels containing higher amounts of NVP as base monomer (75-25xP) led to a slight increase in viability for both HepG2 and HaCaT (Table 3.7). In one experiment a significant ($p<0.05$) proliferation of 10% above the control values occurred for 75-25xP hydrogel extracts exposed to HaCaT cells. The question whether the observed proliferation was in fact triggered by a low concentration of leachable substances in the hydrogel extract or an anomaly regarding the reproducibility of the MTT assay needs to be further investigated. However, research conducted by Smith and colleagues on the cytotoxic effect of crosslinked NVP based hydrogels in indirect contact to primary and continuous cultured keratinocytes also suggests proliferative effects (Smith *et al.,* 2006). Furthermore, Devine *et al.* (2006) previously reported cell proliferative effects of NVP based polymers in solution at the subtoxic concentration range. However, the growth promoting effects of NVP based hydrogels on cells cultured *in vitro* remains to be fully elucidated with various hypotheses previously suggested by Hong *et al.* (1997).

On the other hand, diluted extracts prepared from unwashed hydrogel samples induced a significant ($p<0.05$) loss in cell viability which became more pronounced with an increase in concentration indicating the presence of cytotoxic leachates. Furthermore, the observation at the microscopic level revealed that a high number of damaged cells were present which appeared rounded or lysed. The cell monolayer became visibly disrupted, having lost the ability to adhere to the bottom of the culture plate. This finding correlates with the observed mass loss of hydrogel networks in the swelling experiments (Figure 3.24) and with previous HPLC studies which confirmed the presence of unreacted base monomer and other unbound chemicals in the extracts (Figure 3.27 and Table 3.5). Interestingly, incubation with extract solutions originating from the two different crosslinking agents led to similar results, although the EGDMA type samples appeared slightly less toxic. This may be explained with the aid of the previously obtained swelling data, where EGDMA crosslinked gels had a slower swelling rate leading to a slower release of unbound material from the network by diffusion and displacement processes (Figure 3.24). Moreover, the HepG2 cells appeared generally less susceptible to the cytotoxic effects of the hydrogel extracts. This effect could be related to the metabolic

activity of HepG2 cells which retain several detoxifying enzymes that in turn may protect the cells from cytotoxic insults (Knasmueller *et al.,* 1998). The extracts produced from unwashed samples with high amounts of NVP as base monomers (75-25xP and 75-25xE) showed an elevated level of cell toxicity even at diluted extract concentrations (e.g. the 25% extract concentration led to a loss in cell viability greater than 70% and undiluted extracts resulted in near complete cell death). A decreased level of toxicity was obtained following treatment with extracts produced from unwashed samples with increased amounts of AA compared to the extracts based on hydrogels produced with a higher ratio of NVP. This finding was anticipated as the NVP monomers proved to be cytotoxic in previously conducted studies (Section 3.1.4). Surprisingly, as shown in Figure 3.31, extracts containing leachates of gels with the highest amount of AA (25-75xP and 25-75xE) led to slightly decreased cell viability in comparison to extracts derived from hydrogels containing 50 wt% AA.

3.2.4.2 Elution test (neutral red endpoint)

The elution test in conjunction with a NR endpoint was employed as a second test for measuring viability of hydrogel extract-exposed cells, as it has been previously reported that different cytotoxicity endpoints can give different results depending on the test chemical used (Weyermann *et al.,* 2005). Thus, to increase the reliability of the results obtained, and avoid over- or underestimation of the toxicity of a substance, more than one assay should always be used to determine cell viability in *in vitro* studies (Fotakis and Timbrell, 2006).The NR endpoint is believed to be a suitable candidate for supporting the results generated via elution testing with the MTT endpoint, as the incorporation of NR dye has been previously used as an indicator of cytotoxicity in cell culture systems based on HepG2 and HaCaT cells (Sousa *et al.,* 1998). In order to conduct a comparative study, testing of unwashed and previously washed hydrogel extracts was performed for 24 h at 37^{o}C under similar conditions to those previously outlined in Section 3.2.4.1 with the MTT endpoint. As for the MTT endpoint, the absorbance data obtained for the test extracts was transformed to percentage of untreated control cell values and the NR data is illustrated in Figure 3.32 and summarised in Tables 3.9 and 3.10.

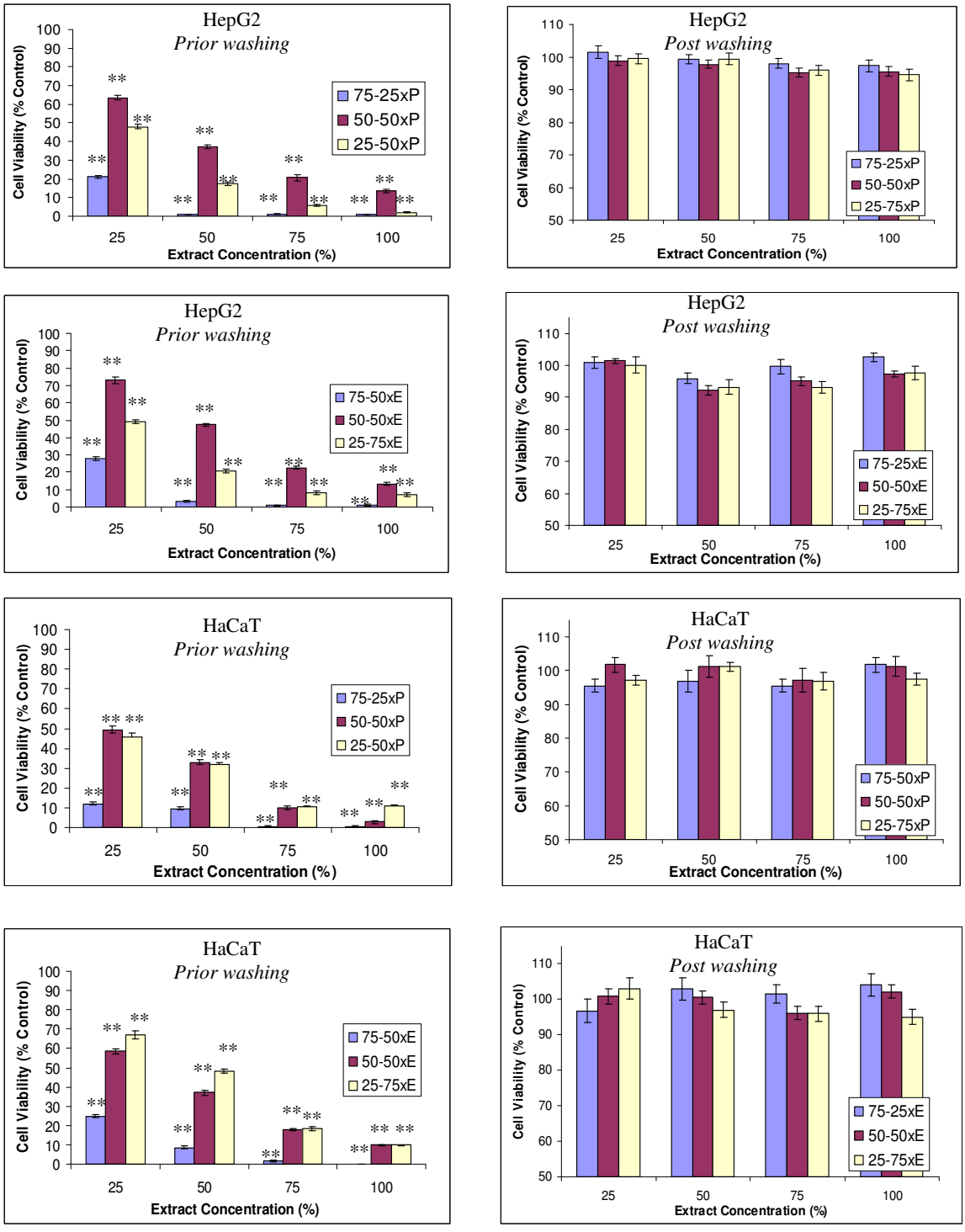

Figure 3.32: Comparison of the effect of washing on the viability of HepG2 and HaCaT cells as assessed in the elution test with the NR endpoint following 24 h exposure at 37°C to various concentrations of extracts of PEGDMA (xP) and EGDMA (xE) crosslinked chemical hydrogels. (n=12 for extracts produced prior washing, n=18 for extracts produced post-washing, ±SEM, * denotes a significant difference from the control **=p<0.01, *=p<0.05).

Table 3.9: Viability (% of control cells) of HepG2 cells after 24 h exposure at 37°C to undiluted extracts of PEGDMA (xP) and EGDMA (xE) crosslinked hydrogels as assessed in the elution test with the NR endpoint (n=12 for extracts produced prior washing, n=18 for extracts produced post-washing ±SEM, * denotes a significant difference from the control **=p<0.01).

Hydrogel Sample	Undiluted Extract before washing	Undiluted Extract post-washing
	% Viability (±SEM)	% Viability (±SEM)
75-25xP	1 (±0.21)**	97 (±1.85)
50-50xP	14 (±0.80)**	96 (±1.61)
25-75xP	2 (±0.27)**	95 (±1.78)
75x25xE	1 (±0.40)**	103 (±1.43)
50-50xE	13 (±0.86)**	97 (±0.94)
25-75xE	7 (±0.91)**	98 (±2.11)

Table 3.10: Viability (% of control cells) of HaCaT cells after 24 h exposure at 37°C to undiluted extracts of PEGDMA (xP) and EGDMA (xE) crosslinked hydrogels cells as assessed in the elution test with the NR endpoint (n=12 for extracts produced prior washing, n=18 for extracts produced post-washing ±SEM, * denotes a significant difference from the control **=p<0.01).

Hydrogel Sample	Undiluted Extract before washing	Undiluted Extract post-washing
	% Viability (±SEM)	% Viability (±SEM)
75-25xP	0 (±0.58)**	102 (±2.18)
50-50xP	3 (±0.75)**	101 (±2.97)
25-75xP	11 (±0.55)**	97 (±1.72)
75-25xE	0 (±0.46)**	104 (±3.11)
50-50xE	10 (±0.45)**	102 (±1.85)
25-75xE	10 (±0.33)**	95 (±2.20)

Figure 3.32 and Tables 3.9 and 3.10 illustrate the effect of 24 h exposure to hydrogel extracts on the viability of HepG2 and HaCaT cells in the elution test (NR endpoint). As illustrated by the relatively small error bars (Figure 3.32) and low SEM values (Tables 3.9 and 3.10) the degree of reproducibility is comparable to that of the data generated via the MTT endpoint (Figure 3.31 and Tables 3.7 and 3.8). Overall, the trend in toxicity profiles obtained following cellular exposure to the hydrogel extracts via the NR endpoint is similar to the trend observed with the MTT endpoint. However, compared to the MTT data, the NR endpoint appears to be slightly more susceptible to the toxicity of extracts from unwashed gels at the higher concentrations (Figures 3.31 and 3.32). It has to

be noted, however, that the concentration of NR dye itself induced microscopic observable changes to the cell morphology after 80 min exposure. However, no evidence was found that any of the tested extracts produced from previously washed hydrogels induced a significant cytotoxic effect on the cell lines. The cell viability values were all found to be in the range of those obtained for the untreated control cells, even for the undiluted concentrations (Tables 3.9 and 3.10). A dose-dependent decrease in viability was only observed for extracts from unwashed gels and this was evident in both cell types. Similar to the MTT data, the greatest reduction in cell viability compared to the control groups was obtained for leachates from unwashed hydrogels with 75 wt% NVP as base monomer (Figures 3.31 and 3.32). For these extracts a complete loss of viability was observed at the higher extract concentrations. Moreover, extracts from gels with higher amounts of AA showed a reduced but still substantial toxicity.

3.2.4.3 Indirect contact (agarose overlay) assay

The cytotoxic potential of leachable substances from unwashed and washed hydrogel matrices was also assessed for HepG2 and HaCaT cells via the agarose overlay assay. Since its introduction, this assay has been extensively used to assess the biocompatibility of polymeric materials (Rickert *et al.,* 2002). The assay requires the establishment of a fully confluent cell monolayer which is covered with a thin layer of agarose. The agarose layer protects the cells from direct contact to the test material as this can induce mechanical stress. As the hydrogel-cell exposure is facilitated by indirect contact, it is possible to evaluate the presence of toxic residues still trapped within the hydrogel matrix which may have not been released during the previously conducted elution tests. In addition, the test allows for a qualitative assessment of cytotoxicity whereby the degree of toxicity can be observed by zones of inhibition and measured objectively by descriptive terms e.g. none, slight, mild, moderate, severe or maximum.

Round discs (Ø = 2cm) of hydrogel samples (preswollen for 5 days in complete culture medium at 37^{o}C) were placed on the solidified agar layer. Unswollen gels tended to dehydrate the agarose. The MTT viability stain was used to facilitate macroscopic determination of the decolouration zones and further microscopic assessment of the morphology of damaged cells. The assay was performed in duplicate and the results were

recorded photographically as shown in Figures 3.33 and 3.34 and were graded as outlined in Table 3.11.

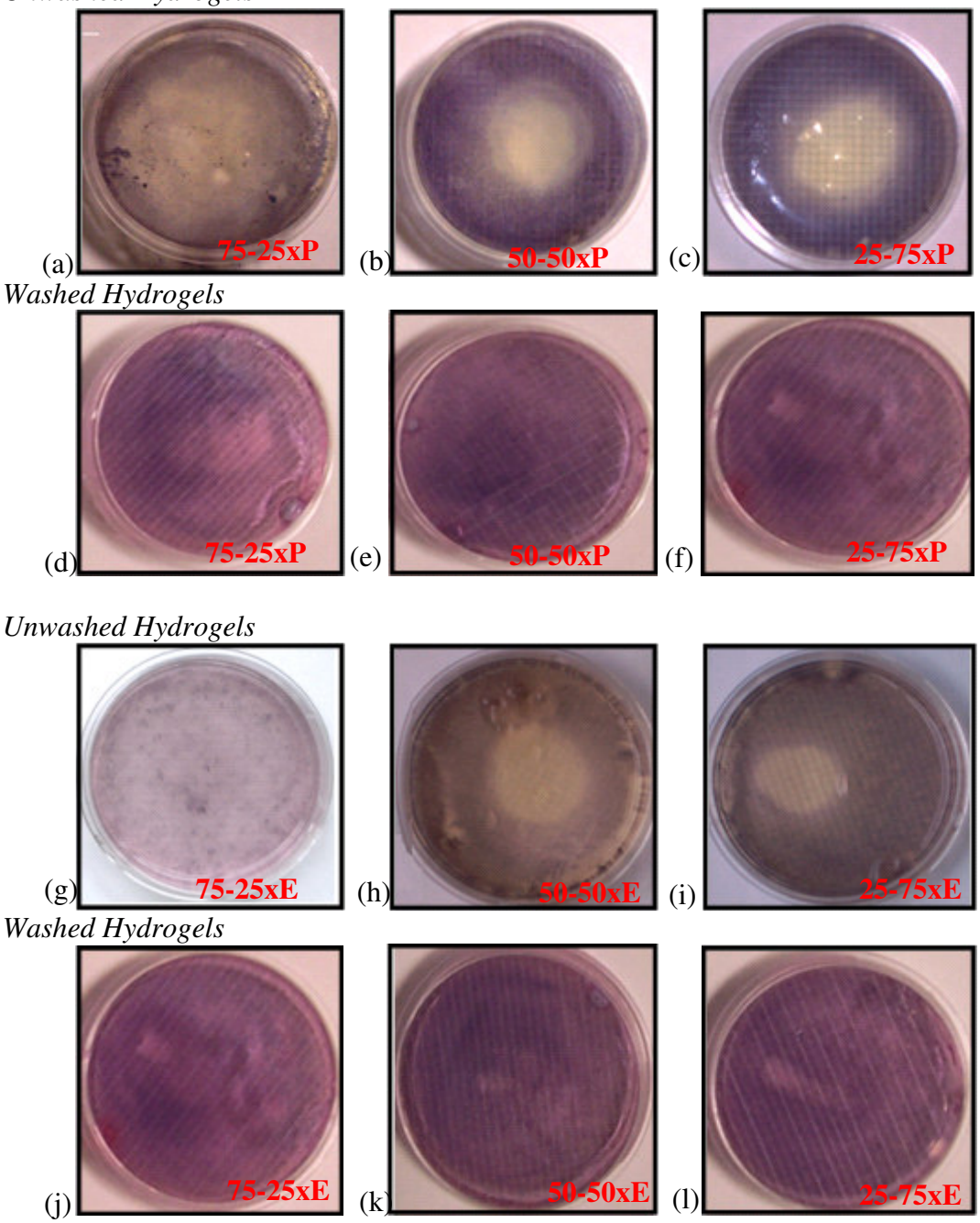

Figure 3.33: The effect of unwashed and washed hydrogel samples crosslinked with either PEGDMA (a-f) or EGDMA (g-l) on the viability of HepG2 cells as assessed via the agarose overlay assay after 24 h exposure at 37°C. Clear zones indicate cellular toxicity.

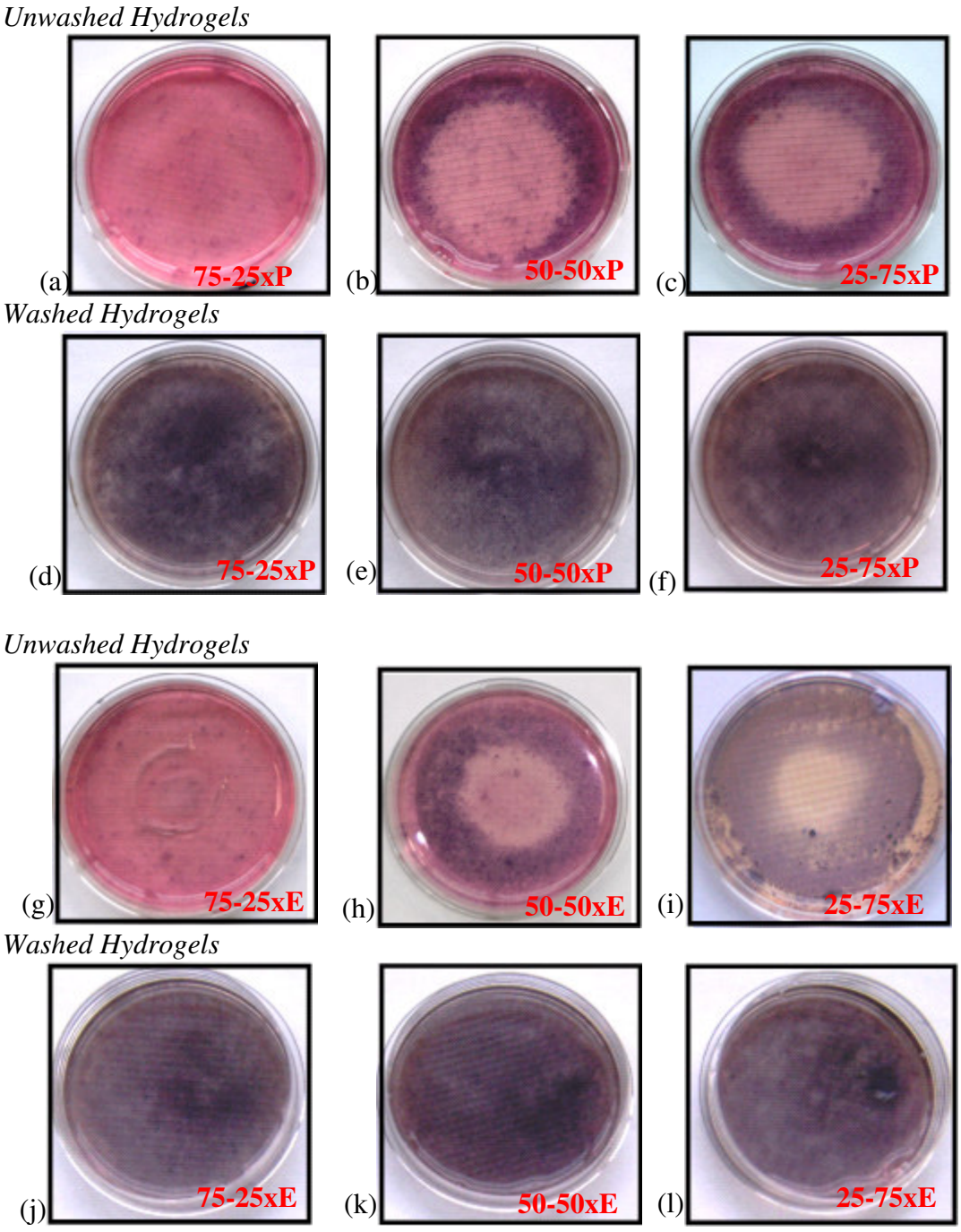

Figure 3.34: The effect of unwashed and washed hydrogel samples crosslinked with either PEGDMA (a-f) or EGDMA (g-l) on the viability of HaCaT cells as assessed via the agarose overlay assay after 24 h exposure at 37°C. Clear zones indicate cellular toxicity.

Table 3.11: Reactivity grades for HepG2 and HaCaT cells following 24 h exposure to unwashed and washed chemical hydrogel samples in the agarose overlay assay.

HepG2 Cells		
Hydrogel Sample	**Grade**	**Cellular toxicity**
Unwashed		
75-25xP	4	Severe toxicity
50-50xP	3	Moderate toxicity
25-75xP	3	Moderate toxicity
75-25xE	5	Maximum toxicity
50-50xE	3	Moderate toxicity
25-75xE	3	Moderate toxicity
Washed		
All samples	0	No Toxicity

HaCaT Cells		
Hydrogel Sample	**Grade**	**Cellular toxicity**
Unwashed		
75-25xP	5	Maximum toxicity
50-50xP	4	Severe toxicity
25-75xP	4	Severe toxicity
75-25xE	5	Maximum toxicity
50-50xE	3	Moderate toxicity
25-75xE	3	Moderate toxicity
Washed		
All samples	0	No toxicity

Figures 3.33 and 3.34 illustrate the effect of swollen hydrogel matrices on HepG2 and HaCaT cell monolayers after 24 h exposure at 37^{o}C. The occurrence of clear zones was a sign of cellular toxicity as dead or damaged cells are not able to metabolise the vital MTT stain into the purple formazan product. The determination of cell toxicity was based on qualitative evaluation of the zone of discolouration from grade 0 (no macroscopic detectable zone of discolouration = no toxicity) to grade 5 (zone of inhibition involves entire dish = maximum toxicity) as outlined in Table 3.11. Overall, tested hydrogels not previously washed for a period of 15 days in PBS released leachate which proved toxic to the underlying HepG2 and HaCaT cells (Figures 3.33a-c and g-i, and 3.34a-c and g-i). Also, microscope examination of the cells exposed to the leachate revealed severe cellular damage as the morphology of the cell layers were completely destroyed with residual cells appearing rounded or lysed. These findings were not surprising as unreacted monomers and other unidentifiable substances were likely present in the network of unwashed hydrogels as indicated in previous swelling experiments and reverse phase HPLC analysis (Sections 3.2.3.2 and 3.2.3.3, respectively). Furthermore, the results correlate with the previously

conducted cytotoxicity evaluation of extracts from chemical hydrogels (Sections 3.2.4.1 and 3.2.4.2). Again, hydrogels containing the highest amounts of NVP as the base monomer exerted the highest amount of cytotoxicity (grade 4-5) as indicated by a lack of cellular formazan production almost covering the entire culture dish (Figures 3.33a and g, 3.34a and g, Table 3.11). In contrast, unwashed gels containing higher amounts of AA induced less cellular toxicity (grade 3-4) independent of cell type and crosslinker used (Figures 3.33c and i, and 3.34c and i, Table 3.11). For both cell types the observed trend in cytotoxicity was similar. However, the HaCaT cell line appeared more susceptible to the adverse effects of the hydrogel leachate especially for PEGDMA crosslinked gels (Figures 3.33b and c).

Similar to the previously conducted MTT and NR assays, the extracts of washed hydrogels did not show any signs of cytotoxicity via the agarose overlay assay for either cell line tested. No macroscopic area of discolouration could be observed for either crosslinker type used (Figures 3.33d-f and j-l, and 3.34d-f and j-l) and all toxicity gradings were classified as grade 0 (Table 3.11). Moreover, microscope examination of cells exposed directly under the hydrogel sample did not reveal any signs of cellular toxicity. This, again, suggests that the residues of unpolymerised monomers and photoinitiator that had been initially present in the gel network were successfully removed during the purification process.

3.2.4.4 Qualitative and quantitative evaluation of cell viability following direct exposure to chemical hydrogels

Microscopic examination

Culturing mammalian cells in direct proximity to a biomaterial is a well established *in vitro* biocompatibility test (Rosenbluth *et al.,* 1965). In contrast to the previously performed cytotoxicity tests, this method allows for direct contact between the cells and the actual material surface. Following microscopic evaluation, important information regarding cell morphology, adhesion, growth and the relationship to the biomaterial's surface conditions can be obtained. In the present study HepG2 and HaCaT cells were seeded below and above the hydrogels and incubated for 24 h at 37^{o}C. During cell seeding, great care was taken to achieve optimum adhesion conditions as the movement of the hydrogel sample has

the potential to disrupt the cells which in turn could be inadvertently misinterpreted as a cytotoxic response. Following exposure the images shown in Figure 3.35 were captured using an inverted microscope attached to a digital camera system (Hamamatsu Photonics 3CCD, Germany).

HepG2 cells

HaCaT cells

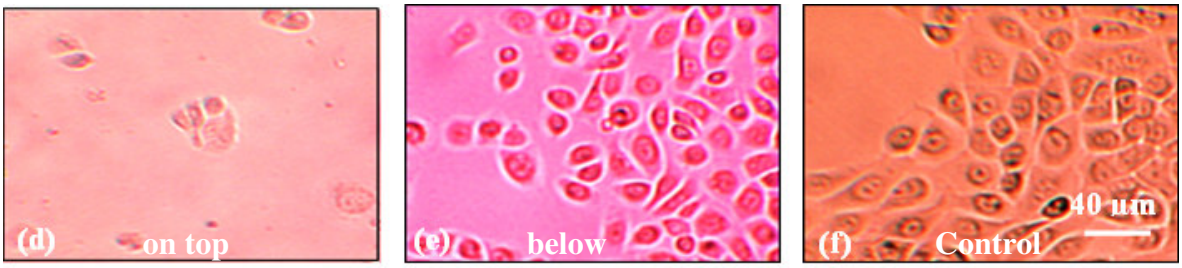

Figure 3.35: Images of the morphology of (a-c) HepG2 and (d-f) HaCaT cells in direct contact with prewashed chemical hydrogels for 24 h. Images a and d were obtained from cells seeded on top of the hydrogels' surface, images b and f were obtained from cells seeded onto culture dishes and covered with the hydrogel.

Figure 3.35 shows representative images of the morphology of HepG2 and HaCaT cells directly exposed to the surface of previously washed hydrogels. Images a and d were obtained by carefully seeding cells on top of the hydrogel to assess the cells' ability to adhere, proliferate and eventually differentiate to express the cell lines characteristic monolayer growth. As visualised in Figure 3.35a and d, the low growth density and altered morphology of both HepG2 and HaCaT cells seeded on top of the hydrogels indicates a lack of adherence. The cells appeared to form aggregates and could not proliferate to their characteristic morphology. The lack of adhesion may be explained by the high water content of the gels as it is known that highly hydrophilic materials inhibit the attachment of cell adhesion proteins (Luck *et al.,* 1998; Haigh, 2002). Moreover, due to the dissociation of hydrogen ions during the purification step, the hydrogels' surfaces express multiple

negative charges. It is believed that negatively charged material surfaces also tend to repel cell adhesion due to the negatively charged surface of cell membranes (Wang *et al.,* 2007b). Furthermore, the high mobility of polymer chains at the gels surface may inhibit cell adhesion. However, these characteristics could be considered beneficial within the context of the hydrogels' wound healing applications as it would allow the gel to be removed with minimal pain or trauma from the wound bed.

Moreover, to simulate the potential wound dressing application, the cells were placed in direct proximity to the samples by conventional seeding onto the bottom of the culture vessel and subsequently overlaying them with a washed hydrogel sample. After a 24 h incubation period the cells adhered to the culture dish and proliferated to a typical cell monolayer comparable to a monolayer obtained for untreated control cells. Even the pressure exerted by direct cell exposure to the hydrogels did not appear to influence cell growth. In this setting the hydrogels were exposed in closest possible proximity to the cells and so this result strongly demonstrates the noncytotoxic nature of the purified hydrogels and additionally supports their use in wound healing applications.

In contrast, cells seeded in direct contact to a preswollen unwashed hydrogel sample had a very different response. After 24 h incubation, all exposed cells appeared rounded or lysed and no signs of cell viability were observed. This again confirmed that unbound residues remaining in the matrices were highly cytotoxic.

Fluorochrome-mediated viability test

The fluorochrome-mediated Fda/EtBr viability test was used to quantitatively confirm the results obtained in the morphology studies, whereby cell viability did not appear compromised when cultures were overlaid with prewashed hydrogel samples (Figure 3.35). This test, first described by Strauss (1991), has become popular for the viability assessment of cells in culture and involves the use of two fluorescent stains FdA and EtBr. Viable cells hydrolyse the FdA and fluoresce green while dead cells absorb the EtBr and their nuclei fluoresce red. The amount of viable or dead cells can be easily quantified by scoring 200 cells from each hydrogel exposure (Fig 3.36 and Table 3.12).

HepG2 cells

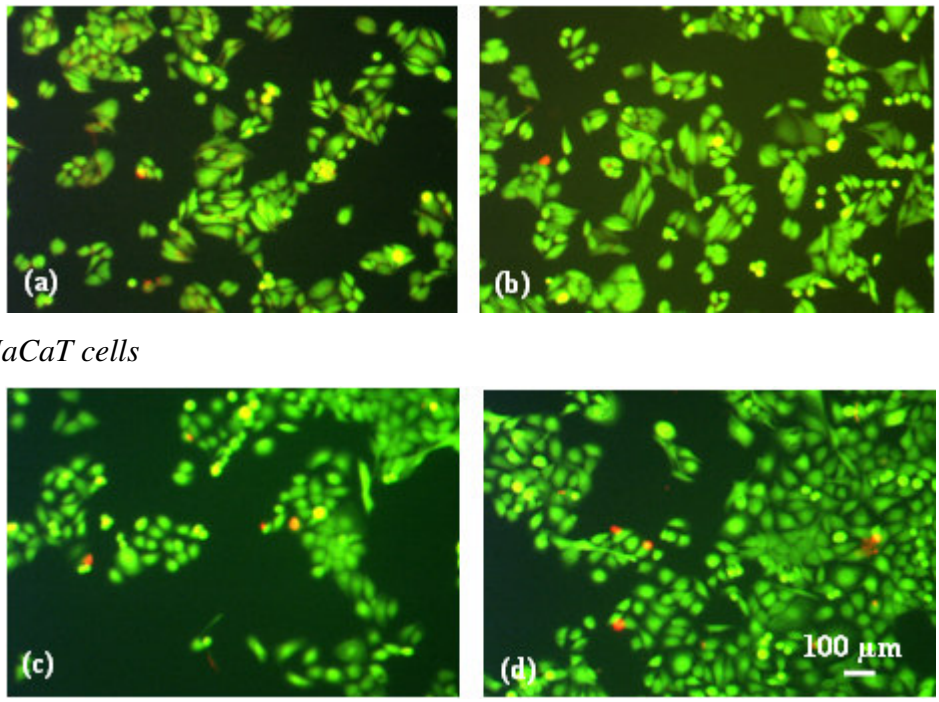

Figure 3.36: Images of (a and b) HepG2 and (c and d) HaCaT cells following the fluorochrome-mediated Fda/EtBr viability test. Images a and c represent untreated control cells, images b and d represent cells seeded onto culture dishes and covered for 24 h with prewashed hydrogel samples. Note: Viable cells exhibit green-fluorescent, red-stained nuclei indicate dead cells.

Table 3.12: Effect of direct contact hydrogel exposure for 24 h on the viability of HepG2 and HaCaT cells via the Fda/EtBr test.

Treatment	% Viable cells ±SEM	
	HepG2 cells	HaCaT cells
Untreated control	97.8 (±0.30)	96.6 (±0.75)
75-25xP	97.6 (±0.37)	98.1 (±0.43)
50-50xP	98.6 (±0.63)	96.8 (±0.41)
25-75xP	98.0 (±0.58)	96.5 (±0.45)
75-25xE	96.9 (±1.05)	97.2 (±0.93)
50-50xE	98.5 (±0.48)	97.0 (±0.98)
25-75xE	98.8 (±0.29)	97.4 (±0.59)

The cell response obtained via the fluorochrome-mediated viability test is illustrated in Figure 3.36 and summarised in Table 3.12. Both the majority of untreated control cells and hydrogel treated cells did not include the red EtBr stain within their nuclei but fluoresced green after excitation$_{515–560nm}$. Only a small number of isolated cells

incorporated the red fluorescent EtBr and were considered as nonviable. Nevertheless, the presence of a small number of red fluorescing cells was also evident in the untreated control population. Thus, this was believed to be indicative for naturally occurring cell death which can be expected for cell cultures grown *in vitro*. The cell count and subsequent statistical analysis presented in Table 3.12 demonstrated that there was no significant difference between the viability of untreated control cells and the hydrogel-exposed cells.

Overall, the results obtained via the fluorochrome-mediated viability assay support the conclusion drawn from the morphological analysis of cells grown underneath a prewashed, cell culture medium conditioned, chemical hydrogel (Figures 3.35 and 3.36 and Table 3.12). Although in direct contact, none of the tested hydrogels negatively interfered with the cells' viability. No interference of growth rates could be observed between the cell monolayer formed during hydrogel exposure and the untreated control monolayer.

3.2.5 Genotoxicity of chemical hydrogels

Like most *in vitro* based genotoxicity test methods, the comet and Ames assays are generally designed to test soluble chemicals for which a known exposure concentration can be prepared. Since the chemical hydrogels were insoluble, their preparation for subsequent genotoxicity testing differs considerably from the preparation of a soluble chemical substance i.e. required preparation of extracts. As it was very difficult to determine the exact extract composition and associated chemical quantities, great care and consistency was required during the extract preparation to obtain the desired level of reproducibility.

The main focus of this study was to determine if the addition of crosslinking agents and the resulting changes in the material properties of chemical-type hydrogels had any impact on their performance at the genetic level. Both crosslinkers belong to the chemical family of methacrylates, some of which have the ability to interfere with the cells genetic material via the alkylation of critical cellular nucleophiles (Johannsen, 2008).

Before extraction, the hydrogel samples were purified by submerging them in PBS for 15 days. To allow for the removal of unbound residuals, the PBS was replaced on a daily basis. After purification, the gels were dried and the final extracts were obtained by incubating the gels for 5 days in 30 ml of either cell culture medium for the comet assay or Ames exposure medium for the Ames test.

Again, the comet and the Ames assay were the chosen test methods to facilitate a comparison between the genotoxic potential of previously evaluated physical hydrogels. Instead of the HCT-8 cell line, which was used for the genotoxicity evaluation of physical hydrogels, the HaCaT skin cell line was used for the following study as the chemical gels may find a future application as wound healing devices. Additionally, HepG2 cells were employed to allow for direct comparison between the results obtained during the evaluation of physical hydrogels (Section 3.1.5.1). The Ames assay was performed with and without the addition of mammalian liver S9 fraction to ensure metabolic competence. Similar to the physical hydrogels, the bacterial strains used to investigate the mutagenic potential of the chemical hydrogels were from the type TA98 and TAMix.

3.2.5.1 The comet assay

For the comet assay, sample extracts of chemical hydrogels were exposed to HaCaT and HepG2 cell lines for 24 h at 37^{o}C. Since the previously performed cytotoxicity evaluation (Section 3.2.4) showed that none of the exposed extract dilutions provoked a significant negative effect on treated cell viability, only undiluted, washed hydrogel extracts were used in the comet assay to assess the extracts' genotoxic potential.

To ascertain that no false positive responses due to cytotoxicity were obtained, the viability of the hydrogel extract treated cells was once more inspected with the trypan blue method shortly before commencing the comet assay. As expected, there was no considerable reduction in cell viability observed. Again, the assay was conducted on duplicate slides with 50 single cells scored per slide. Similar to previous observations for the physical hydrogels, the majority of the data obtained was not normally distributed (Anderson-Darling method) and statistical differences between control and treated cells were evaluated with nonparametric tests. Figure 3.37 and Table 3.13 shows the results obtained following exposure of extracts from washed chemical hydrogels to HepG2 and HaCaT cells in the comet assay.

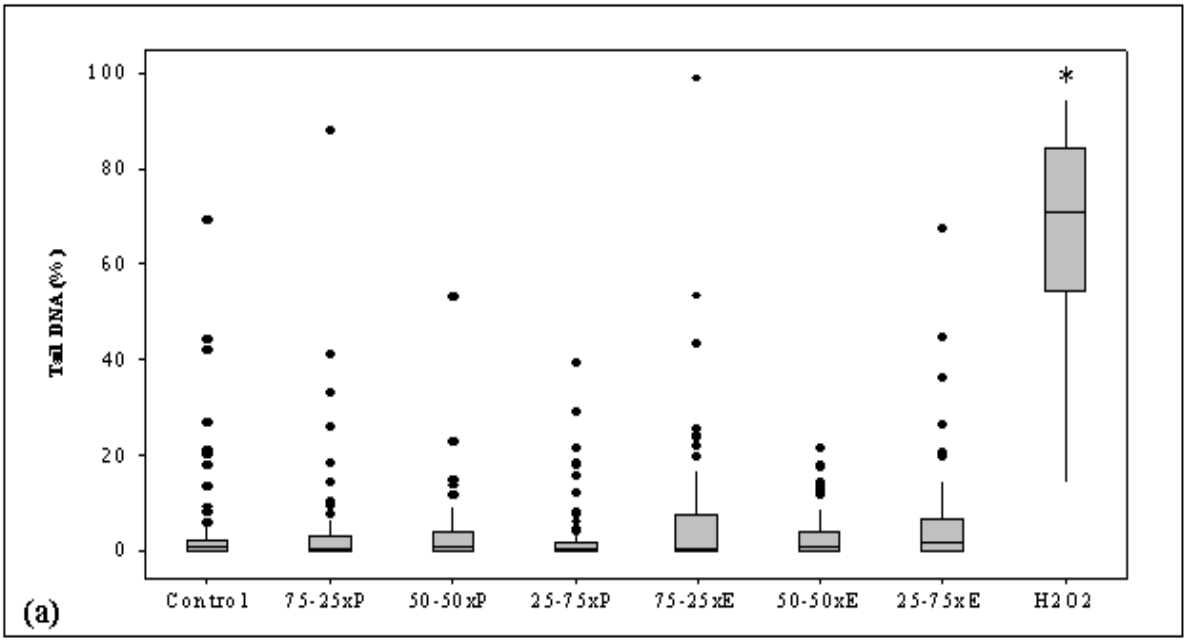

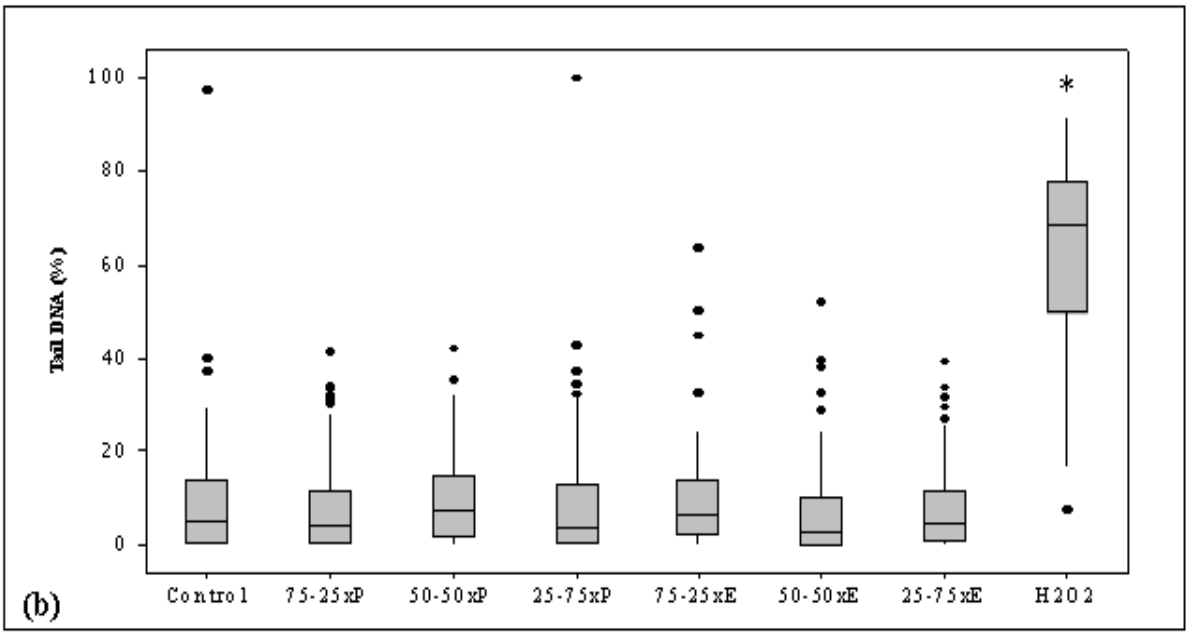

Figure 3.37: Box plot presentation of Tail DNA (%) for HepG2 (a) and HaCaT (b) cells exposed to undiluted, washed chemical hydrogel extracts, negative control (24 h at 37°C) and 100 µM H_2O_2 (40 min at 4°C). Each box corresponds to 100 comets measured on two slides and represents 25-75 percentiles, middle line = median, whisker extends to the maximum/minimum data point within 1.5 box heights from the top/bottom of the box. Dots above and below boxes indicate outliers. * denotes a significant difference from the untreated control ($p<0.05$).

Table 3.13: Tail moment and percentage tail DNA obtained in the comet assay after exposure of HepG2 and HaCaT cells to undiluted, washed chemical hydrogel extracts for 24 h and 100 µM H_2O_2 for 40 min. Results shown are the means (±SEM) of 100 single cells from duplicate slides. * denotes a significant difference from the untreated control ($p<0.05$).

Test Sample	HepG2 Cells		HaCaT cells	
	Tail moment (±SEM)	% Tail DNA (±SEM)	Tail moment (±SEM)	% Tail DNA (±SEM)
Control	0.49 (±0.13)	3.69 (±0.99)	1.41 (±0.27)	8.98 (±1.26)
75-25xP	0.48 (±0.11)	3.89 (±1.08)	1.48 (±0.15)	8.05 (±0.98)
50-50xP	0.38 (±0.08)	3.00 (±0.64)	1.55 (±0.14)	9.69 (±0.92)
25-75xP	0.30 (±0.07)	2.37 (±0.61)	1.31 (±0.19)	9.34 (±1.37)
75-25xE	0.97 (±0.29)	6.46 (±1.60)	1.50 (±0.16)	9.62 (±1.05)
50-50xE	0.35 (±0.05)	2.90 (±0.43)	0.92 (±0.15)	7.04 (±0.99)
25-75xE	0.83 (±0.19)	5.41 (±0.98)	1.00 (±0.11)	7.91 (±0.88)
H_2O_2				
100 µM	18.80 (±1.28)*	68.21 (±1.82) *	32.52 (±1.59) *	62.82 (±1.88) *

None of the undiluted extracts prepared from washed chemical hydrogels caused a significant degree of DNA damage in HepG2 or HaCaT cells as evident from the extent of DNA migration compared to untreated controls (Figure 3.37 and Table 3.13). Indeed, the mean values for tail moment and percentage tail DNA of each tested extract were within the range of the untreated control (Table 3.13).

Interestingly, the HaCaT cells proved to be slightly more susceptible to the positive control than the HepG2 cells, which may be attributed to the higher level of antioxidant defense enzyme levels, probably including catalase activity, present within HepG2 versus HaCaT cells (Dierickx, 1998; Knasmueller *et al.,* 1998). The overall background of observed variation in DNA migration for single cells (indicated by the SEM and outliers in the box plots) may be explained by the fact that the treated cell cultures were in different growth stages. Replicating cells processed in the comet assay can result in the creation of strand breaks or gaps detectable with the comet assay (McGlynn *et al.,* 1999). Also cells undergoing spontaneous apoptosis can also influence the homogeneity of the DNA migration pattern (Choucroun *et al.,* 2001; Kleinsasser *et al.,* 2004). However, these factors were of little concern as they occurred in the untreated control at an equal rate and did not adversely affect the overall performance of the assay.

As observed during the previous evaluation of physical hydrogels, the presence of unbound residuals within the networks resulted in the formation of enhanced DNA migration values due to cytotoxic mechanisms. The lack of genotoxicity from the present investigation indicates, again, that residues of unreacted monomers were successfully reduced via the purification technique. Furthermore, as observed in the comet assay, the introduction of chemical crosslinking agents did not cause a genotoxic effect. Again, the positive control H_2O_2 proved the sensitivity of the assay.

3.2.5.2 The Ames mutagenicity test

As previously outlined for the Ames assay following bacterial exposure to physical hydrogels and the base monomers NVP and AA no elevated rate of induced DNA mutations were observed (Figure 3.20 and Table 3.4). Although the chemical gels have the same monomeric feed compositions as the physical gels, even the addition of small quantities of chemical crosslinker could potentially result in the formation of mutagenic substances within their matrices. Hence, it was necessary to evaluate the potential of these gels to induce single nucleotide point mutations.

The Ames exposure medium was used to extract any residual unbound material left in the gels after purification. Undiluted extracts were used for these investigations, as they appeared nontoxic to the bacterial cells during a conducted cytotoxicity-screen test (Section 2.5.2.1). For comparative purposes, a similar test procedure as described for the physical hydrogel solutions was utilised (2.5.2.2). Both the extracts and respective positive control chemicals (in the absence of S9: 4-NQO:2-NF 500:2000 ηg/ml; in the presence of S9: 2-AmAn 125 μg/ml) were exposed to approximately 10^7 bacteria cells for 90 min.

Figure 3.38 and Table 3.14 show the results obtained with the Ames assay following strain exposure to the various extracts from previously washed chemical hydrogels including the negative controls and appropriate positive control chemicals. Similar to the results obtained for the physical hydrogels, all extracts from washed chemical gels proved nonmutagenic in the Ames assay. The observed reversion response for any of the strains tested (±S9) following exposure to the extracts did not significantly differ from the untreated control.

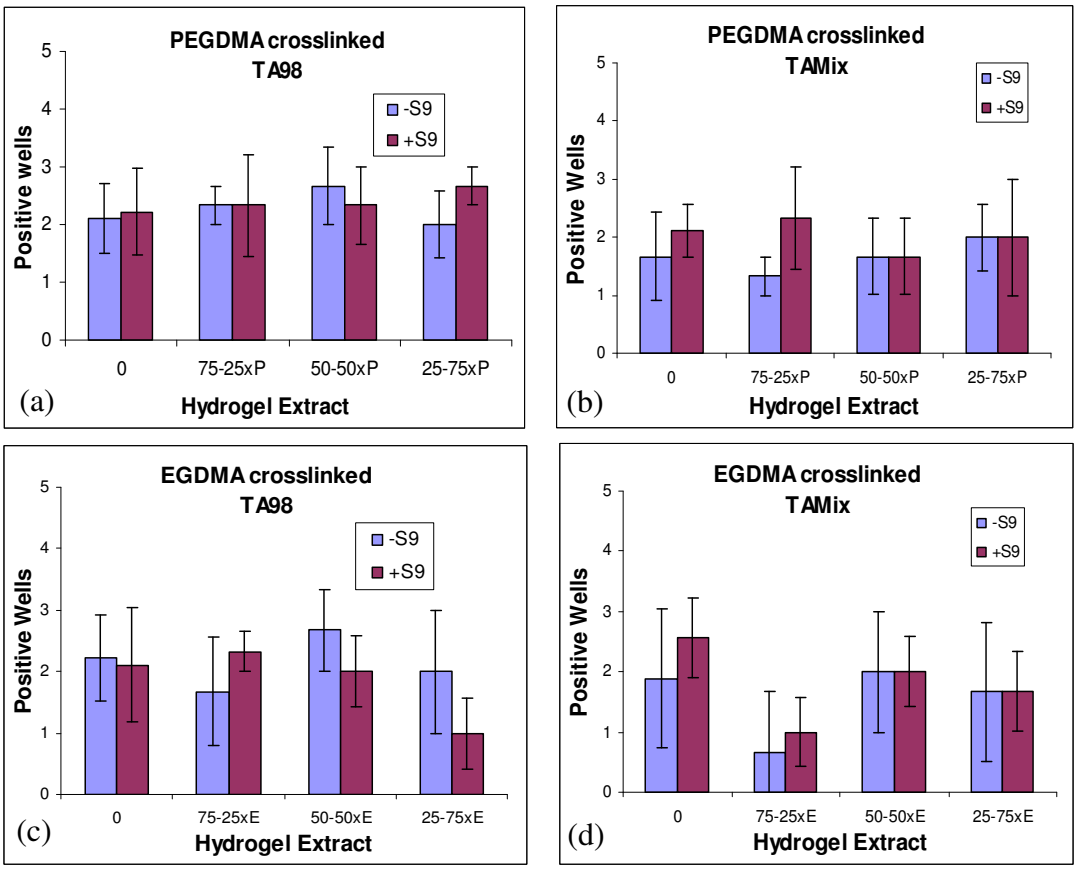

Figure 3.38: Reversion events observed following exposure of *S. typhimurium* strains to extracts from undiluted, washed chemical hydrogels crosslinked with (a and b) PEGDMA or (c and d) EGDMA (c and d). Results obtained are the mean of three independent experiments (±SEM).

Table 3.14: Mean values of positive wells obtained from three experiments (±SEM) via the Ames mutagenicity assay following 90 min cellular exposure to extracts from undiluted, washed chemical hydrogels, untreated and positive controls (±S9). * denotes a significant difference from the untreated control ($p<0.05$).

Sample	TA98 (±SEM)		TAMix (±SEM)	
	-S9	+S9	-S9	+S9
Untreated control	2.44 (±0.82)	2.11 (±0.79)	1.67 (±0.76)	2.11 (±0.45)
75-25xP	2.33 (±0.88)	1.67 (±0.33)	1.33 (±0.33)	2.33 (±0.88)
50-50xP	2.67 (±0.66)	2.33 (±0.66)	0.67 (±0.33)	2.67 (±0.88)
25-75xP	2.00 (±0.58)	2.67 (±0.33)	2.00 (±0.58)	2.00 (±0.10)
Positive control	47.56 (±0.42)*	43.43 (±1.16)*	47.22 (±0.63)*	39.00 (±1.53)*
0	2.22 (±0.69)	2.11 (±0.94)	1.89 (±0.96)	2.56 (±0.66)
75-25xE	1.67 (±0.88)	2.33 (±0.33)	0.67 (±0.66)	1.00 (±0.58)
50-50xE	2.67 (±0.66)	2.00 (±0.57)	2.00 (±1.54)	2.00 (±0.58)
25-75xE	2.00 (±1.00)	1.00 (±0.57.)	1.67 (±0.33)	1.67 (±0.66)
Positive control	47.33 (±0.58)*	43.89 (±1.13)*	47.43 (±0.58) *	44.32 (±1.34) *

Also the presence of the crosslinking agents appeared not to influence the hydrogels mutagenic potential. In agreement with the comet assay, this observation may be based on the fact that the washing procedure removed unbound material from the networks including residuals from the crosslinkers, as the genotoxic effect of methacrylates has been previously documented (Cameron *et al*., 1990; Schweikel *et al.,* 1998; Johannsen, 2008). Dearfield *et al.* (1991) has even suggested that exposure to these chemicals can result in alkylation of critical cellular nucleophiles. In this context, a study performed by Cameron *et al.* (1990) showed that EGDMA tested positive with the mouse lymphoma assay in the presence of S9 liver homogenate. In the current study, the presence of the crosslinking agents appeared not to influence the hydrogels mutagenic potential. This observation was in agreement with the comet assay and may be based on the fact that the washing procedure removed unbound material from the networks including residuals from the crosslinkers. Nevertheless, the concurrent positive controls induced reversion rates exceeding a value of 47 in the absence of S9 liver homogenate and a value of 39 in the presence of S9 for all strains tested.

Overall, the results from this investigation suggest that the tested hydrogel extracts were devoid of any mutagenic effect as no statistical difference between the solvent controls and the hydrogel extracts was established. In addition, no dose-dependent effects were observed. Again, the lack of any mutagenic activity may be related to the purity of the polymer following the removal of leachable material. The positive control chemicals for each strain resulted in the expected increase in the number of revertant colonies, indicating the study was valid (Flückiger-Isler *et al.,* 2004).

3.2.6 Summary

A series of chemically crosslinked copolymers based on NVP and AA were synthesised at different monomeric feed ratios using photopolymerisation. For comparative purposes, two chemical crosslinking agents with varying molecular weights were employed: EGDMA and PEGDMA at a concentration of 0.1 wt% of the total monomer content. After polymerisation, no visual difference between the previously discussed physical hydrogels and the chemical crosslinked gels was evident. Both samples appeared transparent and glass-like in their nonhydrated form. Again, with increasing amounts of AA in the initial

monomeric feed ratio, the surface of the xerogel started to deteriorate and the 25-75xP and 25-75xE samples appeared moist which most likely indicated the presence of unreacted liquid monomers. The FTIR spectra were almost indistinguishable from the spectra of physical hydrogels and the presence of unpolymerised residuals could not be excluded. A change in the spectra due to the addition of a chemical crosslinking agent was not observed. During hydration in PBS, the gels reached high swelling ratios and, after reaching their EWC, were able to retain the swelling medium in their networks without further degradation. When fully swollen, the samples exhibited high moisture contents, thereby resembling a soft tissue-like consistency. Based on the results obtained from the rheological assessment and the compression tests, it can be concluded that the hydrated hydrogels express favourable mechanical properties which strengthens their potential usage in wound healing applications. The nondegradable nature and high elasticity of the swollen gels can provide structural support to damaged tissue.

As these gels were insoluble in aqueous solutions, further purification by washing the hydrogels in PBS was employed to remove residual unbound monomers. Reverse phase HPLC analysis of extracts prepared from unwashed and washed chemical hydrogels was undertaken to estimate the residual monomer content. This study revealed that the washing process proved to be efficient at removing the residual monomers. A marked reduction in the amount of monomers was evident in extracts from washed hydrogels as the amount of unreacted monomers in these extracts was too small to be detected.

The cytotoxic potential of both the unwashed and the washed chemical hydrogels was investigated via direct and indirect exposure of suitable *in vitro* cell culture systems. MTT, NR and fluorescence-based viability endpoints combined with cell morphological examination were employed. Direct and indirect cell exposure to unwashed hydrogels drastically reduced the viability of exposed cell cultures. In contrast, the washing procedure proved very efficient at removing residual cytotoxic monomeric substances from the chemical hydrogel networks, as cells were not affected following direct and indirect exposure to washed gels. In addition, the gels appeared nonadhesive to tissue culture layers with their transparency expected to benefit wound monitoring.

The tested extracts from undiluted, washed chemical hydrogels also proved free of any genotoxic and mutagenic potential as observed with the comet and the Ames assays

respectively. In conclusion, the favourable mechanical properties and the enhanced biocompatibility of the purified chemical hydrogels suggests that these materials have the potential to be used in biomedical applications, more specifically as wound healing devices, that will impact positively on patient health and wellbeing.

3.3 Optimisation and *in vitro* toxicity evaluation of a novel pulsed plasma gas-discharge system intended for low-temperature sterilisation of hydrogels

3.3.1 Preface

In order to minimise acquired infections, all medical devices coming into direct contact with sterile tissue or the vasculature have to be sterilised by an appropriate, validated method (ISO 14937). Recent research has demonstrated that nonsterile devices have a drastic impact on patients' morbidity and mortality rates (Tarafa *et al.,* 2010). Furthermore, the presence of foreign substances may jeopardise the compatibility of the device leading to undesirable tissue reactions and decreased functionality (Cholvin and Bayne, 1998). A variety of sterilisation methods using chemical or physical agents can be considered for the sterilisation of particular medical devices: liquid chemicals based on aldehydes or oxidising agents, radiation (gamma or electron beam), steam, dry heat, plasma and gases such as EtO, ozone and chlorine dioxide have been used to sterilise medical devices (Chamberlain *et al.,* 1998; Rogers, 2005). Apart from inactivating microorganisms, these sterilisation methods can adversely interact with the material of a medical device itself and negatively affect its functionality. For instance, it has been well documented that high temperatures and radiation can degrade a medical polymer's performance and hence lower its biocompatibility (Deng and Shalaby, 1995; Hirata *et al.,* 1995; Nair, 1995). In addition, the compatibility of liquid and gaseous chemical agents with the treated materials requires particular attention because of the corrosive nature of such agents (Tarafa *et al.,* 2010).

Polymeric hydrogels have been found to be problematic to sterilise by conventional techniques in either their dehydrated or hydrated form (Huebsch *et al.,* 2005; Elijarrat-Binstock *et al.,* 2007; Kanjickal *et al.,* 2008). Due to their aqueous nature and the resultant poor mechanical properties many hydrogels are sensitive to heat sterilisation (Stoy, 1999; Jiménez *et al.,* 2008). Furthermore, hydrogels may potentially absorb and trap residues of liquid or gaseous sterilising agents which, in turn, may adversely affect their biocompatibility during the end use (Barbucci *et al.,* 2002). Thus, it is of critical importance that sterilisation processes are developed which do not compromise the functionality and biocompatibility of such sensitive materials.

The limitation of conventional sterilisation methods and the rapid development of polymeric devices have prompted the search for novel sterilisation techniques. Intense interest has developed in technologies based on pulsed electric discharge for the destruction of microorganisms. Initial research proved that pulsed electric discharge is highly efficient with respect to microbial inactivation. In the last decade, various scientific investigations were conducted which confirmed the potential of this technology to inactivate microorganisms on contaminated surfaces (McDonald *et al.,* 2000), in food (Rowan *et al.,* 1999), and in liquids (Marsili *et al.,* 2002; Beveridge *et al.,* 2004; Satoh *et al.,* 2007). Examples of treatments involving pulsed electric discharge technologies include pulsed electric fields (PEF), pulsed UV, and PPGD treatment (McIlvaney *et al.,* 1998). Of these treatment types, PPGD has proven to be a very promising microbial inactivation method as it synergistically employs all the above mentioned biocidal elements in one system (Marsili *et al.,* 2002).

In recent years the interest in gas-discharge plasmas for microbial inactivation has increased with excellent review papers being published in scientific journals (Moisan *et al.,* 2001; Bogaerts *et al.,* 2002; Moisan *et al.,* 2002; Moreau *et al.,* 2008). There are several mechanisms which have been reported to contribute to the deleterious effects of gas-discharge plasmas on microorganisms: interaction of UV-radiation with microbial DNA (Laroussi and Leipold, 2004), damage of microbial cell structures by interaction with reactive species (Ekem, 2006) and nonspecific effects resulting from the formation of pressure shockwaves (Anpilov *et al.,* 2002). Also the formation of PEF can result in charge accumulation at the cell membrane which in turn induces electrostatic stress leading to ruptured cells – a phenomenon known as electroporation (Mendis, 2000).

The present study investigates the suitability of using a novel PPGD technology operated under varying conditions for the microbial decontamination of the chemical hydrogels that were developed in Section 3.2. The PPGD system consisted of a prototype HV pulse generator and a treatment chamber, both specially designed and developed for the low temperature sterilisation of biomaterials by Samtech Ltd. (Glasgow, UK). Within the treatment chamber, PPGD was generated via a multi-needle electrode configuration that was strategically placed over the surface of an aqueous solution which acted as a microbial inactivation medium. Using this PPGD approach a mixture of different biocidal effects was

expected that would ultimately result in the microbial decontamination of materials submerged within the aqueous solution. Depending on the nature of the gas present at the electrodes during treatment, plasma discharge processes will lead to the generation of biocidal elements such as reactive chemical species that can attack the cell surface of microorganisms (Satoh *et al.,* 2007; Moreau, 2008). It was expected that these species would be directed into the aqueous solution by the plasma stream itself and by passive diffusion. The UV-radiation and shockwaves formed during the discharge may also provide additional biocidal effects (Anpilov *et al.,* 2001; Zuckerman *et al.,* 2002). Moreover, with each pulse an electric field will be generated across the liquid with the potential to rupture the cellular envelope of microbial species (Beveridge *et al.,* 2004).

However, as the PPGD system investigated in this study has not been previously used for the inactivation of microorganisms for this particular application, critical electrical and biological properties governing its effective and safe operation needed to be evaluated to determine its suitability for subsequent treatment of chemical hydrogels. Hence, this section outlines preliminary studies which were conducted to obtain the optimal operational parameters needed to achieve maximum microbial inactivation of the aqueous solution (test liquid). Additionally, the toxicological safety of this new microbial decontamination method was investigated to address potential health risks associated with any electrochemical reaction occurring in the discharge-treated test liquid.

Preliminary investigations focused on the pulse formation and observed plasma discharge type and provided an insight into a number of problems associated with the design of the system. It was necessary to modify the original treatment chamber by replacing the PVC spacer with a transparent perspex spacer to allow for visualisation of the discharge process as this was essential for optimisation. Furthermore, the original gas connections on the treatment chamber proved unsuitable for this application and were modified to achieve a more controllable gas flow system. Information gained from the physicochemical characterisation of the plasma-treated test liquid were also used to determine the electrical settings that facilitate optimal microbial inactivation. This information also gave important insights into the possible mechanisms involved in microbial inactivation. Moreover, two bacterial organisms were chosen, namely *E. coli* and *S. aureus*, which represent both Gram negative and Gram positive microbial species, hence,

allowing for comparative studies on species sensitivities and inactivation kinetics for both microbial types. Finally, a preliminary toxicological evaluation of the PPGD-treated test liquid was conducted to ensure the system's suitability for hydrogel treatment whereby the formation and effects of cytotoxic and DNA damaging byproducts were investigated under varying operational settings.

3.3.2 HV pulse characteristics and plasma gas-discharge type

The configuration of the electrodes is a very important parameter for the generation of plasma gas-discharges. Especially when the discharge is directed towards or into a liquid, the placement of the electrodes greatly influences the discharge process and its chemistry. Although Sato *et al.* (1999) and Sunka *et al.* (1999) placed the HV discharge electrode directly into a liquid, and while this arrangement proved effective for the production of hydroxyl radicals compared to discharge into gases, the discharge area was rather small due to the quenching effect of the liquid. Numerous attempts have been made to increase the efficiency of discharge into water by bubbling gases through the discharge region (Espie *et al.,* 2001; Marsili *et al.,* 2002; Rowan *et al.,* 2008). Also the creation of the plasma discharge in the gaseous phase above the liquid has been investigated for the disinfection of contaminated water. Depending on the gases used, this configuration created different types of radicals which subsequently diffused into the liquid media (Satoh *et al.,* 2007).

The present study focuses on the creation of a pulsed plasma gas-discharge above a liquid with a multi-needle electrode, consisting of six sharp pins, used to create the discharge into a gaseous space above an aqueous solution. For the following treatment experiments, the treatment chamber was adjusted to accommodate a volume of 100 ml of aqueous test solution as this volume was found to be sufficient to fully submerge the test hydrogels. The electrodes were adjusted to yield a discharge gap of 5 mm over the surface of the test liquid to obtain a suitable area of discharge. Indeed, this treatment volume and gap distance resulted in a strong and consistent HV discharge, albeit with somewhat reduced impact on the CCS performance, and so was kept constant for all experiments. HV discharges in N_2 and O_2 were investigated as these gases have been found suitable for plasma sterilisation purposes (Satoh *et al.,* 2007). The gases were streamed through the electrode gap during pulsing at varying gas flow rates. Initial experiments, conducted to

determine optimal treatment settings, revealed the unstable nature of the SF_6 pressurised CCS. As shown in Section 2.6.2, Figures 2.5 and 2.6 the CCS was susceptible to internal arcing which was aggravated with increasing charging voltage and pulse repetitions. The arcing caused a molecular breakdown of the SF_6 gas, which in turn caused a failure of the insulating properties of the gas with settlements of debris and arc root burn marks on the switch electrodes. Overall, this had a detrimental impact on the triggering performance and a considerable amount of time was spent maintaining the system in order to restore proper switching ability (Section 2.6.2). Therefore, to minimise the deterioration of the CCS it was decided to utilise the pulse generator at conservative settings by limiting the maximum charging voltage. In accordance with initial treatment range finding tests, it was decided not to utilise the pulse generator above a charging voltage of 18 kV during the time course of this study. The pulse output waveform was monitored on the HV connections of the treatment chamber by using a digital oscilloscope (Tektronix TDS 3022) attached to a resistive probe. A typical voltage and current signal measured with the oscilloscope is shown in Figure 3.39.

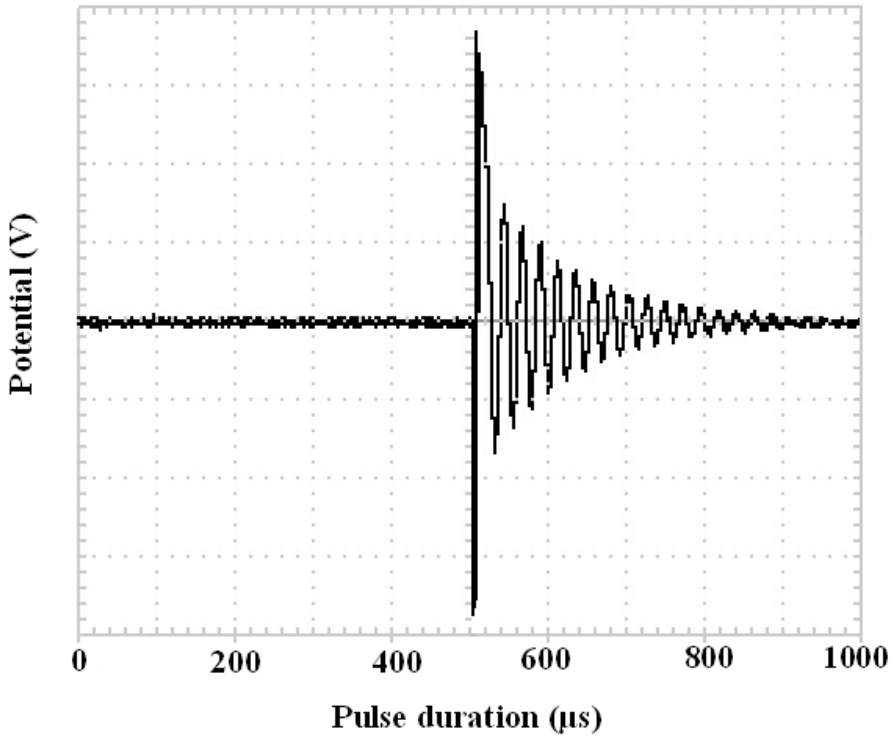

Figure 3.39: Typical waveform of a single pulse produced at the treatment chamber.

Figure 3.39 shows that the pulse is discharged in a bipolar impulse waveform. The pulse duration was found to be approximately 400 to 500 µs and the waveform remained relatively constant during the treatment. According to manufacturer's specification, the energy per pulse measured in joule (J) dissipated into the treatment chamber can be calculated using Equation 3.1, where *C* and *V* are the systems capacitance and the charging voltage, respectively.

$$E = ½ \, x \, C \, x \, V^2$$

(C = 40 nF (~ 4 x 10^{-8} F))

Equation 3.1: Energy per pulse delivered.

Table 3.15 shows the energy per pulse delivered for the PFN charging voltages used throughout this study.

Table 3.15: The PFN charging voltage and corresponding energy per pulse delivered.

Voltage (kV)	Energy per pulse (J)
18	6.48
16	5.12
14	3.92

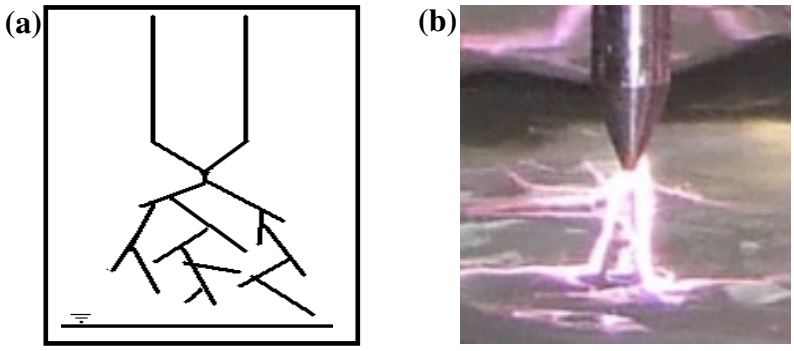

Figure 3.40: Streamer type corona discharge: (a) schematic and (b) observed during treatment in O_2.

As shown in Figure 3.40, for the charging voltage range used in this study, the observed HV discharge was found to be of a positive streamer type corona discharge (Yan *et al.,* 1999; Kanazawa *et al.,* 2002; Tendero *et al.,* 2006). The corona streamers emerged

from the tip of the electrode pins and formed branches which were observed over the entire gap. Although not yet fully understood, van Veldhuizen and Rutgers (2002) suggested that the formation of corona streamers occurs in three steps: initiation of a streamer (usually called inception), propagation and branching. During inception, free electrons, which originate from ionisation through cosmic rays, start moving towards the anode. Within the applied electric field these electrons, known as avalanche electrons, gain velocity. During propagation the avalanche develops into a cloud of positive ions and free electrons, with the high electromagnetic field causing the electrons to collide with gaseous molecules present in the bulk thereby partially transferring their energy, leading to molecule ionisation and the emission of numerous new electrons (van Veldhuizen, 2000). If the voltage is maintained, a conducting path is created between the electrodes and a current will flow through the charged cloud creating the branching effect. However, if the current is high enough it will heat the gas, decrease its density and increase its conductivity. This can lead to a spark breakdown (arcing) through a single conducting channel while no typical streamer branching occurs (van Veldhuizen and Rutgers, 2002).

3.3.3 Critical factors concerning the treatment fluid

The properties of the treatment fluid (also referred to as test liquid) used as medium to submerge the hydrogels during PPGD treatment were of crucial importance. The gas ionisation and subsequent plasma discharge can only occur when an electric field is able to develop from the anode across the liquid towards the cathode. In other words, the treatment fluid must have a high permittivity to allow an electric field to develop between the electrodes. Also, a certain conductivity level was required to conduct an electric current through the liquid. However, the conductivity should be kept low to minimise energy loss and temperature rise occurring through resistive heating (Zhang *et al.,* 2009). For this study a treatment fluid based on deionised water was considered appropriate due to its relatively high permittivity of $\varepsilon = 80.1$ (Kuchling, 2001). PBS was also added to the deionised water to raise the conductivity from 2.5 µS/cm to approximately 1000 µS/cm as this supported the discharge stability (Sato *et al.,* 1999; Anpilov *et al.,* 2004; Satoh *et al.,* 2007; Zhang *et al.,* 2009). With the addition of PBS, the composition of the treatment fluid was 5×10^{-4} M phosphate buffer, 1.35×10^{-4} M potassium chloride and 6.85×10^{-3} M sodium chloride.

Furthermore, the resultant increase in osmolarity provided optimised culture conditions for the microorganism used during subsequent microbial inactivation studies. It was important to achieve favourable bacterial growth conditions within the test liquid since inhibited growth or activated defence mechanisms would influence the inactivation experiments. In addition, it is likely that the inactivation of microbial species would be more difficult with a higher liquid conductivity than used in the present study. Further increasing the conductivity would result in a corresponding decrease in the liquid resistivity, therefore a lower pulse voltage will appear at the load, and the pulse length will also be reduced as a result of ionic conduction through the test liquid.

The following investigations were carried out to characterise the physicochemical changes in the treatment fluid subjected to PPGD treatment. Results obtained from these experiments provided essential information for the establishment of optimised treatment conditions and on the mechanisms involved in bacterial inactivation.

3.3.3.1 Temperature, conductivity and pH

Low temperature sterilisation was desired with regard to the sterilisation of temperature sensitive materials such as hydrogels. The current study used atmospheric corona streamer discharge which is considered a nonthermal plasma type (van Veldhuizen and Rutgers, 2002). However, a certain temperature rise of the treatment fluid resulting from the HV discharge was expected. When a pulse is applied to the test chamber, current flows and some of the energy from the pulse is always converted to heat in a process known as Joule heating.

For the given set of conditions, the rise in temperature within the treatment chamber is mainly dependant on two things. Firstly, temperature increase is dependent on the heat capacity of the contained treatment fluid and chamber components. Secondly, the temperature will be dependent on the presence of the temperature gradient from the chamber to the surrounding environment, since this will result in heat transfer out of the system. Heat is transferred by three separate modes, radiation, convection, and conduction, of which conduction and convection are the predominant processes in the plasma chamber. At thermal equilibrium, the rate of heat transfer into the system by Joule heating will be equal to the rate of heat transfer to the surroundings (Kuchling, 2001).

Besides the sensitivity of hydrogels, the rise in temperature also needs to be considered in terms of microbial inactivation. Thus, it was of the utmost importance to monitor the temperature rise within the chamber during the treatment. The following temperature studies were conducted on 100 ml of the treatment fluid (95 ml dH_20 and 5 ml PBS) with O_2 used as the discharge gas at a constant flow rate of 2.5 l/min. The temperature increase of the treated fluid was monitored with an automated temperature control at 2 min intervals for a total treatment time of 60 min. Investigations on the effect of varying the PFN charging voltage and the pulse repetition rate on the fluid temperature were also conducted. Figure 3.41 illustrates the temperature effect observed at varying charging voltages and pulse repetition rates respectively.

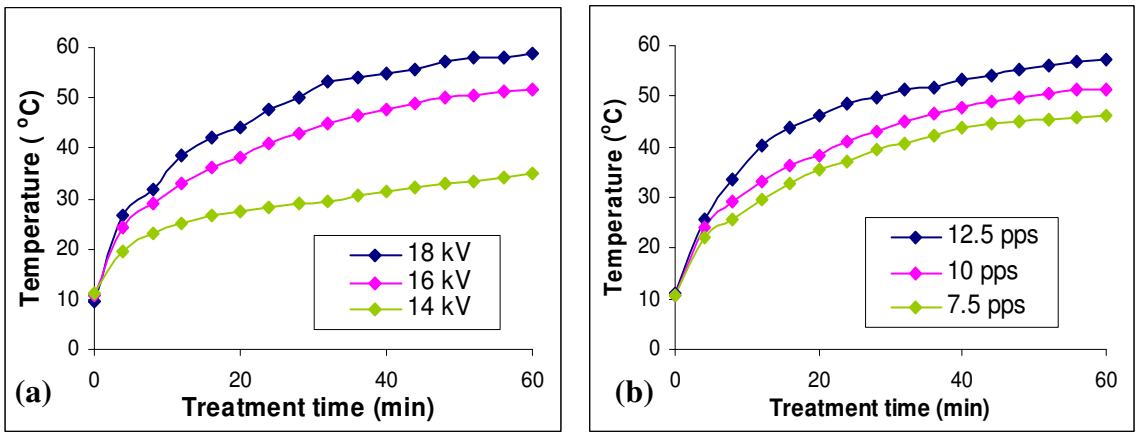

Figure 3.41: Temperature increase observed in the treatment fluid during PPGD treatment with (a) varying PFN charging voltages at a constant pulse frequency of 10 pps and (b) varying pulse frequencies at a constant PFN charging voltage of 16 kV.

Figure 3.41 demonstrates that a significant temperature increase in the treatment fluid was obtained during the PPGD treatment. The temperature increase was strongly dependent on the pulse generator charging voltage and pulse repetition rate. By subjecting the test liquid to a discharge of 18 kV at 10 pps, the temperature rose to 59°C within the treatment time of 60 min. In comparison, for the 16 kV and 14 kV discharge, the temperature reached a maximum of 51.2 and 36.6°C respectively. A similar temperature increase was observed by increasing the pulse frequency while keeping the charging voltage constant at 16 kV. With an increase in the pulse rate there was a corresponding increase in temperature of the test liquid. By treating the solution with 12.5 and 7.5 pps, the

temperature of the fluid reached respective values of 57.4 and 46.3°C. Interestingly, for both tests, a fast temperature increase was observed during the first minutes of treatment. After this initial rise the rate of temperature increase started to slow down, thus indicating that a thermal equilibrium will be approached where the rate of heat input equals the rate of heat transferred from the system by convection and conduction.

The temperature increase of the test liquid seen with prolonged treatment at intense discharge conditions could potentially have a negative impact on the hydrogel's properties. Furthermore, a temperature increase above 40°C may contribute to microbial killing during PPGD treatments. Therefore, these temperature effects had to be considered for subsequent microbial inactivation studies and hydrogel treatments.

As previously mentioned, the conductivity of the treatment fluid is likely to have a direct effect on the electrical pulse characteristics. Hence, the conductivity of test liquid exposed to plasma discharges was monitored to determine if any significant change in the conductivity occurred during treatment. The investigation focused on the effect of two different discharge gases, O_2 and N_2, on the liquid's conductivity. The gases were streamed through the 5 mm electrode-liquid gap at a flow rate of 2.5 l/min. Figure 3.42 shows the change seen in the liquid conductivity during plasma discharge treatment using O_2 and N_2 gas respectively. The PFN charging voltage was kept constant at 16 kV with varying pulse repetition rates investigated.

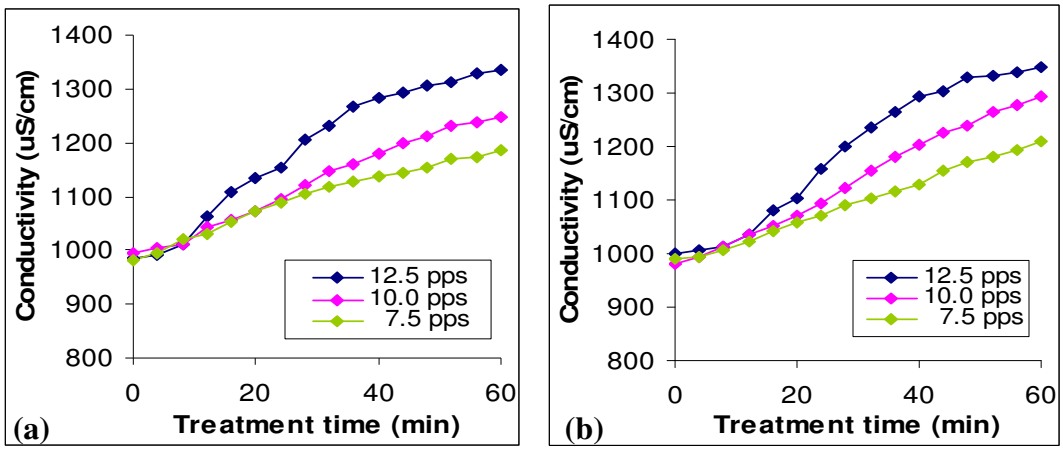

Figure 3.42: Conductivity change of the treatment fluid during PPGD treatment using (a) O_2 and (b) N_2 as discharge gases at a flow rate of 2.5 l/min. The pulse generator was charged to 16 kV while varying pulse repetition rates of 7.5, 10 and 12.5 pps were investigated.

As shown in Figure 3.42, considerable changes in the treatment fluid's conductivity occurred during PPGD using O_2- and N_2-mediated discharges. More specifically, the conductivity of the liquid increased with increasing treatment time and pulse frequency. Compared to the O_2 discharge, the N_2 discharge appeared to cause slightly higher conductivity readings with 1350 µS/cm being the highest value achieved. The increase in conductivity is believed to have occurred as a result of the formation of ionic species during gas ionisation, which readily dissolved into the water. It has been shown previously that, depending on the gas streamed through the electrode gap, streamer corona discharge can produce many chemically active species that have recognised biocidal properties (Clements *et al.,* 1987; Sato *et al.,* 1999; Wenjuan and Xiangli, 2007). If O_2 is streamed between the electrodes during the HV discharge, the O_2 molecules can dissociate to form short lived atomic oxygen. Oda and coworkers showed that the atomic oxygen can then react with other gaseous oxygen to form compounds such as ozone (Oda *et al.,* 2006). If the pulsed HV discharge is directed in or towards an aqueous medium the presence of several chemical species such as free electrons, OH, H·, HO_2· and H_2O_2 can be observed (Joshi *et al.,* 1995). Conversely, by streaming N_2 gas through the electrodes gap, the electrical discharge is able to break the strong triple covalent bond of the N_2 molecule and form activated atomic nitrogen that may also inactivate microorganisms (Rehbein and Cooray, 2001). It is then possible that several oxides of nitrogen are formed during plasma treatment of aqueous liquids when activated nitrogen compounds react with dissolved oxygen and oxygen atoms that could be liberated from the water during the discharge. It is suggested that these nitrogen based compounds will dissolve in aqueous solutions and increase the conductivity level (Zhang *et al.,* 2009). Therefore, a more specific investigation into the generation of chemically active compounds resulting from the discharge will be discussed in subsequent sections (Section 3.3.3.3).

Overall, a significant rise in the treatment fluid's conductivity level was observed for both gas-discharge types. However, this increase did not have a drastic impact on the discharge performance as no changes in the pulse waveform were noticeable by routine oscilloscopic examinations throughout the duration of the experiments. As the increase in water conductivity could have resulted from the diffusion of generated compounds with acidic or basic properties, it was also necessary to closely monitor pH changes in the

treated liquid during the discharge process. Changes in the pH can directly affect the physiology of suspended microorganisms in liquids and at certain levels will contribute to microbial reduction (Rowan, 1999; Black, 2005). Additionally, extreme acidic or alkaline solutions can negatively impact on the performance of many biomaterials (Lemons *et al.,* 1998). Hence, the following study investigated the effect of plasma discharge treatment on the test liquid's pH values with Figure 3.43 showing the effect of O_2- and N_2-mediated plasma discharge on the pH of the test liquid. The PFN charging voltage was 16 kV with varying pulse repetition rates investigated.

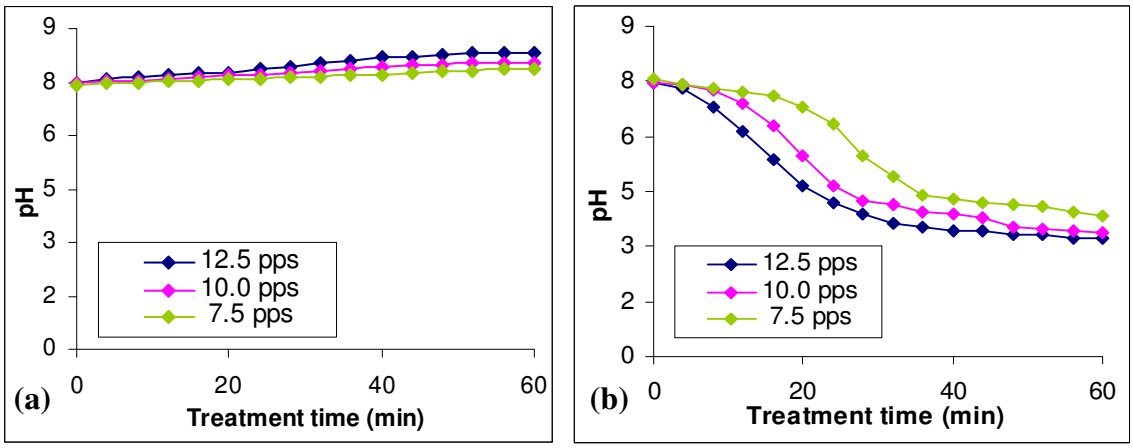

Figure 3.43: Effect of PPGD treatment on the pH of treatment fluid using (a) O_2 and (b) N_2 as discharge gases at a flow rate of 2.5 l/min. The pulse generator was charged to 16 kV while varying pulse repetition rates of 7.5, 10 and 12.5 pps were investigated.

Figure 3.43 shows that the plasma discharge has a notable effect on the pH of the treatment solution. When using O_2 as a discharge gas, the pH values increased slightly in an almost liner fashion, with the pH increase dependent on the pulse frequency. The highest pH value of 8.34 was observed after 60 min plasma treatment with 12.5 pps. When the pulse generator was adjusted to 10 pps and 7.5 pps, the pH increase after a 60 min treatment was found to be 8.06 and 7.87, respectively. The mechanism for this pH change towards alkaline conditions remains to be fully elucidated, but may be due to the formation of dissolved hydroxyl ions resulting from the O_2 discharge contributing to the pH increase.

In contrast to the O_2 discharge, when using N_2 as discharge gas, a drastic drop in pH was observed for all pulse frequencies evaluated with the decrease in pH dependent on the

pulse frequency. The lowest pH value of 3.21 was observed after a 60 min treatment with 12.5 pps, followed by values of 3.40 and 3.82 after treatment with 10 pps and 7.5 pps, respectively. During the first 30 min of treatment, a rapid drop in pH was found for all the evaluated pulse frequencies, as indicated by the negative slope (Figure 3.43b). For the next 30 min the liquid's pH continued to drop, albeit at a lower rate. Also, it appears that a 'saturation level' may have been reached. The formation of nitrogen based compounds has previously been suggested as a possible reason for this notable decrease in pH of the test liquid with research conducted by Wenjuan and Xiangli (2007) proving that activated nitrogen formed during HV discharge in N_2 gas can take part in further aqueous chemical processes to form acidic nitrogen compounds, that are able to dissolve into the aqueous solution and cause a rapid drop in pH. Nevertheless, the chemistry behind the production of such compounds during the plasma discharge, and how they dissolve into the aqueous solution, appears to be relatively complex. Therefore, further analysis of PPGD-treated aqueous solutions using IEC was carried out in this study to accurately determine specific compounds and species which may be responsible for the pH decrease observed during the N_2-mediated discharge.

3.3.3.2 Dissolved ozone concentration

Ozone, from the Greek word 'ozein' meaning 'to smell', is a triatomic oxygen molecule with a strong characteristic odour. Due to its powerful oxidising properties and the fact that it can convert back to oxygen (Summerfelt and Hochheimer, 1997), ozone has been used for a variety of applications such as the purification and disinfection of water (Jyoti and Padnit, 2002), colour removal from solutions (Zhang *et al.,* 2009), food preservation (Rice *et al.,* 1982) and the sterilisation of medical infectious waste (Coronel *et al.,* 2002). In fact, ozone is regarded as one of the most efficient chemical disinfectants currently used in drinking water treatment as it provides adequate inactivation of problematic and rather resistant water borne microorganisms such as protozoa (Gunten, 2003a).

Ozone can be generated by electrical discharges into gases containing oxygen and several scientific investigations are based on the use of pulsed plasma technologies for a large scale ozone production (Simek and Clupek, 2002; Jung and Moon, 2008; Zhang *et al.,* 2009). During PPGD ozone is produced via dissociation of oxygen molecules by

energetic electrons and to a lesser extent by UV light emission. More specifically, free electrons (e^{-1}) which are accelerated by the electric field collide with oxygen molecules thereby transferring some of their dynamic energy. If the transferred energy is high enough, the oxygen molecule dissociates into two single oxygen atoms. As shown in Equation 3.2, those unstable atoms (O) can attach to other oxygen (O_2) molecules to form ozone (O_3). For discharge processes mediated in oxygen, the number of electrons with a given energy determines the amount of ozone produced (Pekárek *et al.,* 2000).

$$e^{-1} + O_2 \rightarrow O + O + e^{-1}$$
$$O_2 + O \rightarrow O_3$$

Equation 3.2: The generation of ozone during electrical discharge.

However, as shown in Equation 3.3, the free electrons and atomic oxygen can further react with the produced ozone molecules to reform oxygen. The ozone decay processes are also enhanced by temperature effects resulting from the discharge itself. Therefore, the net ozone gained during the discharge is the sum of all of the reactions that form and decompose ozone (Alsheyab and Muñozb, 2007).

$$e^{-1} + O_3 \rightarrow O_2 + O + e^{-1}$$
$$O + O_3 \rightarrow 2O_2$$

Equation 3.3: Ozone decay.

Moreover, Takaki (2008) stated that the efficiency of the ozone production by pulsed plasma depends strongly on the ambient temperature and pressure, the gas used and on the discharge settings such as gap width, applied voltage, pulse waveforms, electrode surface and electrode material.

To disinfect the water, the generated ozone must be brought into solution. As well as being actively injected, ozone can enter an aqueous solution by diffusion processes. Although ozone itself has good water solubility, being 12.5 times more soluble than oxygen, its instability in water makes the determination of the molecule within a solution rather complicated. Numerous studies on the complex decomposition of ozone in aqueous

solutions have been performed (Staehelin and Hoigńe, 1985; Gunten, 2003b; Lin and Nakajima, 2003). The half life of ozone in distilled water at 20°C is approximately 20–30 min (Zorlugenç *et al.,* 2008) and its decomposition depends on several factors such as initial ozone concentration, water temperature, pH and dissolved matter (Biń, 2004). As demonstrated in Equation 3.4, in an aqueous solution ozone partly decays into reactive hydroxide radicals (OH·) and superoxide radicals ($O_2{\cdot}^-$) (Staehelin and Hoigńe, 1985; Gunten, 2003b). This reaction is initiated with hydroxide ions (OH^-) and, hence, occurs under alkaline conditions at an elevated rate. Moreover, the produced OH· and $O_2{\cdot}^-$ radicals initiate further reactions with ozone, causing the formation of even more OH· radicals (Gunten, 2003b).

$$O_3 + OH^- \rightarrow HO_2^- + O_2$$

$$O_3 + HO_2\text{-} \rightarrow OH\cdot + O_2{\bullet}^- + O_2$$

Equation 3.4: Further ozone decay.

It has been suggested, that the final products of ozone decay in water are O_2 and H_2O_2 (Lin and Nakajima, 2003).

It is not the action of ozone alone, however, that seems responsible for the chemical based inactivation of microorganisms during plasma discharge processes. Its reactive decay products also play a potential role in disinfection and sterilisation. The hydroxyl and superoxide radicals are known to have potent oxidising properties on microorganisms (Bancroft *et al.,* 1984) and hydrogen peroxide has been used for the oxidative disinfection of water (Wolfe *et al.,* 1989). Table 3.16 shows the oxidising potential of various compounds generated during PPGD processes in O_2.

Table 3.16: Oxidising potential of various compounds generated during plasma discharge in O_2.

Oxidising agent	Oxidising potential
Hydroxyl radical	2.86 V
Ozone	2.07 V
Hydrogen peroxide	1.77 V
Oxygen	1.23 V
Superoxide radical	0.33 V

The sum of the deleterious effects of oxidising substances on microorganisms is often described under the term 'advanced oxidation processes' (AOP) (Jyoti and Padnit, 2002). During AOP, the active compounds can oxidise various essential components of the microbial cells such as unsaturated fatty acids, amino acids and DNA molecules (Montie *et al.,* 2000). Although rather complex in detail, the main antimicrobial action of ozone itself is believed to be exerted on organic compounds such as proteins and unsaturated lipids in the cell membranes of the microorganisms, which ultimately results in the rupture of the membranes, thus affecting cell viability (Pryor, 1994; Hunt and Mariňas, 1999).

In the present study, the efficiency of the PPGD system to produce dissolved ozone in the test liquid was determined using the DPD colorimetric method (Spectroquant® 1.00607). The ozone measurements were conducted for different discharge conditions immediately after the treatment to minimise decay reactions. Firstly, a test was carried out comparing the effects of using O_2 or N_2 as a discharge gas at a flow rate of 2.5 l/min under various discharge intensities (18, 16 and 14 kV pulse generator charge). A second test was used to determine the effect of three gas flow rates (5, 2.5 and 1 l/min) when using O_2 gas under a 16 kV charging voltage at 10 pps. To determine the influence of pulse frequency, a third test examining three pulse repetition rates (12.5, 10 and 7.5 pps) was conducted at a constant charging voltage of 16 kV using 2.5 l/min O_2.

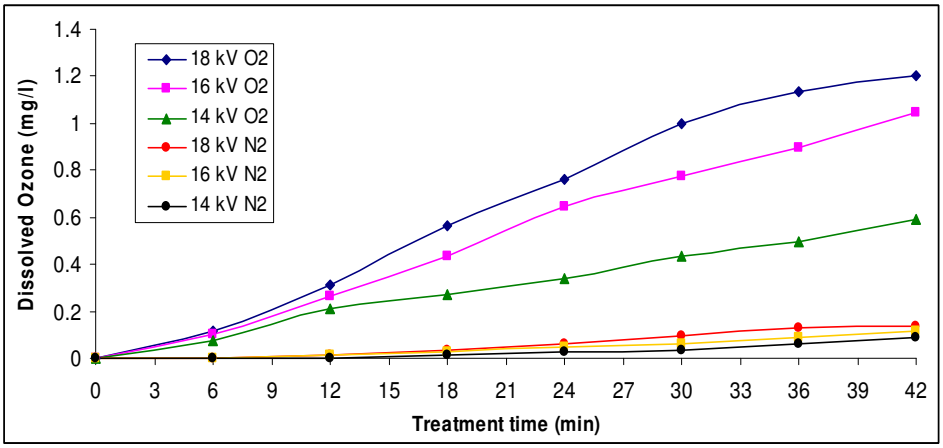

Figure 3.44: Dissolved ozone concentration in the test liquid for varying discharge intensities using O_2 or N_2 gas at a flow rate of 2.5 l/min and a pulse frequency of 10 pps.

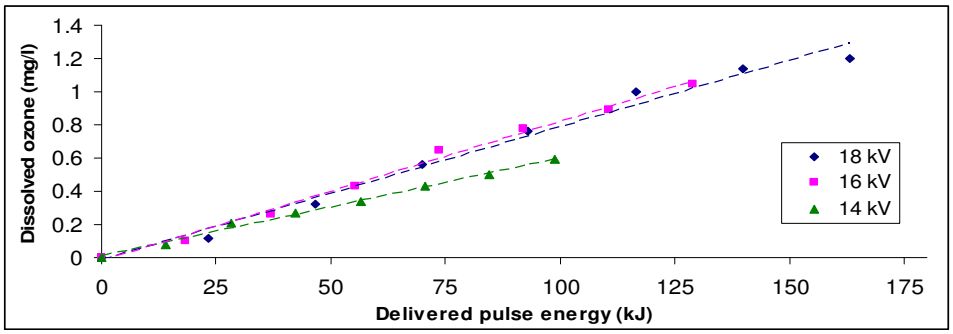

Figure 3.45: Linear plot of dissolved ozone concentration in the test liquid as a function of pulse energy delivered at varying discharge intensities using oxygen gas at a flow rate of 2.5 l/min and a pulse frequency of 10 pps.

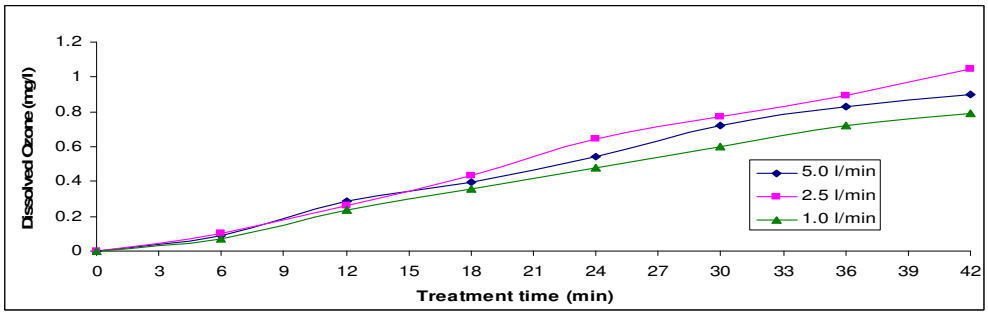

Figure 3.46: Dissolved ozone concentration in the test liquid at varying flow rates using oxygen gas, a PFN charge of 16 kV and a pulse frequency of 10 pps.

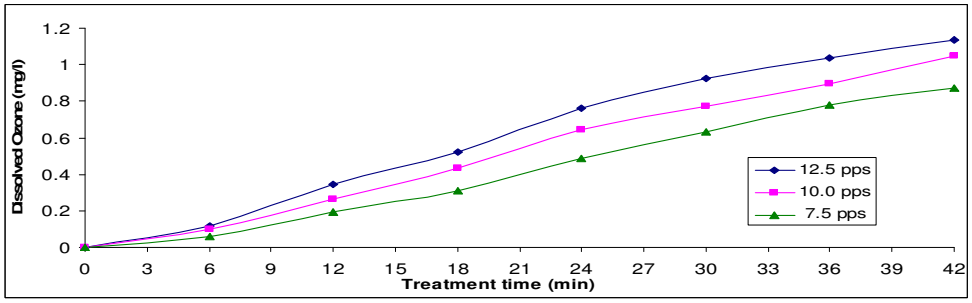

Figure 3.47: Dissolved ozone concentration in the test liquid at varying pulse frequencies using a charging voltage of 16 kV and oxygen flow at 2.5 l/min.

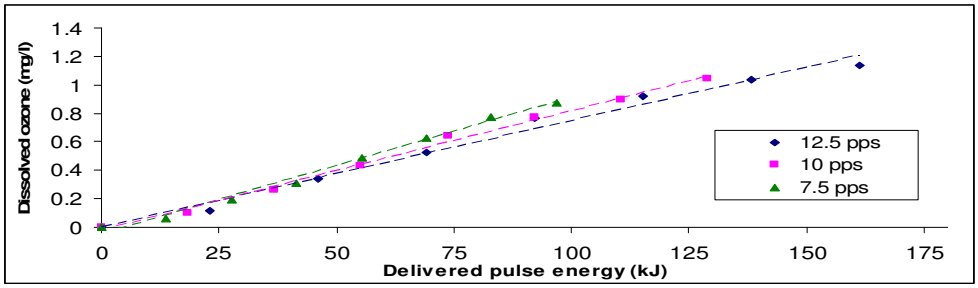

Figure 3.48: Linear plot of dissolved ozone concentration in the test liquid as a function of pulse energy delivered at varying discharge intensities using oxygen gas at a flow rate of 2.5 l/min and a pulse frequency of 10 pps.

As illustrated in Figures 3.44-3.48, the PPGD resulted in the generation of dissolved ozone in the treatment fluid. For all studies, the ozone concentration increased with increasing treatment times. The results illustrated in Figure 3.44 indicate that, depending on the type of discharge gas used, a substantial difference in ozone production was observed. As expected, when streaming oxygen into the discharge chamber, the dissolved ozone concentration was eight times higher than that observed during nitrogen discharge. This effect is the result of an enhanced availability of cleavable O_2 molecules during the discharge.

Although the ozone production during N_2-mediated discharge was found to be rather ineffective, one may still wonder why discharge in N_2 led to ozone formation in the first instance. This can be explained by the configuration of the treatment chamber which is not completely sealed from its outer environment, thus allowing small amounts of O_2 gas into the discharge region from ambient air. Also, the aqueous test solution may represent a possible source for oxygen, dissolved and chemical bound, which can be liberated from the liquid as a result of the plasma discharge.

As ozone concentration increased with an increase in PFN charging voltage, the results obtained demonstrate that a direct relationship between energy per pulse and ozone production existed. The higher the applied discharge energy, the greater the production of ozone during the time duration of the experiment. With varying pulse potency, the concentrations of ozone dissolved in the liquid after 42 min O_2 discharge treatment were found to be 1.2, 1.0 and 0.6 mg/l for applied charging voltages of 18, 16 and 14 kV, respectively.

The linear plot visualised in Figure 3.45 reveals the efficiency of the production of dissolved ozone in relation to the accumulated pulse energy delivered at different charging voltages. Here, it can be seen that although the highest charging voltage of 18 kV led to the highest and fastest production of dissolved ozone, the 16 kV charging voltage appears to be equal or even slightly more energy efficient while 14 kV charging voltage was found to be least efficient. This could be a consequence of a reduced corona streamer formation at 18 kV- and 14 kV-mediated discharges. It has been reported that higher charging voltages tend

to favour undesired arcing effects (van Veldhuizen and Rutgers, 2002). However, 14 kV may not be sufficient to create an adequate corona discharge.

Figure 3.46 details the dissolved ozone concentration achieved using a 42 min PPGD treatment at 16 kV and 10 pps for different oxygen flow rates. Here, the oxygen flow rate of 2.5 l/min produced the highest dissolved ozone concentration of 1.04 mg/l, while a flow of 5 and 1 l/min achieved maximum values of 0.90 and 0.78 mg/l. More specifically, increasing the flow rate from 1 to 2.5 l/min yielded a slight increase in dissolved ozone concentration which can be explained by the fact that the amount of dissociable O_2 molecules at discharge processes was elevated during the treatment. However, increasing the flow rate to 5 l/min did not result in a corresponding increase in the formation of ozonated liquid. It is likely that the elevated gas flow transported a considerable amount of generated ozone molecules out of the treatment zone before they could maintain contact with the liquid interface.

The results in Figure 3.47 illustrate the effect of varying the pulse frequency on the rate of the dissolved ozone concentration. Again, these studies were conducted at a constant PFN charging voltage of 16 kV combined with an O_2 flow rate of 2.5 l/min. Similar to studies conducted with varying charging voltages, for all pulse repetition rates investigated, the increase in dissolved ozone with increasing treatment time was almost linear. Clearly, increasing the pulse frequency will result in an increase in plasma discharges which in turn dissociates available oxygen molecules to create dissolvable ozone and therefore these findings were as was expected. However, interesting results were achieved by transforming the obtained data to a liner plot showing the energy efficiency of varying pulse rates on dissolved ozone production (Figure 3.48). These results showed that the lower the pulse frequency the more energy efficient the generation of dissolved ozone. While the difference in energy efficiency to create dissolved ozone was found to be rather small for the varying pulse repetitions examined, it still deserves adequate consideration. This effect may play a role in the development of future sterilisation applications where an upscaled system may be necessary, requiring much higher magnitudes of energy consumption. From an experimental point of view the increase of energy efficiency towards lower pulse frequencies can be explained by the discharge chemistry. During pulsed discharges at high frequencies, numerous active species are created that in turn can

attack ozone molecules formed by previous discharge processes. Hence, ozone molecules can be effectively degraded before they reach the gas-liquid interface. Therefore, prolonged treatments at lower pulse rates may reduce this effect and allow dissolved ozone to form more efficiently.

Overall, the PPGD treatment was potent to generate up to 1.2 mg/l of dissolved ozone within the 100 ml of treatment fluid when using O_2 gas as the discharge mediator. The ozone production was dependent on several factors, such as treatment time, pulse energy and frequency, and the nature and flow rate of the utilised discharge gas. As expected, the use of O_2 discharge gas for the creation of ozone was superior in comparison to the use of nitrogen. The latter gas produced minor levels of dissolved ozone with concentrations not exceeding 0.14 mg/l at maximum treatment times and discharge conditions. Dissolved ozone levels obtained using O_2 gas were found to be significant in terms of microbial inactivation. It is well established that concentrations as low as 0.2 to 0.6 mg/l can sterilise contaminated drinking water (Evans, 1972) and provide adequate microbial inactivation in secondary effluent waste waters (Masschelein, 1982). The DPD colorimetric method employed for the quantification of dissolved ozone, however, was not suitable to elucidate mechanisms of ozone decay. Preliminary studies undertaken showed that the dissolved ozone levels dropped below detection limit within several hours after the discharge treatment. The time-dependent ozone decay was found to be complex and inconsistent as no reproducible test data could be obtained. In order to determine the treated solution's biocidal and toxicity mechanisms, determination of the decay process' characteristics would be crucial. Thus, future work is required to fully understand the formation of relevant active species resulting from ozone decay after treatment.

3.3.3.3 Products of nitrogen fixation

Under atmospheric conditions, nitrogen in air does not take part in many oxidation reactions (except those associated with microbial activity) because its atoms are bonded by a rather stable triple bond with a dissociation energy of 945.33 kJ/mol at 298 K (Wiberg *et al.,* 2001). However, high energetic electrical discharges occurring in a gas containing N_2 (akin to lightening occurring during a thunderstorm) can lead to activation of the molecule by dissociation and ionisation processes (Rehbein and Cooray, 2001). The activated

nitrogen can react and combine with other compounds to form biologically active products such as NO_x and N_2O. These reactions belong to a process known as nitrogen fixation and play an important role in the biological nitrogen cycle.

During the last decade several laboratory scale studies were conducted to investigate the formation of nitrogen oxides during electrical discharge (Nna Mvondo *et al.,* 2001; Rehbein and Cooray, 2001; Wenjuan and Xiangli, 2007). It was shown by Wenjuan and Xiangli (2007) that in the presence of N_2 gas pulsed HV discharges directed into an aqueous solution can fix nitrogen in the form of dissolved nitric acid (HNO_3) and nitrous acid (HNO_2). As shown in Equation 3.5, the HV discharges can dissociate N_2 molecules and cause the formation of ionic nitrogen (N_2^+).

$$e^{-1} + N_2 \rightarrow 2e^{-1} + N + N^+$$
$$e^{-1} + N_2 \rightarrow 2e^{-1} + N_2^+$$

Equation 3.5: Dissociation of nitrogen and ion formation.

Furthermore, Wenjuan and Xiangli (2007) state that active nitrogen took part in liquid chemical plasma processes to form nitrogen oxides, some of which dissolved in the aqueous solutions as HNO_3 and HNO_2 (Equation 3.6).

$$N_2 + 2H_2O \rightarrow 2NO^{\cdot} + 4H^{\cdot}$$
$$NO^{\cdot} + O^{\cdot} \rightarrow {}^{\cdot}NO_2$$
$$2\,NO_2 + H_2O \rightarrow HNO_2 + HNO_3$$
$$3HNO_2 \rightarrow HNO_3 + 2NO + H_2O$$

Equation 3.6: Formation of nitrogen oxides.

The reactions shown in Equation 3.6 can be influenced by other active species such as OH· radicals produced during the discharge.

In the present study, N_2-mediated discharges reduced the pH of the treatment fluid drastically (Section 3.3.3.1). Inevitably, large pH reductions will play an important contributory role in PPGD-mediated microbial inactivation as it imposes additional lethal stress to the test microorganisms that prefer near neutral conditions for cell survival and

growth (Rowan, 1999; Black, 2005). With the goal of developing a sterilisation technique for hydrogels, the pH change could cause a potential safety hazard depending on the nature of the chemicals generated. Thus, to obtain a conclusive toxicological evaluation of the PPGD process it was necessary to investigate the mechanisms leading to the reduced pH levels. In accordance with research conducted by Wenjuan and Xiangli (2007), the presence of acidic HNO_3 and HNO_2 in the test liquid was examined after plasma treatment using N_2 gas. IEC was used to quantify the amount of NO_3^- and NO_2^- ions which in turn relates to the amount of HNO_3 and, to a lesser extent, HNO_2 produced. More specifically, the amount of NO_3^- directly relates to the amount of HNO_3 because the latter is a typical 'strong acid' which when dissolved in water dissociates completely as shown in Equation 3.7.

$$HNO_3 + H_2O \rightarrow NO_3^- + H_3O^+$$

Equation 3.7: Dissociation reaction of HNO_3 in aqueous solutions.

Thus, no intact HNO_3 molecules will be present in the aqueous solution and all of the nitrogen will exist as NO_3^- in the +V oxidation state which can be detected via IEC.

The determination of HNO_2, however, is more complicated because this is a 'weak acid' and will not fully dissociate in water. In other words, the dissociation reaction shown in Equation 3.8 does not go to completion.

$$HNO_2 + H_2O \rightarrow NO_2^- + H_3O^+$$

Equation 3.8: Dissociation reaction of HNO_2 in aqueous solutions.

Therefore, IEC detects the actual concentration of NO_2^- but may underestimate the amount of undissociated HNO_2. Theoretically, it would be possible to calculate the actual concentration of nitrogen in the +III oxidation state (as undissociated HNO_2 and NO_2^-) using the dissociation constant for nitrous acid and the degree of dissociation. This, however, is further complicated by the fact that HNO_2 is thermally unstable in aqueous solutions. Even at room temperature most of the HNO_2 will eventually be converted to HNO_3 which, once it becomes dissolved in water, will exist entirely in the

form of NO_3^- ions (Cai *et al.,* 2001). However, due to the scope of this project, investigations into the NO_3^- and NO_2^- ion content were deemed sufficient. IEC was used in this study to achieve valuable information regarding the formation of dissolved acidic compounds that led to the reduced pH of the test liquid. IEC is considered to be one of the most powerful techniques for the determination of anions including NO_3^- and NO_2^- (Helaleh and Korenaga, 2000; Gapper *et al.,* 2004). Following species separation in the IEC column, the ions were detected and quantified via a conductivity detector. To minimise the amount of variables, the PFN charging voltage was kept constant at 16 kV by streaming N_2 gas into the discharge gap at a flow rate of 2.5 l/min. The influence of pulse frequency on the creation of fixed nitrogen products was investigated using varying pulse repetition rates of 12.5, 10 and 7.5 pps.

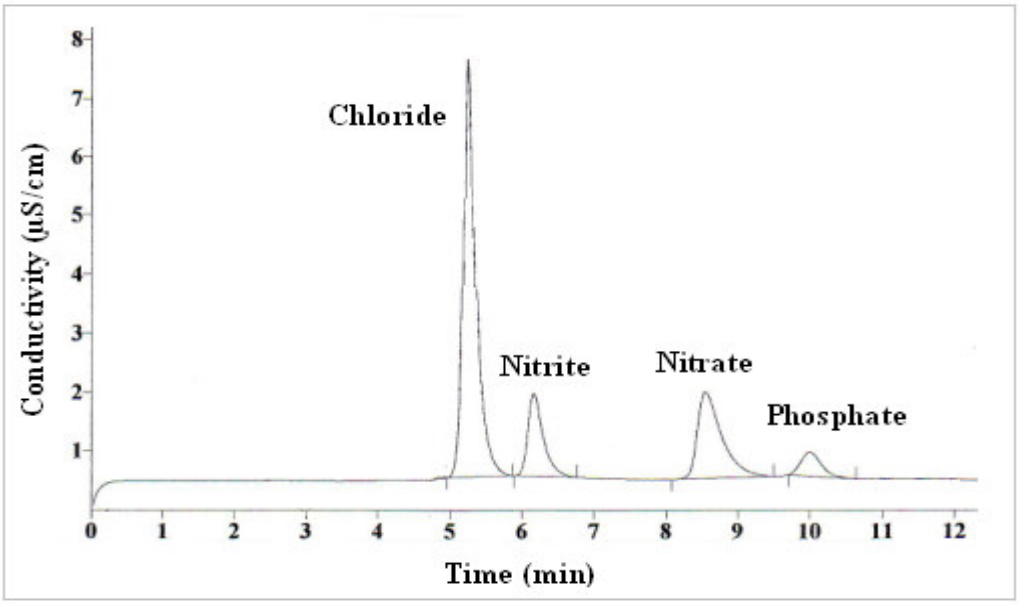

Figure 3.49: Chromatogram obtained during IEC analysis of treatment fluid exposed to prolonged N_2 discharge. Nitrite ions eluted at approximately 6.1 min and nitrate ions eluted at 8.5 min. Additional peaks indicate the presence of chloride and phosphate ions introduced by the PBS.

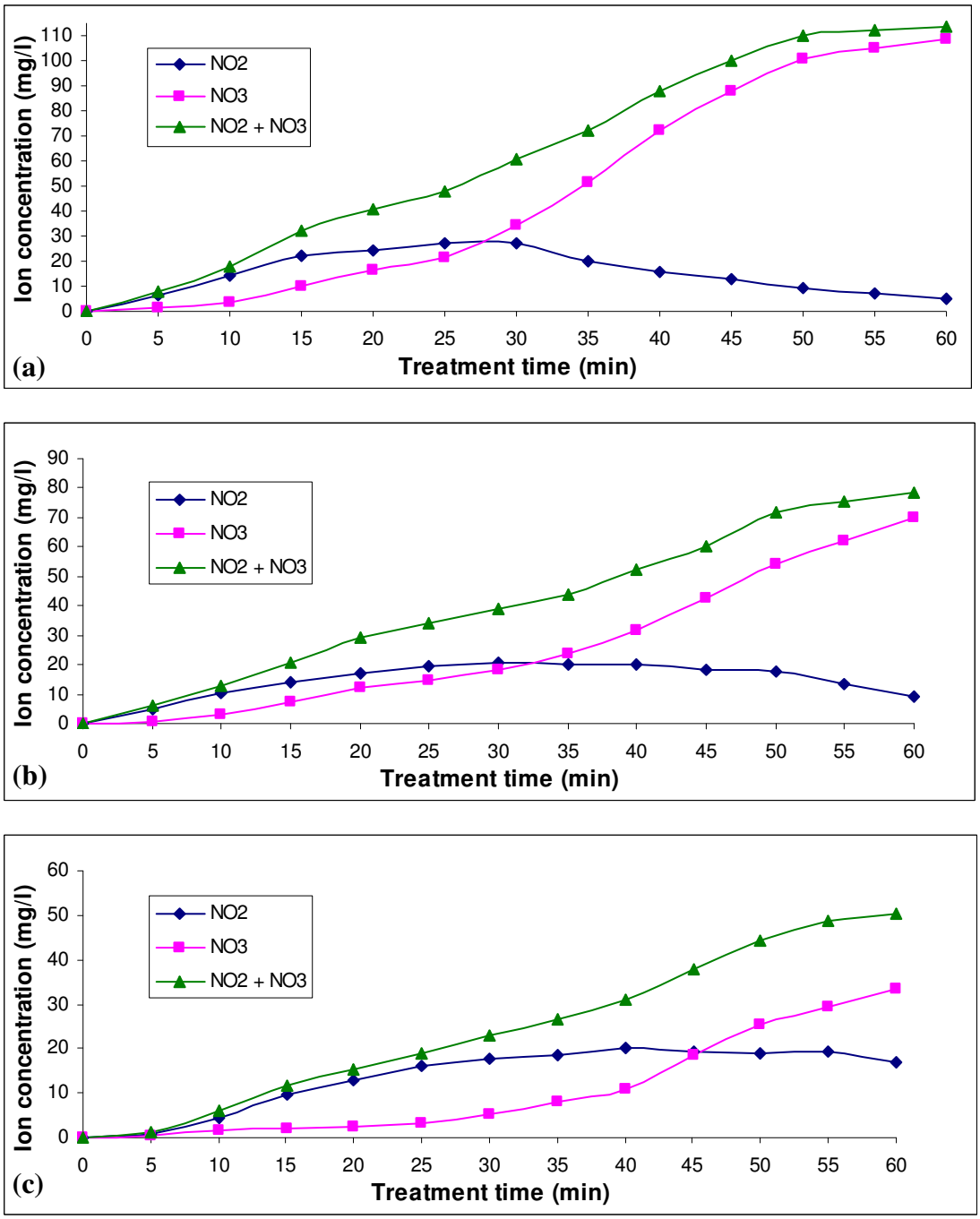

Figure 3.50: The concentration of NO_2^-, NO_3^- and the sum of NO_2^- + NO_3^- in PPGD-treated test liquids using a PFN charging voltage of 16 kV, a N_2 gas flow of 2.5 l/min and varying pulse frequencies of (a) 12.5 pps (b) 10 pps and (c) 7.5 pps.

Figure 3.49 shows an ion exchange chromatogram obtained for PPGD-treated test liquid using N_2 as the discharge gas. The presence of nitrite and nitrate ions was detected with elution times of 6.1 and 8.5 min, respectively. Besides the presence of the two nitrogen containing compounds, PBS-associated chloride and phosphate were also detected having respective elution times of 5.2 and 10.1 min. Figure 3.50 shows that the amount of nitrogen ions generated during the PPGD treatment was dependent on the treatment time. In general, the experiments revealed that with prolonged treatment the NO_3^- species levels were more prominent than levels of NO_2^-. Also the trend of dissolved NO_2^- and NO_3^- levels varied throughout the time course of the experiment. Initially, the production of NO_2^- species dominated above NO_3^-, but with increasing treatment time the concentration of NO_3^- increased far above the levels of nitrites. The NO_3^- increase was almost linear while the slower generation of NO_2^- was found to peak between 25 to 40 min depending on the pulse frequency and started to decline thereafter. In addition, the total nitrogen content of NO_2^- and NO_3^- in the test liquid increased almost linearly with increasing treatment time but the formation of a plateau was indicated at the end of the treatment.

A closer look at Figure 3.50 reveals that varying the pulse repetition rate led to pronounced effects on the generation of fixated nitrogen. The higher the pulse frequency the more nitrate and nitrite was generated. At a maximum treatment time of 60 min, the highest levels of NO_3^- were found to be 108.60 mg/l at a pulse frequency of 12.5 pps, 69.88 mg/l at 10 pps and 33.46 mg/ml at 7.5 pps. The maximum NO_2^- concentration peak was observed between 25 and 40 min of PPGD treatment with 27.03 mg/l for a pulse rate of 12.5 pps, 20.83 mg/l for 10 pps and 20.02 mg/l for 7.5 pps. At the end of the treatment, the residual NO_2^- concentration was found to be 5.04, 8.83 and 16.92 mg/l for respective pulse repetition rates of 12.5, 10 and 7.5 pps.

The results obtained from the IEC analysis proved that nitrogen compounds were fixed in the treatment liquid during N_2 discharge processes. The PPGD was potent to activate the gaseous N_2 molecules which were subsequently oxidised by oxygen species originating from the treatment liquid or from residuals of atmospheric O_2 gas within the discharge region. The oxidised nitrogen dissolved in the liquid and caused the formation of nitric and nitrous acid which dissociated into detectable NO_3^- and NO_2^- ions, respectively. Thus, as discussed in Section 3.3.3.1, the acids generated were the cause of the reduced pH

after plasma treatment using N_2 as discharge gas. The fast reduction of NO_2^- ions after reaching its maximum concentration can be explained via the falling pH values observed after prolonged treatment which in turn may suppress further dissociation of HNO_2. Additionally, oxygen species activated by the plasma treatment could enhance the degradation of the unstable nitrous acid that can be readily oxidised to nitrate products (Cai *et al.,* 2001). This theory is further supported by increased NO_3^- generation rates once the decrease in NO_2^- became observable. The results obtained are comparable to a recent publication by Wenjuan and Xiangli (2007) where HV discharge within liquids formed HNO_3 and HNO_2 when nitrogen was bubbled through the submerged electrode gap. Similar to the present study, the formation of NO_3^- ions dominated the production at NO_2^- ions at prolonged treatment. As expected, by increasing the number of discharges per second an increase in the amounts of fixed nitrogen was detectable in the liquid and also the conversion rate from NO_2^- to NO_3^- appeared to be accelerated.

Due to the pH reducing effect and the presence of NO_2^- and NO_3^- ions in the test liquid, it is believed that the nitrogen fixation process may play a role in the microbial inactivation of PPGD. Nitrite is known to possess antimicrobial properties when dissolved in aqueous solution (Klebanoff, 1993; Casey and Codon, 2000; Anyim *et al.,* 2005).

The amounts of nitrate and nitrite generated were well above the acceptable levels tolerable in drinking water. The European Communities Drinking Water (No. 2) Regulations (2007) state that the nitrite and nitrate content of drinking water must not exceed a value of 0.5 mg/l and 50 mg/l, respectively. Thus, it was important to evaluate the nitrogen fixation from a toxicological perspective since the PPGD method is destined for use in the biomedical field (see also Section 3.3.5). The human toxicity of nitrites and nitrates came to public attention shortly after Comly (1945) reported cases of infant methemoglobinemia (commonly known as blue baby syndrome) associated with well-water containing high amounts of nitrate. Today it is known that nitrite is the main cause for methemoglobinemia as ingested nitrate is largely metabolised and excreted without producing adverse effects unless conditions are favorable for the conversion of nitrate to significant amounts of nitrite e.g. higher pH, presence of certain intestinal flora. Nitrites cause the conversion of hemoglobin to methemoglobin which cannot bind and transport oxygen to tissues and cells throughout the body (Locey, 2005). Nitrate and nitrite are

generally not classified as human carcinogens. However, under certain conditions nitrite and nitrate may combine with amines in the body to form nitrosamines (Vermeer *et al.,* 1998) which in turn are believed to be involved in carcinogenesis (Lin, 1990; Huang *et al.,* 1996).

3.3.3.4 Electrode erosion and residual degradation products

Degradation of electrodes during HV discharge processes is a common phenomenon and has been studied for many years (Augis *et al.,* 1971; Fujimoto and Toshima, 1972; Gray and Pharney, 1974). Electrode degradation is a major problem, limiting the performance and lifetime of electrodes and further restraining the choice of electrode material. Degradation is caused by erosion events resulting from the interactions of electrical discharges with the surface of the electrodes. Physical and chemical processes such as particle ejection, vapourisation, sputtering and oxidation events have been identified as contributors to electrode erosion. Particle ejection results from ion bombardment of the electrode. Heat generated during ion bombardment can cause the outer metal surface of the electrode to melt and nano- to microscale droplets of the molten metal can be ejected with further discharges (Gray and Pharney, 1974; Lasagni *et al.,* 2004). Loss of electrode material through vapourisation occurs when local molten metal spots are further heated until boiling temperature is reached (Coulombe and Meunier, 2000). Another possible mechanism of electrode erosion is sputtering. Sputtering describes the ejection of metal atoms by collision events, with accelerated ions and fast atoms that are generated in the electrode gap during the discharge (Mason and Pichilingi, 1994; Walker *et al.,* 2005). Discharge processes in the presence of oxygen can result in oxidation processes of the electrode material which increases the erosion rate. More specifically, electrode bombardment with oxygen radicals and ions generated during plasma discharges can greatly contribute to oxidation reactions (Shiki *et al.,* 2007).

The HV electrode used in the present study was arranged in a multi-needle configuration. The entire electrode including the needles was composed of stainless steel BS316S11, with the elemental composition described in Section 2.6.5.4. To demonstrate electrode erosion effects experienced throughout this study, microscopic images of the discharge needles before and after prolonged PPGD treatment are shown in Figure 3.51.

During PPGD treatment, the lower earthed electrode, composed of aluminium alloy 6082 (Section 2.6.5.4), was protected from direct discharge effects via the aqueous solution. However, during prolonged usage the formation of a deposit layer upon the entire electrode surface was evident. Microscopic images of the surface topography of the earthed electrode before and after prolonged PPGD treatment are shown in Figure 3.52.

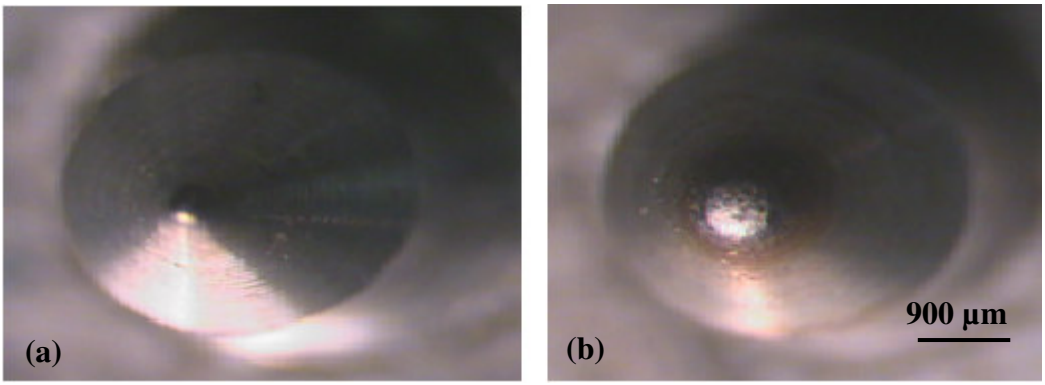

Figure 3.51: Unused needle tip of the HV electrode (a). Etched and shortened needle tip after prolonged usage (b).

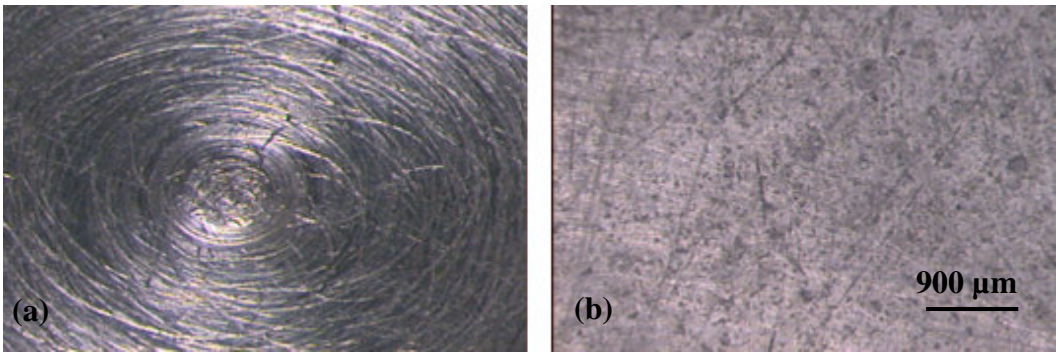

Figure 3.52: Surface of unused earthed electrode (a). Evidence of deposit formation on earthed electrode after prolonged usage (b).

As shown in Figure 3.51, the creation of plasma discharge resulted in a slow but steady shortening of the individual needle electrodes via erosion mechanisms. All the needle tips became rounded while displaying a crater-like surface morphology. The observed damage was believed to result from a mixture of complex electrode erosion events including particle ejection, vapourisation and sputtering. Furthermore, colour changes indicative for oxidative damage were also evident. Oxidative damage was believed

to be mainly caused by active species generated during discharges in the presence of gaseous O_2 molecules. As most mechanisms leading to electrode erosion are temperature dependent, a way to conserve the electrodes would be to reduce PFN charge and pulse frequency. Also reducing the use of O_2 as discharge gas may diminish oxidative damage. However, the discharge settings used in the present study were not found to degrade the electrode material at a problematic rate. In general, the electrode life span was found to be satisfactory and no major problems in relation to the discharge efficiency were noticed. Periodically, eroded electrode needles were simply exchanged with a set of new needles. As shown in Figure 3.52, prolonged PPGD treatment resulted in the formation of a deposit layer on the lower earthed electrode. The deposit layer appeared to be composed of some form of salts possibly originating from oxidised Al and from residuals of the PBS used to adjust the conductivity of the test liquid. Al is known to be a reactive element and forms oxides immediately upon exposure to oxygen species. Several scientific investigations are concerned with the formation of Al oxides during electrical discharges in aqueous solutions (Gedenkov *et al.,* 2000; Curran and Clyne, 2005; Xin *et al.,* 2005). Although the deposit layer could potentially interfere with electrical discharge characteristics no alteration of the discharge conditions following prolonged treatment were observed in the present study. Periodically, the deposit layer was removed by polishing the electrode surface with abrasive paper (grit size: P800 – P1000).

Material degradation resulting from electrode erosion is not the sole concern when electrical discharges are used for the treatment of drinking water or health care products. More specifically, toxic degradation products released from the electrodes can contaminate the treatment object and impose a health hazard. Thus, the presence of electrode degradation products within the PPGD-treated test liquid was investigated. Several scientific investigations have been published on the harmful effect of metal ions released from Al or stainless steel electrodes during electrical discharges in aqueous solutions and most of the research was conducted on electropermeabilisation (electroporation) equipment used for biomolecular cell manipulations. More specifically, the release of Al^{2+} and Al^{3+} was reported during electrical discharges from Al containing electroporation electrodes (Friedrich *et al.,* 1998; Kotnik *et al.,* 2001; Lukeš *et al.,* 2006). Further investigations

confirmed the release of Fe^{2+} and Fe^{3+} ions from stainless steel electrodes (Stapulionis,1999; Tomov and Tsoneva, 2000).

In the present study, metal contamination within the test liquid was evaluated for both O_2- and N_2-mediated discharges with a constant charging voltage of 16 kV and a pulse frequency of 10 pps. To allow for a broad and extensive treatment range, two time points were chosen which were 30 and 90 min. The results for PPGD-treated test liquids were compared to a test liquid (untreated control) which was exposed to the chamber for the duration of the longest test run i.e. 90 min. In accordance with the elemental composition of both electrode types (Section 2.6.4), the PPGD-treated test liquid was analysed for the content of four indicator elements, namely Al, Fe, Cr and Mn. Table 3.17 shows the results obtained from the metal analysis in PPGD-treated water.

Table 3.17: Concentration of indicator elements in PPGD-treated test liquid.

Determination	Untreated control	30 min O_2 treated	90 min O_2 treated	30 min N_2 treated	90 min N_2 treated	PV value*
Al (µg/l)	<20	5515	27150	6546	26330	200
Fe (µg/l)	<20	98	747	147	500	200
Cr (µg/l)	<5	34	195	44	121	50
Mn (µg/l)	<5	20	90	34	112	50
pH	7.52	7.69	8.28	4.53	3.09	N/A
Conduct.(µS/cm)	981	1159	1353	1192	1394	N/A

*PV value is the parametric value taken from European Communities Drinking Water (No. 2) Regulations (2007) and was included for comparative purposes.

The concentration of contaminants in the untreated control was below the detection limit for all metal elements tested (Table 3.17). With increasing PPGD treatment the concentration of electrode contaminants increased. Both discharge gases led to comparable contaminate production. More specifically, for the 30 min PPGD treatment the N_2 discharge resulted in slightly higher metal levels, but after 90 min higher contaminate levels were obtained following O_2 discharge treatment. Al was by far the most abundant element for all treatments investigated followed by Fe, Cr and Mn. The highest levels of Al were 27150 and 26330 µg/l for 90 min of PPGD treatment in O_2 and N_2 respectively. The

highest concentrations of suspended Fe were found to be 747 and 500 µg/l following discharges mediated for 90 min in O_2 and N_2.

During PPGD treatment electrode material was released into the test liquid. The fact that all metals investigated were detected indicates that elements from both the stainless steel HV electrode and the Al earthed electrode were released. The observed contaminate concentration was dependent on the treatment time suggesting that, with every delivered HV, pulse material was freed from the electrodes. Varying the discharge gas did not seem to have a major effect on the examined metal levels. Surprisingly, Al contaminate from the earthed electrode was most abundant even though this electrode was shielded from direct effects of the discharge. This supports the assumption that the deposit layer was composed of oxidised Al which was released into the liquid during treatment (Gedenkov *et al.,* 2000). Furthermore, research conducted by Kotnik *et al.* (2001) and Lukeš *et al.* (2006) suggests that Al^{2+} and Al^{3+} are released from the electrodes by electrolytic action and electrode erosion events.

Greater levels of Fe were detected compared to those of Cr and Mn, which was in accordance with the elemental composition of stainless steel. However, in comparison with the tolerated metal levels in drinking water recommended by the European Communities Drinking Water (No. 2) Regulations (2007), the Al contaminate was of major concern. After a 30 min treatment at 16 kV and 10 pps, the Al concentration was 32 times the recommended value while the detected levels originating from the HV electrode were below the tolerated limits. Following PPGD exposure for 90 min, all elements were found to exceed the tolerated levels. The Al contamination was most critical with levels exceeding 135 times the maximum tolerated levels. Nevertheless, it must be highlighted that the 90 min treatment was chosen as an extreme point and it is unlikely that in practice microbial inactivation treatment will greatly exceed 30 min duration. However, even with 30 min treatment, the release of electrode material, in particular Al, may impose a risk factor which was considered in subsequent toxicity evaluations of the test liquid and treated hydrogel samples.

3.3.4 The antimicrobial effect of various PPGD conditions

The antimicrobial action of pulsed HV discharges in aqueous solution has been known for more than three decades (Zhuk, 1971) with vast interest in this phenomenon increasing particularly in the late 1990s (Gorayachev *et al.,* 1998; Efremov *et al.,* 2000; Rowan *et al.,* 2001). In contrast to pure electrical discharge processes, pulsed HV discharges involving a suitable gas for the generation of plasmas to inactivate pathogenic microorganism suspended within an aqueous solution have not received extensive attention to date. Espie *et al.* (2000, 2001) conducted research on plasma discharge in liquids using bacterial and yeast cells and concluded that this technology can be utilised in areas such as potable water applications, liquid waste management, and sewage treatment. A follow-on study performed by Marsili *et al.* (2002) from the same research group compared the biocidal efficiency of PEF and plasma gas-discharges in liquids using a range of food related microorganisms. Here, plasma discharges especially those using O_2 containing gases were found to inactivate the test organisms at a superior rate than PEF. Anpilov *et al.* (2002, 2004) investigated the use of PPGD in liquids for the inactivation of *E. coli* and concluded that a multi-electrode configuration was preferable. Since then, the research emphasis concerned with plasma discharges directed into liquids moved towards elucidating the mechanisms involved in microbial inactivation and important process parameters (Baroch *et al.,* 2006; Kolikov *et al.,* 2007; Akishev *et al.,* 2008; Rowan *et al.,* 2008). Recently, studies of plasma gas-discharge in or above liquids became more orientated on practical applications including antimicrobial treatment of poultry wash water (Rowan *et al.,* 2007) and the chemical free disinfection of water (Satoh *et al.,* 2007).

In the present study, initial inactivation studies were conducted using microbial species suspended in the treatment liquid to gain valuable process information and subsequently optimise the PPGD system for the sterilisation of hydrogels. The Gram negative bacteria *E. coli* and the Gram positive *S. aureus* were the chosen strains as they represent a broad range of potentially pathogenic bacteria. Indeed, Gram negative and Gram positive bacteria differ genetically, morphologically and metabolically (including adaptive stress responses) and it is these combined properties that make some bacteria more sensitive to the external environment than others. The identity of each strain was confirmed as previously outlined in Section 2.7.1, using morphological, physiological and

biochemical tests. The two bacterial strains used in this study exhibited characteristic morphological, physiological and biochemical properties associated with each organism (Table 3.18).

Table 3.18: Confirmation of microbial test strain identity.

Test bacteria	Typical characteristic demonstrated during tests
Escherichia coli (ATCC 25922)	Gram negative rods, motile, IMViC positive, catalase positive, growth on MacConkey agar, API 20 E profile, lactose and glucose positive with gas production
Staphylococcus aureus (ATCC 25923)	Gram positive cocci in grape-like clusters, catalase positive, oxidase negative, nonmotile, DNAse positive, coagulase positive, black colony development on Baird Parker agar and characteristic API 20 STAPH profile

The selected bacterial strains outlined in Table 3.18 were inactivated with PPGD under various operating conditions in order to determine their susceptibility and treatment response so as to inform and guide subsequent investigations into antimicrobial hydrogel treatments. The inactivation studies were performed with all test organisms suspended in 100 ml of cooled treatment fluid. A dense bacterial suspension with cell numbers as high as 1×10^7 cfu/ml was used as a starting point to simulate extreme microbial contamination. The electrode-liquid gap was kept constant at 5 mm. The effect of varying the applied PFN charging voltage, the pulse frequency and the nature and amount of the gas were examined. The total treatment time was 30 min and cell enumerations were obtained at 2 min intervals by the spread plate and pour plate technique before and during the PPGD process (Section 2.7.3). Nonselective nutrient agar plates were used as they were devoid of antibiotic supplements and dyes that may inhibit the recovery of sublethal damaged cells. The inoculated nutrient agar plates were further incubated at 37^oC for a minimum of 24 h, where survivors were expressed in terms of $\log_{10}$ cfu/ml. Moreover, the inactivation rate constant k obtained using the Chick-Watson model of microbial inactivation (Section 2.7.3, Equation 2.5) determined the susceptibility of the test organisms to varying PPGD treatment conditions. All studies were carried out in triplicate with duplicate plates for each set of exposures.

3.3.4.1 Effect of applied voltage on O_2- and N_2-mediated PPGD

The effect of varying the PFN charging voltage on the bacterial decontamination efficiency using O_2- and N_2-mediated discharge was initially investigated over a wide range of applied charging voltages (10-25 kV). However, to minimise thermal effects and problems associated with the durability of the CCS, the treatment was limited to a maximum charging voltage of 18 kV. Bacterial cell densities of 1 x 10^7 cfu/ml of *E. coli* and *S. aureus* were prepared in 100 ml of treatment fluid as outlined in Section 2.7.2 and the cultures were subjected to varying PFN charges of 14 kV (3.92 J/pulse), 16 kV (5.12 J/pulse) and 18 kV (6.48 J/pulse) at 10 pps and a constant gas flow rate of 2.5 l/min using O_2 and N_2 gases.

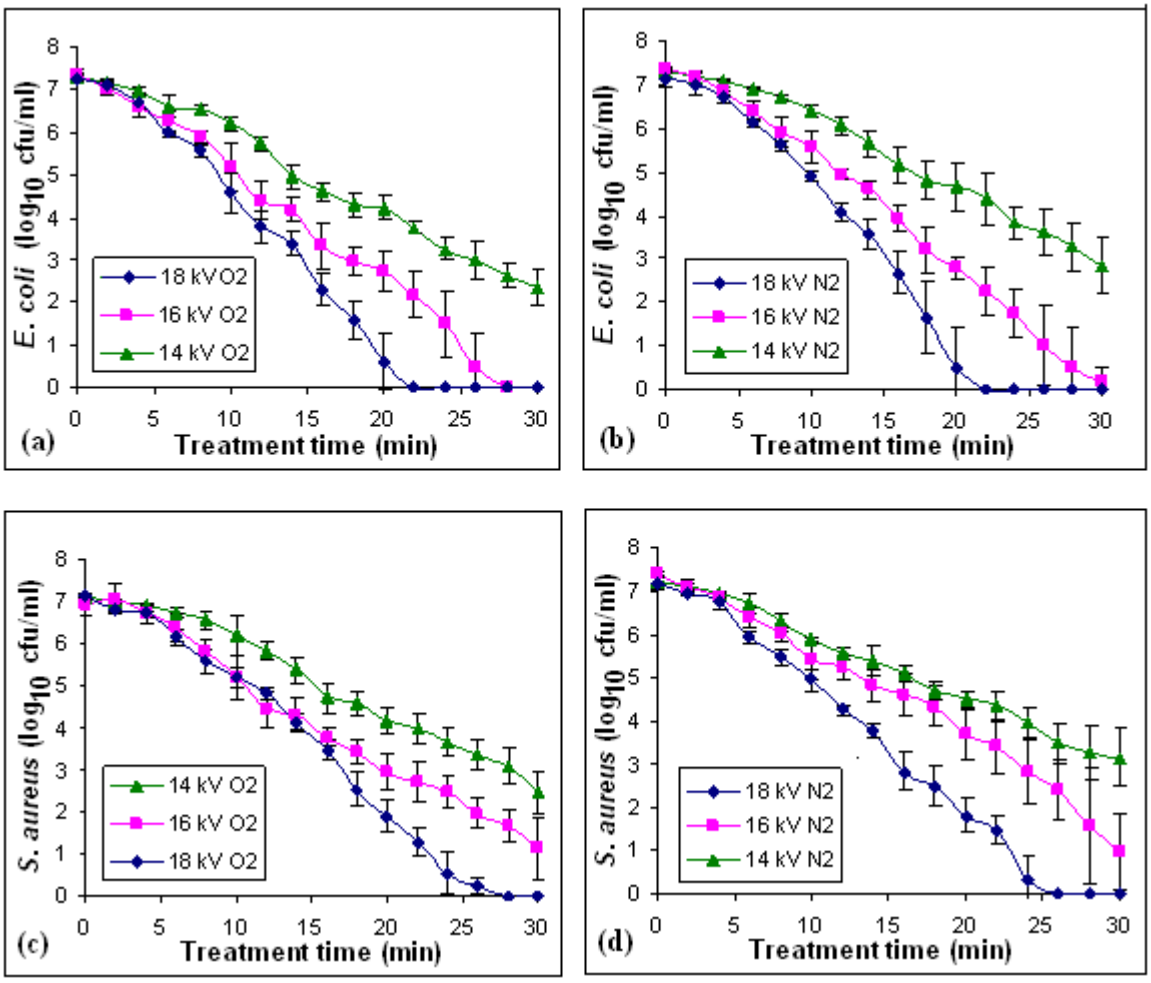

Figure 3.53: The effect of varying the PFN charging voltage (18, 16 and 14 kV) on the inactivation of (a and b) *E. coli* and (c and d) *S. aureus* using O_2- and N_2-mediated PPGD. Results are the mean of three replicates (±SD) at a constant pulse rate of 10 pps and gas flow rate of 2.5 l/min.

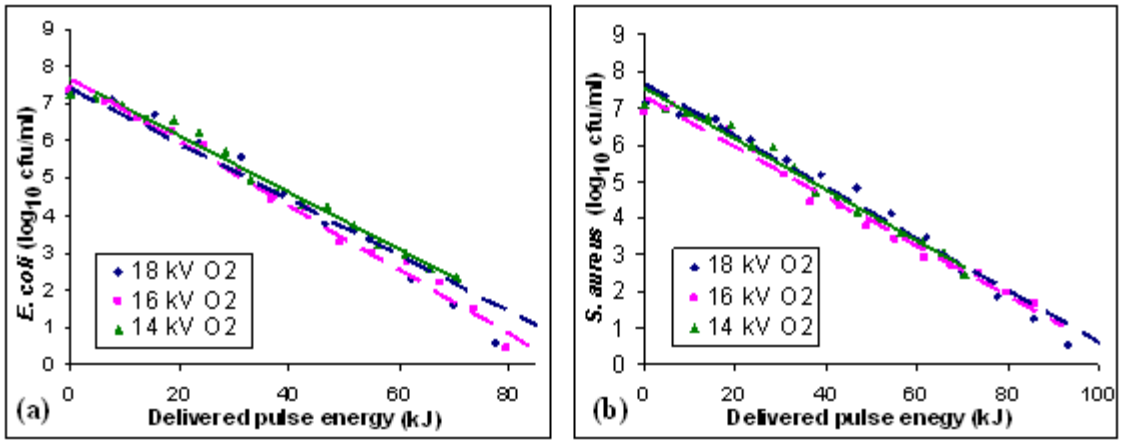

Figure 3.54: The microbial inactivation efficiency of PPGD on (a) *E. coli* and (b) *S. aureus* as a function of pulse energy delivered at varying PFN charging voltages (18, 16 and 14 kV). O_2 gas was used at a flow rate of 2.5 l/min with constant a pulse frequency of 10 pps.

Table 3.19: Inactivation rate constant *k* values (±SD) for *E. coli* and *S. aureus* exposed to PPGD at varying PFN charging voltages. The discharge gas was utilised at a flow rate of 2.5 l/min with constant a pulse frequency of 10 pps.

PPGD treatment	**Inactivation rate constant *k* for varying PFN charges**	
	O_2 discharge	**N_2 discharge**
E. coli		
18 kV	0.0485 (±0.0035)	0.0478 (±0.0033)
16 kV	0.0358 (±0.0029)	0.0346 (±0.0038)
14 kV	0.0250 (±0.0030)	0.0231 (±0.0037)
S. aureus		
18 kV	0.0398 (±0.0026)	0.0405 (±0.0022)
16 kV	0.0301 (±0.0017)	0.0276 (±0.0045)
14 kV	0.0228 (±0.0023)	0.0201 (±0.0026)

The PPGD inactivation experiments illustrated in Figure 3.53 show that a strong reduction in the surviving microbial cell density was evident for both organisms tested. It was observed, that after an initial shoulder effect, the microbial densities decreased significantly ($p<0.05$) and almost in a linear fashion with increasing treatment time. In general, the Gram negative *E. coli* (Figures 3.53a and b) appeared more susceptible to the antimicrobial effects of the PPGD treatment than the Gram positive *S. aureus* (Figures 3.53c and d). Increasing the PFN charging voltage resulted in a significantly ($p<0.05$) accelerated microbial inactivation in all experiments conducted. More specifically, after applying charging voltages of 18 kV a full 7 log-order inactivation was achieved for all parameters tested. For this setting, the required time to fully inactivate the organisms

suspended in 100 ml of test liquid was below 22 and 26 min for *E. coli* and *S. aureus* respectively, regardless of which discharge gas was used. The use of O_2 gas was found to be more potent than N_2 gas in terms of microbial inactivation and this effect was specifically observed for the 16 and 14 kV treatments. A full 7 log-order reduction for *E. coli* was obtained within 30 min of O_2- and N_2-mediated discharge treatments using a PFN charge of 16 kV. Utilising a 14 kV O_2 discharge the maximum inactivation achieved was 5.03 and 4.67 log-orders for *E. coli* and *S. aureus*, respectively. These trends were again observed by determining the inactivation rate constants representative for each microorganism under specific discharge conditions (Table 3.19). The values of the obtained inactivation constants significantly ($p<0.05$) increased with an increase in applied charging voltages. Again, it was observed that the use of O_2 gas was more biocidal than N_2 gas at treatment voltage below 18 kV. Moreover, Gram negative strains exhibited increased rates of inactivation in comparison to the Gram positive strains tested.

Figure 3.54 shows the variation of *E. coli* and *S. aureus* cell density as a function of input energy to demonstrate the net efficiency of differing PFN charges and it can be seen that for the settings used, the energy required to inactivate a certain microbial density was almost independent of the PFN charging voltage. Although the 18 kV treatment led to a more rapid reduction in cell viability, it was not more energy efficient than the 16 or 14 kV. In fact, a close look over the whole treatment range reveals that the 16 kV setting appears to result in a slightly more energy efficient inactivation of both organisms. Furthermore, this graph allows for a direct comparison between the pulse energy required to fully inactivate the two different types of bacteria within the treatment liquid. It is noticeable that approximately 110 kJ are required to achieve a $\geq$7 log-order inactivation of the Gram positive *S. aureus* while less than 100 kJ was necessary to obtain a similar inactivation scale for *E. coli*.

The results obtained in Figure 3.53 confirmed the biocidal activity of the PPGD system used in the present study. Furthermore, the inactivation rate constants shown in Table 3.19 proved useful for comparing the sensitivity of both microbial species to the PPGD. However, as the Chick-Watson model is based on pseudo first-order kinetics it would underestimate the shoulder effects seen on the inactivation graphs (Figure 3.53). Overall, the discharge resulted in a significant and fast reduction of viable microorganisms

suspended within the 100 ml of test liquid. The treatment efficiency was dependent on various parameters such as PFN charging voltage, the nature of the discharge gas, and the type of microorganisms used. In accordance with previous investigations, it is likely that several mechanisms contribute to the biocidal effects of pulsed plasma discharges, some of which have yet to be fully elucidated (Anapilov *et al.,* 2001; Marsili *et al.,* 2001; Satoh *et al.,* 2007). The formation of pulsed electric fields during HV discharges across liquids has been reported to cause detrimental effects to the bacterial cell wall (Beveridge *et al.,* 2004). However, electrode configurations leading to discharges into a gas rather than directly into the liquid are believed to minimise the effects of electric fields (Espie *et al.,* 2000). The active species generated in the gaseous phase, which subsequently dissolve into the liquid, are expected to play a major role in the microbial inactivation process (Anpilov *et al.,* 2002, 2004; Satoh *et al.,* 2007). In Sections 3.3.3.2 and 3.3.3.3, the presence of ozone and reactive nitrogen was observed within the test liquid after PPGD treatment and it was suggested that several other active species may be generated by the system. The concentration of these species increased with prolonged treatment and was dependent on the type of discharge gas used. The time-dependent increase in the quantity of active species detected may explain the delayed cell inactivation at the start of the treatment which was indicated by the shoulder effect (Figure 3.53). It appears that a sufficient amount of radicals is required to initiate microbial inactivation. On the other hand, the increasing amount of active species formed during prolonged treatment caused the observed acceleration of bacterial inactivation.

Lerouge *et al.* (2001) suggests that the nature and composition of the gas used for the generation of the plasma is a determining factor of its biocidal effectiveness as it dictates the types of active species formed. In the current study, it appears that active species generated during O_2 discharge were superior in microbial decontamination than those generated during N_2 discharges. This effect was also observed by Satoh *et al.* (2007) and it was suggested that oxygen based radicals such as O_3, H_2O_2 and ·OH have a more lethal effect on bacteria cells than compounds containing nitrogen atoms. The rate of microbial inactivation obtained while using N_2 as a discharge gas is likely to be related to the presence of nitric and nitrous acid which in turn drastically reduced the pH of the treatment solution (Section 3.3.3.1). Several investigations have stated that, depending on

the microorganism treated, an acidic milieu present during plasma discharge treatment can enhance the microbial reduction rate (Espie *et al.,* 2001; Satoh *et al.,* 2007; Rowan *et al.,* 2008).

Furthermore, antimicrobial activity has been attributed to shockwaves and UV-radiation resulting from the corona discharge (Anpilov *et al.,* 2001; Zuckerman *et al.,* 2002). However, for the treatment volume and electrode setup used in this study UV-radiation effects are believed to play only a minor role because of the limited penetration properties of biocidal UV light in liquids (Hu *et al.,* 2008). Although difficult to determine, the effect of high pressure shockwaves created during HV plasma discharges cannot be underestimated. A publication by Zuckerman *et al.* (2002) demonstrated the excellent microbial inactivation potential of those shockwaves in aqueous solutions. However, the exact mechanism of bacterial destruction is not fully understood. In addition, the shockwaves facilitate the mixing of treated water, delivering reactive species to all parts of the treatment system (Anpilov *et al.,* 2001).

Although the PPGD system was designed to be used as a nonthermal disinfection method, certain temperature increases of the test liquid during treatment were unavoidable. The temperature rose as a result of Joule heating and this is demonstrated in Figure 3.41 of Section 3.3.3.1. The liquid temperature increased significantly above the optimal growth condition for *E. coli* and *S. aureus* (37^{o}C) within the 30 min treatment at 16 and 18 kV. This effect could have contributed also to the microbial inactivation of the organisms studied. Also, the manifestation of adverse effects towards microbial cell viability resulting from metal residuals introduced by electrode erosion cannot be excluded. It was shown in Section 3.3.3.4, that within 30 min of PPGD treatment, the Al concentration rose to a noteworthy value within the treatment liquid and previous investigations have demonstrated the toxic effects of Al on microorganisms (Guida *et al.,* 1991; Piña and Cervantes, 1996). However, in relation to the present study more information is needed to determine whether the metal contamination levels seen played a significant role in the inactivation rate of the microbial species.

In general, it appeared that the Gram positive *S. aureus* was less susceptible to the lethal action of the plasma discharge than the Gram negative *E. coli*. This effect was also observed by Rowan *et al.* (2008) and it was suggested that the differences in complexity of

the cell envelopes associated with Gram negative and Gram positive bacteria may have been responsible. Gram positive cell walls are simple structures but have thick peptidoglycan layers (10-20 layers thick) which support the cell walls. On the other hand, Gram negative cell walls have complex structures but thinner peptidoglycan layers (only one to two layers thick). Consequently, Gram negative cell envelopes may be more permeable and subsequently less resistant to a chemical insult (Zhang *et al.,* 2006). Furthermore, it is well known that *S. aureus* grows in grape-like clusters which provide a protective environment for organisms in the center of these clusters. This may allow for the prolonged survival of some organisms within the protective cluster.

Moreover, less energy was required to inactivate the Gram negative bacterium as can be seen from the linear plots in Figure 3.54, illustrating the relationship between microbial inactivation and delivered energy in kJ. Surprisingly, the energy efficiency of the treatment procedure was almost independent from the varying PFN charging voltages investigated. Therefore, it seems that the only major benefit of higher PFN charges is a more rapid inactivation. However, this rapid inactivation is at the cost of introducing increased thermal effects into the treatment chamber. Additionally, the electrical elements of the PPGD system such as the CCS deteriorated at a faster rate when used at the elevated charging voltages.

3.3.4.2 Effect of varying pulse frequency

Studies were also carried out on *E. coli* and *S. aureus* to determine the effect of varying the pulse frequency on the PPGD disinfection performance and experimental pulse frequencies of 7.5, 10 and 12.5 pps were chosen. To obtain comparable results, a constant PFN charging voltage of 16 kV was used in combination with discharge mediated in O_2 and N_2 gases at a flow rate of 2.5 l/min. As previously described, both bacterial types were prepared to obtain a starting cell population of 1 x 10^7 cfu/ml in 100 ml of precooled treatment fluid. The findings of this study are illustrated in the inactivation plots shown in Figure 3.55. In addition, the relationship between the varying frequencies and their energy efficiency towards microbial inactivation are shown in Figure 3.56. Furthermore, the treatment specific inactivation constants calculated by the Chick-Watson model are given in Table 3.20.

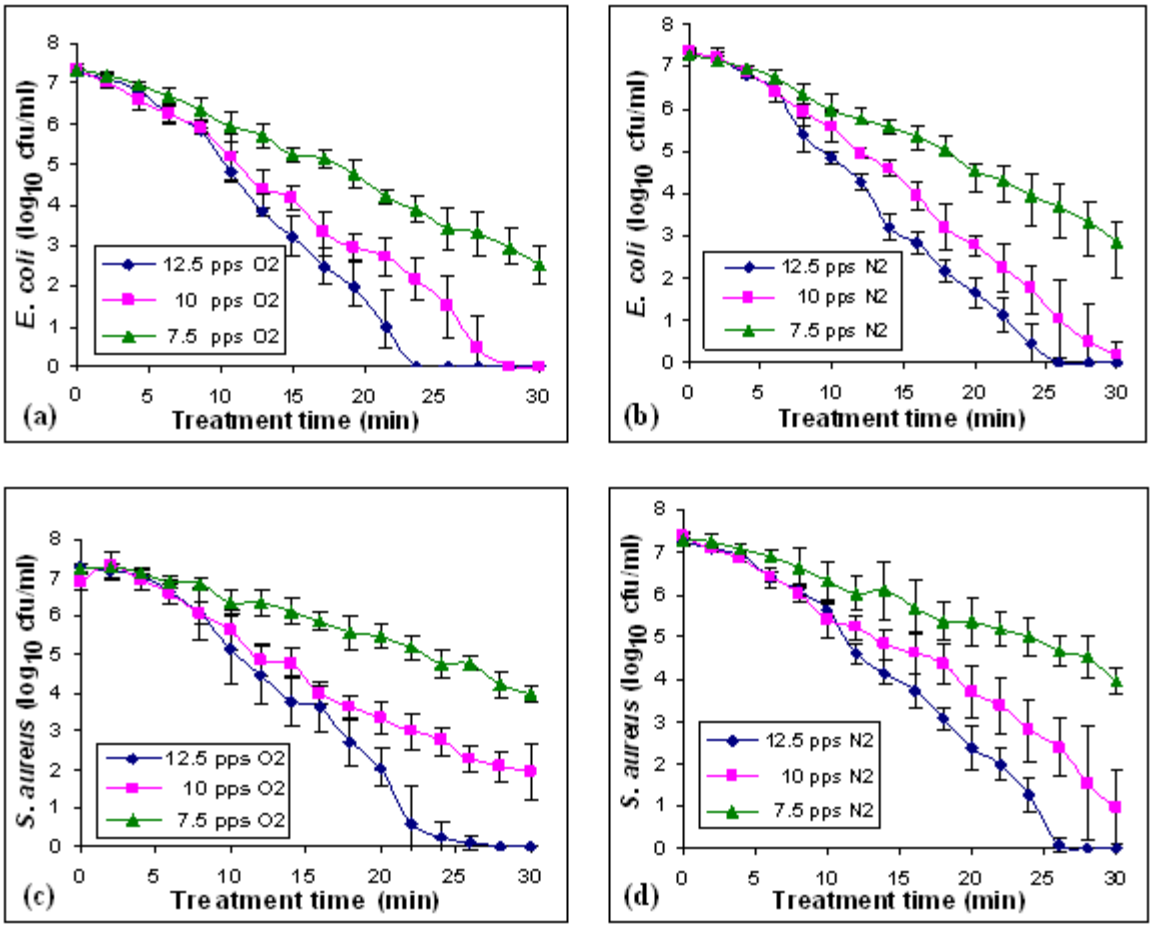

Figure 3.55: The effect of varying the pulse frequency (12.5, 10 and 7.5 pps) on the inactivation of (a and b) *E. coli* and (c and d) *S. aureus* using O_2- and N_2-mediated PPGD. Results are a mean of three replicates (±SD) at a constant PFN charge of 16 kV and gas flow rate of 2.5 l/min.

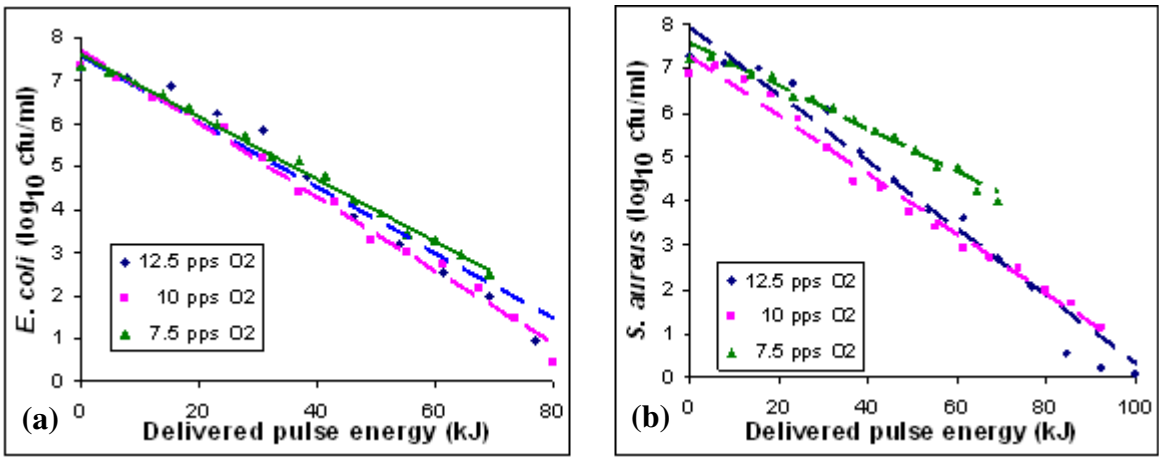

Figure 3.56: The microbial inactivation efficiency of PPGD on (a) *E. coli* and (b) *S. aureus* as a function of pulse energy delivered at varying pulse frequencies (12.5, 10 and 7.5 pps). O_2 gas was utilised at a flow rate of 2.5 l/min with constant PFN charge of 16 kV.

Table 3.20: Inactivation rate constant *k* values (±SD) for *E. coli* and *S. aureus* exposed to PPGD with varying pulse frequencies. Discharge gas was utilised at a flow rate of 2.5 l/min with constant PFN charging voltage of 16 kV.

PPGD treatment	Inactivation rate constant *k* for varying pulse frequencies	
	O_2 discharge	N_2 discharge
E. coli		
12.5 pps	0.0475 (±0.0054)	0.0434 (±0.0022)
10.0 pps	0.0358 (±0.0029)	0.0346 (±0.0038)
7.5 pps	0.0226 (±0.0024)	0.0203 (±0.0041)
S. aureus		
12.5 pps	0.0430 (±0.0029)	0.0381 (±0.0021)
10.0 pps	0.0301 (±0.0017)	0.0276 (±0.0045)
7.5 pps	0.0155 (±0.0016)	0.0147 (±0.0017)

The results shown in Figure 3.55 and Table 3.20 demonstrate the effect of varying the pulse frequency on the antimicrobial properties of the PPGD treatment. It was observed that increasing the pulse frequency results in a significantly ($p<0.05$) increased inactivation rate. Similar to the results illustrated in Figure 3.53, a pronounced shoulder effect at the start of the treatment was seen in Figure 3.55. Again, the presence of this shoulder effect indicated that a certain level of PPGD treatment is needed to initiate the inactivation of the microorganisms. Once sufficient treatment was provided, microbial inactivation occurred constantly until complete cell death was achieved.

For experiments using 12.5 pps, a strong biocidal activity was evident with both types of bacteria being completely inactivated (≥7 log-order reduction) within the 30 min treatment time. As indicated by the inactivation constants obtained, for these treatments the susceptibility of *E. coli* and *S. aureus* was comparable while O_2-mediated discharge proved slightly more potent than N_2 discharge (Table 3.20). More specifically, the respective inactivation constants for *S. aureus* were slightly but significantly ($p<0.05$) below those obtained for the 12.5 pps treatment of *E. coli* (Table 3.20). Also, a closer look at the final inactivation (20-28 min) of the Gram positive *S. aureus* subjected to 12.5 pps (Figures 3.55c and d) reveals an accelerated rate of inactivation which is believed to be related to temperature effects. In comparison, reducing the pulse rate to 7.5 pps resulted in a significantly ($p<0.05$) decreased microbial inactivation rate compared to 12.5 and 10 pps treatments as shown by the inactivation graphs and the *k* values (Figure 3.55 and Table 3.20). Similar to the previously discussed inactivation test, it was clear that the *S. aureus*

bacterium was more resilient to the biocidal effects of the PPGD than the *E. coli* organism. Again, the use of O_2 gas appeared to be superior to N_2 gas for the inactivation of the organisms. After a 30 min treatment with 7.5 pps, the *E. coli* bacterium was reduced by a log-order of 4.84 and 4.42 for O_2 and N_2, respectively, while *S. aureus* was reduced by a log-order 3.25 and 3.12 for O_2 and N_2, respectively. The *k* values obtained for these studies further strengthened these findings and confirmed that O_2 gas was more potent for microbial inactivation than N_2.

Figure 3.56 illustrates the difference in electrical energy required to achieve the microbial reduction at varying pulse frequencies. It is clearly shown that over the whole frequency range tested, the *E. coli* bacterium requires less energy than *S. aureus* to become fully inactivated. Again, for both bacteria types, the 10 pps treatment was found to be the most energy efficient setting, while the 12.5 pps treatment was found to be slightly less efficient. The 7.5 pps treatment was considerably less effective, particularly for the inactivation of the Gram positive test bacteria. Theoretically, it requires accumulated pulse energies of approximately 110 and 155 kJ for the 7.5 pps treatment to achieve a 7 log-order inactivation of *E. coli* and *S. aureus*, respectively.

Overall, it was not surprising to observe that higher pulse frequencies were able to inactivate the microorganisms at a faster rate as the energy input into the treatment chamber was directly proportional to the repetition rate of the pulse. Therefore, the increased reduction rate can be explained by the fact that the bacteria were exposed to elevated discharge energies per increment of treatment time. Although the 12.5 pps rate led to a faster microbial reduction it was not found to be more energy efficient than the 10 pps rate. These findings were comparable to results obtained in the previous investigation where increasing the PFN charge from 16 to 18 kV resulted in an increased microbial reduction but without a remarkable difference in energy efficiency (Figures 3.53 and 3.54). However, decreasing the pulse rate to 7.5 pps had a severe impact on the biocidal properties of the PPGD. While conducting studies on the inactivation of the Gram positive test species *S. aureus*, a remarkable reduction in inactivation efficiency was observed. Thus, it appears that a certain pulse frequency is required to obtain optimum inactivation. Moreover, these findings are in accordance with Sections 3.3.3.2 and 3.3.3.3 where an increase in the pulse frequency led to an elevated production of dissolved reactive oxygen

and nitrogen species. However, in contrast, treatments with 12.5 pps were not found to be more energy efficient than treatments using 10 pps. Also, the introduction of temperature effects observed towards the end of the treatment with 12.5 pps could not substantially influence this result. Therefore, at the utilised 16 kV PFN charge, a 10 pps frequency appears to be favourable for the treatment of heat sensitive materials and these settings was considered during the following inactivation studies using chemical hydrogels.

3.3.4.3 Effect of various discharge gases and flow rates

The impact of varying gas flow rates on the biocidal properties of the PPGD treatment was also investigated since it has the potential to affect the rate of reactive species generated (Lerouge *et al.,* 2001). For comparative purposes, O_2 and N_2 were used as the discharge gases at a flow rate of 1, 2.5 and 5 l/min while a constant PFN charging voltage of 16 kV combined with a pulse repetition rate of 10 pps was maintained. The tests were performed in accordance with previous inactivation experiments, with *E. coli* and *S. aureus* dispersed in 100ml of precooled treatment liquid at a final cell concentration of 1 x 10^7 cfu/ml.

It was previously determined (Section 3.3.3.2, Figure 3.46) that varying the gas flow rate of O_2 during the PPGD treatment influenced the amount of dissolved ozone detectable within the treatment fluid. Here, the highest amount of dissolved ozone was generated using an O_2 gas flow of 2.5 l/min. Furthermore, a study into the antimicrobial effects of PPGD by Espie *et al.* (2001) suggests that the gas flow rate plays an important part in physically mixing the treatment liquid and thus supports the distribution of biocidal species to all parts of the treatment system. Thus, it was important to establish how changes in the gas flow rates contribute to the cell inactivation achieved via the PPGD treatment.

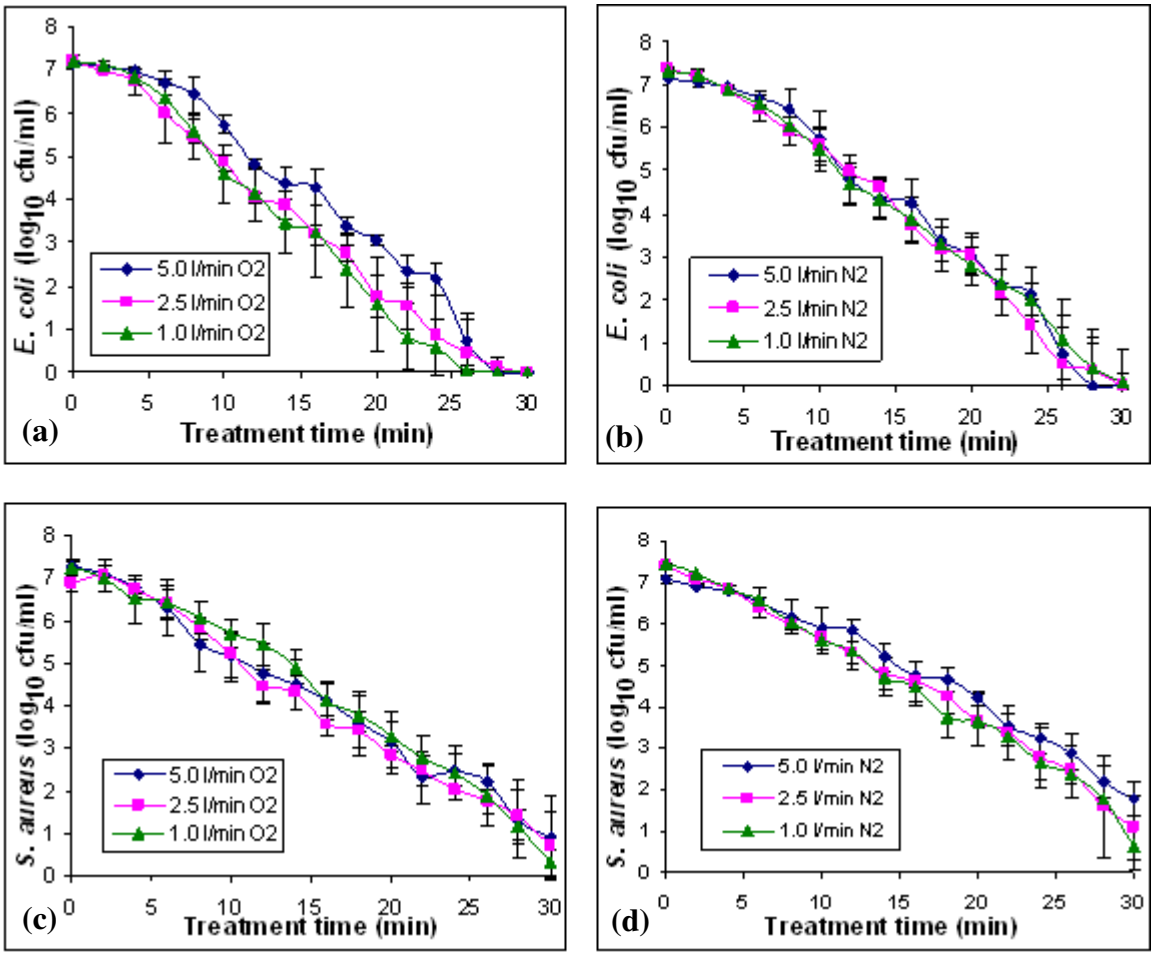

Figure 3.57: The effect of varying the gas flow of O_2 and N_2 (5, 2.5 and 1 l/min) on the PPGD inactivation of (a and b) *E. coli* and of (c and d) *S. aureus*. Results are the mean of three replicates (±SD) at a constant PFN charge of 16 kV and a pulse repetition rate of 10 pps.

Table 3.21: Inactivation rate constant *k* values (±SD) for *E. coli* and *S. aureus* exposed to PPGD with varying gas flow rates. The discharge was utilised at constant PFN charging voltage of 16 kV and 10 pps delivered.

PPGD treatment	**Inactivation rate constant *k* for varying gas flow rates**	
	O_2 discharge	**N_2 discharge**
E. coli		
5.0 l/min	0.0349 (±0.0012)	0.0319 (±0.0044)
2.5 l/min	0.0383 (±0.0037)	0.0356 (±0.0019)
1.0 l/min	0.0434 (±0.0046)	0.0366 (±0.0023)
S. aureus		
5.0 l/min	0.0295 (±0.0033)	0.0267 (±0.0033)
2.5 l/min	0.0320 (±0.0018)	0.0277 (±0.0045)
1.0 l/min	0.0313 (±0.0043)	0.0295 (±0.0019)

Figure 3.57 demonstrates the effect of varying the gas flow rate on the inactivation efficiency of PPGD. For all treatments there was little difference in microbial reduction observed when the gas flow rates of O_2 and N_2 gases were varied. The results obtained were comparable to the 16 kV at 10 pps treatments obtained in the previous studies where varying PFN charge and the pulse repetition rates were investigated (Figures 3.53 and 3.55). Even gas flow rates as low as 1 l/min proved efficient for reducing the microbial load. However, a closer look at *E. coli* treatments with O_2 gas (Figure 3.57a) reveals that the gas flow of 5 l/min was less efficient than the gas flow rate of 1 l/min ($p<0.05$). This finding is in accordance with previous observations described in Section 3.3.3.2, where a reduced amount of dissolved ozone was detected at this flow rate. It was suggested that the reactive species generated using a 5 l/min flow rate may be transported out of the treatment zone before they could reach the liquid interface and dissolve. This effect, however, was neither observed for *E. coli* treatments using various N_2 flow rates nor for experiments using *S. aureus*. Here, no significant difference between the inactivation potential of different gas flow rates could be established. Therefore, for the experimental settings investigated, it appeared that varying the flow rate had only a minor impact on the biocidal properties of the PPGD system (Figure 3.57 and Table 3.21).

This finding is somewhat comparable to a study conducted by Satoh *et al.* (2007) where varying the gas flow rates of air, O_2 and N_2 from 0.5 to 4 l/min did not drastically affect the antimicrobial performance of PPGD. Considering the cost of using purified gases, the 1 l/min treatment appears to be the most economical flow rate while also achieving effective microbial inactivation of both Gram negative and Gram positive test species. However, subsequent hydrogel sterilisation experiments will be performed at a flow rate of 2.5 l/min as this setting appeared most efficient in the production of ozone (Section 3.3.3.2). Furthermore, increased temperature effects resulting from the use of low gas flows cannot be excluded due to the reduced ventilating capacities.

3.3.5 *In vitro* toxicity evaluation of PPGD-treated test liquid

Since the PPGD treatment investigated in the current study is a novel sterilisation method, verification of its toxicological safety is necessary. In this context, the biocidal species generated within the PPGD-treated test liquid requires particular attention as they could

potentially be toxic to humans. Once removed from the discharge source, it was hoped that the majority of activated compounds may eventually lose their high energy and recombine to less toxic byproducts. Nevertheless, an extended biocidal activity of the liquid could be disadvantageous in terms of sterilisation of chemical hydrogels intended for biomedical applications. Due to the hydrophilic nature of hydrogels it is possible that residuals of the treatment liquid may be absorbed into the gel matrices whereby extended biocidal effects could interfere with the overall biocompatibility of the hydrogels. In addition, elemental metal contaminates released during electrode degradation processes may diffuse into the hydrogel and cause some concern regarding hydrogel biocompatibility.

Although the antimicrobial efficacy of PPGD in the presence of an aqueous medium has been investigated (Satoh *et al.,* 2007; Rowan *et al.,* 2007, 2008), a systematic study addressing the safety of this method is lacking. Therefore, to obtain valuable information on the suitability and sustainability of the PPGD method for the microbial disinfection of chemically crosslinked hydrogels, the cytotoxic and DNA damaging potential of the PPGD-treated test liquid was under investigation. The test liquid was evaluated via the previously employed *in vitro* testing approach involving direct exposure of HaCaT cells to PPGD-treated test liquid using both NR and MTT viability endpoints in addition to the comet and Ames genotoxicity tests. The HaCaT cell line was chosen for toxicity testing as it represents characteristics of the human skin (Boukamp *et al.,* 1988), the organ on which PPGD sterilised hydrogels are intended to find a use as wound healing device.

Before conducting the toxicity assays, 100 ml of the test liquid were treated for 30 min with PPGD using an applied charging voltage of 16 kV and a pulse frequency of 10 pps. For comparative purposes, both O_2- and N_2-mediated discharges were used at a gas flow rate of 2.5 l/min. The PPGD-treated test liquid was then exposed to the test systems directly after treatment, or the treated test liquid was incubated for 7 days at room temperature prior to cellular exposure in order to allow reactive species to decay to less toxic residuals.

3.3.5.1 Cytotoxicity evaluation of PPGD-treated test liquid

The potential of the PPGD-treated test liquid to induce adverse effects on HaCaT cells grown in culture was evaluated via the direct contact assay using both the MTT and NR endpoints. More specifically, test liquid exposed to O_2- and N_2-mediated discharges was prepared for subsequent 24 h cell exposure via dilution in complete cell culture medium. To ensure sufficient cell nutrient content in the exposure medium, the maximum concentration tested was 40% with the results obtained expressed as percentage of untreated control cell viability. The control solutions were prepared with dilutions of untreated test liquid in cell culture medium. The effect of PPGD-treated test liquid on cytocompatibility was either evaluated directly after PPGD treatment or after incubating the treated liquid for 7 days at room temperature. The mean percentage viability ±SEM of replicate results were then calculated for each cell line.

Figures 3.58 and 3.59 suggest that following 24 h cell exposure to PPGD-treated test liquid, there was a pronounced effect on the viability of HaCaT cells in the direct contact assay with MTT and NR endpoints, respectively. Overall, the trend in toxicity profiles observed via the MTT endpoint was similar to the trend observed in the NR endpoint although the latter assay appeared more sensitive to the cytotoxic effects of the PPGD-treated test liquid. In both assays a significant ($p<0.01$), dose-dependent decrease in cell viability was observed. Cell exposure to O_2 discharge-treated test liquid resulted in lower cell viability values compared to cell exposure to test liquids produced using N_2 gas. Furthermore, cellular exposure to the test liquids immediately after PPGD treatment led to elevated cytotoxic effects in both assays and for both gas-discharge types. In contrast, incubating the test liquid at room temperature for an additional 7 days before cell exposure appeared to detoxify the samples. This detoxifying effect was most pronounced for the O_2-treated liquids as here the difference in cell viability values obtained for direct exposure compared to exposure after the 7 days incubation was greatest. More specifically, as shown in Figures 3.58a and 3.59a, direct exposure to the highest test liquid concentration (40%) prepared with O_2 discharge-treated test liquid reduced the cell viability to 21% in the MTT and 4% in the NR endpoints. In comparison, when incubated for 7 days before exposure, the same concentration resulted in cell viability values of 29% and 39% in the MTT and NR endpoints respectively (Figures 3.58b and 3.59b).

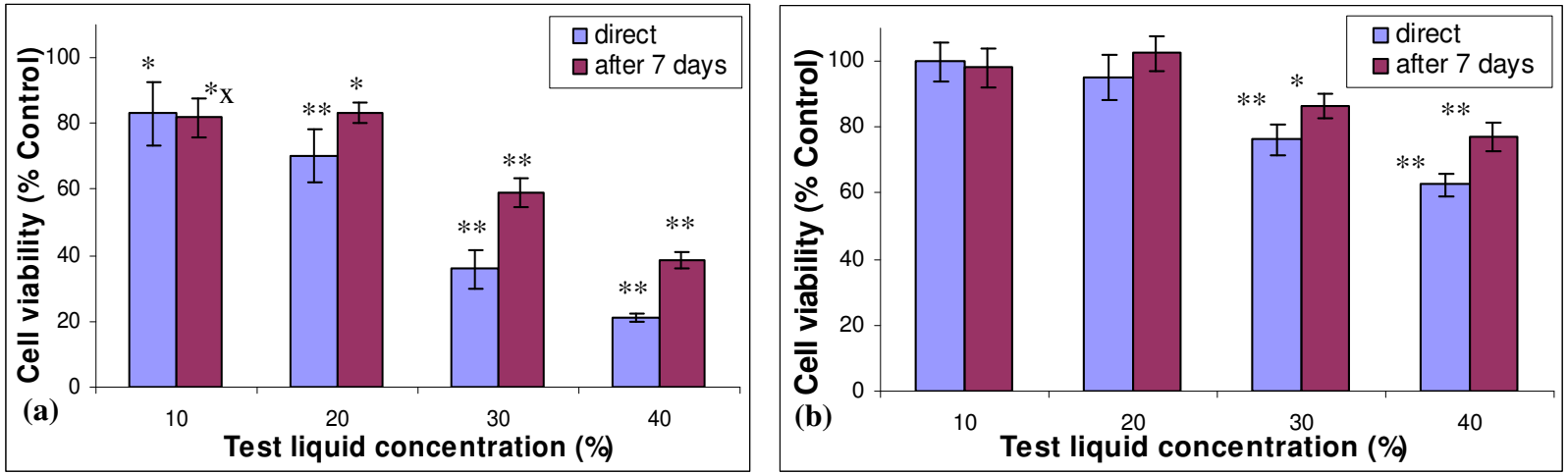

Figure 3.58: Effect of (a) O_2- and (b) N_2-mediated PPGD-treated test liquid on the viability of HaCaT cells following 24 h exposure at 37°C as assessed by the direct contact assay using the MTT endpoint (n=18 ±SEM, * denotes a significant difference control **=p<0.01, *=p<0.05).

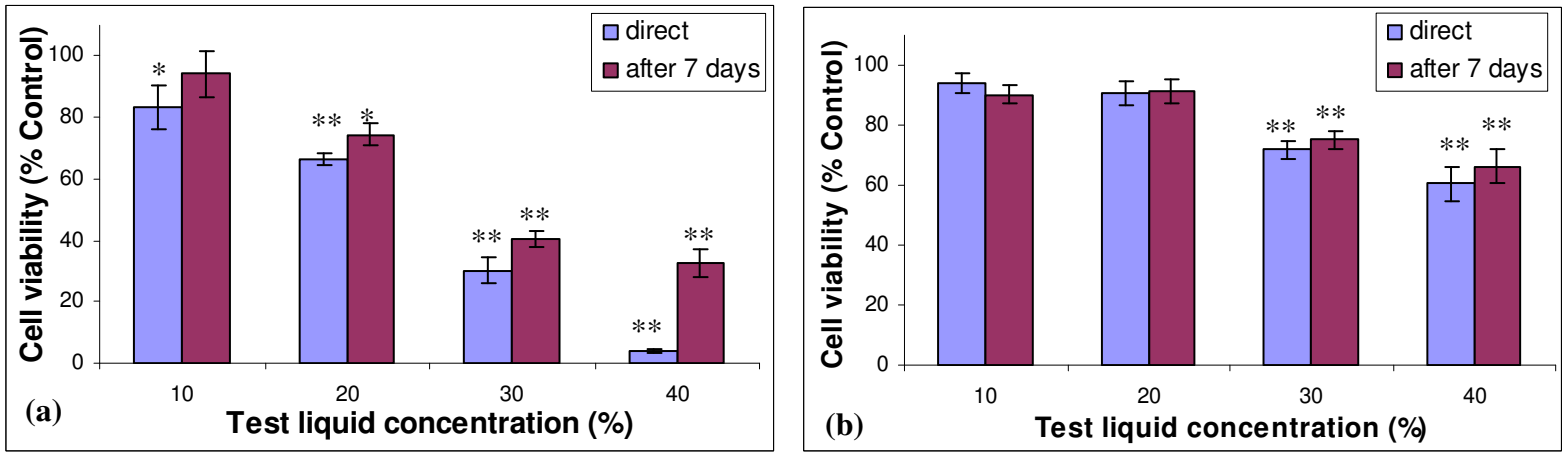

Figure 3.59: Effect of (a) O_2- and (b) N_2-mediated PPGD-treated test liquid on the viability of HaCaT cells following 24 h exposure at 37°C as assessed by the direct contact assay using the NR endpoint (n=18 ±SEM, * denotes a significant difference control **=p<0.01, *=p<0.05).

Direct exposure to the highest N_2-treated test liquid concentration (40%) resulted in reduced cell viability values of 67 and 61% while exposure after the 7 days incubation resulted in viability values of 77 and 66% for both the MTT and NR endpoints, respectively.

Not surprisingly, similar to the previously observed biocidal activity on indicator bacteria (Section 3.3.4), the PPGD-treated test liquid also appeared cytotoxic to HaCaT cells even at concentrations below 40% and this effect was dependent on the gas type used for the discharge. The use of O_2 gas during the preparation of the test liquid was found to enhance the cytotoxic potential of the liquid. Although the observed cell death might be a sum of various effects associated with the plasma treatment, it was believed that the generated reactive chemical species had a major contribution. This assumption is further strengthened by the fact that 7 days delayed exposure to the test liquid had a detoxifying effect, in particular for O_2 gas-treated samples, which would allow some of the radical species generated to dissipate and combine to form less toxic substances.

The presence of dissolved ozone within HV discharge-treated liquids has been previously confirmed in Section 3.3.3.2 using the DPD colorimetric method with the production of this reactive chemical being enhanced by the use of O_2 as a discharge gas. More specifically, as previously shown in Figure 3.44, the concentration of dissolved ozone was almost 0.8 mg/l measured immediately after PPGD treatment using a charging voltage of 16 kV at 10 pps and an O_2 flow of 2.5 l/min. It was suggested that the presence of ozone is likely to be accompanied by various other oxidising radicals such as H_2O_2, OH·, and $O2^{\cdot -}$ resulting from ozone decay and additional gas activation during HV discharge processes (Staehelin and Hoigńe, 1985; Gunten, 2003b; Lin and Nakajima, 2003). Similar to its deleterious action on microorganisms, ozone and associated free radicals damage mammalian cells mainly by oxidation of fatty acids, DNA, proteins, amines, and thiols (Mehlman and Borek, 1987). Furthermore, a study conducted by Whiteside and Hassan (1988) showed that ozone can lead to the inactivation of intracellular antioxidant enzymes such as catalase and superoxide dismutase thereby enhancing its toxic effects on subcellular structures. Several studies have also investigated the cytotoxic effects of dissolved ozone using mammalian cells in culture (Diaz-Llera *et al.,* 2002; Larini and Bocci, 2005; Zhou *et al.,* 2008) and H_2O_2 was thought to be a major intermediate causing

such toxicity (Oosting *et al.,* 1991). However, the effects of ozone much depend on the concentration of antioxidants present in the extracellular fluid (the cell culture medium) thus making the comparison between other studies difficult (Larini and Bocci, 2005; Zhou *et al.,* 2008).

In Section 3.3.3.3, the presence of nitrate and nitrite ions was detected in the test liquid post-PPGD treatment using N_2 gas as a discharge mediator (Figure 3.50). It was suggested that these ions indicate the presence of dissociated nitric and nitrous acid which drastically decreased the pH of the test liquid (Figure 3.43). Moreover, it was believed that reactive nitrogen compounds and the resulting acidic conditions played a contributing role in the observed microbial inactivation during N_2-mediated PPGD (Section 3.3.4). However, in relation to the observed cytotoxic potential of the PPGD-treated test liquid on HaCaT cells, the test liquid's acidity was not believed to play a significant role as the buffering capacity of the cell culture medium was able to neutralise such pH changes even at the higher exposure concentrations of 40%. Indeed, such medium associated buffering capacity may have contributed to the reduced cytotoxic potential of N_2 discharge-treated test liquid in comparison to O_2 discharge-treated liquid.

Although the pharmacokinetics of nitrite and nitrate ions have been studied for decades, the molecular mechanisms of their toxicity still remain to be fully elucidated. More specifically, most of the scientific investigations concerned with the toxicity of those nitrogen compounds have been conducted on experimental animals *in vivo*, with the aim to predict human toxicity. Hence, only a limited amount of studies have examined the effect of nitrate and nitrite exposure at the cellular level using mammalian cell culture models. Although many scientific investigations suggests that reactive oxygen species such as peroxinitrite (Chow and Hong, 2002) or nitric oxide (Iijima *et al*., 2002) play a role in nitrate and nitrite toxicity, the identification of the specific molecular mechanisms still remain the subject of debate. Nonetheless, two independent studies conducted by Bharadwaj *et al*. (2005) and Jondeau *et al*. (2006) provide initial information on the cytotoxic potential of nitrate on human HepG2 cells in culture. After conducting a NR assay, Bharadwai *et al.* (2005) concluded that no significant impact on HepG2 cell viability was observable following 24 h exposure of 1000 mg/l nitrate dissolved in cell culture medium. Similarly, Jondeau *et al*. (2006) conducted a range of 20 h exposure tests and

showed that a minimum concentration of approximately 2500 mg/l nitrate in cell culture medium was required to cause a 50% reduction in cell viability. The cytotoxic potential of sodium nitrite on human gastric epithelial cells was also investigated by Sun *et al*. (2006) using a cell proliferation assay with only the highest dose of 2300 mg/l sodium nitrite inducing a mild cytotoxic effect after 72 h exposure.

In the present study the nitrate and nitrite concentrations detected were found to be 18 and 21 mg/l, respectively following PPGD treatment using a charging voltage of 16 kV at 10 pps and a N_2 flow of 2.5 l/min (Figure 3.50). Here, particular concern is the concentration of nitrite which is well above the maximum tolerated value (0.5 mg/l) for drinking water within the European Communities (No. 2 Regulations 2007). However, considering the aforementioned studies, it is unlikely that even the combined action of nitrate and nitrite have caused the observed adverse effects on HaCaT cell viability. Nevertheless, there is a possibility that generated reactive nitrogen compounds other than nitrate and nitrite may have contributed to the observed cytotoxicity. Indeed, when dissolved in an aqueous solution the NO_2^- ions are unstable and can decay into smaller reactive nitrogen molecules which will eventually be oxidised to form less reactive NO_3^- ions (Cai *et al.,* 2001). As a consequence, such decay into less reactive nitrogen compounds may explain the slightly reduced cellular toxicity observed after exposing the cells to test liquid which was preincubated for 7 days following PPGD treatment with N_2 discharge (Figures 3.58 and 3.59).

Another factor that could have affected the HaCaT cell viability is the presence of metallic electrode degradation products within the PPGD-treated test liquid. In Section 3.3.3.4 it is shown (Table 3.17) that the metal elements investigated (Al, Fe, Cr and Mn) were released into the test liquid during PPGD treatment (Table 3.17). Al was by far the most abundantly released element followed by Fe. During 30 min PPGD treatment at 16 kV and 10 pps, the Al released reached a concentration in the range of 5525-6546 µg/l which was in excess of the drinking water tolerated value of 200 µg/l (European Communities No. 2 Regulations 2007). It has been suggested that the element is released in the form of Al^{2+} and Al^{3+} ions (Kotnik *et al.,* 2001; Lukeš *et al.,* 2006). In recent decades Al has gained a lot of attention as it has been reported that the element is a possible etiological factor in neurological disorders such as Alzheimer's disease (Perl and Brody, 1980;

Harrington *et al.,* 1994) and dialysis encephalopathy (Stakey, 1987; Deloncle and Guillard, 1990). Hence, several *in vitro* studies have investigated the cytotoxic potential of Al compounds on cells derived from the nervous system (Campbell *et al.,* 2001; Ohyashiki *et al.,* 2002; Toimela *et al.,* 2004).

Investigations more comparable to the present study which conducted research on metal ions released from electrodes during electroporation treatments, have shown that Al ions can be freed from the electrodes during electroporation and gain access into mammalian cells in culture, interfering severely with essential biochemical processes and macromolecules such as DNA and proteins (Loomis-Husselbee *et al.,* 1991; Stapulionis, 1999). Moreover, Kotnik *et al.* (2001) investigated the cytotoxic effect of Al and Fe ions on DC-3F hamster fibroblast cells by simulating cellular environment conditions typically observed after electroporation treatments i.e. using a 1 h exposure at room temperature and an ion concentration range of 0–2.5 mM (2.5 mM approximately corresponds to 1.4 x10^5 µg/l Fe and 6.75 x 10^4 µg/l of Al). This study showed that following the 1 h exposure, Fe^{2+} and Fe^{3+} significantly reduced the viability of mammalian cells in culture while Al^{3+} had no effect. It was suggested that biologically active ferrous ions could generate free radicals which in turn attack cellular components (Tomov and Tsoneva, 2000). Compared to the present study, the upper-end ion concentrations used by Kotnik *et al.* (2001) were higher than those determined for HaCaT cells exposure (at the 40% dilution approximately 20 and 2000 times higher for Al and Fe, respectively). However, as a much longer cell exposure time was used in the present study, cytotoxic effects resulting from the metal elements, especially Al, cannot be excluded.

Overall, it is likely that a combined action of reactive species and metal ions resulted in the cytotoxic effects observed on HaCaT cells exposed to PPGD-treated test liquid. Clearly, when exposing cell cultures to vehicles containing a mixture of different substances, toxic responses originating from additive or even synergistic effects cannot be ruled out.

3.3.5.2 Genotoxicity evaluation of PPGD-treated test liquid

As previously outlined in Sections 3.3.3.2 and 3.3.3.3, electrochemical reactions generated by the plasma discharge resulted in the formation of biocidal substances based on reactive

oxygen and nitrogen species and metal ions. In terms of the safety evaluation of the PPGD method, a specific hazard may be associated with such reactive species and/or metal ions as they may possess the ability to alter the genetic material.

During the last two decades numerous investigations have focused on elucidating the DNA damaging mechanisms of several reactive oxygen and nitrogen species (Sandhu and Birnboim, 1997; Yu and Anderson, 1997; Halliwell, 1999; Ohshima, 2003). It has been observed that cell exposure to dissolved ozone leads to a dose-dependent increase in DNA damage (Diaz-Llera *et al.,* 2002; Ito *et al.,* 2005). Furthermore, research conducted by Ito *et al.* (2005) showed that ozone molecules can directly cause DNA base modification. However, it appeared that ozone itself was not fully responsible for the extent of DNA damage observed and it was further suggested that reactions with unsaturated fatty acids and available thiol groups caused the production of reactive intermediaries with H_2O_2 as one of the final products (Diaz-Llera *et al.,* 2002; Ito *et al.,* 2005). This, in turn, traces the DNA damage back to the actions of the OH· radical which is generated from H_2O_2, possibly via the redox cycle properties of transition metals either free or bound to macromolecules such as DNA (Spencer *et al.,* 1995; Diaz-Llera *et al.,* 2002; Ohshima, 2003; Ito *et al.,* 2005).

Several nitrogen oxides have also shown genotoxic and mutagenic potential in *in vitro* tests (Victorin, 1994; Halliwell, 1999; Ohshima, 2003). In contrast to nitrate, *in vitro* studies have revealed the DNA damaging potential of nitrite (Routledge *et al.,* 1994; Spencer *et al.,* 2000; Knaapen *et al.,* 2005). Furthermore, nitrite has been shown to induce base pair substitutions in the Ames assay (Balimandawa *et al.,* 1994). Also, nitrous acid has the potential to induce point mutations by deamination of DNA bases (Victorin, 1994; Oldreive *et al.,* 1998) and cause DNA strand breaks in mammalian cells (Halliwell, 1999).

In addition, metal byproducts released from the electrodes require consideration as they could influence the production of the aforementioned reactive species (e.g. redox cycling) or even directly interact with DNA molecules (Bal and Kasprzak, 2002; Kasprzak, 2002; Moriwaki *et al.,* 2008). During PPGD, Al was the most abundant metal released into the test liquid (Table 3.17) and although it has been shown that Al can induce oxidative stress in mammalian cells (Kaneko *et al.,* 2007), information regarding the genotoxic and mutagenic potential of this element on mammalian cells is scarce.

Therefore, in this study, the DNA damaging and mutagenic potential of the treatment liquid was investigated using the comet and Ames assays respectively. Before initiating the comet assay procedure, subcytotoxic concentrations of both O_2 and N_2 discharge-treated test liquid were determined via the trypan blue exclusion method (viability ≥80%). The test liquid was then directly exposed to the HaCaT cells for 12 h at 37^{o}C. To ensure optimal assay conditions 100 μM H_2O_2 was also used as a positive control. Again, the assay was conducted on duplicate slides with 50 single cells scored per slide.

The potential of the PPGD-treated test liquid to induce nucleotide point mutations in the Ames assay was also tested using concentrations predetermined not to be biocidal to the test bacteria (as previously outlined for the prescreen test described in Section 2.5.21). As recommended by the assay manufacturer, the exposure was conducted for 90 min using approximately 10^7 bacteria cells thus allowing for two cell divisions and the assay was performed in the presence and absence of liver S9 fraction to account for bioactive metabolites. The average number of wells containing revertants, as indicated by a change in the colour of the indicator medium, was then calculated. Positive control chemicals (in the absence of S9: 4-NQO:NF 500:2000 ηg/ml; in the presence of S9: 2-AmAn 125 μg/ml) were used to ensure optimal assay conditions.

Figure 3.60 and Table 3.22 show the results obtained via the comet assay following HaCaT cell exposure to both O_2 and N_2 PPGD-treated test liquid. The box plots shown in Figure 3.60a indicate that, compared to the untreated control, none of the test sample concentrations composed of O_2 discharge-treated liquid caused significantly elevated percentage tail DNA values. A reduced median and 75 percentile for the percentage DNA distribution was obtained for the highest tested O_2-mediated discharge concentration (20%). However, an increased amount of outliers was obtained for this concentration which may be indicative of cytotoxic effects. The general trend observed in Figure 3.60a is further reflected in Table 3.14 where the entire concentration range of O_2 discharge-treated test liquid displayed DNA migration values which did not significantly differ from untreated control values. Interestingly, Table 3.22 reveals a dose-dependent but not significant increase in tail moment values obtained.

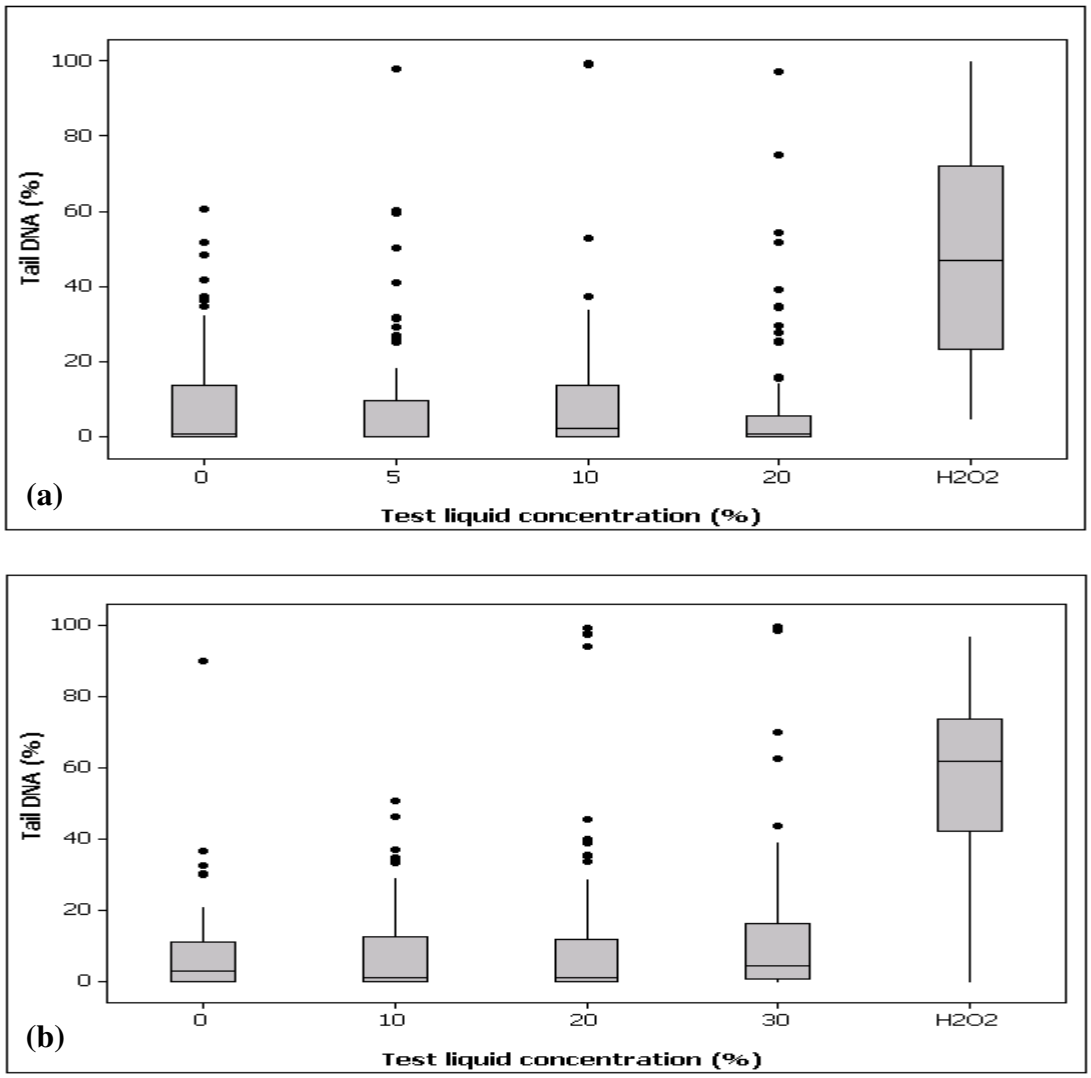

Figure 3.60: Box plot presentation of percentage tail DNA obtained following HaCaT cell exposure to increasing concentrations of (a) O_2- and (b) N_2-mediated PPGD-treated test liquid (12 h at 37^{o}C) and 100 µM H_2O_2 (40 min at 4^{o}C). Each box corresponds to 100 comets measured on two slides and represents 25-75 percentiles, middle line = median, whisker extends to the maximum/minimum data point within 1.5 box heights from the top/bottom of the box. Dots above and below boxes indicate outliers. * denotes a significant difference from the control ($p<0.05$).

Table 3.22: Tail moment and percentage tail DNA obtained in the comet assay after exposure of HaCaT cells to increasing concentrations of PPGD-treated test liquid for 12 h and 100 µM of H_2O_2 for 40 min. Results shown are the means (±SEM) of 100 single cells from duplicate slides. * denotes a significant difference from the untreated (0%) control ($p<0.05$).

Conc. test liquid (%)	O_2 discharge Tail moment (±SEM)	O_2 discharge % Tail DNA (±SEM)	N_2 discharge Tail moment (±SEM)	N_2 discharge % Tail DNA (±SEM)
0	1.07 (±0.23)	8.49 (±1.35)	1.22 (±0.26)	7.13 (±1.22)
5	1.05 (±0.20)	10.17(±1.97)	---	---
10	1.35 (±0.33)	9.40 (±1.65)	0.81 (±0.11)	7.81 (±1.12)
20	1.66 (±0.44)	8.51 (±2.03)	1.36 (±0.35)	10.29 (±2.07)
30	---	---	1.98 (±0.47)	11.73 (±1.83)
H_2O_2				
100 µM	14.47 (±0.93)*	67.54 (±2.67)*	19.06 (±1.25.)*	55.77 (±2.31)*

Similar results were obtained following comet assay experiments using N_2 discharge-treated liquids (Figure 3.60b and Table 3.22). Again, the percentage tail DNA values obtained following exposure did not significantly differ from the untreated control values (Table 3.14). However, Figure 3.60b does reveal that the highest liquid concentration (30%) caused a slightly elevated percentage tail DNA median and 75 percentile compared to the lower concentrations and the negative control. This effect was also illustrated in Table 3.22 where again a dose-dependent but not significant increase in the mean tail moment values were observable, with the highest tail moment value obtained for the 30% test liquid dilution (1.98).

The positive control (100 µM H_2O_2) produced the expected response. Here, a 40 min exposure at 4°C resulted in significantly ($p<0.05$) elevated DNA migration values with mean percentage tail DNA and tail moment values being approximately 8 times and 13-20 times higher that the respective values obtained for untreated control cells (Table 3.22).

Interestingly, the reactive oxygen and nitrogen species and metal ions generated by the PPGD did not yield significantly elevated DNA migration values in the comet assay. Noticing the amount of outliers shown in Figure 3.60, it appears that the dose-dependent but insignificant increase in tail moment value is a result of cytotoxic effects to single cells (as discussed in Section 3.1.5.1) rather than a direct adverse effect on the cells genetic material. It appears that the level of reactive species was too low to cause a detectable

insult on the HaCaT cells' DNA. A comet assay study conducted by Diaz-Llera *et al.* (2002) showed that a dissolved ozone concentration of 42 mg/ml incubated for 1 h was required to induce detectable DNA damage on human leukocytes in culture. However, in the current study, the level of dissolved ozone generated by the PPGD within 30 min of treatment did not exceed 1 mg/ml. An investigation conducted by Spencer *et al.* (2000) observed significant DNA strand breakage upon treating human respiratory tract cells in culture with 46 mg/l nitrite at exposure times exceeding 60 min. Within the present study, potentially harmful nitrite concentrations above 27 mg/ml could be generated following prolonged PPGD treatment at high energetic discharge conditions. Additionally, it needs to be mentioned that constitutes of culture medium may act as free radical scavengers thus influencing the outcome of the *in vitro* assays used.

Table 3.23: Mean values of positive wells (±SEM) obtained from three experiments in the Ames mutagenicity assay following 90 min exposure to increasing concentrations of PPGD-treated test liquids and positive controls (±S9). * denotes a significant difference from the untreated (0%) control ($p<0.05$).

Conc. test liquid (%)	**TA98 (±SEM)**		**TAMix (±SEM)**	
	-S9	**+S9**	**-S9**	**+S9**
O_2 discharge treatment (direct)				
0	1.50 (±0.43)	1.00 (±0.00)	1.80 (±0.88)	1.33 (±0.30)
35	1.67 (±0.33)	1.33 (±0.33)	2.67 (±0.33)	1.33 (±0.88)
45	1.67 (±0.33)	0.67 (±0.33)	3.33 (±0.88)*	1.33 (±0.33)
55	2.00 (±0.58)	1.00 (±0.58)	9.00 (±2.47)*	2.00 (±0.58)
65	2.33 (±0.88)	1.33 (±0.88)	8.33 (±1.45)*	1.67 (±0.66)
Positive control	48.00 (±0.00)*	39.00 (±1.15)*	48.00 (±0.00)*	41.67 (±1.20)*
O_2 discharge treatment (after 7 days)				
0	1.50 (±0.61)	1.33 (±0.33)	1.67 (±0.33)	2.00 (±0.58)
35	1.67 (±0.88)	1.67 (±0.66)	2.00 (±0.00)	1.33 (±0.33)
45	0.67(±0.66)	1.67 (±0.33)	2.33 (±0.33)	0.67 (±0.66)
55	1.00 (±0.58)	1.00 (±0.58)	1.67 (±0.88)	0.67 (±0.33)
65	1.33 (±0.88)	2.33 (±0.66)	2.67 (±0.58)	1.00 (±0.00)
Positive control	47.00 (±0.88)*	36.00 (±3.05)*	48.00 (±0.00)*	34.00 (±2.30)*
N_2 discharge treatment (direct)				
0	2.33 (±0.66)	0.67 (±0.30)	1.67 (±0.88)	1.67 (±0.33)
35	2.67 (±0.88)	0.33 (±0.33)	0.00 (±0.00)	2.00 (±0.58)
45	2.00 (±0.58)	1.67 (±0.88)	1.00 (±0.58)	1.67 (±0.88)
55	1.67 (±0.66)	1.00 (±1.00)	1.67 (±0.66)	1.33 (±0.33)
65	4.00 (±0.58)	1.33 (±0.33)	0.67 (±0.66)	2.00 (±0.00)
Positive control	41.33 (±3.48)*	36.33 (±2.03)*	48.00 (±0.00)*	40.00 (±2.08)*

Table 3.23 shows the results obtained via the Ames test, expressed as mean values of positive wells. The majority of samples tested had no mutagenic activity when compared to the positive controls. However, a weak but significant ($p<0.05$) mutagenic response was detected for the TAmix strain exposed O_2 discharge-treated samples at concentrations between 45% and 65%, but only in the absence of S9 and only for PPGD-treated test liquid samples evaluated directly after PPGD treatment (Table 3.15). Interestingly, the mutagenicity disappeared when the strain exposure was performed following a 7 day preincubation of the sample at room temperature.

The positive control chemicals produced the expected mutagenic response comparable to previously conducted Ames assays in Sections 3.1.5.2 and 3.2.5.2.

No increased reversion frequencies were detected following exposure of N_2 discharge-treated test liquid to any of the *S. Typhimurium* Ames test strains. In contrast, O_2 discharge-treated test liquid caused a positive result in the Ames assay via the induction of missense mutations (TAmix) in the absence of S9. In this instance, the observed increase in reversion frequency was not very high thus implying weak mutagenicity. It is believed that the mutagenic effect may be introduced by the formation of dissolved ozone. This assumption is strengthened by the negative results obtained for strain exposure to O_2 discharge-treated test liquid which was tested following a 7 day incubation period to allow for ozone decay.

The negative results seen with the addition of S9 may be related to a possible detoxifying action of the liver homogenate on reactive oxygen species. Partially comparable, an Ames test by Monarca *et al.* (2000) demonstrated the mutagenic potential of dissolved ozone at a concentration of 3 mg/l.

Since this is one of the first studies to evaluate the toxicological aspects of PPGD, little directly comparable data is readily available. However, two independent studies by Reyns *et al.* (2004) and Gusbeth *et al.* (2009) evaluated the DNA damaging potential of aqueous solutions after antimicrobial PEF treatment. Gusbeth *et al.* (2009) concluded that PEF treatment used under biocidal conditions did not induce genotoxic or mutagenic byproducts in PBS buffer solutions and tap water. On the other hand, Reyns *et al.* (2004) observed a mutagenic effect of PEF-treated PBS buffer (TA97 and TA102 strains) and grape juice (TA102 and TA104 strains) via the Ames assay. It was suggested that the

genetic insult was caused by reactive oxygen species generated during electrolytic processes.

3.3.6 Summary

Important electrical and antimicrobial aspects of the PPGD system were investigated to gain a valuable insight into the optimum PPGD conditions required for effective sterilisation of chemical hydrogels. The HV discharge was directed above a set volume (100 ml) of aqueous solution which serves as a protective inactivation medium for the treatment of hydrogels. A multi-needle electrode configuration was used to create the discharge into O_2 and N_2 gases. The pulsed plasma created was found to be a streamer type corona discharge and electrical measurements suggested a stable and reproducible pulse waveform. Depending on the discharge conditions employed, the internal elements of the PPGD were subject to material wear, and maintenance was required after prolonged usage. In order to minimise the extent of the maintenance required, it was decided to utilise the system at settings not exceeding a PFN charge of 18 kV and a pulse repetition rate of 12.5 pps. Initial physicochemical examinations of the discharge-treated test liquid helped to elucidate mechanisms involved in microbial inactivation. Although this microbial inactivation method was designed to be nonthermal, a temperature increase of the test liquid was observed with an increase in applied voltage and pulse frequency. Furthermore, an increase in conductivity of the treatment liquid was evident after O_2- and N_2-mediated discharges. The action of plasma discharges resulted in an alteration of the pH value of the treatment fluid depending on which gas was used to facilitate the discharge. Oxygen discharge increased the pH ($\leq$8.58) while the use of nitrogen as a discharge gas resulted in a rapid pH drop to acidic levels ($\geq$3.21). These findings suggested that the plasma discharge resulted in the generation of active chemical species which dissolved in the treated liquid and in turn caused the aforementioned chemical changes. Thus, further studies were undertaken to detect the presence of biocidal chemical species which are generally associated with plasma discharge processes. It was shown that the HV discharges had the potential to dissociate O_2 and N_2 molecules and to form active species which entered the test liquid. The presence of dissolved ozone was detected and quantified in the test liquid after O_2-mediated discharges and it was suggested that this compound was

accompanied by several other reactive oxygen species such as H_2O_2, OH· and $O_2^{\bullet -}$. IEC was used to detect and quantify the presence of dissolved NO_2^- and NO_3^- after N_2-mediated discharges. It was suggested that these reactive nitrogen species originated from dissociated nitric and nitrous acids which in turn were thought responsible for the observed drop in pH.

The degradation of electrode material was visually observed throughout the investigation. More specifically, the stainless steel discharge needles of the HV electrode were subjected to erosion events and needed to be exchanged after prolonged use. Moreover, extended PPGD treatment resulted in the formation of deposits on the lower Al earthed electrode which were possibly composed of oxidised Al and residual salt from the treatment liquid. Following these observations, it was necessary to investigate if electrode degradation products were released into the treatment liquid. Chemical analysis of the test liquid proved that the concentration of all metal elements investigated (Al, Fe, Cr, Mn) increased with increasing PPGD treatment. Most concerning was the amount of Al released into the test liquid following 30 min of treatment which was found to be more than 30 times the tolerated value for EU drinking water.

Initial microbial inactivation studies were conducted using Gram negative *E. coli* and Gram positive *S. aureus* as indicator organisms. To investigate the antimicrobial performance of the PPGD system under extreme conditions, a high cell density of the organisms (1×10^7 cfu/ml) was prepared in 100 ml of the treatment liquid and subsequently treated under various discharge conditions. The microbial reduction rate was examined by varying the electrical parameters such as PFN charging voltages (14-18 kV) and pulse repetition rates (7.5-12.5 pps) in conjunction with varying flow rates of O_2 and N_2 gas (1-5 l/min). Over the 30 min treatment time, it was observed that the rate of microbial inactivation was directly dependent on the electrical settings. The higher the PFN charge and the pulse repetition rate, the faster the destruction of the test bacteria. In general, the Gram negative *E. coli* appeared more susceptible to the lethal effects of the discharge than the Gram positive *S. aureus*. Additionally, O_2-mediated discharge proved more efficient towards the destruction of bacteria than N_2 gas, although no noteworthy difference was observed while using varying gas flow rates. Complete inactivation ($\geq$7 log-order) of both organisms was achieved for treatments using high-end discharge conditions. The lowest microbial reduction at the end of the 30 min treatment was found to be of a 3.12 log-order

for *S. aureus* subjected to an applied charging voltage of 14 kV and 10 pps using N_2 discharge. Although the microbial destruction evoked during PPGD processes is a result of various biocidal effects, it was suggested that dissolved active chemical species could play a major role.

A preliminary toxicological evaluation of PPGD-treated test liquids showed that the electrochemical processes involved in the formation of electrode degradation products and antimicrobial reactive species also led to the induction of considerable cytotoxicity to HaCaT mammalian cells in culture. The cytotoxic potential was reduced by a 7 day preincubation step as it allowed reactive species such as ozone to decay into less harmful products. No significant DNA damaging effects were observed via the comet assay. However, a weak mutagenic response was detected in the Ames assay following direct exposure of O_2 discharge-treated test liquid to TAmix strains without S9 mix. This mutagenic effect disappeared by introducing the 7 day preincubation step prior to exposure thus indicating the dissipation of reactive species.

3.4 Microbial inactivation of hydrogels using the PPGD method and its impact on physicochemical characteristics and biocompatibility

3.4.1 Preface

The limitations of conventional sterilisation methods relating to temperature sensitive hydrogels have prompted the search for more suitable sterilisation techniques (Stoy, 1999; Jiménez *et al.,* 2008). Several alternative methods for the microbial decontamination of hydrogels have been investigated. A study conducted by Huebsch *et al.* (2005) examined the possibility of sterilising *N*-isopropylacrylamide hydrogels with UV-radiation. Despite prolonged treatment times (up to 15 h), this method proved unsuccessful as it could not prevent regrowth of microorganisms and furthermore caused progressive degradation of the polymer molecules. Elijarra-Binstock *et al.* (2007) examined the effect of gamma radiation, EtO and autoclave sterilisation on hydrogel sponges of hydroxyethyl methacrylate crosslinked with EGDMA and showed that all of the investigated sterilisation techniques influenced the hydrogels mechanical properties, with gamma radiation and EtO being more appropriate than autoclaving, as the latter method was unsuitable for hydrogels with EWC above 70%. Calvet *et al.* (2008) investigated the effect of gamma radiation and H_2O_2 plasma sterilisation (Sterrad® 100S) on poly(ethylene glycol) (PEG) based hydrogels. Both techniques led to a slight oxidation of the polymer, however, the H_2O_2 plasma sterilisation approach was found to be more convenient throughout this investigation. A similar study evaluated the effect of EtO, H_2O_2 plasma (Sterrad®100S), and gamma sterilisation on PEG based hydrogels (Kanjickal *et al.,* 2008). Here, the three sterilisation methods studied had varying degrees of success on the PEG hydrogels and it was believed that the formation of free radicals influenced the gels properties. The EtO and gamma sterilisation led to the introduction of increased crosslinking whereas the H_2O_2 plasma method broke down crosslinks within the polymer. Jiménez *et al.* (2008) evaluated a novel high pressure CO_2-based cold sterilisation process on a poly(acrylic acid-acrylamid) based hydrogel. Although this technique proved suitable for the inactivation of test bacteria without influencing the gels physicochemical properties, a long treatment time exceeding 4 h was required.

To-date no literature exists regarding the use of PPGD for the sterilisation of hydrogels. Therefore, the remaining focus of this study was to investigate the efficacy and

safety of the novel PPGD system for 'low temperature' sterilisation of hydrogels. Based on the findings discussed in the previous sections, the hydrogel treatment was conducted at optimised treatment settings with a PFN charging voltage of 16 kV, a pulse frequency of 10 pps and a gas flow rate of 2.5 l/min. The treatment included O_2- and N_2-mediated discharges on representative samples of fully hydrated chemical 75-25xP hydrogels. During treatment the samples were completely submerged in aqueous test liquid. This protected the hydrogels from the deleterious effects associated with direct exposure to the corona discharge but allowed the gels to access any antimicrobial species formed in the test liquid. The antimicrobial efficacy of the method was verified by contaminating the samples with *E. coli* and *S. aureus* prior to treatment. Furthermore, the impact of the PPGD treatment on the gels' mechanical properties was evaluated using oscillatory plate rheometry, compressive failure analysis and surface analysis. Finally, the biocompatibility of the PPGD-treated samples was also investigated.

3.4.2 PPGD-mediated inactivation of microorganisms preloaded onto hydrogels

The following study was employed to evaluate the suitability of the PPGD method for the microbial decontamination of chemical hydrogels. The purified 75-25xP hydrogel type was chosen as a representative sample due to its favourable mechanical qualities and satisfactory *in vitro* biocompatibility. The microbial inoculation was accomplished by submerging the hydrogel samples in a PBS solution containing either *E. coli* or *S. aureus* organisms for 90 min at a cell density of approximately 1 x 10^9 cfu/ml. Following inoculation, unbound bacteria were recovered as per Section 2.9.3 and the hydrogels were submerged in PPGD-treated test liquid adjusted to obtain a final treatment volume of 100 ml. The PPGD treatment was conducted using optimised electrical conditions (16 kV, 10 pps) with O_2 and N_2 used as discharge gases at a flow rate of 2.5 l/min. The microbial recovery and subsequent enumerations were obtained at 4 min treatment intervals before and during the process. Microbial survivors were expressed in terms of $\log_{10}$ cfu/cm^2 while the inactivation rate constant k was calculated using the Chick-Watson model of microbial inactivation (Section 2.7.3 Equation 2.5). All studies were carried out in duplicate with duplicate plates for each set of exposures. The results obtained from the PPGD treatment of

microbial contaminated hydrogels are shown in Figure 3.61 and respective *k* values are given in Table 3.24.

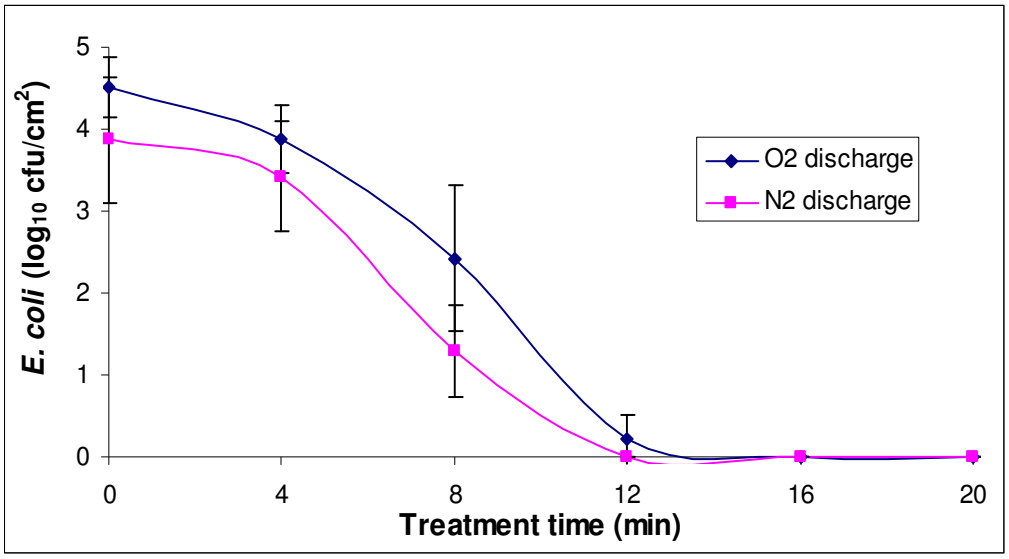

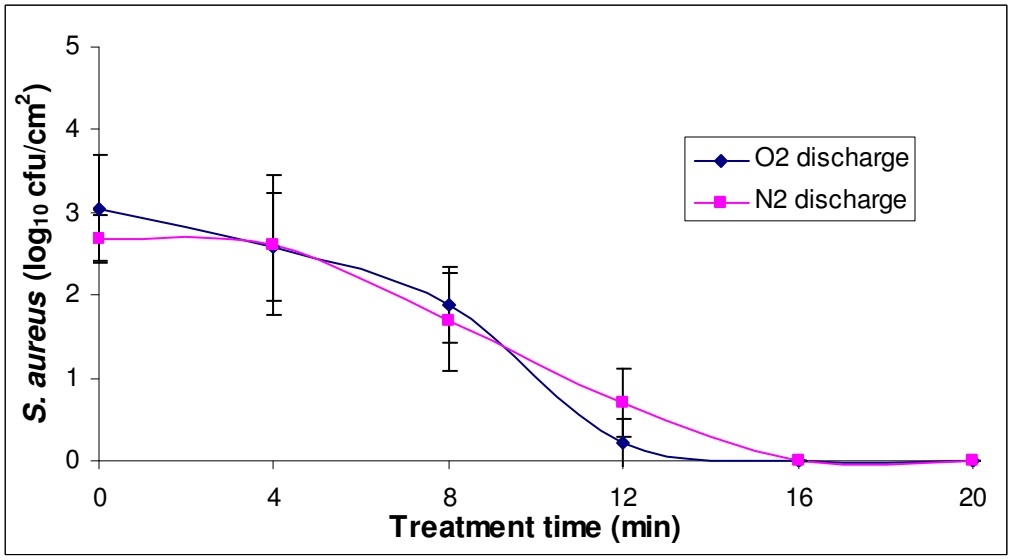

Figure 3.61: The antimicrobial effect of PPGD on 75-25xP hydrogels inoculated with (a) *E. coli* and (b) *S. aureus*. Results are the mean of two replicates (±SD) with PPGD performed at a constant PFN charge of 16 kV and a pulse frequency of 10 pps. O_2 and N_2 was injected at a flow rate of 2.5 l/min.

Table 3.24: Inactivation rate constant *k* values obtained from PPGD treatment of *E. coli* and *S. aureus* inoculated hydrogels. Results are the mean of two replicates (±SD) with PPGD performed at a constant PFN charge of 16 kV and a pulse frequency of 10 pps. O_2 and N_2 were injected at a flow rate of 2.5 l/min.

Test Strain	Inactivation rate constant *k* for PPGD-treated hydrogels	
	O_2 discharge-treated	N_2 discharge-treated
E. coli	0.0697 (±0.0014)	0.0725 (±0.0010)
S. aureus	0.0750 (±0.0055)	0.0759 (±0.0033)

Figure 3.61 reveals that PPGD treatment was effective at inactivating microorganisms on the surface of the hydrogels. Both *E. coli* and *S. aureus* were completely inactivated within 12-16 min of treatment. Following inoculation, a significantly ($p<0.05$) greater cell attachment was observed with the *E. coli* bacterium which in turn led to higher log-order reduction for this organism. More specifically, the microbial log-order reduction values obtained for *E. coli* were 4.51 and 3.87 cfu/cm^2 while the reduction values for *S. aureus* were 3.05 and 2.69 cfu/cm^2 for O_2- and N_2 -mediated gas-discharges, respectively. Although higher log reduction values were observed for O_2-mediated discharge than for those using N_2 as treatment gas, no conclusive statistical analysis was obtainable due to variations in attached cell numbers at the start of the treatment. Furthermore, no significant difference could be determined for the obtained *k* inactivation rates which were found to be in the range of 0.0697-0.0759.

Bacterial adhesion to the hydrogel surface, facilitated during the inoculation step, was dependent on the microbial organism used. The Gram negative *E. coli* showed a higher affinity of attachment to the hydrogel surface and this is possibly related to the net surface charge and hydrophilicity of the hydrated polymer (Reid and Busscher, 1992; Andrews *et al.,* 2001). This effect, in conjunction with an overall low degree of reproducibility, made an objective comparison of the achieved microbial reduction between the two different test strains difficult. Nevertheless, the PPGD treatment led to a rapid and complete inactivation of microorganisms as observed via the spread plate method. Within a treatment time of 16 min no culturable bacteria could be recovered from the hydrogels. Also, the test liquid appeared free from viable test organisms. The inactivation profiles were somewhat similar to those obtained in Section 3.3.4, with an almost linear decrease in the number of active microbial cells with increased treatment time. Interestingly, a more pronounced shoulder

effect was observed for treatments conducted on *S. aureus*. This effect resulted in higher *k* values for this organism compared to *E. coli* due to the fact that these values were based on linear parts of the inactivation profile. As previously mentioned, different phenomena associated with the PPGD, such as reactive species, PEF, UV-radiation and pressure shockwaves, were responsible for the microbial destruction (Anapilov *et al.,* 2001; Marsili *et al.,* 2001; Satoh *et al.,* 2007). Again, the exact mechanism of microbial inactivation during PPGD treatment could not be elucidated. However, temperature effects were not considered to have contributed to microbial cell death, as the temperature of the test liquid did not exceed 36^{o}C for the PPGD treatment parameters used in the current section.

A thorough review suggested that no previous studies investigated the use of PPGD directed towards liquids as a potential sterilisation technique for biomaterials or other medical devices. Therefore, a direct comparison of the findings with existing studies was not possible. However, direct exposure to H_2O_2 gas-mediated low pressure glow discharge plasma was recently used for microbial decontamination of hydrogels (Calvet *et al.,* 2008; Kanjickal *et al.,* 2008). In these studies the commercially available and by the Food and Drug Administration (FDA) approved plasma steriliser Sterrad® 100S was found to be effective for the sterilisation of hydrogels. Nevertheless, as this method was based on the exposure of bacterial cells to reactive oxygen species in their gaseous form, the induction of adverse material changes could not be excluded (Calvet *et al.,* 2008; Kanjickal *et al.,* 2008).

3.4.3 The impact of PPGD treatment on the material properties of hydrogels

When employing a novel method for the microbial decontamination of materials intended for the medical field it is of utmost importance to evaluate its impact on the materials' properties. Evidently, the treatment process must be compatible with the device so that its functionality is not significantly compromised. The PPGD mechanism associated with inactivation of microbes can potentially impact the hydrogel surface or even its mechanical properties. The reactive chemical species generated during the discharge could affect the gel's surface and even diffuse into the gel matrix. Research has shown that exposure to reactive species generated in plasmas can affect polymers via events such as surface ablation or etching, crosslinking and the introduction of functional groups e.g. hydroxyl or

carbonyl groups (Wang *et al.,* 2008; Hu and Chen, 2009). Additionally, the fragile network of swollen hydrogels may be negatively affected by exposure to PEF and high pressure shockwaves.

A mechanical analysis composed of oscillatory plate rheology and compressive failure analysis was conducted to evaluate the impact of the PPGD system on the hydrogels' material properties as similar approaches have been previously used to detect material changes in medical polymers post-sterilisation (Elijarrat-Binstock *et al.,* 2007; Yakacki *et al.,* 2008). Furthermore, the surface topography was evaluated via ScEM. The hydrogels were subjected to O_2- and N_2-mediated PPGD under optimised electrical settings (16 kV charging voltage, 10 pps, and a gas flow rate of 2.5 l/min). Although a 16 min treatment proved sufficient for the microbial decontamination of highly contaminated hydrogels, a 30 min treatment was chosen for subsequent mechanical testing to allow for extreme treatment conditions.

3.4.3.1 Mechanical testing

Oscillatory plate rheology and compressive failure analysis were carried out on PPGD-treated hydrogel samples in accordance with the method previously discussed in Section 3.2.3.4. The results were compared to untreated hydrogels. Figure 3.62 illustrates the G' obtained during the rheological study, while Figure 3.63 shows the compressive failure data achieved for compression analysis.

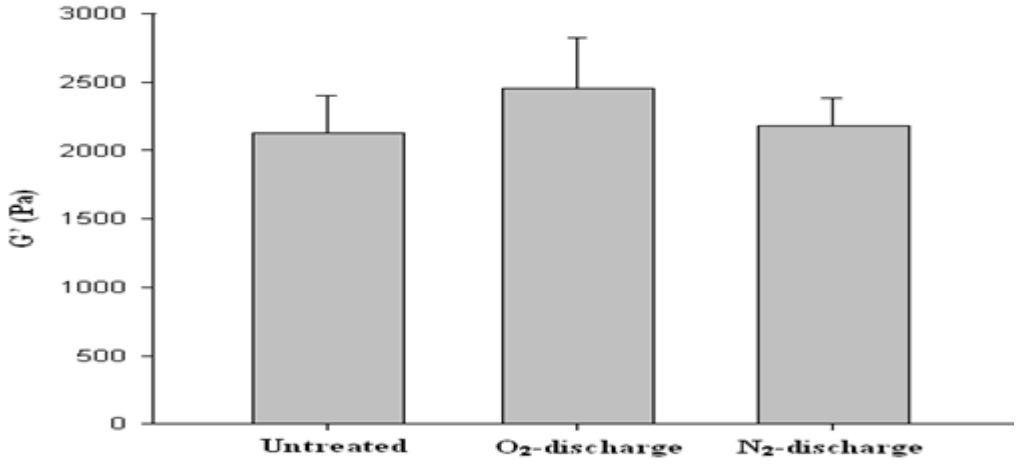

Figure 3.62: Storage modulus values of untreated and PPGD-treated 75-25xP hydrogels.

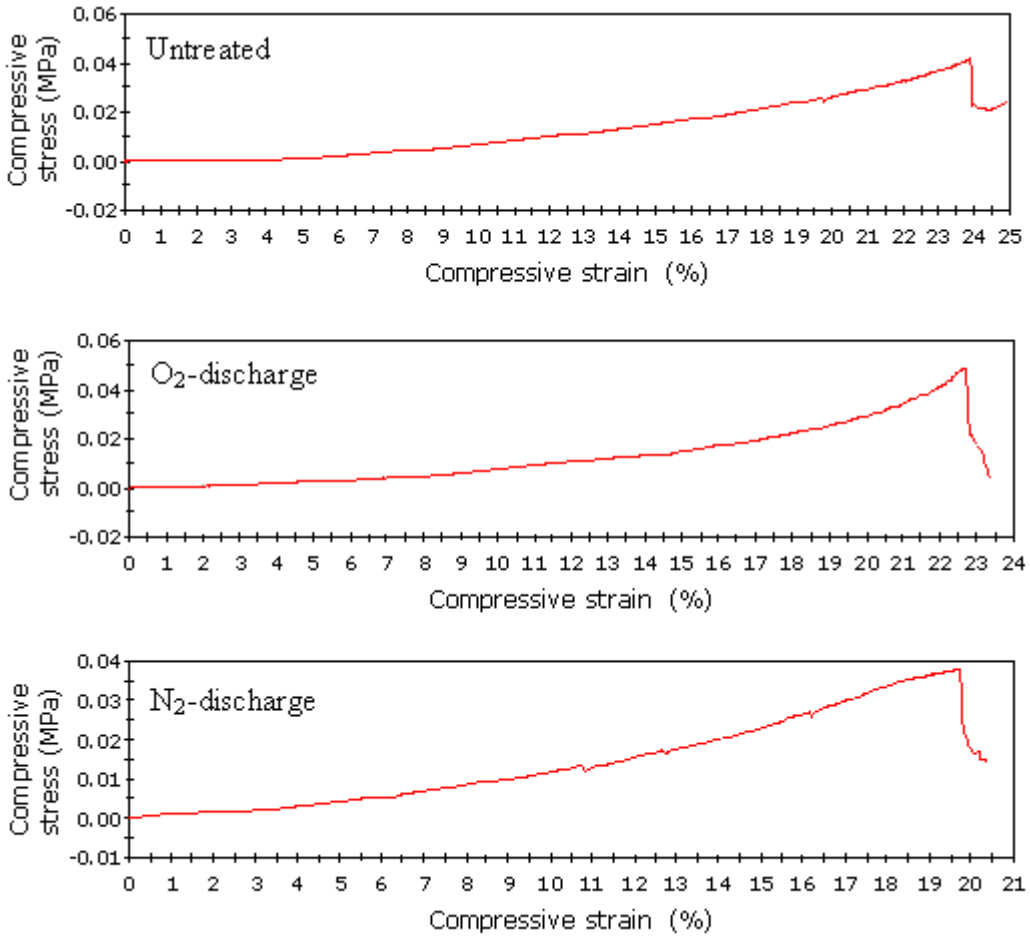

Figure 3.63: Results obtained during compression testing of PPGD-treated chemical hydrogels.

During the rheological analysis respective G' values of 2456 and 2177 Pa were obtained for O_2 and N_2 discharge-treated 75-25xP hydrogels, while the untreated sample reached a G' value of 2129 Pa (Figure 3.62). Compared to the untreated control, the G' values obtained from PPGD appeared slightly elevated; however, no statistical difference was determined between the three samples.

As shown in Figure 3.63, for each of the samples tested, the percentage compressive strain increased with increasing compressive stress load. The compressive strain values, indicative for sample deformation, were found in the narrow range of 19.8 to 23.3 % for all samples tested. After being subjected to similar compressive forces, the samples began to deform rapidly. More specifically, the obtained critical compressive

stress values were 0.0409 MPa for the untreated 75-25xP hydrogel, while values of 0.0482 and 0.0387 were obtained for O_2 and N_2 discharge-treated samples, respectively.

The mechanical testing approach employed for assessing the impact of PPGD treatment on a representative hydrogel sample did not reveal any adverse changes in the bulk properties of the gels. The PPGD exposure had no significant effect on the hydrogel strength as observed via the oscillatory plate rheology and compressive failure analysis. The test liquid protected the submerged samples from the thermal effects of the discharge, while exposure to PEF and shockwaves, mediated through the liquid, did not affect the gel strength. Although the presence of reactive chemical species was previously determined in the test liquid for both O_2- and N_2-mediated discharges, they did not induce a detectable weakening effect on the polymer. However, this could be due to the fact that the active compounds were not able to diffuse into the matrix but rather reacted with the gels' surface. In this context, recent investigations proved that direct exposure to H_2O_2 plasma using the Sterrad® 100S sterilisation method can alter the surface properties of hydrogels. Kanjickal *et al.* (2007) noticed a decrease in surface roughness and an elevated presence of peroxy radicals post-plasma treatment, while surface observations conducted by Calvet *et al.* (2008) showed a reduction in total oxygen content but a notable increase in carboxylic groups. To determine whether the PPGD treatment had a visual effect on the surface of the hydrogels, ScEM analysis was used in the current study.

3.4.3.2 Surface topography analysis

Being the point of cell-tissue interaction, the surface of a biomaterial is a critical determinant for its biocompatibility. It is commonly recognised that surface attributes, such as chemistry and topography, strongly dictate and influence the biological reaction to materials in contact with living tissue. On the other hand, the biological performance of a material can be modified following a degradation of its surface (LaBerge, 1998). It has been shown that direct plasma exposure to polymeric surfaces, including those of hydrogels, can cause alteration to surface properties and topography (Kanjickal *et al.*, 2007; Calvet *et al.,* 2008; Liu *et al.,* 2009). Although hydrogels treated in the present study were protected from the direct plasma discharge by the test liquid, a degradation of the surface resulting from mechanical or chemical insults imposed by the treatment cannot be

excluded. In the present study, ScEM was used to evaluate the impact of PPGD treatment on the gel's surface topography as this technique has proven to be a valuable tool for determining changes in the surface and texture of polymeric materials post-sterilisation (Lerouge *et al.,* 2002; Lee *et al.,* 2008; Cottam *et al.,* 2009; Nardo *et al.,* 2009). Topographical images obtained by ScEM provide much more information than light microscopy because of its better resolution, greater depth of field, and absence of light scattering from the surface (Lacefield and Clare, 1998). Optimally, such a surface analysis should be performed on samples which are preserved in the same state as used during their application. However, due to their high EWC and resulting delicate mechanical properties, it was not possible to analyse the hydrogel samples via ScEM in their hydrated state. To allow for analysis the samples had to be dehydrated post-PPGD treatment. This introduced structural alterations by folding the surface thus making an objective evaluation difficult.

Figure 3.64 shows ScEM micrographs obtained from untreated and O_2 discharge-treated hydrogels in their dehydrated form (xerogels). No structural changes were seen in the surface topography post-PPGD treatment as determined via the ScEM images. At the lower magnification (a and c) both of the gel surfaces appeared wrinkled and folded. At higher magnifications the surface topography revealed crater-like formations. Again, these formations were seen on the untreated and O_2 discharge-treated xerogels, thus they were not believed to be indicative of PPGD induced surface degradation.

Although reactive chemical species were generated during the PPGD which may have the potential to react with the polymer surface, it was not possible to visualise any structural defects via the ScEM surface analysis, however, the folds induced during dehydration of the hydrogels made it difficult to conduct an objective evaluation of the images. Nevertheless, conclusive surface topography studies using atomic force microscopy have been conducted to determine the impact of H_2O_2 plasma sterilisation on dehydrated hydrogels (Kanjackal *et al.,* 2008). In this study a significant increase in surface roughness was detected following the sterilisation treatment. It was suggested that this effect was caused by reactive species which induced chain cleavage of polymer molecules expressed at the gel surface. Furthermore, a ScEM study by Lerouge *et al.* (2002) showed that plasma-based sterilisation techniques (Sterrad® 100S and Plazlyte™) caused drastic changes to the surface appearance of polymeric medical devices.

Untreated 75-25xP

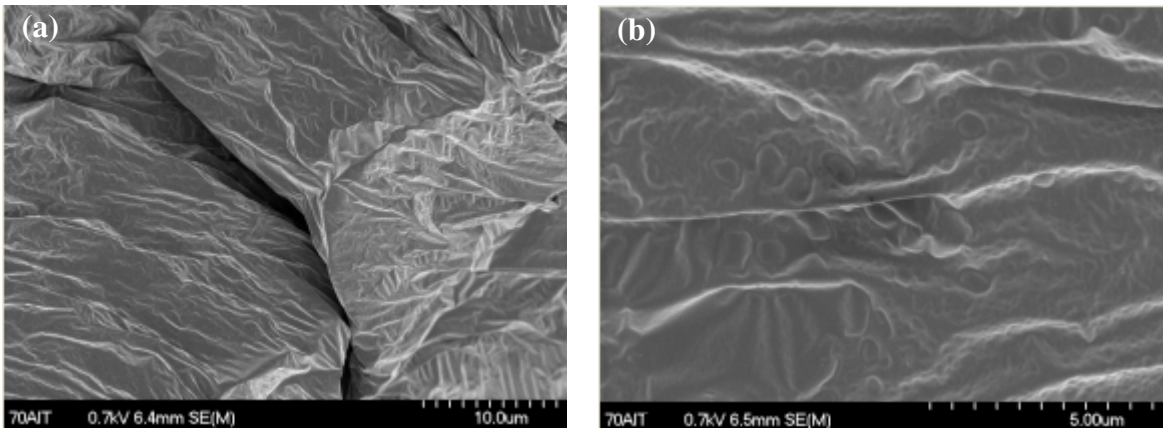

O_2 discharge-treated 75-25xP

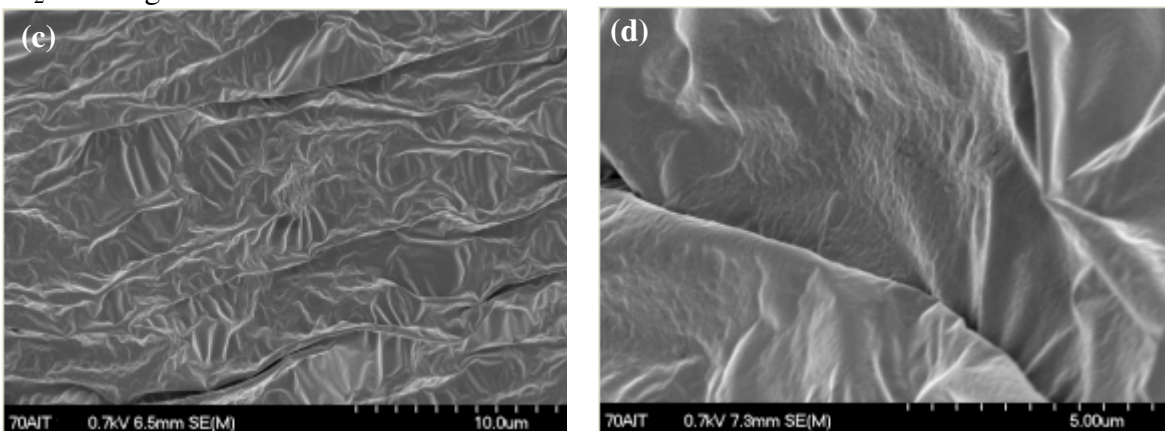

Figure 3.64: ScEM micrographs of (a and b) untreated xerogels and (c and d) O_2 discharge-treated xerogels.

For the present study, however, more information relating to the hydrogels' surface state was required to fully elucidate the effect of PPGD as it appears that a single technique may not be adequate for complete surface characterisation. Although a wide variety of analytical methods for the surface characterisation of polymeric biomaterials are available, few techniques are able to provide surface data that is of direct relevance to the biological application of the material. Most methods including ScEM operate in high vacuum and are therefore of limited relevance to the biomaterial's application. Thus, it appears that besides the employment of multiple techniques, the obtained data must be extrapolated from the analytical environment in order to generate valuable surface characterisation.

3.4.4 PPGD effects on hydrogel biocompatibility

In addition to verifying the antimicrobial efficacy of the PPGD method, it is of critical importance to evaluate whether the treatment introduced substances or modified the hydrogels in such a way that their biocompatibility may be compromised. It was shown in previous sections that reactive species formed in the test liquid post-PPGD treatment which can also adversely affect cell structure and function (Figures 3.58 and 3.59). Indeed, such reactive species can potentially enter the hydrophilic gel matrix, thereby causing the material to become incompatible with biological systems. Furthermore, the introduction of dangerous chemical alterations into the polymer network cannot be excluded. Thus, the biological safety of the hydrogels was re-evaluated after PPGD treatment. More specifically, the cytotoxicity and genotoxicity of a representative hydrogel sample (75-25xP) was determined following 30 min PPGD exposure at optimised electrical settings (16 kV charging voltage, 10 pps, and a gas flow rate of 2.5 l/min). Although the PPGD method is expected to inactivate microbial contamination on hydrogel surfaces in a much shorter exposure time (Section 3.4.2), a 30 min PPGD exposure was chosen for the toxicological impact assessment as to account for extreme microbial contamination by stress hardened and spore forming organisms. For comparative purposes O_2- and N_2-mediated discharge treatments were utilised as they led to the formation of different species within the test liquid. Following treatment, the hydrogels were rinsed with sterile PBS to remove excess test liquid. Test extracts were prepared by incubating the samples in 15 ml of culture medium or Ames exposure medium for 3 days at 37^{o}C and 125 rpm agitation. An untreated hydrogel was also prepared and provided control extracts.

3.4.4.1 Cytotoxicity of PPGD-treated hydrogels

As the hydrogels may find future application as wound healing devices, it is important to ensure that no cytotoxic potential is introduced during the manufacturing and subsequent sterilisation treatment. To-date no biocompatibility evaluation on medical materials has been conducted post-PPGD treatment. Thus, the effect of PPGD treatment on the hydrogels' cytocompatibility was determined via extract tests and agarose overlay assays. For these studies the HaCaT cell line was used as it represents important characteristics of the human skin (Boukamp *et al.,* 1988), the organ which is often the first site of contact for

wound healing devices. The elution test was conducted using MTT and NR endpoints and the results for undiluted extracts obtained from PPGD-treated hydrogels were compared to extracts from untreated control gels following a 24 h cell exposure at 37°C. In addition, the agarose overlay assay was conducted using round discs (Ø = 2cm) of 75-25xP type hydrogel samples which were exposed for 12 h immediately after PPGD treatment and following a preincubation step of 7 days. This exposure type was chosen to determine whether reactive species absorbed into the gel matrix can degrade to less harmful products over time. Figure 3.65 illustrates the data obtained via the extract test. The agarose overlay assay results are shown in Figure 3.66 and were graded in Table 3.25.

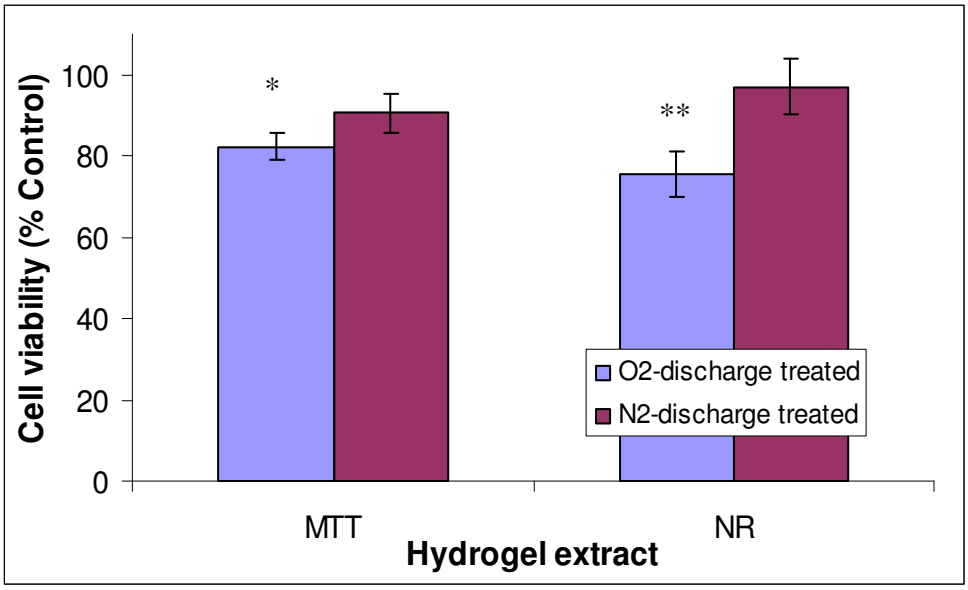

Figure 3.65: The effect of extracts from PPGD-treated 75-25xP type hydrogels on HaCaT cell viability as assessed using the MTT and NR assay following 24 h exposure at 37°C (n=18, ±SEM, * denotes a significant difference from the control **=p<0.01, *=p<0.05).

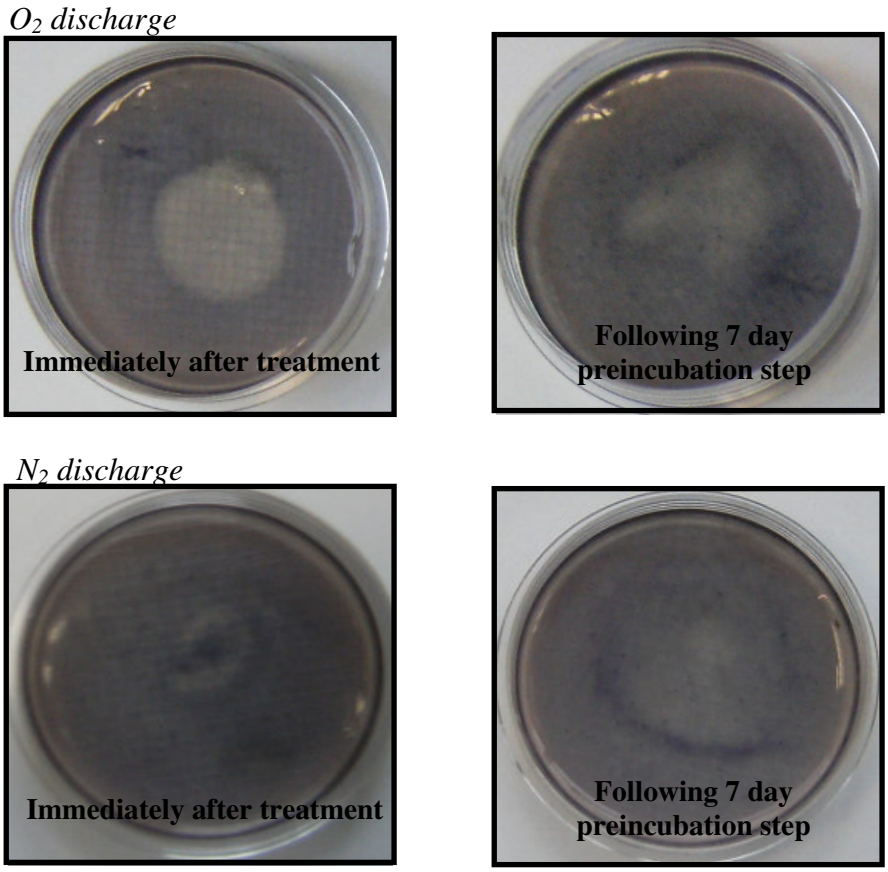

Figure 3.66: The effect of PPGD-treated 75-25xP type hydrogels on HaCaT cell viability as assessed via the agarose overlay assay after 12 h exposure at 37°C. Clear zones indicate cellular toxicity.

Table 3.25: Reactivity grades for HaCaT cells following 12 h exposure to PPGD-treated hydrogels in the agarose overlay assay.

Exposed immediately after treatment		
Discharge type	**Grade**	**Cellular Toxicity**
O_2 discharge	3	Moderate Toxicity
N_2 discharge	1	Slight toxicity

Exposed following 7 day preincubation		
Discharge type	**Grade**	**Cellular Toxicity**
O_2 discharge	2	Mild Toxicity
N_2 discharge	1	Slight toxicity

The extract test shown in Figure 3.65 revealed that the PPGD treatment had an impact on the hydrogels cytocompatibility. Following 24 h exposure, the hydrogel extracts obtained from O_2 discharge-treated hydrogels induced significant cell death in the MTT

($p<0.05$) and NR ($p<0.01$) assay. Although extracts obtained from N_2 discharge-treated gels caused a mild reduction in cell viability, the values obtained were not found to be statistically significant. The residual viability values were 83% and 75% for extracts obtained from O_2 discharge-treated gels and 90% and 96% for extracts from N_2 discharge-treated gels in the MTT and NR assays, respectively.

In the agarose overlay assay, indirect exposure to PPGD-treated hydrogels caused a varying degree of cellular damage to the underlying HaCaT cells as indicated by the formation of the clear zones in Figure 3.66 and graded in Table 3.25. The highest degree of cellular toxicity (grade 3) was observed following exposure to O_2 discharge-treated gels immediately after the PPGD treatment. This cytotoxicity was reduced to grade 2 when a 7 day preincubation step was included before cell exposure. In comparison, the N_2 discharge-treated hydrogels appeared less toxic in the agarose overlay assay. Only slight cellular toxicity (grade 1) was observed directly under the gel specimen following immediate and delayed exposure to N_2 discharge-treated hydrogels.

Based on the results obtained from the cytotoxicity analysis it appears that the reactive species generated, in particular during O_2-mediated PPGD, were able to enter the gel matrix and cause an impact on the material's biocompatibility. Conducive to findings extensively discussed in Section 3.3.5.1, the generation of cytotoxic species depended on the type of discharge used. Reactive species produced during O_2 discharge treatment caused a negative impact on the bioperformance of the gels, while N_2 discharge introduced only minor effects on the utilised cells. Hence, based on these results, it appears that N_2-mediated discharge is superior to O_2-mediated discharge in terms of material biocompatibility.

Moreover, the 7 day preincubation step somewhat detoxified the samples and this effect was primarily seen for treatments involving O_2 discharge. This phenomenon supports the theory that chemically reactive oxygen species, such as ozone that can decay to less harmful products, were the main cause of cellular toxicity.

Furthermore, Duffy and her colleagues described the introduction of toxic metal residues to ophthalmic surgery instruments resulting from a commercial plasma sterilisation method (Plazlyte^{TM}) which was related to an epidemic outbreak of toxic corneal endothelial cell destruction (Duffy *et al.,* 2000). In the current study, the presence

of metal contaminates originating from electrode erosion processes was determined within the PPGD-treated test liquid (Table 3.17). Although Al residues reached a critical level within the test liquid following 30 min of PPGD, it is questionable whether these contaminates were absorbed by the hydrogels during the process. Nevertheless, to ensure the hydrogels' use in wound healing applications further research is needed to elucidate possible implications also resulting from the potential presence of metal contaminates.

Overall, these findings compare favourably to a study conducted by Ikarashi *et al.* (1995), who evaluated the cytotoxicity of medical polymers after vapor-phase H_2O_2 sterilisation, whereby residues of reactive oxygen species caused a deterioration of the polymer's cytocompatibility and it was advised to allow for an appropriate aeration time post-sterilisation to mediate the decay of reactive species.

Similarly, the preincubation step in this study had a positive effect on the PPGD-treated hydrogel's biocompatibility and allowed for the decay of reactive species. Therefore, an additional incubation period post-PPGD should be a mandatory requirement before the gels can be used in biomedical applications. Moreover, although somewhat time and labour intensive, it is believed that chemical species introduced by the PPGD treatment can be efficiently removed by a second hydrogel purification step in suitable solvents such as PBS.

As the treatment settings used were based on extreme microbial contamination, further research aiming to reduce the intensity of the PPGD treatment would be worthwhile. Practically, before the PPGD treatment is commenced, the level of microbial contamination could be drastically reduced by stringent aseptic manufacturing and/or by the implementation of a preclean step to allow gross removal of infectious agents from the gel's surface.

3.4.4.2 Genotoxicity of PPGD-treated hydrogels

As previously mentioned, the formation of active chemical species in the test liquids during HV discharge treatment could potentially introduce hazardous alterations to the polymer network. Furthermore, O_2 discharge-treated test liquid provoked a weak positive result in the Ames assay in Section 3.3.5.2 and possible mechanisms were discussed. Hence, it was necessary to evaluate the safety of PPGD treatment on the

hydrogels from a genotoxicological perspective. In this section, the comet assay and the Ames assay were used to screen undiluted extracts prepared from O_2 and N_2 discharge-treated hydrogels for the presence of genotoxic/mutagenic substances. Again, the comet assay was conducted with HaCaT cells exposed for 12 h at 37°C to undiluted PPGD-treated hydrogel extracts, whose cytotoxicity was predetermined via the trypan blue exclusion method (viability ≥80%), using duplicate slides per test extract with 50 cells scored per slide. In addition, 100 µM H_2O_2 was used as a positive control to which cells were exposed for 40 min at 4°C. In accordance with previous tests, the Ames assay strains (approximately 10^7 bacteria cells) were exposed for 90 min to hydrogel extracts prepared in Ames exposure medium with metabolic competence enhanced by the addition of S9 fraction. Appropriate positive control chemicals were included to ensure optimal assay conditions (in the absence of S9: 4-NQO:NF 500:2000 ηg/ml; in the presence of S9: 2-AmAn 125 µg/ml).

The results obtained for the comet assay are illustrated in Figure 3.67 and Table 3.26 while the results for the Ames assay are shown in Table 3.27.

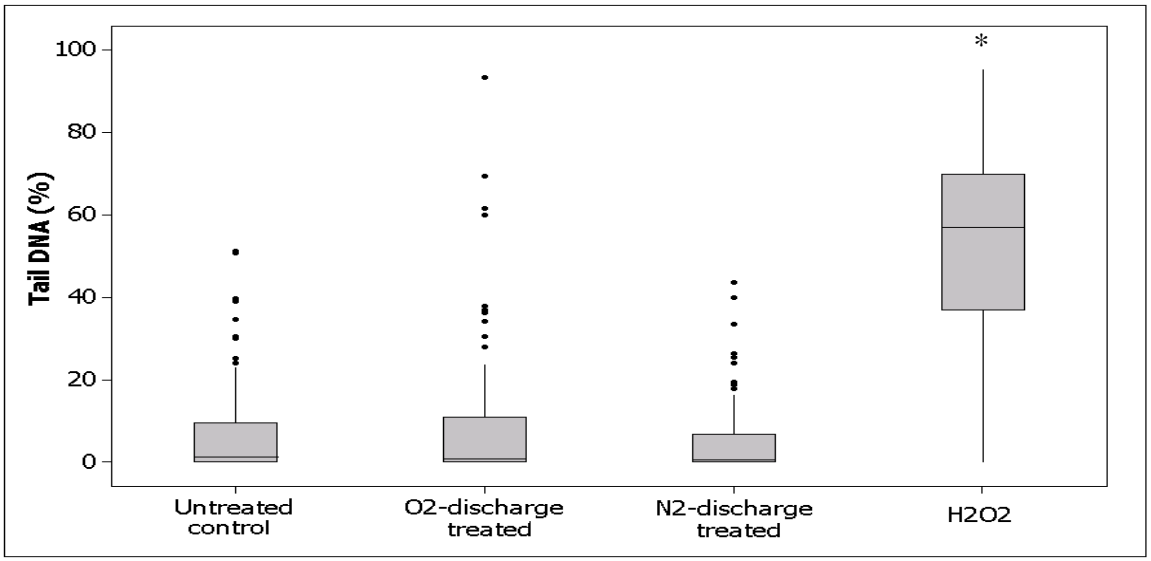

Figure 3.67: Box plot presentation of percentage tail DNA obtained following HaCaT cell exposure to extracts from PPGD-treated 75-25xP type hydrogels (12 h at 37°C) and 100 µM H_2O_2 (40 min at 4°C). Each box corresponds to 100 comets measured on two slides and represents 25-75 percentiles, middle line = median, whisker extends to the maximum/minimum data point within 1.5 box heights from the top/bottom of the box. Dots above and below boxes indicate outliers. * denotes a significant difference from the control ($p<0.05$).

Table 3.26: Tail moment and percentage tail DNA values obtained in the comet assay after exposure of HaCaT cells to extracts from PPGD-treated 75-25xP type hydrogels (12 h at 37°C) and 100 µM H_2O_2 (40 min at 4°C). Results shown are the means (±SEM) of 100 single cells from duplicate slides. * denotes a significant difference from the control ($p<0.05$).

Treatment	Tail moment	% Tail DNA
Control	1.03 (±0.27)	8.08 (±1.11)
O_2 discharge	1.36 (±0.48)	7.25 (±1.07)
N_2 discharge	0.92 (±0.37)	6.25 (±1.03)
H_2O_2 100 µM	16.14 (±0.91)*	53.09 (±2.53)*

Table 3.27: Mean values of positive wells (±SEM) obtained from three experiments in the Ames mutagenicity assay following 90 min exposure to extracts from PPGD-treated 75-25xP type hydrogels and positive controls (±S9). * denotes a significant difference from the control ($p<0.05$).

Hydrogel Extract	TA98		TAMix	
	-S9	+S9	-S9	+S9
Untreated Control	2.00 (±1.15)	2.33 (±0.33)	1.67 (±0.88)	1.00 (±0.58)
O_2 discharge	1.67 (±0.33)	1.67 (±0.66)	1.33 (±0.66)	1.67 (±0.33)
N_2 discharge	2.67 (±0.33)	1.33 (±0.66)	2.67 (±0.33)	1.67 (±0.33)
Positive control	47.00 (±1.00)*	36.00 (±3.15)*	47.67 (±0.33)*	32.67 (±2.50)*

The box plots illustrated in Figure 3.67 and the data summarised in Table 3.26 indicate that none of the hydrogel extracts tested caused a significant increase in DNA migration via the comet assay. Following 12 h exposure to extracts from O_2 and N_2 discharge-treated hydrogels maximum the percentage DNA and tail moment values were equivalent to 7.25 and 1.36, respectively. However, a slightly elevated number of outliers were detected for extracts from O_2 discharge-treated hydrogels which was associated with minor cytotoxic effects. In contrast, the positive control (100 µM H_2O_2) produced significantly ($p<0.05$) elevated DNA migration values which were similar to those seen in previous tests. Here, the mean percentage tail DNA and tail moment values were approximately 7 and 16 times greater than the respective values obtained for untreated control cells.

Furthermore, no mutagenic activity was observed following extract exposure to the Ames strains (Table 3.27). The mean values of positive wells obtained following TA98 and

TAMix exposure (±S9) to extracts from PPGD-treated hydrogels were in the same range as those obtained from exposure to extracts prepared from untreated hydrogels. Moreover, the positive control chemicals produced a mutagenic response in all strains tested (±S9) comparable to the previously conducted Ames test (Sections 3.1.5.2, 3.2.5.2 and 3.3.5.2).

Overall, the PPGD did not induce a detectable genotoxic/mutagenic alteration to the PPGD-treated hydrogels as assessed via the comet and Ames assays. However, it should be considered that in this study the cells were exposed albeit to undiluted extracts of PPGD-treated hydrogels but the extract medium may have acted as a free radical scavenger, thus influencing the findings. This concern is strengthened by the fact that a weak mutagenic result was observed in Section 3.3.5.2 during exposure of O_2 discharge-treated test liquid to the TA98 Ames strain. As this effect was only observed in the absence of S9 it led to the hypothesis that the liver homogenate may have inactivated residues of reactive species such as ozone. As the mutagenic potential of the test liquid was not observable following implementation of a 7 day incubation step, the need for an appropriate incubation time period allowing for the decay of reactive species post-PPGD treatment of hydrogels must be further stressed. Nevertheless, further research using direct hydrogel exposure methods may be required to fully elucidate whether the PPGD imposes hazardous changes to the material.

3.4.5 Summary

In this section the efficacy and safety of PPGD treatment on fully hydrated chemical hydrogels of the 75-25xP type was investigated. It was shown that the PPGD method proved highly effective for the antimicrobial treatment of chemical hydrogels. Within 16 min of treatment, using settings previously determined as optimal, no bacterial survivors were recovered from hydrogels previously inoculated with microbial densities up to 4.6 cfu/cm^2. Both the Gram negative *E. coli* and the Gram positive *S. aureus* tester strains were successfully inactivated with O_2- and N_2-mediated discharges at comparable rates.

Using extreme conditions of 30 min PPGD exposure, preliminary results obtained during oscillatory plate rheology and compressive failure analyses suggested that the PPGD did not have an impact on the hydrogels' mechanical properties. More specifically, there was no significant difference between the gel strength values of PPGD-treated and

untreated hydrogels. Also, using ScEM, no topographical changes of the gels' surface were determined post-PPGD treatment. However, a prerequisite for performing ScEM was to dehydrate the hydrogels which introduced substantial surface shrinkage and folding thus making an objective analysis difficult.

The impact of the PPGD treatment on biocompatibility was also evaluated with *in vitro* based cyto- and genotoxicologial assessment methods. The cytotoxic potential of PPGD-treated hydrogels was determined using MTT and NR based extract tests and an agarose overlay assay. It was observed that O_2 discharge caused a reduction in cytocompatibility while the effects of N_2 discharge were minor. It was suggested that reactive species were the prime cause for the observed cytotoxicity. This hypothesis was further strengthened by the fact that a 7 day preincubation step led to a marked detoxification.

The PPGD treatment did not induce any genotoxic changes detectable via the comet and the Ames assay. The tested extracts from PPGD-treated hydrogels appeared free of any genotoxic and mutagenic substances. However, it was remarked that the extract medium could potentially scavenge reactive species and thus influence the outcome of the assays. Hence, further research using direct contact methods is advised.

Chapter 4: Conclusion

4.1 Overall conclusion

The aim of this study was to evaluate the functional properties and the *in vitro* biocompatibility of novel physical and chemical hydrogels intended for use in biomedical applications. Additionally, the suitability of a novel prototype HV electro-technology for the nonthermal sterilisation of such hydrogels was also investigated.

Following a thorough literature review and in accordance with research previously conducted in our laboratories, NVP and AA were the base materials selected as their hydrophilic and fast copolymerisation characteristics made them ideal candidates for the synthesis of copolymeric hydrogels.

In the early stages of development, a series of physical hydrogels were synthesised at a variety of different monomeric concentrations using photopolymerisation. Initially, the photopolymerisation employed proved fast and effective in producing solid, water-soluble xerogels and preliminary functional characterisation indicated potential use as a lubricous biomaterial coating. However, chemical analysis revealed that critical levels of unreacted monomers remained in the hydrogel matrix which could not be removed via post-polymerisation purification or washing due to the soluble nature of such physical hydrogels. As a biomaterial must be biocompatible to be considered for biomedical applications, the physical hydrogels were subjected to a cyto- and genotoxicological assessment. Although no definite genotoxicological response was determined, the hydrogels proved cytotoxic to *in vitro* cultured ileocecal adenocarcinoma (HCT-8) and hepatoma (HepG2) cells of human origin. The reduced cell-compatibility was linked to the unpolymerised residues. These findings indicate that further optimisation of the polymerisation process is required, aiming to decrease the amount of unreacted residues and, thus, enhance the biocompatibility of the physical networks. However, as this was beyond the scope of this study, the research emphasis shifted towards the synthesis, characterisation and toxicological evaluation of chemical hydrogels that, due to their water-insoluble nature, can be purified post-polymerisation.

For the synthesis of chemical hydrogels, identical monomeric compositions and polymerisation conditions as previously employed for the physical gels were chosen while incorporating EGDMA and PEGDMA to facilitate crosslinking of the gel networks. Chemical analysis determined that unreacted, cytotoxic residuals were removed by a

simple washing procedure using aqueous solutions. Moreover, in depth functional characterisation revealed that these hydrogels achieved high moisture contents thereby resembling a soft and natural living tissue-like consistency, while still maintaining structural integrity. Combined with their nondegradable nature and high elasticity, these properties strengthen the materials' potential usage in regenerative medicine such as wound healing, where they could provide structural support and a moist healing environment for damaged tissue. In addition, their transparency is expected to benefit uncomplicated wound monitoring. Investigation of the hydrogels' cytocompatibility using human keratinocyte (HaCaT) and hepatoma (HepG2) cells did not indicate any cellular injury via direct and indirect contact exposure. Direct contact also revealed that these hydrogels were nonadhesive to tissue culture layers, a characteristic that would allow the gels to be removed with minimal pain or trauma from the wound bed. Furthermore, the hydrogel extracts tested proved entirely free of any genotoxic and mutagenic potential as observed via *in vitro* genotoxicity tests.

To reduce the risk of infection, biomaterials including wound healing devices, require proper microbial decontamination before use. Limitations of conventional disinfection methods for treating fragile polymeric devices highlighted the need for alternative methods to eradicate microbial contamination without impacting on the materials functionality. Once appropriate hydrogels were developed, the remaining part of the study focused on determining the suitability of a novel PPGD technology as an antimicrobial treatment method for such delicate and heat sensitive materials. As the PPGD system was delivered as prototype design and has not been previously used for disinfection purposes, studies into its applicability were not without significant technical challenges and optimisation. Various discharge conditions using O_2 and N_2 gases were examined during the search for optimal operational settings which gave an important insight into the physicochemical mechanisms responsible for the system's antimicrobial action. Following successful optimisation, a wide range of preliminary experiments on microbial test organisms (*E. coli* and *S. aureus*) suspended in treatment liquid confirmed that the PPGD method had great potential for low temperature disinfection of biomaterials and medical devices. However, preliminary studies into the toxicological safety of this novel treatment

method showed that the reactive species generated and electrode degradation products can potentially influence the biocompatibility of the treated devices.

Further experiments on bacterial contaminated chemical hydrogels revealed that the PPGD method led to fast and effective elimination of all viable microbial organisms investigated. Preliminary material characterisation suggested that the treatment did not have a negative impact on the gels' functionality. However, studies of the biocompatibility of PPGD-treated hydrogels indicated that reactive species generated during the discharge can adversely influence the biocompatibility of hydrogels. This effect was predominately seen with discharges mediated by O_2 gas. Due to their absorbing capacity, biocidal species can gain entry into the gel network. Preliminary studies showed that the cytotoxic effects of these reactive species are reduced simply by preincubating the hydrogels under aseptic atmospheric conditions for 7 days prior to biocompatibility testing. It must be stated, however, that such studies were carried out at PPGD treatment regimes that were aimed at extreme microbial contamination conditions and may not reflect the actual treatment time required for actual hydrogel sterilisation which potentially may be much lower. Furthermore, a number of additional suggestions were made aiming to minimise the impact of PPGD treatment on the hydrogels' biocompatibility such as the implementation of an additional washing procedure.

4.2 Future studies

The findings from this study have comprehensively addressed the aim(s) of the project. However, a number of areas have emerged that will direct future related studies, such as (but not limited to):

1. To explore a wider range of polymerisation conditions for physical NVP-AA based hydrogels in order to minimise unreacted residues and, in turn, to improve their overall biocompatibility.

2. To ensure further development of chemical NVP-AA based hydrogels with the final goal to achieve a marketable wound healing device. These studies may include investigations into custom-designed drug delivery applications e.g. the effective

delivery of local anesthetics, anti-inflammatory, antimicrobial agents etc. Moreover, suitable *in vivo* studies involving clinical trials are required as they provide a superior understanding of the materials' biocompatibility and constitute a necessity for regulatory approval.

3. To investigate the potential of the PPGD system for the inactivation of complex ranges of infectious species including spore forming bacteria (e.g. *Geobacillus stearothermophilus*), protozoa, viruses and even proteinaceous particles (prions) from biomedical materials.

4. To investigate the viability of PPGD-treated microbial pathogens attached to hydrogels using relevant fluorescent probes as not all potentially pathogenic bacteria treated with PPGD may be capable of growth on artificial agar media.

5. To further investigate if the physicochemical and biocompatibility properties of biomaterials including chemical hydrogels are adversely affected by exposure to PPGD sterilisation regimes and how to minimise such impacts. These could include using combinations of less severe PPGD exposure regimes and the addition of suitable hydrogel washing procedures aimed at removing residual biocidal species.

6. To compare the efficacy of PPGD treatment with other conventional industrial approaches including EtO and e-beam sterilisation approaches using a standard battery of microorganisms typically used for sterility testing.

References

ACGIH (1986) American Conference of Government Industrial Hygienists Documentation of the threshold limit values and biological exposures indices, 5th ed., ACGIH, Cincinnati, US 14

ACGIH (1991) American Conference of Government Industrial Hygienists Documentation of the threshold limit values and biological exposures indices, 6th ed., ACGIH, Cincinnati, US 26-29

Ajji, Z., Othman, I., Rosiak, J.M. (2005) Production of a hydrogel wound dressings using gamma radiation. Nuclear Instruments and Methods in Physics Research Section B: Beam Interactions with Materials and Atoms 229 375-80

Akishev, Y., Grushin, Y.M., Karalnik, V., Trushkin N., Kholodenko, V., Chugunov, V., Kobzev, E., Zhirkova, N., Irkhina I., Kireev, G. (2008) Atmospheric-pressure, nonthermal plasma sterilization of microorganisms in liquids and on surfaces. Pure and applied chemistry 80 1953-1969

Albertini B., Cavallari C., Passerini N., Gonzalez-Rodriguez M.L., Rodriguez L. (2003) Evaluation of β-lactose, PVP K12 and PVP k90 as excipients to prepare piroxicam granules using two wet granulation techniques. European journal of pharmaceutics and biopharmaceutics 56 479-487

Alderborn, G. (2002) Tables and compaction, in Pharmaceutics; the science of dosage form design- 2nd ed., Editor: Aulton, M.E., Elsevier Science

Alla, S.G.A., El-Din, H.M.N., El-Naggar, A.W.M (2007) Structure and swelling-release behaviour of poly(vinyl pyrrolidone) (PVP) and acrylic acid (AAc) copolymer hydrogels prepared by gamma irradiation. European Polymer Journal 43 2987–2998

Alsheyab, M.A.T., Muñozb, A.H. (2007) Optimisation of ozone production for water and wastewater treatment Desalination 217 1–7

Ames, B. N., McCann, J., Yamasaki, E. (1975) Methods for detecting carcinogens and mutagens with the Salmonella/mammalian microsome mutagenicity test. Mutation Research 31 347-364

Andrews, C.S., Denyer, S.P., Hall, B., Hanlon, G.W., Lloyd, A.W. (2001) A comparison of the use of an ATP-based bioluminescent assay and image analysis for the assessment of bacterial adhesion to standard HEMA and biomimetic soft contact lenses. Biomaterials 22 3225-3233

Anpilov, A.M., Barkhudarov1, E.M., Bark, Y.U., Zadiraka, Y.V., Christofi, M., Kozlov, Y.N., Kossyi1, I.A., Kop'ev1, V.A., Silakov, V.P., Taktakishvili, M.I., Temchin, S.M. (2001) Electric discharge in water as a source of UV radiation, ozone and hydrogen peroxide. Journal of Physics.D: Applied Physics 34 993-999

Anpilov, A.M., Barkhudarov, E.M., Christofi, N., Kop'ev, V.A., Kossyi, I.A., Taktakishvili, M.I., Zadiraka Y. (2002) Pulsed high voltage electric discharge disinfection of microbially contaminated liquids. Letters in Applied Microbiology 35 90-94

Anpilov, A.M., Barkhudarov, E.M., Christofi, N., Kop'ev, V.A., Kossyi, I.A., Taktakishvili I.M., Zadiraka, Y.Z. (2004) The effectiveness of a multi-spark electric discharge system in the destruction of microorganisms in domestic and industrial wastewaters. Journal of Water and Health 02 267-277

Anyim, M., Benjamin, N., Wilks, M. (2005) Acidified nitrite as a potential antifungal agent. International Journal of Antimicrobial Agents 26 85-87

Ashman, L.E., Menashi, W.P. (1972) Treatment of surface with low-pressure plasma. US Patent 3,701,628

Augis, J.A., Gibson, F.J., Gray, E.W (1971) Plasma and electrode interactions in short gap discharges in air: II. Electrode effects. International Journal of Electronics 30 315

Ayliffe, G. A.J. (1997) Sterilization, disinfection, and cleaning of medical devices and equipment: Guidance on decontamination from the Microbiological Advisory Committee to Department of Health Medical Devices Agency. Journal of Hospital Infection 35 73-75

Babich, H., Borenfreund, E. (1990) Applications of the neutral red cytotoxicity assay to *in vitro* toxicology. Alternatives to Laboratory Animals 18 129-144

Bae, Y.H., Huh, K.M., Kim, Y., Park, K.H. (2000) Biodegradable amphiphilic multiblock copolymers and their implications for biomedical applications Journal of Controlled Release 64 3-13

Bal, W., Kasprzak, K.S. (2002) Induction of oxidative DNA damage by carcinogenic metals. Toxicology Letters 127 55-62

Balimandawa, M., de Meester, C., Léonard, A. (1994) The mutagenicity of nitrite in the Salmonella/microsome test system. Mutation Research/Genetic Toxicology 321 7-11

Balls, M., Bridges, J., Southee, J. (1991) Animals and alternatives in toxicology. Macmillan Education

Bancroft, K, Chrostowski, P., Wright, R.L., Suffet, I. (1984) Ozonation and oxidation competition values. Water Research 18 473–478

BASF (1980) Effects of Kollidon 30 on the bone marrow chromosome aberration in Chinese hamster. Unpublished report from BASF. Gewerbehygiene and Toxikologie, Ludwigshafen, Germany. Submitted to the World Health Organization by BASF

Barker, S., Murray, D., Zheng, J., Li, L., Weinfeld, M. (2005) A method for the isolation of covalent DNA–protein crosslinks suitable for proteomics analysis. Analytical Biochemistry 344 204–215

Baroch, P., Takeda, T., Oda, M., Saito, N., Takai, O. (2006) Degradation of bacteria using pulse plasma discharge in liquid medium. 27th International Power Modulator symposium 482- 485

Barbouti, A., Doulias, P.T., Nousis, L., Tenopoulou, M., Galaris, D. (2002) DNA damage and apoptosis in hydrogen peroxide exposed jurat cells: Bolus addition versus continuous generation of H_2O_2. Free Radical Biology and Medicine 33 691–702

Barbucci, R., Lamponi, S., Borzacchiello, A., Ambrosio, L., Fini M., Torricellic, P., Giardino R. (2002) Hyaluronic acid hydrogel in the treatment of osteoarthritis Biomaterials 23 4503–4513

Benamer, S., Mahlous, M., Boukrif, A., Mansouri, B., Larbi Youcef, S. (2006) Synthesis and characterisation of hydrogels based on poly(vinyl pyrrolidone) Nuclear Instruments and Methods in Physics Research Section B: Beam Interactions with Materials and Atoms 248 284-290

Bernhard, D., Schwaiger, W., Crazzolara, R., Tinhofer, I., Kofler, R., Csordas, A. (2003) Enhanced MTT-reducing activity under growth inhibition by resveratrol in CEM-C7H2 lymphocytic leukemia cells. Cancer Letters. 195:193–199

Beveridge, J.R., Wall, K., MacGregor, S.J., Anderson, J.G., Rowan, N.J. (2004) Pulsed electric field inactivation of spoilage microorganism in alcoholic beverages. Proceedings of the IEEE 92

Bharadwaj, L., Dhami, K., Schneberger, D., Stevens, M., Renaud, C., and Ali, A. (2005) Altered gene expression in human hepatoma HepG2 cells exposed to low-level 2,4-dichlorophenoxyacetic acid and potassium nitrate. Toxicology *In Vitro* 19 603-619

Billiet, L., Fournier, D., Prez, F.D. (2009) Step-growth polymerization and 'click' chemistry: The oldest polymers rejuvenated. Polymer 50 Pages 3877-3886

Bińi, A.K. (2004) Ozone dissolution in aqueous systems treatment of the experimental data Experimental Thermal and Fluid Science 28 395–405

Biondi, M., Ungaro, F., Quaglia, F., Netti, P.A. (2008) Controlled drug delivery in tissue engineering. Advanced Drug Delivery Reviews 60 229-242

Bithell, R.M. (1982) Package and sterilizing process for same. US Patent No. 4,321,232

Black, J.G. (2005) Microbiology: Principles and Explorations, 6th ed., John Wiley and Sons Inc.

Black J. (1992) Biological performance of materials, 2nd ed., Editor: Dekker Inc., New York, US

Bogaerts, A., Neyts, E., Gijbels, R., van der Mullen, J. (2002) Gas discharge plasmas and their applications. Spectrochimica Acta Part B: Atomic Spectroscopy 57 609-658

Boucher, R.M.G. (1980) Seeded gas plasma sterilization method. US Patent No. 4,297,286

Boukamp, P., Petrussevska, T.T., Breitkreutz, D., Hornung, J., Markham, A., Fusenig, N.E. (1988) Normal keratinization in a spontaneously immortalized aneuploid human keratinocyte cell line. The Journal of Cell Biology 106 761-771

Bordi, F., Paradossi, G., Rinaldi, C., Ruzick, B. (2002) Chemical and physical hydrogels: two case systems studied by quasi elastic light scattering. Physica A 304 119-128

Borenfreund, E., Puerner, J.A. (1985) Toxicity determined *in vitro* by morphological alterations and neutral red absorption. Toxicology Letters 24 119-124

Borzacchiello, A., Ambrosio, L (2009) Structure-property relationships in hydrogels, in Hydogels – biological properties and applications. Editor: Barbucci R., Springer, Milan, Italy 9-20

Brannon-Peppas, L. (1997) Polymers in controlled drug delivery. Medical Plastic and Biomaterials Magazine, November issue

Braybrook, J.H. (1997) Biocompatibility Assessment of Medical Devices and Materials. John Wiley & Sons Ltd, West Sussex England

Brumfield, R.C., Naff, J.T., Robinson, A.T.W. (1970a) Containers and process for asepsis. US Patent No 3,490,580

Brumfield, R.C., Naff, J.T., Robinson, A.T.W. (1970b) Microwave reactors and process for asepsis. US Patent No 3,551,090

Byrant, S.J., Nuttelman, C.R., Anseth, K.S. (2000) Cytocompatibility of UV and visible light photoinitiating systems on cultured NIH/3T3 fibroblasts *in vitro*. Journal of Biomaterial Science, Polymer 11 439-57

Cabane, B., Lindell, K., Engstrom, S., Lindman, B. (1996). Microphase separation in polymer surfactant systems. Macromolecules 29 3188–3197

Calvet, J.L., Grafahrend, D., Klee, D., Möller, M. [(2008) Sterilization effects on starPEG coated polymer surfaces: characterization and cell viability. Journal of Materials Science: Materials in Medicine 19 1631-1636

Cai, Q., Zhang, W., Yang, Z. (2001) Stability of nitrite in Wastewater and its determination by ion chromatography. Analytical Sciences 17 917-920

Cameron, T.P., Seifried, H.E., Rogers-Back, A.M., Lawlor, T.E., Harbell, J.W., Dunkel, V.C. (1990) Genotoxicity of multifunctional acrylates in the salmonella/mammalian-microsome assay and mouse lymphoma tk+/-assay Environmental and Molecular Mutagenesis 17 264–271

Campbell, A., Hamai, D., Bondy, S.C. (2001) Differential Toxicity of Aluminum Salts in Human Cell Lines of Neural Origin: Implications for Neurodegeneration NeuroToxicology. 22 63-71

Casey, P., Condon, S. (2000) Synergistic lethal combination of nitrite and acid pH on a verotoxin-negative strain of *Escherichia coli* O157. International Journal of Food Microbiology 55

Cenni, E., Ciapetti, G., Granchi, D., Aricola C.R., Sarvarino L., Stea, S., Montanaro, L., Pizzoferrato, A. (1999) Established cell lines and primary cultures in testing medical devives *in vitro.* Toxicology *in Vitro* 13: 801-810

Chamberlain V.C., Lambert B., Tang, F.W. (1998) Sterilization effects, in Handbook of Biomaterials Evaluation. Editor: Scientific, Technical, and Clinical Testing of Implant Materials 2nd ed., von Recum, A.F., Macmillan, New York 253-261

Charles, S.W., Cullen, F.C., Owen, N.L., Williams, G.A. (1987) Infrared spectrum and rotational isomerism of acrylic acid. Journal of Molecular Structure 157 17-29

Chen, H., Chang, X., Du, D., Li, J., Xu, H., Yang, X. (2006) Microemulsion-based hydrogel formulation of ibuprofen for topical delivery. International Journal of Pharmaceutics 315 52-58

Chick, H. (1908) An investigation of the laws of disinfections. Journal of Hygiene 92-157

Cholvin, N.R., Bayne, N.R. (1998) General compatibility, in Handbook of biomaterials evaluation: Scientific, Technical, and Clinical Testing of
Implant Materials 2nd ed., Editor: von Recum, A.F., Macmillan, New York, 507–522

Choucroun, P., Gillet, D., Dorange, G., Sawicki, B., Dewitte, J.D. (2001) Comet assay and early apoptosis Mutation Research 478:89–96

Chow, C.K., Hong, C.B. (2002) Dietary vitamin E and selenium and toxicity of nitrite and nitrate. Toxicology 180 195-207
Ciarkowski, A.A., Mueller, E. (1998) Preclinical testing guidelines, in Handbook of biomaterials evaluation. Scientific, Technical, and Clinical Testing of Implant Materials 2nd ed., Editor: von Recum, A.F., Macmillan, New York, US 775-790

Clements, J.S., Sato, M., Davis, R.H. (1987) Preliminary Investigation of Prebreakdown Phenomena and Chemical Reactions Using a Pulsed High-Voltage Discharge in Water Industry Applications. IEEE Transactions on IA-23 224 – 235

Clontz, L., (1998) Microbial limit and bioburden tests: Validation approaches and global requirements .CRC Press LLC Florida, US

Cohrrsen, J.J., Covello, V.T. (1989) Risk analysis: A guide to principles and methods for analyzing health and environmental risks. Council on Environmental Quality. Washington DC

Collins, A.R. (2004) The comet assay for DNA damage and repair: principles, applications, and limitations. Molecular Biotechnology 26 249-61

Collins, A.R., Dobson, V.L., Dusinka, M., Kennedy, G., Stetina, R. (1997) The comet assay: what can it really tell us? Mutation Research 375 183-193

Collins, A.R., Oscoz1, A.A., Brunborg, G., Gaivão, I., Giovannelli, L., Kruszewski, M., Smith, C.C., Štětina, R. (2008) The comet assay: topical issues. Mutagenesis 23 143-151

Comly, H.H. (1945) Cyanosis in infants caused by nitrates in well-water. Journal of the American Medical Association 129 112-116

Coronel, B., Duroselle, P., Behr, H., Moskovtchenko, J.F., Freney, J. (2002) *In situ* decontamination of medical wastes using oxidative agents: a 16-month study in a polyvalent intensive care unit. Journal of Hospital Infection 50 207-212

Cottam, E., Hukins, D.W.L., Lee, K., Hewitt, C., Jenkins, M.J. (2009) Effect of sterilisation by gamma irradiation on the ability of polycaprolactone (PCL) to act as a scaffold material. Medical Engineering and Physics 31 221-226

Coulombe S., Meunier, J.L. (2000) Theoretical prediction of non-thermionic arc cathode erosion rate including both vaporization and melting of the surface. Plasma Sources Science and Technology 9 239

Cowan, S.T., Steel, K.J. (2003) Cowan and Steel's manual for the identification of medical bacteria, 3rd ed., Editor: Barrow, G.I., Feltham, R.K.A., Cambridge University Press, UK

Curran, J.A., Clyne, T.W. (2005) Thermo-physical properties of plasma electrolytic oxide coatings on aluminium. Surface and Coatings Technology 199 168– 176

Custodio, J., Palmeira, C., Moreno, A., Wallace, K. (1998) Acrylic acid induces the glutathione-independent mitochondrial permeability transition *in vitro*. Toxicology Science 43 19-27

Dang, J.M., Leong, K.W. (2006) Natural polymers for gene delivery and tissue engineering, Review article. Advanced Drug Delivery Reviews 58 487-499

Das, T., (2000) The year 2000: looking back and looking forward. Indian Journal of Ophthalmology 48 1-2

Dearfield, K., Harrington-Brock, K., Doerr, C.L., Rabinowitz, J.R., Moore, M.M. (1991) Genotoxicity in mouse lymphoma cells of chemicals capable of michael addition. Mutagenesis 6 519–525

Deligkaris, K., Tadele, T.S., Olthuis, W., van den Berg, A. (2010) Hydrogel based devices for biomedical applications. Sensors and Actuators. B: Chemical, In Press, Accepted Manuscript

Deloncle, R., Guillard, O., 1990. Mechanism of Alzheimer's disease: arguments for a neurotransmitter-aluminum complex implication. Neurochemical Research 15 1239-1245

Demling, R.H., DeSanti L., Orgill, D.P. (2000) Moist healing and wound care including burns-Advantages and current approaches. Available online: www.burnsurgery.com/Documents/moist_healing_wound_care.*doc*

Deng, M., Shalaby, S.W. (1995) Effects of c irradiation, gas environments, and post-irradiation aging on ultrahigh molecular weight polyethylene. Journal of Applied Polymer Science 58 2111–21119

Devery, S., Tomkins P.T. (1999) Alkali sensitive DNA strand breaks and evidence of repair in primary cells and tissue comparable cell lines after UV and clastogen exposure. Mutagenesis 14 641

Devine, D.M., Higginbotham, C.L. (2003) The synthesis of a physically crosslinked NVP based hydrogels. Polymer 44 7851-7860

Devine, D.M., Higginbotham, C.L. (2005) Synthesis and characterisation of chemically crosslinked N-vinyl pyrrolidinone (NVP) based hydrogels. European Polymer Journal 41 1272-1279

Devine, D.M., Devery, S.M., Lyons, J.G., Geever, L.M., Kennedy, J.E., Higginbotham C.L. (2006) Multifunctional polyvinylpyrrolidinone-polyacrylic acid copolymer hydrogels for biomedical applications. International Journal of Pharmaceutics 326 50–59

Diaz-Llera, S., Gonzalez-Hernandez, Y., Prieto-Gonzalezand, E.A., Azoy, A. (2002) A genotoxic effect of ozone in human peripheral blood leukocytes. Mutation Research 517 13-20

Dierickx, P.J. (1998) Cytotoxicity testing of 114 compounds by the determination of the protein content in HepG2 hepatoma cell cultures. Toxicology *In Vitro* 3 189-193

Duffy, R.E., Brown, S.E., Caldwell, K.L., Lubniewski, A., Anderson, N., Edelhauser, H., Holley, G., Tess, A., Divan, H., Helmy, M., Arduino, M., Jarvis, W.R. (2000) An epidemic of corneal destruction caused by plasma gas sterilization. The toxic cell destruction syndrome investigative team. Archives of Ophthalmology 118 1167-1176

Duthie, S.J., Collins, A.R. (1996) The influence of the cell growth, detoxifying enzymes and DNA repair on hydrogen peroxide-mediated DNA damage (measured using the comet assay) in human cells. Free Radical Biology & Medicine 22 717-724

Efremov, N.M., Adamiak, B.Y., Blochin, V.I., Dadashev, S.J., Dmitriev, K.I., Semjonov, V.N., Levashov, V.F., Jusbashev, V.F. (2000) Experimental investigation of the action of pulsed electric discharges in liquids. IEEE Transactions in Plasma Science 28 224–229

Ekem, N., Akan, T., Akgun, Y., Kiremitci, A., Pat, S., Musa, G. (2006) Sterilization of Staphylococcus aureus by atmospheric pressure pulsed plasma. Surface and Coatings Technology 201 993-997

Elijarrat-Binstock, E., Bentolila, A., Kumar, N., Harel, H., Domb, A. (2007) Preparation, characterization, and sterilization of hydrogel sponges for ionophoretic drug-delivery use. Polymers for Advanced Technologies 18 720-730

Espie, S., Marsili, L., MacGregor, S.J., Anderson, J.G. (2000) Plasma inactivation of microorganisms in liquids. Proceedings of XIIIth. International Conference on Gas Discharges and their Applications 688–691

Espie, S.; Marsili, L.; Macgregor, S.J.; Anderson, J.G. (2001) Investigation of microbial cell inactivation using plasma dischargetreatment of liquids. Pulsed Power Plasma Science IEEE Conference Record – Abstracts

EU Directive 2001/83/EC Current good laboratory practice

EU directive 2003/94/EC Current good manufacturing practice

EU Directive 2004/23/EC Quality and safety for the donation, procurement, testing, processing, preservation, storage, distribution of human tissues and cells

EU Directive 93/42/EEC The medical device directive
Evans, F.L., (1972) Ozone in water and wastewater treatment. Ann Arbor Science Publishers Inc.

Fang, Z., Qiu, Y., Sun, Y., Wang, H., Edmund, K. (2008) Experimental study on discharge characteristics and ozone generation of dielectric barrier discharge in a cylinder–cylinder reactor and a wire–cylinder reactor Journal of Electrostatics 66 421–426

Feairheller, W.R., Kanton, J.E (1967) The vibrational spectra of acrylic acid and sodium acrylate. Spectrochimical Acta Part A: Molecular Spectroscopy 23 2225-2232

Flückiger-Isler, S., Baumeister, M., Braun, K., Gervais, V., Hasler-Nguyen, N., Reimann, R., Van Gompel, J., Wunderlich, H.G., Engelhardt, G. (2004) Assessment of the performance of the Ames II^{TM} assay: a collaborative study with 19 coded compounds. Mutation Research 558 181–197

Fonder, M.A., Lazarus, G.S., Cowan, D.A., Aronson-Cook B., Kohli, A.R., Mamelak, A.J. (2008) Treating the chronic wound: A practical approach to the care of nonhealing wounds and wound care dressings. Journal of the American Academy of Dermatology 58 185-206

Fotakis, G., Timbrell, J.A. (2006) *In vitro* cytotoxicity assays: comparison of LDH, neutral red, MTT and protein assay in hepatoma cell lines following exposure to cadmium chloride. Toxicology Letters 160 171-177

Fraser, S.J., Gillete, R.B., Olson, R.L (1974) Sterilizing and packaging process utilizing gas plasma. US Patent No. 3,851,436

Fraser, S.J., Gillete, R.B., Olson, R.L (1976) Sterilizing process and apparatus utilizing gas plasma. US Patent No. 3,948,601

Frazier, J.M. (1992) *In vitro* toxicity testing–Applications to safety evaluation. Marcel Dekker Inc., 17-20

Freshney, R.I. (1987) Culture of animal cells: a manual of basic technique. Liss Inc., New York, US107-126

Friedrich, U., Stachowicz, N., Simm A, Fuhr, G., Lucas, K., Zimmermann, U. (1998) High efficiency electrotransfection with aluminium electrodes using microsecond controlled pulses. Bioelectrochemistry and Bioenergetics 47 103-111

Fryburg, G.C. (1956) Enhanced Oxidation of Platinum in Activated Oxygen. Journal of Chemical Physics 24 175

Fujimoto, R., Toshima, S. (1972) Electrode erosion by pulsed discharges in liquid. Electrical Engineering Japan 92 29-35
Fujimori, K., Trainor, G.T. (1983) Effect of viscosity in the radical polymerization of acrylic acid in the presence of poly(4-vinylpyridine) in methanol. Polymer Bulletin 9 204-207

Gad, S.C. (1988) Product safety evaluation handbook. Marcel Dekker Inc., New York, US 15-22

Gad, S.C. (2000) *In vitro* toxicology 2nd ed., Taylor and Francis 94-128

Gapper, L.W., Fong, B.Y., Otter, D.E., Indyk, H.E., Woollard, D.C. (2004) Determination of nitrite and nitrate in dairy products by ion exchange LC with spectrophotometric detection. International Dairy Journal 14 881-887

Gee, P., Aron, D.M., Ames, B.N. (1994) Detection and classification of mutagens: a set of base specific salmonella tester strains. The Proceedings of the National Academy of Sciences Online 91 11606–11610

Geever, L., Cooney, C.C., Lyons, J.G., Kennedy, J.E., Nugent, M.J.D., Devery, S.M., Higginbotham, C.L. (2008) Characterisation and controlled drug release from novel drug-loaded hydrogels. European Journal of Pharmaceutics and Biopharmaceutics 69 1147-1159

Geever, L., Cooney, Devine, D.M., Kennedy, J.E., Nugent, M.J.D., Lyons, J.G., Higginbotham, C.L. (2006) The synthesis, characterisation, phase behaviour and swelling of temperature sensitive physically crosslinked poly(1-vinyl-2-pyrrolidinone)/poly(N-isopropylacrylamide) hydrogels. European Polymer Journal 42 69-80

Gnedenkov, S.V., Khrisanfova, O.A., Zavidnaya, A.G., Sinebrukhov, S.L., Kovryanov, A.N., Scorobogatova, T.M., Gordienko, P.S. (2000) Production of hard and heat-resistant coatings on aluminium using a plasma micro-discharge. Surface and Coatings Technology 123 24–28

Goryachev, V.L., Rutberg, F.G., Fedyukovich, V.N. (1998) Electric-discharge method of water treatment. Status of the problem and prospects. Applied Energy. Russian Journal of Fuel Power and Heat Systems 36 35-49

Gray, E.W., Pharney, J.R. (1974) Electrode erosion by particle ejection in low-current arcs. Journal Applied Physics 45 667

Griffith, L.G (2000) Polymeric biomaterials. Acta Materialia 48 263-277

Grosskinsky, U. (2006) Biomaterial regulations for tissue engineering. Desalination 199 265-267

Guess, W.L., Rosenbluth, S.A., Schmidt, B., Autian, J. (1965) Agar diffusion method for toxicity screening of plastics on cultured cell monolayers. Journal of Pharmaceutical Sciences 54 1545–1547

Gueven, O., Sen, M. (1991) Preparation and characterization of poly (N-vinyl-2 Pyrrolidone) Hydrogels. Polymer 32 2491-2495

Guida, L., Saidi, Z., Hughes, M.N., Poole, R.K. (1991) Aluminium toxicity and binding to Escherichia coli. Archives of Microbiology 156 507-12

Gunten U. (2003b) Ozonation of drinking water: Part I. Oxidation kinetics and product formation Water Research 37 1443–1467

Gunten U. (2003a) Ozonation of drinking water: Part II. Disinfection and by-product formation in presence of bromide, iodide or chlorine Water Research 37 1469–1487

Gupta, P., Vermani, K., Garg, S. (2002) Hydrogels: from controlled release to pH-responsive drug delivery. Drug Discovery Today 7 569-579

Gupta, K., Rispin, A., Stitzel, K., Coecke, S., Harbell, J. (2005) Regulatory toxicology and pharmacology 43 219-22

Gusbeth, C., Frey, W., Volkmann, H., Schwartz, T., Bluhm, H.J. (2009) Pulsed electric field treatment for bacteria reduction and its impact on
hospital wastewater. Chemosphere 75 228-233

Haigh, R., Fullwood, N., Rimmer, S. (2002) Synthesis and properties of amphiphilic networks 2: a differential scanning calormetric study of poly(dodecyl methacrylate-stat-2,3 propandiol-1-methacrylate-statethandiol dimethacrylate) networks and adhesion and spreading of dermal fibroblasts on these materials. Biomaterials 23 3509-3516

Halliwell, B. (1999) Oxygen and nitrogen are pro-carcinogens. Damage to DNA by reactive oxygen, chlorine and nitrogen species: measurement, mechanism and the effects of nutrition. Mutation Research (443) 37–52

Hamidi, M., Azadi, A., Rafiei, P. (2008) Hydrogel nanoparticles in drug delivery Advanced Drug Delivery Reviews 60 1638–1649

Harrington, C.R., Wischik, C.M., McArthur, E.K., Taylor, G.A., Edwardson, J.A., Candy, J.M. (1994) Alzheimer's disease-like changes in tau protein processing: association with aluminium accumulation in brains of renal dialysis patients. Lancet 343 993-997

Hart, S.P., Dransfield, I., Rossi A.G. (2008) Phagocytosis of apoptotic cells. Methods 44 280-285

Hartmann, A., Speit, G. (1997) The contribution of cytotoxicity to DNA-effects in the single cell gel test (comet assay). Toxicology Letters 90 183-188

Haslett, C. (1992) Resolution of acute inflammation and the role of apoptosis in tissue fate of granulocytes. Clinical Science 83 639-648

Hawksworth, G.M. (1994) Advantages and Disadvantages of Using Human Cells for Pharmacological and Toxicological Studies. Human and Experimental Toxicology 13 568-573

Helaleh, M.I.H., Korenaga, T (2000) Ion chromatographic method for simultaneous determination of nitrate and nitrite in human saliva Journal of Chromatography B 744 433–437

Heller, M.A., Howe, L.N. (1998) Legal Aspects, in Handbook of biomaterials evaluation. Scientific, Technical, and Clinical Testing of Implant Materials 2nd ed., Editor: von Recum, A.F., Macmillan, New York, US 775-790

Hennink, W.W., van Nostrum C.F. (2002) Novel crosslinking methods to design hydrogels. Advanced Drug Delivery Reviews 54 13–36

Hillery, A.M., Lloyd, A.W., Swarbrick, J. (2001) Drug delivery and targeting – for pharmacists and pharmaceutical scientists. Taylor and Francis, London 15-120

Himly, N., Darwis, D., Hardiningsih, L. (1993) Poly(n-vinylpyrrolidone) hydrogels: Hydrogel composites as wound dressing for tropical environment. Radiation Physics and Chemistry 42 911-914

Hirata, N., Matsumoto, K.I., Inishita, T., Takenaka, Y., Suma, Y., Shintani, H. (1995) C-ray irradiation, autoclave and ethylene oxide sterilization to thermosetting polyurethane: sterilization to polyurethane. Radiation Physics and Chemistry 46 377–381

Hodgson, E. (2004) A textbook of modern toxicology, 3th ed., John Wiley and Sons Inc., 266

Hoffman, A.S. (2002) Hydrogels for biomedical applications. Advanced drug delivery reviews 43 3-12

Honda, K., Motoki, R., Sakuma, H., Watanabe, M. (1966) Complications following the use of plasma expander, especially polyvinylpyrrolidone. International Surgery 45:549-547

Hong, Y., Chirila, T.V., Fitton, H., Ziegelaar, B.W., Constable, I.J. (1997) Effect of crosslinked poly(1-vinyl-2-pyrrolidinone) gels on cell growth in static cell cultures. Biomedical Materials and Engineering 7 35-47

Hori, K., Sotozono, C., Hamuro, J., Yamasaki, K., Kimura, Y., Ozeki, M., Tabata, Y., Kinoshita, S., (2007) Controlled-release of epidermal growth factor from cationized gelatin hydrogel enhances corneal epithelial wound healing. Journal of Controlled Release 118 169-176

Hu, M., Chen, J., Chen, C. (2008) Inactivation of Escherichia coli using remote low temperature glow discharge plasma. Plasma Science Technology 10 619-622

Hu, M., Chen, J. (2009) Inactivation of Escherichia coli and properties of medical poly(vinyl chloride) in remote-oxygen plasma. Applied Surface Science 255 5690-5697

Huang, Y.G., Ji, J.D., Hou, Q.N. (1996) A study on carcinogenesis of enogenous nitrite and nitrosamine, and prevention of cancer. Mutation Research/Fundamental and Molecular Mechanisms of Mutagenesis 358 28 7-14

Huebsch, N., Gilbert, M., Healy, K.E. (2005) Analysis of sterilization protocols for peptide-modified hydrogels. Journal of Biomedical Materials Research Part B: Applied Biomaterials 74b 440-447

Hunt, N.K., Mariňas, B.J. (1999) Inactivation of Escherichia coli with ozone: Chemical and inactivation kinetics. Water Research 33 2633-2641

Iijima, K., Henry, E., Moriya, A., Wirz, A., Kelman, A. W., and McColl, K. E. (2002) Dietary nitrate generates potentially mutagenic concentrations of nitric oxide at the gastroesophageal junction. Gastroenterology 122 1248-1257

Ikarashi, Y., Tsuchiya, T., Nakamura, A. (1995) Cytotoxicity of medical materials sterilized with vapour-phase hydrogen peroxide. Biomaterials 16 177-183

ISO 10993-1:2009 Biological evaluation of medical devices Part 1: Evaluation and testing within a risk management process

ISO 10993-3:2003 Biological evaluation of medical devices Part 3: Tests for genotoxicity, carcinogenicity and reproductive toxicity

ISO 10993-4:2002/Amd 1:2006 Biological evaluation of medical devices Part 4: Selection of tests for interactions with blood

ISO 10993-5:2009 Biological evaluation of medical devices Part 5: Tests for *in vitro* cytotoxicity

ISO 10993-6:2007 Biological evaluation of medical devices Part 6: Tests for local effects after implantation

ISO 10993-9:2009 Biological evaluation of medical devices Part 9: Framework for identification and quantification of potential degradation products

ISO 10993-10:2002/Amd 1:2006 Biological evaluation of medical devices Part 10: Tests for irritation and delayed-type hypersensitivity

ISO 10993-11:2006 Biological evaluation of medical devices Part 11: Tests for systemic toxicity

ISO 10993-13:1998 Biological evaluation of medical devices Part 13: Identification and quantification of degradation products from polymeric medical devices

ISO 10993-14:2001 Biological evaluation of medical devices Part 14: Identification and quantification of degradation products from ceramics

ISO 10993-15:2000 Biological evaluation of medical devices Part 15: Identification and quantification of degradation products from metals and alloys

ISO 10993-16:1997 Biological evaluation of medical devices Part 16: Toxicokinetic study design for degradation products and leachables

ISO 10993-17:2002 Biological evaluation of medical devices Part 17: Establishment of allowable limits for leachable substances

ISO 10993-18:2005 Biological evaluation of medical devices Part 18: Chemical characterization of materials

ISO/TS 10993-19:2006 Biological evaluation of medical devices Part 19: Physico-chemical, morphological and topographical characterization of materials

ISO/TS 10993-20:2006 Biological evaluation of medical devices Part 20: Principles and methods for immunotoxicology testing of medical devices

ISO 14937:2009 Sterilization of health care products. General requirements for characterization of a sterilizing agent and the development, validation and routine control of a sterilization process for medical devices

ISO EN DIN 9001 (2000) Standard, Quality management systems

ISO EN DIN 13485 (2003) Standard, Medical devices quality management systems

Ito, K., Inoue, S., Hiraku, Y., Kawanishi, S. (2005) Mechanism of site-specific DNA damage induced by ozone. Mutation Research 585 60-70

Jacobs, P.T., Lin, S.M. (1987) Hydrogen peroxide plasma sterilization system. US Patent No. 4,643,876

Jaruga, P., Speina, E., Gackowski, D., Tudek, B. and Olinski, R. (2000) Endogenous oxidative DNA base modifications analysed with repair enzymes and GC/MS technique Nucleic Acids Research. 28 E16-E16

Jiang, H., Su, W., Mather, P.T., Bunning, T.J. (1999) Rheology of highly swollen chitosan/polyacrylate hydrogels. Polymer 40 4593–4602

Jianqi, F., Lixia, G. (2002) PVA/PAA thermo-crosslinking hydrogel fiber: preparation and pH-sensitive properties in electrolyte solution. European Polymer Journal 38:1653-1658

Jin, S., Liu, M., Zhang, F., Chen, S., Niu A. (2006) Synthesis and characterization of pH-sensitivity semi-IPN hydrogel based on hydrogen bond between poly(N-vinylpyrrolidone) and poly(acrylic acid). Polymer 47 1526–1532

Jimenez, A., Zhang, J., Matthes, M.A. (2008) Evaluation of CO_2-based cold sterilization of a model hydrogel. Biotechnology and Bioengineering 101 1344-1352

Johannsen, F.R., Vogt, B., Waite, M., Deskin R. (2008) Mutagenicity assessment of acrylate and methacrylate compounds and implications for regulatory toxicology requirements. Regulatory Toxicology and Pharmacology 50 322-35

Jondeau, A., Dahbi, L., Bani-Estivals, M. H., Chagnon, M.C. (2006) Evaluation of the sensitivity of three sublethal cytotoxicity assays in human HepG2 cell line using water contaminants. Toxicology 226 218-228

Jones, A., Vaughan, D. (2005) Hydrogel dressings in the management of a variety of wound types: A review Journal of Orthopaedic Nursing 9 1-11

Joshi, A.A., Locke, B.R., Arce, P., Finney, W.C. (1995) Formation of hydroxyl radicals, hydrogen peroxide and aqueous electron bypulsed streamer corona discharge in aqueous solution. Journal of Hazardous Material 41 3

Jung, J.S., Moon, J.D. (2008) Corona discharge and ozone generation characteristics of a wire-plate discharge system with a glass-fiber layer. Journal of Electrostatics 66 (2008) 335–341

Jyoti K.K., Padnit, A.B (2002) Ozone and cavitation for water disinfection Biochemical Engineering Journal 18 9-10

Kaczmarek, H., Szalla, A., Kaminska, A., (2001) Study of poly(acrylic acid)-poly(vinylpyrrolidinone) complex and their photostability. Polymer 42 6057-59

Kamath, K.R., Park, K. (1993) Biodegradable hydrogels in drug delivery. Advanced Drug Delivery Reviews 11 59-84

Kanazawa, S., Ito, T., Shuto, Y., Ohkubo, T., Nomoto, Y., Mizeraczyk, J. (2002) Characteristics of laser-induced streamer corona discharge in a needle-to-plate electrode system Journal of Electrostatics 55 343-350

Kaneko, N., Sugioka, T., Sakurai, H. (2007) Aluminum compounds enhance lipid peroxidation in liposomes: Insight into cellular damage caused by oxidative stress Journal of Inorganic Biochemistry 101 967-975

Kanjackal, D., Lopina, S., Evancho-Chapman, M., Schmidt, S., Donovan, D. (2008) Effects of sterilization on poly(ethylene glycol) hydrogels. Journal of biomedical materials research. Part A 87 608-617

Kappas, A. (1990) Mechanisms of environmental mutagenesis-carcinogenesis. Plenum Press, New York, US

Karsa, D., Stephenson, R. (1996) Chemical aspects of drug delivery systems. Cambridge. The Royal Society of Chemistry 4

Kasprzak, K.S. (2002) Oxidative DNA and protein damage in metal-induced toxicity and carcinogenesis. Free Radical Biology and Medicine 32 958-967

Kavanagh, G.M., Ross-Murphy, S.B. (1998) Rheological characterisation of polymer gels. Progress in Polymer Science., Vol. 23, 533-562, 1998

Kawahara, T., Nomura, Y., Tanaka, N., Teshima, W., Okazaki, M., Shintani, H. (2004) Leachability of plasticizer and residual monomer from commercial temporary restorative resins. Journal of Dentistry 32 277-283

Kawanishi, S., Hiraku, Y., Oikawa, S. (2001). Mechanism of guanine-specific DNA damage by oxidative stress and its role in carcinogenesis and aging. Mutation Research. 488 65–76

Kessler, F.K., Laskin, D.L., Borzelleca, J.F., Carchman, R.A. (1980) Assessment of somatogenotoxicity of povidone-iodine using two *in vitro* assays. Journal of Environmental Pathology and Toxicology 4 327-335

Kindernay, J., Blazková, A., Rudá, J., Jancovicová, V., Jakubíková Z. (2002) Effect of UV light source intensity and spectral distribution on the photopolymerisation reactions of a multifunctional acrylated monomer. Journal of Photochemistry and Photobiology A: Chemistry 151 229-236

Kirsch, P., Dati, F., Freisberg, K.O., Birnstiel, H., Mirea, D., Zeller, H. (1972) Report on a study on the effects of Kollidon 90 when applied orally to rats over a 25-day period. Unpublished report from BASF Gewerbehygiene and Toxikologie, Ludwigshafen, Germany. Submitted to the World Health Organization by BASF

Kirsch, P., Dati, F., Freisberg, K.O., Hempel, K.J., Mirea, D., Peh, J., Deckardt, K., Zeller, H. (1975a) Report on a study on the effects of polyvinylpyrrolidone (kollidon 90) when applied orally to dogs over a 28-day toxicity test period. Unpublished report from BASF Gewerbehygiene and Toxikologie, Ludwigshafen, Germany. Submitted to the World Health Organization by BASF

Kirsch, P., Deckardt, K., Mirea, D., Hempel, K. J., Merkle, J. (1975b) Report on testing of Kollidon CE5050 for toxicity when administered to rats over a 28-day period. Unpublished report from BASF. Gewerbehygiene and Toxikologie, Ludwigshafen, Germany. Submitted to the World Health Organization by BASF

Klebanoff, S.J. (1993) Reactive nitrogen intermediates and animicobal acticity: Role of nitrite. Free Radical Biology and Medicine 14 351-360

Kleinsasser, N.H, Wallner, B.C., Harreus, U.A., Kleinjung, T., Folwaczny, M., Hickel, R., Kehe, K., Reichel, F.X. (2004) Genotoxicity and cytotoxicity of dental materials in human lymphocytes as assessed by the single cell microgel electrophoresis (comet) assay Journal of Dentistry 32 229-34

Klimisch, H.J., Deckardt, K., Gembardt, C., Hildebrand, B., Kuttler, K., Roe, F.J. (1997a) Subchronic inhalation and oral toxicity of *N*-vinylpyrrolidone-2. Studies in rodents. Food Chemistry Toxicology 35 1061-1074

Klimisch, H.J., Deckardt, K., Gembardt, C., Hildebrand, B., Kuttler, K., Roe, F.J. (1997b) Long-term inhalation toxicity of N-vinylpyrrolidone-2 vapours. Studies in rats. Food Chemistry Toxicology 35 1041-1060

Knasmueller, S., Parzefall, W., Sanyal, R., Ecker, S., Schwab, M., Uhl, M., Mersch-Sundemann, V.G., Williamsn, Hietsch G., Langer, T., Darroudi, F., Natarajan, A.T. (1998) Use of metabolically competent human hepatoma cells for the detection of mutagens and antimutagens. Mutation Research 402 182-202

Knapp, A.G.A., Voogd, C.E., Kramers, P.G.N. (1985) Mutagenicity of vinyl compounds. Mutation Research 147 303

Knaapen, A.M., Schins, R.P., Borm P.J., van Schooten, F.J. (2005)Nitrite enhances neutrophil-induced DNA strand breakage in pulmonary epithelial cells by inhibition of myeloperoxidase. Carcinogenesis 26 1642-1648

Kohn, J., Langer, R. (1984) A new approach to the development of bioerodible polymers for controlled release applications employing naturally occurring amino acids, in Polymeric materials. Science and Engineering. American Chemical Society, Washington, DC 51 119–121

Kohn, J., Langer, R. (1987) Polymerization reactions involving the side chains of a-L-amino acids, American Chemistry Society 109 817–820

Kolikov, V.A., Kurochkin, V.E., Panina, L.K., Rutberg, A.F., Rutberg1, F.G., Snetov1, V.N., Stogov, Y.U. (2007) Prolonged microbial resistance of water treated by a pulsed electrical discharge. Technical Physics 52 2 163-270

Kokabi, M., Sirousazar, M., Hassan, Z.M. (2007) PVA–clay nanocomposite hydrogels for wound dressing. European Polymer Journal 43 773-781

Kopeček, J., Yang, Y. (2007) Hydrogels as smart biomaterials. Polymer International 56 1078-1098

Korkina L., Kostyuk V., Guerra, L. (2009) Biohydrogles for the *in vitro* re-construction and *in situ* regeneration of human skin, in Hydogels - biological properties and apllications. Editor: Barbucci, R., Springer, Milan, Italy 97-109

Kost, J., Langer, R. (2001) Responsive polymeric delivery systems. Advanced Drug Delivery Reviews 46 125-148

Kotnik, T., Miklavcˇic, D., Lluis M. (2001) Cell membrane electropermeabilization by symmetrical bipolar rectangular pulses Part II: Reduced electrolytic contamination. Bioelectrochemistry 54 91-95

Kulicke, W.M., Nottelmann, H. (1989) Polymers in aqueous media –Performance through association. Editor: Glas J.E., American Chemical Society, Washington D.C., US 15-44

Kurtz, S.M., Muratoglu, O.K., Evans, M., Edidin, A.A. (1999) Advances in the processing, sterilization, and crosslinking of ultra-high molecular weight polyethylene for total joint arthroplasty. Biomaterials 20 1659-1688

Kuchling H (2001) Taschenbuch der physik. 17. ed., Fachbuchverlag Leipzig, Germany

LaBerge, J.E., Venugopalan, R., Lucas, L.C. (1998) Friction and wear, in Handbook of Biomaterials Evaluation. Scientific, Technical, and Clinical Testing of Implant Materials 2nd ed., Editor: von Recum, A.F., Macmillan, New York, US 171-194

Lacefield, W., Clare, A. (1998) Ceramics and glasses, in Handbook of biomaterials evaluation. Scientific, Technical, and Clinical Testing of Implant Materials 2nd ed., Editor: von Recum, A.F., Macmillan, New York, US 143-154

LaPorte, R. (1997) Hydrophilic polymer coatings for medical devices - stucture/properties, development, manufacture and applications. Lancaster: Technomic publishing Co. Inc., Florida, US

Larini, A., Bocci, V. (2005) Effects of ozone on isolated peripheral blood mononuclear cells. Toxicology *In Vitro*. 19 55-61

Laroussi, M., Leipold, F. (2004) Evaluation of the roles of reactive species, heat, and UV radiation in the inactivation of bacterial cells by air plasmas at atmospheric pressure. International Journal of Mass Spectrometry 233 81–86

Laroussi, M. (2005) Low temperature plasma-based sterilization: overview and state-of-art. Plasma Processes and Polymers 2 391-400

Lasagni, A., Soldera, F., Mücklich, F. (2004) Quantitative investigation of material erosion caused by high pressure discharges in air and nitrogen. Zeitschrift für Metallkunde **95** 102

Lau, C., Mi, Y. (2002) A study of blending and complexiation of poly(acrylic acid)/poly (vinyl pyrrolidinone). Polymer 43 823-9

Lee, M.H., Kim, H.L., Kim, C.H., Lee, S.H., Kim, J.K., Lee, S.J., Park J.C. (2008) Effects of low temperature hydrogen peroxide gas on sterilization and cytocompatibility of porous poly(d,l-lactic-co-glycolic acid) scaffolds. Surface and Coatings Technology 202 5762-5767

Lee, T. W., Robinson, J. R. (2000) The science and practice of pharmacy, 2nd ed., Lippinocott Williams and Wilkin 903-929

Lee, P.I., Kim, C.J. (1985) Probing the mechanisms of drug release from hydrogels. Journal of Controlled Release 2 277-288

Lemons, J.E., Venugopalan R., Lucas L.C. (1998) Corrosion and biodegradation, in handbook of biomaterials evaluation. Scientific, Technical, and Clinical Testing of Implant Materials 2nd ed., Editor: von Recum, A.F., Macmillan, New York, US 155-170

Lerouge S., Wertheimer M.R., Yahia L.H. (2001) Plasma sterilisation: A review of parameters, mechanisms and limitations. Plasmas and polymers 16 175-188

Lerouge, S., Tabrizian, M., Wertheimer, M.R., Marchand, R., Yahia, L.H. (2002) Safety of plasma-based sterilization: Surface modifications of polymeric medical devices induced by Sterrad® and Plazlyte™ processes. Bio-Medical Materials and Engineering 12 3-13

Lin, C.C., Anseth, K.S. (2009) PEG hydrogels for the controlled release of biomolecules in regenerative medicine. Pharmaceutical Research 26 3

Lin, C.C., Metters, A.T. (2006) Hydrogels in controlled release formulations: Network design and mathematical modeling. Advanced Drug Delivery Reviews 58 1379-1408

Lin, J., Nakajima, T (2003) An AM1 study of decomposition of aqueous ozone Journal of Molecular Structure: Theochem 625 (2003) 161–167

Lin J.K. (1990) Nitrosamines and potential carcinogens in man. Clinical Biochemistry 23 67-71

Lin, S.Y., Chen, K.S., Run-Chu, L. (2001) Design and evaluation of drug loaded wound dressing having thermoresponsive, adhesive, absorptive and easy peeling properties. Biomaterials 22 2999-3004

Liu, H., Zhang, H., Chen, J. (2009) Surface analysis of long-distance oxygen plasma sterilized PTFE film. Applied Surface Science 255 8115–8121

Locey B.J. (2005) Nitrides, in Encyclopedia of Toxicology 2nd ed., Editor: Wexler, P. Academic Press

Loeb, L.A., Preston, B.D. (1986) Mutagenesis by apurinic/apyrimidinic sites. Annual Review Genetics. 20 201–230

Long, T.E., Turner, S.R. (2000) Step-growth polymerization. Applied Polymer Science: 21st Century 979-997

Loomis-Husselbee, J.W., Cullen, P.J., Irvine, R.F., Dawson, A.P. (1991) Electroporation can cause artifacts due to solubilization of cations from the electrode plates. Biochemical Journal 277 883-885

Loo-Teck Ng, Salesh Swami (2005) IPNs based on chitosan with NVP and NVP/HEMA synthesised through photoinitiator-free photopolymerisation technique for biomedical applications. Carbohydrate Polymers 60 523-528

Lovell, P., Omori, T. (2008) Statistical issues in the use of the comet assay. Mutagenesis 23 171 -182

Lü, W., Ding, W. (2005) Dynamic Monte Carlo simulation of chain growth polymerization and its concentration effect Science in China Series B: Chemistry 48 5
459-465

Lu, F. C. (1991) Basic toxicology fundamentals, target organs, and risk assessment, 2nd Ed., Hemisphere Publishing Corporation New York, US 93-110

Luck, M., Paulke, B.R., Schroder, W., Blunk, T., Muller, R.H. (1998) Analysis of plasma protein adsorption on polymeric nanoparticles with different surface characteristics. Journal of Biomedical Material Research 39 478-485

Lukeš, P., Člupek, M., Babický, V., Šunka, P., Skalný, J.D., Štefečka, M., Novák, J., Málková, Z. (2006) Erosion of needle electrodes in pulsed corona discharge in water. Czechoslovak Journal of Physics 56 916-924

Lullmann-Rauch, R. (1979) Drug-induced lysosomal storage disorders. Front Biology 48: 49-130

Madden, L.A., Anderson, A.J., Shah, D.T., Asrar, J. (1999) Chain termination in polyhydroxyalkanoate synthesis: involvement of exogenous hydroxy-compounds as chain transfer agents. International Journal of Biological Macromolecules 25 43-53

Mallapragada S.K., Narasimhan B. (1998) Drug delivery systems, in Handbook of biomaterials evaluation. Scientific, Technical, and Clinical Testing of Implant Materials 2nd ed., Editor: von Recum, A.F., Macmillan, New York, US 425-438

Mason, R.S., Pichilingi, M. (1994) Sputtering in a glow discharge ion source - pressure dependence: Theory and experiment. Journal of Physics D: Applied Physics 27 2363

Masschelein, W. J. (1982) Ozonation manual for water and wastewater treatment. John Wiley & Sons

Mathur, A.M., Moorjani, K.S., Scranton, A.B. (1996) Methods for Synthesis of Hydrogel Networks: A Review. Polymer Reviews 36 405-430

Marsili, L., Espie, S., Anderson, J.G., MacGregor, S.J., Rowan, N.J. (2002) Plasma inactivation of food–related microorganisms in liquids. Radiation Physics and Chemistry 65 507-513

Martens, P.A., Galliani, V., Graham, G., Caputo, R.A. (1998) Sterilization of medical products using gas plasma technology, in Sterilization of drugs and devices. Editors: Nordhauser, F.M., Olson, W.P., Interpharm Press, Inc., Illinois, US 157-195

McDonald, K.F., Curry, R.D., Clevenger, T.E., Unklesbay, K., Eisenstark, A., Golden, J. and Morgan, R.D. (2000) A comparison of pulsed and continuous ultraviolet light sources for the decontamination of surfaces. IEEE Transactions on Plasma Science 28 1581–1587

McGlynn, A.P., Wasson, G., O'Connor, J., McKelvey-Martin, V., Downes, C.S. (1999) The bromodeoxyuridine comet assay. Cancer Research 59:5912-5916

McIlvaney, L., MacGregor, S.J., Anderson, J.G., Rowan, N.J., Fourarce, R.A., Farish, O. (1998) Electrotechnologies for food pasteurization and sterilisation. Proceedings of the IEE. Symposium Pulsed Power 98

McNamee, J.P., McLean, J.R.N., Ferrarotto, C.L., Bellier, P.V. (2000) Comet assay: rapid processing of multiple samples. Mutation Research/Genetic Toxicology and Environmental Mutagenesis 466 63-69

Mehdinia, A., Ghassempour, A., Rafati, H., Heydari, R. (2007) Determination of *N*-vinyl-2-pyrrolidone and *N*-methyl-2-pyrrolidone in drugs using polypyrrole-based headspace solid-phase microextraction and gas chromatography–nitrogen-phosphorous detection. Analytical Chimica Acta 587 182-88

Mehlman, M.A., Borek, C. (1987) Toxicity and biochemical mechanisms of ozone. Environmental Research 42 36-53

Mehyar, G.F., Liu, Z., Han, J.H. (2008) Dynamics of antimicrobial hydrogels in physiological saline. Carbohydrate Polymers 74 92-98

Menashi, W.P. (1968) Treatment of surfaces. US Patent No. 3,383,163

Mendes, G.C.C., Brandao, T.R.S., Silva, C.L.M. (2007) Ethylene oxide sterilization of medical devices: A review. American Journal of Infection Control 35 574-581

Mendis, D.A., Rosenberg, M. Azam, F. (2000) A note on the possible electrostatic disruption of bacteria. Plasma Science, IEEE Transactions on 28 1304–1306

Meyvis, T.K., Stubbe, B.G., van Steenbergen, M.J., Hennink, W.E., de Smedt, S.C., Demeester J. (2002) A comparison between the use of dynamic mechanical analysis and

oscillatory shear rheometry for the characterisation of hydrogels. International Journal of Pharmaceutics 244 163-168

Miller, J.S., Shen, C.J., Legant, W.R., Baranski, J.D., Blakely, B.L., Chen, C.S. (2010) Bioactive hydrogels made from step-growth derived PEG–peptide macromers. Biomaterials 31 3736-3743

Moisan, M., Barbeau, J., Crevier, M.C., Pelletier, J., Nicolas, P., Saoudi, B. (2002) Plasma sterilization. Methods and mechanisms. Pure and Applied Chemistry 74 349–358

Moisan, M., Barbeau, J., Moreau, S., Pelletier, J., Tabrizian, M., Yahia, L.H. (2001) Low-temperature sterilization using gas plasmas: a review of the experiments and an analysis of the inactivation mechanisms. International Journal of Pharmaceutics 226 1–21

Monarca, S., Feretti, D., Collivignarelli, C., Guzzella, L., Zerbini, I., Bertanza, G., Pedreazzani, R. (2000) The influence of different disinfectants on mutagenicity and toxicity of urban wastewater. Water Research 34 4261-4269

Montie, T.C., Kelly-Wintenberg, K., Roth, J. (2000) An overview of research using the one atmosphere uniform glow discharge plasma (OAUGDP) for sterilization of surfaces and materials. IEEE Transactions on Plasma Science 28 41–50

Moore, M.M., Amtower, A., Doerr, C.L., Brock, K.H., Dearfield, K.L. (1988) Genotoxicity of acrylic acid, methyl acrylate, ethyl acrylate, methyl methacrylate and ethyl methacrylate in L5178Y mouse lymphoma cells. Environmental and Molecular Mutagenesis 11 49–63

Moreau, S., Moisan, M., Tabrizian, M., Barbeau, J., Pelletier, J., Ricard A.(2000) Using the flowing afterglow of plasma to inactivate Bacillus subtilis spores: influence of the operating conditions. Journal of Applied Physics 88 1166–1174

Moreau, M., Orange, N., Feuilloley, M.G.J. (2008) Non-thermal plasma technologies: New tools for bio-decontamination. Biotechnology advances 26 610-617

Moreira, A.J., Mansano, R.D., Pinto, T.dJ.A., Ruas, R., Zambon L.dS, Silva, M.Vd., Verdonck P.B. (2004) Sterilization by oxygen plasma. Applied Surface Science 235 151-155

Moriwaki, H., Osborne, M.R., Phillips, D.H. (2008) Effects of mixing metal ions on oxidative DNA damage mediated by a Fenton-type reduction Toxicology *In Vitro* 22 36-44

Morley, N., Rapp A., Dittmar H., Salterl L., Gould, D., Greulich, K.O., Curnow, A. (2006) UVA-induced apoptosis studied by the new apo/necro-Comet-assay which distinguishes viable, apoptotic and necrotic cells. Mutagenesis 21 105-114

Mosmann, T. (1983) Rapid colorimetric assay for cellular growth and survival: Application to proliferation and cytotoxicity assays. Journal of Immunological Methods 65 55-63

Mrad, O., Saunier, J., Aymes Chodur, C., Rosilio, V., Agnely, F., Aubert, P, Vigneron, J., Etcheberry, A., Yagoubi, N. (2010) A comparison of plasma and electron beam-sterilization of PU catheters. Radiation Physics and Chemistry 79 93-103

Murakami, K., Aoki, H., Nakamura, S., Nakamura, S.I., Takikawa, M., Hanzawa, M, Kishimoto, S., Hattori, H., Tanaka, Y., Kiyosawa, T., Sato, Y., Ishihara, M. (2010) Hydrogel blends of chitin/chitosan, fucoidan and alginate as healing-impaired wound dressings. Biomaterials 31 83-90

Nair, P.D. (1995) Currently practised sterilization methods–some inadvertent consequences. Journal of Biomaterials Applications 10 121–35

Napper, D.H., Hunter, R.J. (1972) Surface chemistry and colloids, 7th ed., Editor: Keker, M., Universal Press: Baltimore, US

Nardo, Ld., Alberti, R., Cigada, A., L'Hocine, Y., Tanzi, M.C., Farè, S (2009) Shape memory polymer foams for cerebral aneurysm reparation: Effects of plasma sterilization on physical properties and cytocompatibility. Acta Biomaterialia 5 1508-1518

Nguyen, K.T., West, J.L. (2002) Photopolymerizable hydrogels for tissue engineering applications. Biomaterials 23 4307–4314

Nna Mvondo, D., Navarro-Gonzalez, R., McKay, C.P., Coll, P., Raulin, F. (2001) Production of nitrogen oxides by lightning and coronae discharges in simulated early Earth, Venus and Mars environments. Advanced Space Research 27217-23

Northup, S.J., Cammack, J.N. (1998) Mammalian cell culture models, in Handbook of biomaterials evaluation. Scientific, Technical, and Clinical Testing of Implant Materials 2nd ed., Editor: von Recum, A.F., Macmillan, New York, US 325-339

Nuttelman, C.R., Rice, M.A., Rydholm, A.E., Salinas, C.N., Shah, D.N., Anseth, K.S. (2008) Macromolecular Monomers for the Synthesis of hydrogel niches and their application in cell encapsulation and tissue engineering. Progress in Polymer Science 33 167-179

Oda, T., Yamashita, Y., Takezawa, K., Ono, R. (2006) Oxygen atom behaviour in the nonthermal plasma. Thin Solid Films 669-673

O'Hare, S., Atterwill, C.K. (1995) *In vitro* toxicity testing protocols. Methods in molecular biology. Humana Press Inc., New Jersey, US

Ohshima, H. (2003) Genetic and epigenetic damage induced by reactive nitrogen species: implications in carcinogenesis. Toxicology Letters 140 99-104

Ohyashiki, T., Satoh, E., Okada, M., Takadera, T., Sahara, M. (2002) Nerve growth factor protects against aluminum-mediated cell death. Toxicology 176 195-207

Oldreive, C., Zhao, K., Paganga, G., Halliwell, B., Rice-Evans, C. (1998) Inhibition of nitrous acid-dependent tyrosine nitration and DNA base deamination by flavonoids and other phenolic compounds. Chemical Research in Toxicology 11 1574-1579

Olinski, R., Zastawny, T.H., Foksinski, M., Barecki, A., Dizdaroglu, M. (1995) DNA base modifications and antioxidant enzyme activities in human benign prostatic hyperplasia. Free Radical Biology and Medicine 18 807-813

Olive, P. L., Banath, J. P., Durand R.E. (1990) Heterogeneity in radiation induced DNA damage and repair in tumor and normal cells measured using the comet assay. Radiation Research 122: 86-94

Oosting, R.S., van Rees-Verhoef, M., Verhoef, J., van Golde, L.M.G., van Bree, L. (1991) Effects of ozone on cellular ATP levels in rat and mouse alveolar macrophages. Toxicology 70 195-202

Okano, T. (1998) Biorelated Polymers and Gels – Controlled release and Applications in Biomedicla Engineering. San Diego: Academic Press

Östling, O., Johanson, K.J. (1984). Microelectrophoric study of radiation induced DNA damage in individual mammalian cells. Biochemical and Biophysical Research Communications 123 291-298

Panayiotou, M., Freitag, R. (2005) Synthesis and characterisation of stimuli responsive poly(N,N'-diethylacylamide) hydrogels. Polymer 46 615-621

Park, K., Shalaby, W.S.W., Park, H. (1993) Biodegradable hydrogels for drug delivery. Technomic Publishing Inc., Basel, Germany

Park, H., Park, K. (1996) Hydrogels in Bioapplications, in Hydrogels and Biodegradable Polymers for Bioapplications. Editors: Ottenbrite, R.M., Huang, S.J., Park, K., American Chemical Society, Washington, D.C., US 2-10

Peeples, R.E., Anderson, N.R. (1985) Microwave coupled plasma sterilization and depyrogenation II. Mechanisms of action, Journal of parenteral science and technology 39 9–14

Pekárek, S., Rosenkranz1, J., Kříha, V. (2000) Ozone generation in gas flow enhanced hollow needle to plate electrical discharge in air. Czechoslovak Journal of Physics 50 385-388

Peppas, N.A., Bures, P., Leobandung, W., Ichikawa, H. (2000) Hydrogels in pharmaceutical formulations. European Journal of Pharmaceutics and Biopharmaceutics 50 27-46

Peppas, N.A. (1986) Hydrogels in medicine and pharmacy, CRC Press 1

Peppas, N.A., Khare, A.R. (1993) Preparation, structure and diffusional behavior of hydrogels in controlled-release. Advanced Drug Delivery Reviews 11 1-35

Perl, D.P., Brody, A.R. (1980) X-ray spectrometric evidence of aluminum accumulation in neurofibrillary tangle-bearing neurons. Science 208 297-299

Petersen, A.B., Gniadecki, R., Vicanova, J., Thorn, T., Wulf, C.H. (2000) Hydrogen peroxide is responsible for UVA-induced DNA damage measured by alkaline comet assay in HaCaT keratinocytes. Journal of Photochemistry and Photobiology B: Biology 59 123-131

Piña, R.G., Cervantes, C. (1996) Microbial interactions with aluminium. BioMetals 9 319-316

Pryor, W.A. (1994) Mechanisms of radical formation from reactions of ozone with target molecules in the lung. Free Radical Biology and Medicine 17 451-465

Purna, S.K., Babu, M. (2000) Collagen based dressings—a review. Burns 26 54-62

Qiu, Y., Park, K. (2001) Environment-sensitive hydrogels for drug delivery Advanced Drug Delivery Reviews 53 321-339

Ramakrishna, S., Mayer, J., Wintermantel, E., Leong, K. W. (2001) Biomedical application of polymer-composite material: A Review. Composites Science and Technology 61: 1189-1224

Ratner, B. D., Hoffman, A. S. Schoen, F. J. Lemons, J. E. (1996) Biomaterials science – an introduction to materials in medicine. Academic Press. San Diego, US

Ratner, B.D., Hoffman A.S (1976) Synthetic hydrogels for biomedical applications, in Hydrogesl for medical and related application. Editor: Andrade, F.D., ACS Symposium Series, 31 American Chemistry Society, Washington, D.C., US 311-336

Ravichandran, P., Shantha, K.L., Panduranga Rao, K. (1997) Preparation, swelling characteristics and evaluation of hydrogels for stomach specific drug delivery international Journal of Pharmaceutics 154 89-94

Razzak, M.T., Darwis, D., Sukirno, Z. (2001) Irradiation of poly(vinyl alcohol) and poly(vinyl pyrrolidone) belended hydrogel for wound dressing. Radiation Physics and Chemistry 62 107-113

Recum, A.F., Jenkins, M.E., Recum, H.A. (1998) Introduction: Biomaterials and biocompatibility, in Handbook of biomaterials evaluation. Scientific, Technical, and Clinical Testing of Implant Materials 2nd ed., Editor: Recum, A.F., Macmillan, New York, US 1-36

Reid, G., Busscher, H.J. (1992) Importance of surface properties in bacterial adhesion to biomaterials, with particular reference to the urinary tract. International Biodeterioration and Biodegradation 30 105-122

Redtenbacher J. (1843) Ueber die zerlegungsprodukte des glycerinoxydes durch trockene destillation. Annalen der Chemie und Pharmacie 47 113–148

Rehbein, N., Cooray, V. (2001) NO_X production in spark and corona discharges Journal of Electrostatics 51 333-339

Reyns, K.F.M.A., Diels A.M.J., Michiels C.W. (2004) Generation of bactericidal and mutagenic components by pulsed electric field treatment. International Journal of Food Microbiology 93 165-173

Rice, R.G., Farquhar, J.W., Bollyky, L.J. (1982) Potential Applications of ozone for increasing storage time of perishable food. Ozone Science and Engineering 4 147-164

Rickert, D., Lendlein, A., Kelch, S., Fuhrmann, R., Franke, R.P. (2002) Detailed evaluation of the agarose diffusion test as a standard biocompatibility procedure using an image analysis system. Influence of plasma sterilization on the biocompatibility of a recently developed photoset-polymer. Biomedizinische Technik 47 285-289

Rimondini, L., Fini, M., Giardino, R. (2005) The microbial infection of biomaterials: A challenge for clinicians and researchers. A short review. Journal of Applied Biomaterials and Biomechanics 3 1-10

Robinson, B.V., Sullivan, F.M., Borzelleca, J.F., Schwartz, S.L. (1990) A critical review of the kinetics of polyvinylpyrroolidone (povidone). Lewis publishers, Washington D.C., US

Rogers, W. (2005) Sterilisation of polymers and healthcare products. Rapra Technology Ltd., Shrewsbury, UK

Rosiak, J.M., Rucinska-Rybus A., Pekala, W. (1989) Method of manufacturing of hydrogel dressings Patent USA, No. 4, 871, 490

Rosiak, J.M., Yoshii, F. (1999) Hydrogels and their medical applications. Nuclear Instruments and Methods in Physics Research Section B: Beam Interactions with Materials and Atoms 151 56-64

Rosenbluth, S.A., Weddington, G.R., Guess, L.W., Autian, J. (1965) Tissue culture method for screening toxicity of plastics to be used in medical practice. Journal of Pharmaceutical Science 54 156-159

Rossi, F., Kylian, O., Hasiwa, M. (2006). Decontamination of surfaces by low pressure plasma discharges. Plasma Processes and Polymers 3 431-442

Routledge, M., Mirsky, F.J., Wink, D.A., Keefer, L.K., Dipple, A. (1994) Nitrite-induced mutations in a forward mutation assay concentration and pH. Mutation Research/Genetic Toxicology 322 341-346

Rowan, N.J. (1999) Evidence that inimical food-preservation barriers alter microbial resistance, cell morphology and virulence. Trends in Food Science and Technology 10 261-270

Rowan, N.J., MacGregor, S.J., Anderson, J.G., Fouracre, R.A., McIlvaney, L. and Farish, O. (1999) Pulsed-light inactivation of food-related micro-organisms. Applied and Environmental Microbiology 65 1312–1315

Rowan, N.J., MacGregor, S.J., Anderson, J.G., Cameron, D. and Farish, O. (2001) Inactivation of Mycobacterium paratuberculosis by pulsed electric fields. Applied and Environmental Microbiology 67 2833–2836

Rowan, N.J., Espie, S., Harrower, J., Anderson, J.G., Marsili, L., MacGregor, S.J. (2007) Pulsed-Plasma Gas-Discharge Inactivation of Microbial Pathogens in Chilled Poultry Wash Water. Journal of food protection 70 2805-2810

Rowan, N.J., Espie, S., Harrower, J., Farrell, H., Marsili, L., Anderson, J.G. MacGregor, S.J. (2008) Evidence of lethal and sublethal injury in food-borne bacterial pathogens exposed to high-intensity pulsed-plasma gas discharges. Letters in Applied Microbiology 46 80-86

Rudin, A. (1999) Step-Growth Polymerizations. Elements of Polymer Science and Engineering, 2nd 155-188

Russel, W., Burch, R. L. (1959) The Principle of Humane Experimental Technique. Methuen, London, UK 238

Rzaev, Z., Dincer, S., Piskin, E. (2007) Functional copolymers of *N*-isopropylacrylamide for bioengineering applications. Program of Polymer Science 32 534-595

Sadtler (1980) The infrared spectra atlas of monomers and polymers. Sadtler research laboratories Philadelphia, Pennsylvania, US

Sandhu, J.L., Birnboim, H.C. (1997) Mutagenicity and cytotoxicity of reactive oxygen and nitrogen species in the MN-11 murine tumor cell line. Mutation Research/Fundamental and Molecular Mechanisms of Mutagenesis 379 241-252

Satish, C.S., Satish, K.P., Shivakumar, H.G. (2006) Hydrogels as controlled drug delivery systems: Synthesis, crosslinking, water and drug transport mechanism. Indian Journal of Pharmaceutical Science 68 133-140

Sato, M., Ohgiyama, T., Clements, J.S. (1999) Formation of chemical species and their effects on microorganisms using a pulsed high-voltage discharge in water. IEEE Transactions on Industry. Applications 32 1 106-112

Satoh, K., MacGregor, S.J., Anderson J.G., Woolsey G.A, Fouracre, R.A. (2007) Pulsed plasma disinfection of water containing *Escherichia coli*. Japanese Journal of Applied Physics 46 1137-1141

Schacht, E.H. (2004) Polymer chemistry and hydrogel systems. Journal of Physics: Conference Series 3 22–28

Scheffner, D. (1955) Tolerance and side-effects of various kollidons administered by mouth and their behavior in the gastrointestinaltract (translation from German), Doctor Thesis, University of Heidelberg

Schweikl, H., Schmalz, G., Rackebrandt, K. (1998) The mutagenic activity of unpolymerized resin monomers in *Salmonella typhimurium* and V79 cells. Mutation Research/Genetic Toxicology and Environmental Mutagenesis 415 119-130

Seet, K.K., Juodkazis, S., Jarutis, V., Misawa, H. (2006) Feature-size reduction of photopolymerized structures by femtosecond optical curing of SU-8. Applied Physics Letters 89

Siepmann, J., Göpferich, A. (2001) Mathematical modelling of bioerodible, polymeric drug delivery systems. Advanced Drug Delivery Reviews 48 229 -247

Simmon, V.F., Baden, J.M. (1980) Mutagenic activity of vinyl compounds and derived epoxides. Mutation Research 78 227-231

Simo, C., Cituefentes, A., Gallardo A. (2003) Drug delivery: polymers and drugs monitored by capillary electromigration methods. Journal of Chromatography B. 797 37-49

Singh, N.P. (1996) Microgel electrophoresis of DNA from individual cells. Principles and methodology; in Technologies for detection of DNA Damage and mutations. Editor: Pfeifer, G.P., Plenum, New York, US 2-24

Singh, N.P., McCoy, M.T., Tice, R.R., Schneider, E.L. (1988) A simple technique for quantitation of low levels of DNA damage in individual cells. Experimental Cell Research 175 184-191

Shantha, K.L., Harding, D.R.K. (2003) Synthesis, characterisation and evaluation of poly[lactose acrylate-N-vinyl-2-pyrrolidinone] hydrogels for drug delivery European Polymer Journal 39 63-68

Shiki, H., Motoki, J., Takikawa, H., Sakakibara, T., Nishimura, Y., Hishida, S., Okawa, T., Ootsuka, T. (2007) Electrode Erosion in Pulsed Arc for Generating Air Meso-Plasma Jet under Atmospheric Pressure IEEJ Transactions on Fundamentals and Materials. 127 567-573

Simek, M., Clupek, M. (2002) Efficiency of ozone production by pulsed positive corona discharge in synthetic air Journal of Physics D: Applied Physiks 35 1171-1175

Sinha, R., Islam, M., Bhadra, K., Kumar, G.S., Banerjee, K., Maiti, M. (2005) The binding of DNA intercalating and non-intercalating compounds to a-form and protonated form of poly(rC)Epoly(rG): Spectroscopic and viscometric study. Bioorganic and Medicinal Chemistry 14 800–814

Smith, L.E., Rimmer, S., MacNeil, S. (2006) Examination of the effects of poly (N-vinylpyrrolidinone) hydrogels in direct and indirect contact with cells Biomaterials 27 2806-2812

Sousa, G., Delescluse, C., Pralavorio, M., Perichaud, M., Avon, M., Lafaurie M., Rahmani, R. (1998) Toxic effects of several types of antifouling paints in human and rat hepatic or epidermal cells. Toxicology Letters 96-97 41-46

Sparrow, J. R., Vollmer-Snarr, H. R., Zhou, J., Jang, Y. P., Jockusch, S., Itagaki, Y., Nakanishi, K. (2003) A2E-epoxides damage DNA in retinal pigment epithelial cells. vitamin E and other antioxidants inhibit A2E-epoxide formation. J. Biology. Chemistry 278 18207-18213

Spaulding E.N. (1972) Chemical Disinfection and Antisepsis in the hospital. Journal of Hospital Research 9 5-31

Spencer, J.P.E., Jenner, A., Chimel, K., Aruoma, O.I., Cross, C.E., Wu, R., Halliwell, B. (1995) DNA strand breakage and base modification induced by hydrogen peroxide treatment of human respiratory tract epithelial cells. FEBS Letters 374 233-236

Spencer, J.P., Whiteman, M., Jenner, A., Halliwell, B. (2000) Nitrite-induced deamination and hypochlorite-induced oxidation of DNA in intact human respiratory tract epithelial cells. Free Radical Biology and Medicine 28 1039-1050

Stacy, G., MacDonald, C. (2001) Immortilisation of primary cells, in Cell culture Methods for *in vitro* Toxicology. Editors: Stacy, G., Doyel, A., Ferror, M., Academic Publisher

Staehelin, J., Hoigńe, J. (1985) Decomposition of ozone in water in the presence of organic solutes acting as promoters and inhibitors of radical chain reactions. Environ Science and Technology 19 1206–1213

Stakey, B.J. (1987) Aluminum in renal disease: current knowledge and future developments. Annals of Clinical Biochemistry 24 337–344

Stammen, J.A., Williams, S., Ku, D.N, Guldberg, R.E. (2001) Mechanical properties of a novel PVA hydrogel in shear and unconfined compression. Biomaterials 22 799–806

Stapulionis, R. (1999) Electric pulse-induced precipitation of biological macromolecules in Electroporation. Bioelectrochemistry and Bioenergetics 48 249-254

Steelman, V.M. (1992) Issues in sterilization and disinfection. Urologic Nursing 12 123-127

Stoop, R. (2008) Smart biomaterials for tissue engineering of cartilage. Injury 39 77-87

Stoy, V.A (1999) Hydrogels, in Enceclopedia of pharmaceutical technology volume 18th ed., Editor: Swarbrick J., Boylan J.C. Marcel Dekker Inc., New York, US 91-119

Strauss, G.H.S (1991) Non-random cell killing in cryopreservation: Implications for the performance of the battery of leucocyte tests (BLT) I. Toxic and immunotoxic effects. Mutation Research Environmental/Mutagenesis 252 1-16

Summerfelt S. T, Hochheimer J.N. (1997) Review of ozone processes and applications as an oxidizing agent in aquaculture. The Progressive Fish-Culturist 59 94-105

Sun, J., Aoki, K., Wang, W., Guo, A., Misumi, J. (2006) Sodium nitrite-induced cytotoxicity in cultured human gastric epithelial cells. Toxicology *In Vitro* 20 (2006) 1133–1138

Sung, J.H., Hwang, M.R., Kim, J.O., Lee, J.H., Kim, Y.I., Kim, J.H., Chang, S.W., Jin, S.G., Kim, J.A., Lyoo, W.S., Soo, S.H., Ku, S.K., Yong, C.S., Choi, H.G. (2010) Gel characterisation and in vivo evaluation of minocycline-loaded wound dressing with enhanced wound healing using polyvinyl alcohol and chitosan. International Journal of Pharmaceutics, In Press, Corrected Proof

Sunka, P., Babicky, V., Clupek, M., Lukes, P., Simek, M., Schmidt, J., Cernak, M., (1999) Generation active species by electrical discharges in water. Plasma Sources Science and Technology 8 258

Száraz, I., Forsling W. (2000) A spectroscopic study of the solvation of 1-vinyl-2-pyrrolidone and poly(1-vinyl-2-pyrrolidone) in different solvents. Polymer 41 4831–4839

Takaki, K., Hatanaka, Y., Arimaa, K., Mukaigawaa, S., Fujiwara, T. (2008) Influence of electrode configuration on ozone synthesis and microdischarge property in dielectric barrier discharge reactor. Vacuum 83 1 128-132

Tarafa, P.J., Jiménez, A., Zhang, J., Matthews, M.A. (2010) Compressed carbon dioxide (CO_2) for decontamination and tissue scaffolds. Journal of Supercritical Fluids 53 192-199

Tendero, C., Tixier, C., Tristant, P., Desmaison, J., Leprince, P. (2006) Atmospheric pressure plasmas: A review. Spectrochimica Acta Part B: Atomic Spectroscopy 61 12-30

Tensmeyer, L.G. (1976) Method of killing microorganisms in the inside of a container utilizing a laser beam induced plasma US Patent No. 3,955,921

Tensmeyer, L.G. (1977) Method of killing microorganisms in the inside of a container utilizing a plasma initiated by a focused laser beam and sustained by an electromagnetic field. US Patent No. 4,042,325

Tice, R.R., Agurell, E., Anderson, D., Burlinson, B., Hartmann, A., Kobayashi, H., Miyamae, Y., Rojas, E., Ryu, J.C., Sasaki, Y. F. (2000). Single cell gel/comet assay: guidelines for *in vitro* and *in vivo* genetic toxicology testing. Environmental and Molecular Mutagenesis 35 206–221

Timbrell, J.A. (2009) Principles of biochemical toxicology, 4th ed., Taylor and Francis Washington, DC, US 190-210

Toimela, T., Mäenpää, H., Mannerström, M., Tähti, H. (2004) Development of an *in vitro* blood-brain barrier model-cytotoxicity of mercury and aluminum. Toxicology and Applied Pharmacology 195 73-82

Tomov, T., Tsoneva, I. (2000) Are the stainless steel electrodes inert? Bioelectrochemistry 51 207-209

Tsai W.T. (2007) The decomposition products of sulfur hexafluoride (SF_6): Reviews of environmental and health risk analysis. Journal of Fluorine Chemistry, 128 1345-1352

Tunney, M.M., Gorman, S.P. (2002) Evaluation of a poly(vinyl pyrollidone)-coated biomaterial for urological use. Biomaterials 23 4601-4608

Twentymann, P.R., Luscombe, M. (1987) A study of some variables in tetrazolium dye (MTT) based assay for cell growth and chemosensitivity. British Journal Cancer 56 279-385

Uhrich, K.E., Cannizzaro, S.M., Langer, R.S., Shakesheff, K.M. (1999) Polymeric systems for controlled drug release. Chemistry Review 99 3181-3198

Urban, V.M., Machado, A.L., Oliveira, R.V., Vergani, C.E., Pavarina, A.C., Cass, Q.B. (2007) Residual monomer of reline acrylic resins. Effect of water-bath and microwave post-polymerization treatments. Dental Aaterials 23 363–368

US EPA (1984) US Environmental Protection Agency. Health and environmental effects erofile for 2-propenoic acid (acrylic acid). Office of Research and Development, US EPA, Cincinnati, US 25

Vamvakas, S., Vock, E.H., Lutz, W.K. (1997) On the role of DNA double-stand breaks in toxicity and carcinogenesis. Critical Reviews in Toxicology 27 155-157

van Veldhuizen E.M., Rutgers, W.R. (2002) Pulsed positive corona streamer propagation and branching. Journal of Physics D: Applied Physics 35 2169-2179

van Veldhuizen, E.M. (2000) Electrical Discharges for Environmental Purposes - Fundamentals and Applications, Huntington, Nova Science Publishers, Inc., New York, US

Vermeer, I.T., Pachen, D.M., Dallinga, J.W., Kleinjans, J.C., van Maanen, J.M. (1998) Volatile N-nitrosamine formation after intake of nitrate at the ADI level in combination with an amine-rich diet. Environmental Health Perspective 106 459–463

Victorin, K. (1994) Review of the genotoxicity of nitrogen oxides. Mutation Research/Reviews in Genetic Toxicology 317 43-55

Viljanen, E.K., Langer, S., Skrifvars, M., Vallittu, P.K. (2006) Analysis of residual monomers in dendritic methacrylate copolymers and composites by HPLC and headspace-GC/MS. Dental materials 22 845–851

Walker, L.R., Lin H.T., Levina, I., Brady, M.P., Lykowski, J. (2005) SEM and EPMA analysis of spark plug electrode erosion microscopy and microanalysis 11 1614-1615

Wan, L.S., Xu, S.K., Huang, X.J., Wang, Z.G., Wang, J.L. (2005) Copolymerization of acrylonitrile with N-vinyl-2-pyrrolidone to improve the hemocompatibility of polyacrylonitrile Polymer 46 7715-7723

Wang, M., Xu, L., Hu, H., Zhai, M., Peng, J., Nho, Y., Li, J., Wei, G. (2007a) Radiation synthesis of PVP/CMC hydrogels as wound dressing. Nuclear Instruments and Methods in Physics Research Section B: Beam Interactions with Materials and Atoms 265 385-89

Wang, C.C., Lu, J.N., Young, T.H. (2007b) The alteration of cell membrane charge after cultured on polymer membranes. Biomaterials 28 625-631

Wang, C., Chen, J., Li, R. (2008) Studies on surface modification of poly (tetrafluoroethylene) film by remote and direct Ar plasma. Applied Surface Science 254 2882-2888

Watson, H.E. (1908) A note on the variation of the rate of disinfection with change in the concentration of disinfectant. Journal of Hygiene 8 536-542

Weiner, M., Kotkoskie L. (1996) Excipient toxicity and safety –drugs and pharmaceutical science. Marcel Dekker, New York 123- 321

Wenjuan, B., Xiangli, Y. (2007) Nitrogen Fixation into HNO_3 and HNO_2 by Pulsed High Voltage Discharge. Plasma Science Technology 9 288-291

Weyermann, J., Lochmann, D., Zimmer, A. (2005) A practical note on the use of cytotoxicity assays. International Journal of Pharmaceuticals. 288 369-376

Wiberg, E., Wiberg, N., Holleman, A.F. (2001) Inorganic chemistry. Academic Press, Munich, Germany

Whiteman, M., Hong, H.S., Jenner, A., Halliwell, B. (2002) Loss of oxidized and chlorinated bases in DNA treated with reactive oxygen species: implications for assessment of oxidative damage *in vivo*. Biochemical and Biophysical Research Communications 296 883-889

Whiteside, C., Hassan, M. (1988) Role of oxyradicals in the inactivation of catalase by ozone. Free Radical Biology and Medicine 5 305-312

Wichterle, O., Lim, D. (1960) Hydrophilic gels for biological use. Nature 185 117-118

Williams, D.F. (1987) Definitions in biomaterials. Proceeding of a consensus conference of the european society for biomaterials. Elsevier press. New York, US

Williams D.F., Cunningham J. (1979) Materials in clinical dentistry. Oxford university press

Williams, C.G., Malik, A.N., Kim, T.K., Manson, P.N., and Elisseeff, J.H. (2005) Variable cytocompatibility of six cell lines with photoinitiators used for polymerizing hydrogels and cell encapsulation. Biomaterials 26 1211-1218

Williams, P.L., James, R.C., Roberts, S.M. (2000) Principles of Toxicology – Environmental and industrial applications, 2nd ed., Weinheim: John Wiley & Sons Inc., 273-279

Wilsnack, R.E., Meyer, R.J., Smith, J.G. (1973) Human cell culture toxicity testing of medical devices and correlation to animal tests. Biomaterials, Medical Devices and Artificial Organs 1 543–562

Winter, G.D. (1962) Formation of the scab and the rate of epithelization of superficial wounds in the skin of the young domestic pig Nature 193 293-4

Winter, G.D. (1965) A note on wound healing under dressing with special reference to perforated film dressing. Journal of Investigative Dermatology 45 299-302

Wolfe, R.L., Stewart, M.H., Liang, S., McGuiri, M.J. (1989) Disinfection of model indicator organisms in a drinking water pilot plant using Peroxone. Applied Environmental Microbiology 55 2230-2241

Wu, X.S. (1996) Controlled drug delivery systems (Part I) Lancaster: Technomic Publishing Co. Inc., Pennsylvania, US 8-52

Yakacki, C.M., Lyons, M.B., Rech, B., Gall, K., Shandas, R. (2008) Cytotoxicity and thermomechanical behavior of biomedical shape-memory polymer networks post-sterilisation. Biomedical Materials 3 1-9

Yan, K., Yamamoto, T., Kanazawa, S., Ohkubo, T., Nomoto, Y., Chang, J.S. (1999) Control of flow stabilized positive corona discharge modes and NO removal characteristics in dry air by CO2 injections. Journal of Electrostatics 46 207-219

Yanfeng, C., Min, Y. (2001) Swelling kinetics and stimuli responsiveness of poly(DMAEMA) hydrogels prepared by UV-irradiation. Radiation Physics and Chemistry 61 65-68

Yaung, J.F., Kwei, T.K. (1998) pH sensitive hydrogels based on polyvinypyrrolidinin-polyacrylic acid (PVP-PAA) semi interpenetrating networks (semi-IPN): swelling and controlled release. Journal of Appliesd Polymer Science 69 921-30

Yin, L., Zhao, Z., Hu, Y., Ding, J., Cui, F., Tang, C., Yin, C. (2008) Polymer–protein interaction, water retention, and biocompatibility of a stimuli-sensitive superporous hydrogel containing interpenetrating polymer networks. Journal of Applied Polymer Science 108 1238-48

Yu, T.W., Anderson D. (1997) Reactive oxygen species-induced DNA damage and its modification: A chemical investigation. Mutation Research/Fundamental and Molecular Mechanisms of Mutagenesis 379 201-210

Zeiger, E. (1987) Carcinogenicity of mutagens: Predictive Capability of the Salmonella Mutagenesis Assay for Rodent Carcinogenicity. Cancer Research 47 1287-1296

Zeiger, E., Anderson, B., Haworth, S., Lawlor, T., Mortelmans, K., Speck W. (1987) Salmonella mutagenicity tests: III. Results from testing of 255 chemicals. Environmental Mutagenesis 9 1-110

Zeller, H., Englehardt C. (1977) Testing of kollidon 30 for mutagenic effects in male mice after a single intraperitoneal application, Dominant lethal test. Unpublished report from BASF. Gewerbehygiene and Toxikologie, Ludwigshafen, Germany. Submitted to the World Health Organization by BASF

Zhang, J., Davis, TA, Matthews MA, Drews MJ, LaBerge M, An YH (2006) Sterilization using high-pressure carbon dioxide. Journal of Supercritical Fluuids 38 354-372

Zhang, L., Sun, B., Zhu, X. (2009) Organic dye removal from aqueous solution by pulsed discharge on the pinhole. Journal of Electrostatics 67 62–66

Zhao, L., Xu, L., Mitomo, H., Yoshii, H. (2003) Synthesis of pH-sensitive PVP/CM-chitosan hydrogels with improved surface property by irradiation. Carbohydrate Polymer 64 473-80

Zhou, N., Fu, Z., Sun, T. (2008) Effects of different concentrations of oxygen – ozone on rats' astrocytes *in vitro*. Neuroscience Letters 441 178-182

Zhuk, E.G., (1971) Water disinfection by pulse electric discharges. Journal of Microbiology, Epidemiology and Immunology 48 99-103

Zorlugenç, B, Zorlugenç, F.K., Öztekin, S, Evliya, B. (2008) The influence of gaseous ozone and ozonated water on microbial flora and degradation of aflatoxin B1 in dried figs. Food and Chemical Toxicology 46 3593-3597

Zucco, F., De Angelis, I., Testai, E., Stammati, A. (2004) Toxicology investigations with cell culture systems: 20 years after. Toxicology *In Vitro* 18 153-163

Zuckerman, H., Krasik, Y.E., Felsteiner, J (2002) Inactivation of microorganisms using pulsed high-current underwater discharges. Innovative Food Science and Emerging Technologies 3 329-336

Appendices

Appendix I: Relevant data

XENOMETRIX
by Endotell

Certificate of Analysis

Product:	TA98 *hisD3052*
Lot No.:	S48
Date of Manufacture:	08/07
Storage:	-70°C

For investigational use only

Test	Result	Acceptance
Spontaneous Reversion Rate[1]	<8 positive wells	Passed*
Induced Reversion Rate[1] 2-NF (2 µg/ml)	>25 positive wells	Passed*
Histidine Synthesis[2]	Auxotrophic	Passed
rfa/Crystal Violet Sensitivity[2]	Sensitive	Passed
uvrB/Resistance to Ultraviolet Light[2]	Sensitive	Passed
pKM101/Ampicillin Resistance[2]	Resistant	Passed
Nucleotide sequence of *hisD3052* of frozen permanent culture	According to published data	Passed

Quality Control Department

References:
1. Gee et. al. (1998) Mutat. Res. 412. 115-130.
2. Maron and Ames (1983) Mutat. Res. 113: 173 - 215.

* Consistent with historical data.

FOR DETAILED INFORMATION ON OUR TEST METHODOLOGIES, PLEASE CONTACT OUR QUALITY CONTROL DEPARTMENT AT ++41-61-482 14 34.

Xenometrix GmbH
by Endotell
Gewerbestrasse 25
CH-4123 Allschwil

Tel ++41·61·482 14 34
Fax ++41·61·482 20 72
email info@xenometrix.ch
www.xenometrix.ch

XENOMETRIX
by Endotell

Certificate of Analysis

Product:	TAMix (TA7001 - TA7006 equimolar mixture)
Lot No.:	S41
Date of Manufacture:	11/06
Storage:	-70°C

For investigational use only

Test	Result	Acceptance
Spontaneous Reversion Rate[1]	<8 positive wells	Passed*
Induced Reversion Rate[1] 4NQO (500 ng/ml)	>25 positive wells	Passed*
Histidine Synthesis[2]	Auxotrophic	Passed
rfa/Crystal Violet Sensitivity[2]	Sensitive	Passed
uvrB/Resistance to Ultraviolet Light[2]	Sensitive	Passed
pKM101/Ampicillin Resistance[2]	Resistant	Passed
Nucleotide sequences of *his* loci of frozen permanent cultures	According to published data[3]	Passed

Quality Control Department

References:

1. Gee et. al. (1998) Mutat. Res. 412. 115-130.
2. Maron and Ames (1983) Mutat. Res. 113: 173 - 215.
3. Gee et al. (1994) Proc. Natl. Acad. Sci. USA 91. 11606- 11610.

* Consistent with historical data.

FOR DETAILED INFORMATION ON OUR TEST METHODOLOGIES, PLEASE CONTACT OUR QUALITY CONTROL DEPARTMENT AT ++41-61-482 14 34.

Xenometrix GmbH
by Endotell
Gewerbestrasse 25
CH-4123 Allschwil

Tel ++41·61·482 14 34
Fax ++41·61·482 20 72
email info@xenometrix.ch
www.xenometrix.ch

City Analysts Limited
Environmental Laboratories

City Analysts Limited,
Pigeon House Road,
Ringsend,
Dublin 4.

Tel: (01) 613 6003 /6 /9
Fax: (01) 613 6008
Email:info@cityanalysts.ie
www.cityanalysts.ie

Certificate of Analysis

Customer: Athlone Institute of Technology

Customer Address: Dublin Road
Athlone
Co Westhmeath

Report Reference: 09-03781-AIT
Date Received: 15/10/2009

Customer Contact: Dominik Kirf

Sample Description: Sample 1-untreated control
Sample Type: Treated Water
Date Sampled: 15/10/2009
Lab Reference Number: 70659

Site/Method Ref.	Analysis Start Date	Parameter	Result	Units	PV Value	Accreditation Status
D/3001	23/10/2009	Aluminium, Total	<20	ug/l	200 µg/l	INAB
D/3001	23/10/2009	Chromium, Total	<5	ug/l	50 µg/l	INAB
D/3001	23/10/2009	Iron, Total	<20	ug/l	200 µg/l	INAB
D/3001	23/10/2009	Manganese, Total	<5	ug/l	50 µg/l	INAB

Note:
NAC & ATC - No abnormal change and acceptable to customers.
PV Value is the parametric value, taken from European Communities, (Drinking Water) (No. 2) Regulations, 2007. S.I. No. 278 of 2007, and relates only to drinking water samples.
Site D = Analysed at City Analysts Dublin. Site L = Analysed at City Analysts Limerick

Template 1146
Revision 009

City Analysts Limited,
Pigeon House Road,
Ringsend,
Dublin 4.

Tel: (01) 613 6003 /6 /9
Fax: (01) 613 6008
Email:info@cityanalysts.ie
www.cityanalysts.ie

City Analysts Limited

Environmental Laboratories

Certificate of Analysis

Customer: Athlone Institute of Technology

Customer Address: Dublin Road
Athlone
Co Westhmeath

Report Reference: 09-03781-AIT
Date Received: 15/10/2009

Customer Contact: Dominik Kirf

Sample Description: Sample 2-30min N2
Sample Type: Treated Water
Date Sampled: 15/10/2009
Lab Reference Number: 70660

Site/Method Ref.	Analysis Start Date	Parameter	Result	Units	PV Value	Accreditation Status
D/3001	27/10/2009	Aluminium, Total	6546	ug/l	200 µg/l	NON
D/3001	23/10/2009	Chromium, Total	44	ug/l	50 µg/l	INAB
D/3001	23/10/2009	Iron, Total	147	ug/l	200 µg/l	INAB
D/3001	23/10/2009	Manganese, Total	34	ug/l	50 µg/l	INAB

Note:
NAC & ATC - No abnormal change and acceptable to customers.
PV Value is the parametric value, taken from European Communities, (Drinking Water) (No. 2) Regulations, 2007. S.I. No. 278 of 2007, and relates only to drinking water samples.
Site D = Analysed at City Analysts Dublin. Site L = Analysed at City Analysts Limerick

Template 1146
Revision 009

City Analysts Limited,
Pigeon House Road,
Ringsend,
Dublin 4.

Tel: (01) 613 6003 /6 /9
Fax: (01) 613 6008
Email:info@cityanalysts.ie
www.cityanalysts.ie

City Analysts Limited

Environmental Laboratories

Certificate of Analysis

Customer: Athlone Institute of Technology

Customer Address: Dublin Road
Athlone
Co Westhmeath

Report Reference: 09-03781-AIT
Date Received: 15/10/2009

Customer Contact: Dominik Kirf

Sample Description: Sample 3-30min O2
Sample Type: Treated Water
Date Sampled: 15/10/2009
Lab Reference Number: 70661

Site/Method Ref.	Analysis Start Date	Parameter	Result	Units	PV Value	Accreditation Status
D/3001	27/10/2009	Aluminium, Total	5515	ug/l	200 µg/l	NON
D/3001	23/10/2009	Chromium, Total	34	ug/l	50 µg/l	INAB
D/3001	23/10/2009	Iron, Total	98.3	ug/l	200 µg/l	INAB
D/3001	23/10/2009	Manganese, Total	20	ug/l	50 µg/l	INAB

Note:
NAC & ATC - No abnormal change and acceptable to customers.
PV Value is the parametric value, taken from European Communities, (Drinking Water) (No. 2) Regulations, 2007. S.I. No. 278 of 2007, and relates only to drinking water samples.
Site D = Analysed at City Analysts Dublin. Site L = Analysed at City Analysts Limerick

Template 1146
Revision 009

City Analysts Limited
Environmental Laboratories

City Analysts Limited,
Pigeon House Road,
Ringsend,
Dublin 4.

Tel: (01) 613 6003 /6 /9
Fax: (01) 613 6008
Email:info@cityanalysts.ie
www.cityanalysts.ie

Certificate of Analysis

Customer: Athlone Institute of Technology

Customer Address: Dublin Road
Athlone
Co Westhmeath

Report Reference: 09-03781-AIT
Date Received: 15/10/2009

Customer Contact: Dominik Kirf

Sample Description: Sample 4- 3x30min O2
Sample Type: Treated Water
Date Sampled: 15/10/2009
Lab Reference Number: 70662

Site/Method Ref.	Analysis Start Date	Parameter	Result	Units	PV Value	Accreditation Status
D/3001	27/10/2009	Aluminium, Total	27150	ug/l	200 µg/l	NON
D/3001	27/10/2009	Chromium, Total	195	ug/l	50 µg/l	INAB
D/3001	27/10/2009	Iron, Total	747	ug/l	200 µg/l	INAB
D/3001	27/10/2009	Manganese, Total	90	ug/l	50 µg/l	INAB

Note:
NAC & ATC - No abnormal change and acceptable to customers.
PV Value is the parametric value, taken from European Communities, (Drinking Water) (No. 2) Regulations, 2007. S.I. No. 278 of 2007, and relates only to drinking water samples.
Site D = Analysed at City Analysts Dublin. Site L = Analysed at City Analysts Limerick

Template 1146
Revision 009

City Analysts Limited,
Pigeon House Road,
Ringsend,
Dublin 4.

Tel: (01) 613 6003 /6 /9
Fax: (01) 613 6008
Email:info@cityanalysts.ie
www.cityanalysts.ie

City Analysts Limited

Environmental Laboratories

Certificate of Analysis

Customer: Athlone Institute of Technology

Customer Address: Dublin Road
Athlone
Co Westhmeath

Report Reference: 09-03781-AIT
Date Received: 15/10/2009

Customer Contact: Dominik Kirf

Sample Description: Sample 5- 3x30min N2
Sample Type: Treated Water
Date Sampled: 15/10/2009
Lab Reference Number: 70663

Site/Method Ref.	Analysis Start Date	Parameter	Result	Units	PV Value	Accreditation Status
D/3001	27/10/2009	Aluminium, Total	26330	ug/l	200 µg/l	NON
D/3001	27/10/2009	Chromium, Total	121	ug/l	50 µg/l	INAB
D/3001	27/10/2009	Iron, Total	500	ug/l	200 µg/l	INAB
D/3001	27/10/2009	Manganese, Total	112	ug/l	50 µg/l	INAB

Note:
NAC & ATC - No abnormal change and acceptable to customers.
PV Value is the parametric value, taken from European Communities, (Drinking Water) (No. 2) Regulations, 2007. S.I. No. 278 of 2007, and relates only to drinking water samples.
Site D = Analysed at City Analysts Dublin. Site L = Analysed at City Analysts Limerick

Template 1146
Revision 009

Appendix II: Relevant publications

Conference Publications

Kirf D., Higginbotham C.L., Rowan N.J Devery S.M. (2008) Cyto- and genotoxicological evaluation of novel hydrogels for biomedical applications. Annual Meeting of the United Kingdom Environmental Mutagen Society. University of Northumbria, Newcastle, UK

Kirf D., Higginbotham C.L., Rowan N.J., Devery S.M. (2008). Biocompatibility assessment of novel NVP-AA copolymeric hydrogels sterilised via pulsed plasma gas discharge. Institute of Chemistry of Ireland: Annual Congress – Nanotechnology. Athlone Institute of Technology, Athlone, Ireland

Kirf D., Higginbotham C.L., Rowan N.J., Devery S.M. (2009) Toxicological evaluation of a novel hydrogel drug delivery device sterilised via pulsed plasma gas discharge. 22nd European Conference on Biomaterials. Lausanne, Switzerland

Kirf D., Higginbotham C.L., Rowan N.J., Devery S.M. (2009) Toxicological evaluation of Novel hydrogels sterilized using a pulsed plasma gas discharge technology. 2nd International Congress on Biohydrogels. Viareggio, Italy

Kirf D., Higginbotham C.L., Rowan N.J., Devery S.M. (2009) Impact of high voltage induced gas discharge sterilisation on the biocompatibility of NVP based hydrogels. Materials Ireland Annual Conference. Tyndall National Institute at University College Cork, Ireland

Journal publications

Mutagenesis vol. 24 no. 1, p. 110, 2009
Abstracts of the 31st Annual Meeting of the United Kingdom Environmental Mutagen Society, 15–18 June 2008. Held jointly with the Nordic Environmental Mutagen Society at the University of Northumbria, UK

40. Cyto- and geno-toxicological evaluation of multifunctional hydrogels for biomedical and drug delivery applications

Kirf, D., Rowan, N.J., Devery, S.M., Higginbotham, C.L.

Centre for Biopolymer and Biomolecular Research, Athlone Institute of Technology, Dublin Road, Athlone, Co. Westmeath, Ireland

Biocompatibility testing of biomaterials forms an integral part of preclinical product evaluation as well as being a prerequisite for regulatory approval. Hence, the main aim of the present study is to determine the biocompatibility of novel hydrogels intended for biomedical and drug delivery applications.

Superabsorbent hydrogels or copolymers of varying concentrations of *N*-vinylpyrrolidone and acrylic acid were prepared using either ethylene glycol dimethacrylate or polyethylene glycol 400 dimethacrylate as crosslinkers in conjunction with UV_{340nm} photopolymerization and the photoinitiator Irgacure® 184. Initial swelling/degradation studies in conjunction with headspace-linked GC/MS analysis of the gel matrices revealed that trace amounts of residual monomeric material still remained following the polymerization process. Consequently, the hydrogels were washed for a sufficient period in physiological saline to facilitate removal of such impurities.

In vitro biocompatibility testing was then performed in accordance with ISO 10993 guidelines to determine the cytotoxic and genotoxic potential of the hydrogels following indirect contact with human keratinocytes (HaCaT) and human hepatoma (HepG2) cells, chosen as model cell lines. More specifically, the agarose diffusion assay and elution test in conjunction with MTT and Neutral Red endpoints showed no indication of substantial cell death following treatment with hydrogels previously washed of any un-reacted monomer. The reduction in viability of treated cells did not exceed 10% of untreated control cell viability. In addition, no genotoxic effect was detected for either cell line following polymer exposure as evidenced by DNA migration patterns in the alkaline Comet assay upon comparison of average tail moment values for untreated control cells (<1.0) with those for the positive control agent 100 μM H_2O_2 at 37°C for 1 h (>13.0). Initial investigations at the nucleotide level in the Ames assay, with Salmonella typhimurium TA98 and a mix of TA7001-TA7006 tester strains with and without metabolic activation again provides no evidence of mutagenic activity associated with such polymeric hydrogels.